MPInterconsulting

ULTRASONICS - SONOCHEMISTRY - INNOVATION

PIEZOELECTRIC TRANSDUCERS MODELING AND CHARACTERIZATION

August 2004

MPInterconsulting
ULTRASONICS - SONOCHEMISTRY - INNOVATION

SERIES OF BOOKS RECOMENDED BY MPI

Keywords: Ultrasonics, Piezoelectric, Transducers, Converters Resonance, Impedance, Active and Reactive Power, Optimal Operating Regimes, Converter Quality Parameters.

Every engineer working in high power ultrasonics with piezoelectric transducers and ultrasonic power supplies would need to know precise answers on topics presented in this book. Instead of spending years of work and enormous amounts of money in establishing proper R&D ultrasonic lab, it is much faster and easier to consult this book which presents synthesis of author's results during more than 25 years in highly professional R&D environment.

PIEZOELECTRIC TRANSDUCERS MODELING AND CHARACTERIZATION

Author: Miodrag Prokic
Published 2004 in Switzerland by MPI
266 pages,

Book can be ordered from:

MP Interconsulting
Marais 36
2400, Le Locle
Switzerland
mpi@bluewin.ch

Phone/Fax: +41- (0)-32-9314045
email: mpi@mpi-ultrasonics.com
http://www.mpi-ultrasonics.com
http://mastersonic.com

CONTENTS:

PIEZOELECTRIC TRANSDUCERS MODELING AND CHARACTERIZATION

1. Piezoelectric Converters Modeling and Characterization

Here are pictures of products that are related to modeling and characterization techniques presented in this paper. All of such devices and components can be measured, modeled and characterized using (more or les) the same methodology and the same terminology.

There are many possibilities to present and analyze equivalent models of piezoelectric converters. The analysis presented here will primarily cower modeling of high-power piezoelectric, Langevin, sandwich-converters (applicable in ultrasonic cleaning, plastic welding, sonochemistry and other power industrial applications), and the same analysis can easily be extended to cover much wider field of different piezoelectric transducers and sensors (but this was not the main objective of this paper). For electrical engineering needs (as for instance: when optimizing ultrasonic power supplies, in order to deliver maximal ultrasonic power to a mechanical load) we need sufficiently simple and practical (lumped parameter), equivalent models, expressed only using electrical (and easy measurable or quantifiable) parameters (like resistance, capacitances, inductances, voltages and currents). Of course, in such models we should (at least) qualitatively know which particular components are representing purely electrical nature of the converter, and which components are representing mechanical or acoustical nature of the converter, as well as to know how to represent mechanical load. For here described purpose, the best lumped parameter equivalent circuits that are fitting a typical piezoelectric-converter impedance (the couple of series and parallel resonance of an isolated vibration mode) are shown to be Butterworth-Van Dyke (**BVD**) and/or its electrical dual-circuit developed by Redwood (booth of them derived by simplifying the Mason equivalent circuit and/or making the best piezoelectric impedance modeling based on experimental results and electromechanical analogies). In this paper the two of mutually equivalent (above mentioned, **and later slightly modified**), dual electrical models will be used to present a piezoelectric converter operating in its series and/or parallel resonance, Fig. 1.

Above described objective has been extremely simplified after electronics industry developed Network Impedance (Gain-Phase) Analyzers (such as HP 4194A and similar instruments). Practically, for the purpose of modeling, it is necessary to select one single converter's operating mode (to select a frequency window which captures only the mode of interest, or the single couple of series and parallel resonance belonging to that mode) and let Impedance Analyzer to perform electrical impedance measurements by producing sweeping frequency signal in the selected frequency interval (and by measuring voltage and current passing on the converter connected to the input of Impedance Analyzer). The next step (implemented in Impedance Analyzers) is to compare the measured impedance parameters with theoretically known converter model (lumped parameters model, already programmed as an modeling option inside of Impedance Analyzer), and to calculate model parameters (practically performing the best curve fitting that places measured impedance values into theoretical impedance model). This way, in a few (button pressing) steps we are able to get numerical values of all (R, L, C) electrical components relevant (only) for selected converter mode and selected frequency range (and this is in most cases the most important for different engineering purposes, such as: optimizing ultrasonic power supplies, realizing optimal resonant frequency and output power control, optimizing converters quality…). We are also able to compare (using modern impedance analyzers) how close are measured impedance values (of a real converter), and values resulting from impedance curve fitting process. In cases of well-designed converters (and converters with sufficiently high mechanical quality factor) we are able to get almost 100% correct modeling in a selected frequency window (meaning that all measured and calculated R, L and C, lumped model parameters, are numerically almost 100% correct).

The objectives of this paper are:

1. To explain the most important (and simplified, practical and easy quantifiable), electrical lumped-parameters equivalent circuits, suitable to represent piezoelectric converter in its series and/or parallel resonance, for purposes such as converters characterization, qualification and optimization, for different electrical design purposes, as well as to explain qualitatively converter models regarding higher frequency harmonics, and

models when converter transforms mechanical input into electrical output (operating as a receiver or sensor).

2. To establish the very general concept of mechanical loading of piezoelectric converters (where mechanical load is presented in normalized form using the mechanical-load units comparable to internal resistance of the converter-driving electric circuit, or ultrasonic power supply).

3. To analyze the optimal power transfer of piezoelectric converters (when transforming electrical input into mechanical output), operating in series and parallel resonance, and to explain mechanical loading process and losses in both situations.

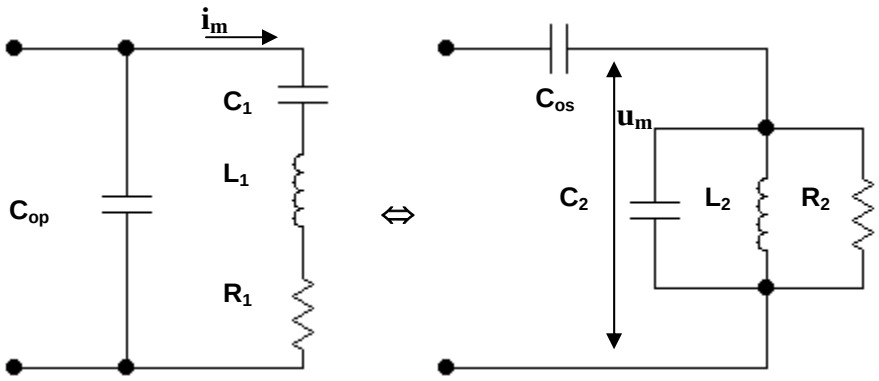

Fig. 1 Piezoelectric Converter (One-Port), Dual, BVD Models valid in the close vicinity of an isolated couple of converters series and parallel resonances

The Fig. 1 presents two of the most widely used lumped-parameters piezoelectric converter impedance models (mutually equivalent, **BVD** = **B**utterworth-**V**an **D**yke, dual-circuits models), valid for isolated couple of series and parallel resonances (of a non-loaded). In fact, on the fig Fig. 1 are presented the simplest models applicable for relatively high mechanical quality factor piezoelectric converters, where thermal dissipative elements in piezoceramics could be neglected. The more general models (again mutually equivalent), representing real piezoelectric (non-loaded) converters with dissipative dielectric losses and internal resistive electrode-elements (**R_{op} (=) Leakage AC and DC resistance, $R_{os1} \approx R_{os2}$ (=) Dielectric resistive loss of piezoceramics**) in piezoceramics are presented on the Fig. 2. For high quality piezoceramics **R_{op}**, is in the range of 10 MΩ - 50 MΩ, and **R_{os1}**, **R_{os2}** are in the range between 50 Ω and 100 Ω, measured at 1 kHz, low signal (and can be calculated from piezoceramics **tanδ** value, or using HP 4194A, and similar Impedance Analyzers). In most of cases of high quality piezoceramics we can neglect **R_{op}** as too high resistance, and **R_{os1}**, **R_{os2}**, as too low values, but we should also know that dielectric and resistive losses are becoming several times higher when converter is driven high power, in series or parallel resonance, comparing them to low signal measurements.

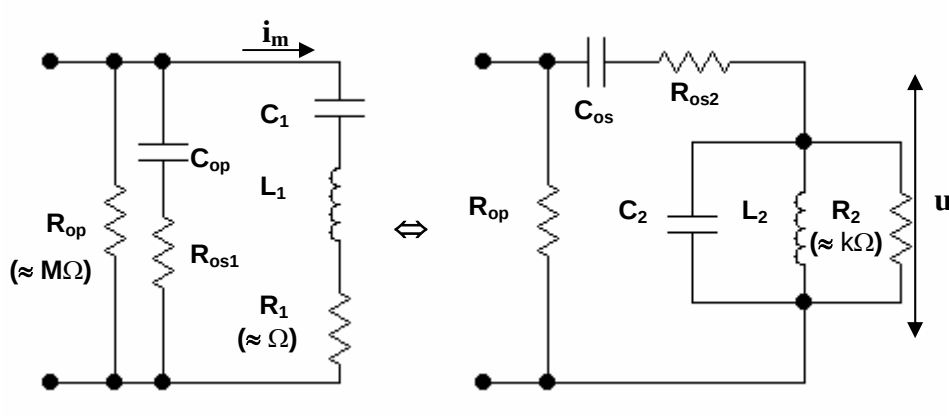

Fig. 2 BVD Piezoelectric Converter Models with dissipative elements

The other dissipative power losses (R_1 and R_2) are belonging to the mechanical circuit branch and come from converter joint losses, from planar friction losses between piezoceramics and metal parts, from mounting elements and from material hysteresis-related losses (internal mechanical damping in all converter parts). The models from the Fig. 2 can be schematically simplified if we introduce abbreviated electric-elements symbolic presenting dissipative (real) inductances and capacitances together with their belonging resistances, using only one symbol, as for instance: For any electric combination (or connection) between one capacitance and one resistance we shall introduce the symbol **C***, and for any electric combination between one inductance and one resistance we shall introduce the symbol **L*** (since we can always find exact circuit transformations between two elements in serial and parallel connection). Doing this way, models presented on Fig. 2 will be simplified as given on the Fig. 3, and applicable circuit equivalents (used in Fig. 3) are presented on the Fig. 4.

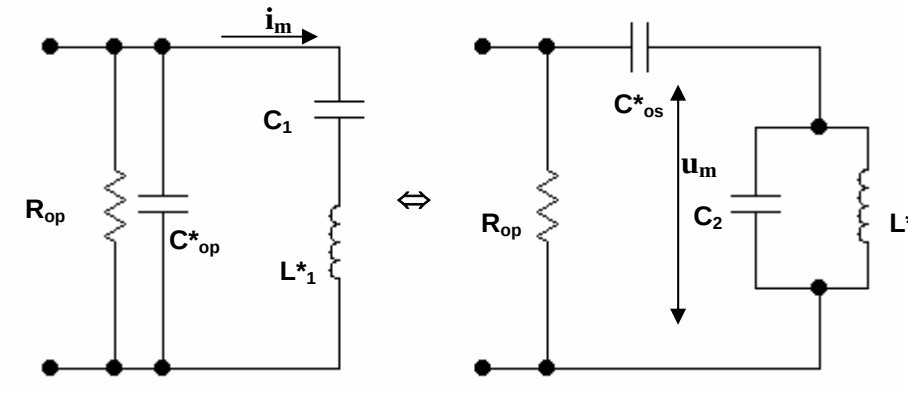

Fig. 3 Simplified BVD Piezoelectric Converter Models
(L* and C* are presenting real inductances and capacitances with internally integrated, dissipative elements: Fully equivalent to models on Fig. 2)

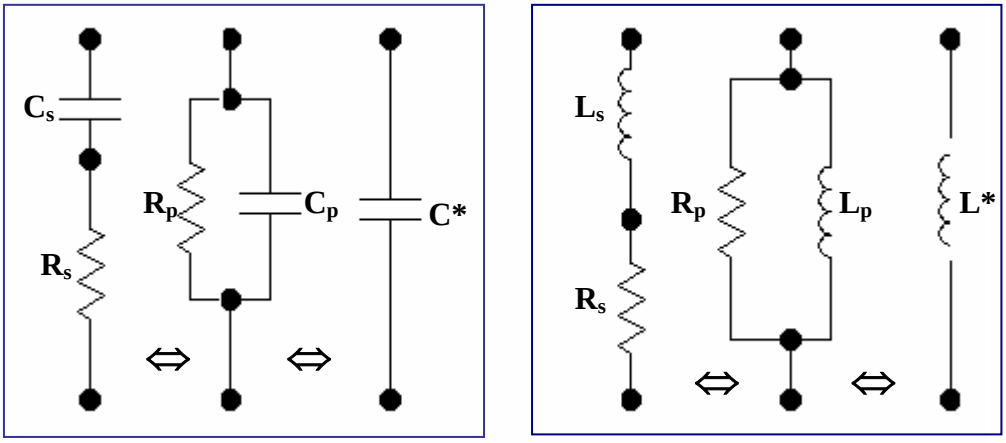

$R_p = R_s(1+1/Q_s^2), R_s = R_p/(1+1/Q_p^2)$	$R_p = R_s(1+Q_s^2)$, $R_s = R_p/(1+Q_p^2)$
$C_p = C_s/Q_s^2$, $C_s = C_p Q_p^2$,	$L_p = L_s(1+1/Q_s^2), L_s = L_p/(1+1/Q_p^2)$
$Q_s = \omega C_s R_s$, $Q_p = 1/\omega R_p C_p$, $\omega = 2\pi f$	$Q_s = \omega L_s/R_s$, $Q_p = R_p/\omega L_p$, $\omega = 2\pi f$

Fig. 4 Circuit Equivalents & Simplifications (explaining models from Fig. 3)

The other elements on the Fig. 2 are: **$C_{os} \approx C_{op}$ (=) Clamped, static capacitance/s of piezoceramics**, **$C_{1/2}$, $L_{1/2}$ (=) motional mass and stiffness elements of converter's mechanical oscillating circuit/s** (see Fig. 7 to find approximate mathematical relations between all model parameters)**.** We could also add in series to any of input converter terminals the cable (and winding) resistance, since every real converter has input electrodes, soldered or bonded (electrical) joints, and a cable (presently neglected parameters).

The influence of an external acoustic load on the converters' modeling is presented on the Fig. 5, by introducing loading resistances **R_{L1}** and **R_{L2}**, as the closest and very much simplified equivalent of the real converter loading (in reality loading resistances **R_{L1}** and **R_{L2}**, sometimes should be treated as complex impedances as the most general case).

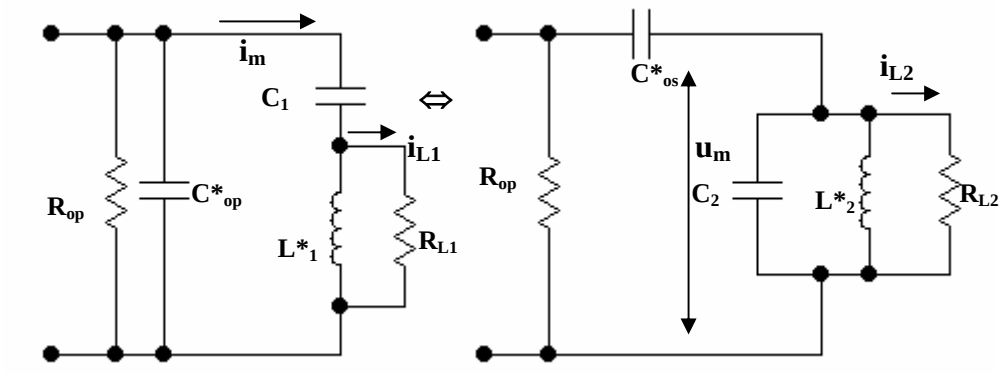

Fig. 5 Alternative BVD Models of Loaded Piezoelectric Converters

Based on equivalent electric circuits presented on Fig. 4, we can easily place parallel-loading resistances from Fig. 5 in series with inductances, just by calculating new equivalent frequency-dependant elements-values. In literature regarding the same problematic it is very usual to see that left-side piezoelectric converter-model from Fig. 5 has loading resistance in series with motional inductance and capacitance, and for the model on the right side of the Fig. 5 is usual that loading resistance is found in parallel with motional inductive and capacitive circuit elements (but using Electric Circuit Theory we can easily play with any of parallel or series elements combination, as presented on the Fig. 4). It is also clear that loading nature or load-resistance would change, depending how and where we place it (in situations, like in series connection/s with motional inductance, load resistance would increase with load-increase (starting from very low value), and in case of placing it in parallel with motional inductance (as presented on Fig. 5), load resistance would decrease with load-increase (starting from very high value)).

In all above given converter models (Figs. 1,2,3,5), we can recognize motional current $\boldsymbol{i_m}$ *and motional voltage* $\boldsymbol{u_m}$ *as the most important mechanical-output power/amplitude controlling parameters of piezoelectric converters in series and parallel resonance. When converter is operating in series resonance, in order to control its output power and/or amplitude we should control its motional current* $\boldsymbol{i_m}$*, and in the regime of parallel resonance, output power and/or amplitude are directly proportional to the motional voltage* $\boldsymbol{u_m}$*. More precisely,* ***when we compare two operating regimes of the same converter, when converter is producing the same output power (in series and/or parallel resonance)****, we can say that converter operating in series resonance is able to deliver to its load high output force (or high pressure) and relatively low velocity, and when operating in parallel resonance it is able to deliver high output velocity and relatively low force (knowing that output converter power is the product between velocity and force delivered on its front emitting surface). Here we are using the electromechanical analogy system:* ***(CURRENT ⇔ FORCE) & (VOLTAGE ⇔ VELOCITY)****. When we are talking about converter's series-resonance frequency zone, this is the case of motional* ***Current-Force*** *resonance (where converter's impedance has low values), and when we are talking about converter's parallel-resonance frequency zone, this is the case of motional* ***Voltage-Velocity*** *resonance (where converter has high impedance values). Automatically, if we realize by electrical means high motional current (current resonance, equal to series resonance), the converter will produce high motional force (it will operate in a force resonance). Also, if we realize by electrical means high motional voltage (voltage resonance, equal to parallel resonance), the converter will produce high motional velocity (it will operate in a velocity resonance). All above conclusions, for the time being, are based only on the analogy* ***(CURRENT ⇔ FORCE) & (VOLTAGE ⇔ VELOCITY)****, and later on, some more (experimental) supporting facts will be presented.*

It is also important to underline which circuit-elements (in all above found circuits, Figs. 1,2,3,5) are representing purely electrical elements of a piezoelectric converter, and which elements are only given as functional (and analog) electrical equivalents of converter's mechanical parts and its mechanical properties (including loading elements), see Fig.6.

It is very important to know that mechanical converter-loading, presented on Figs. 5 & 6, is equally and coincidently influencing changes, both in series and parallel converter impedance, basically reducing equivalent mechanical quality factor/s of a loaded converter (or coincidently increasing its series resonant-impedance and decreasing parallel resonant-impedance). ***This is the principal reason why (in this paper) an isolated couple of series and parallel resonances is treated as the same, single and unique oscillating-mode that can be driven in its current or voltage resonance, and produce force or velocity-dominant mechanical output. It is also shown to be possible to drive an ultrasonic converter high power, extremely efficiently, in any frequency (continuously) between its series and parallel resonance (when special converter reactive impedance-compensation is used).*** Since there is certain frequency shift between each couple of series and parallel resonances, and since most of today's converters (made by big players in ultrasonic industry worldwide) operate either in series or parallel resonance, in literature regarding converters modeling and converters measurements, many authors are talking about different vibration modes or different harmonics.

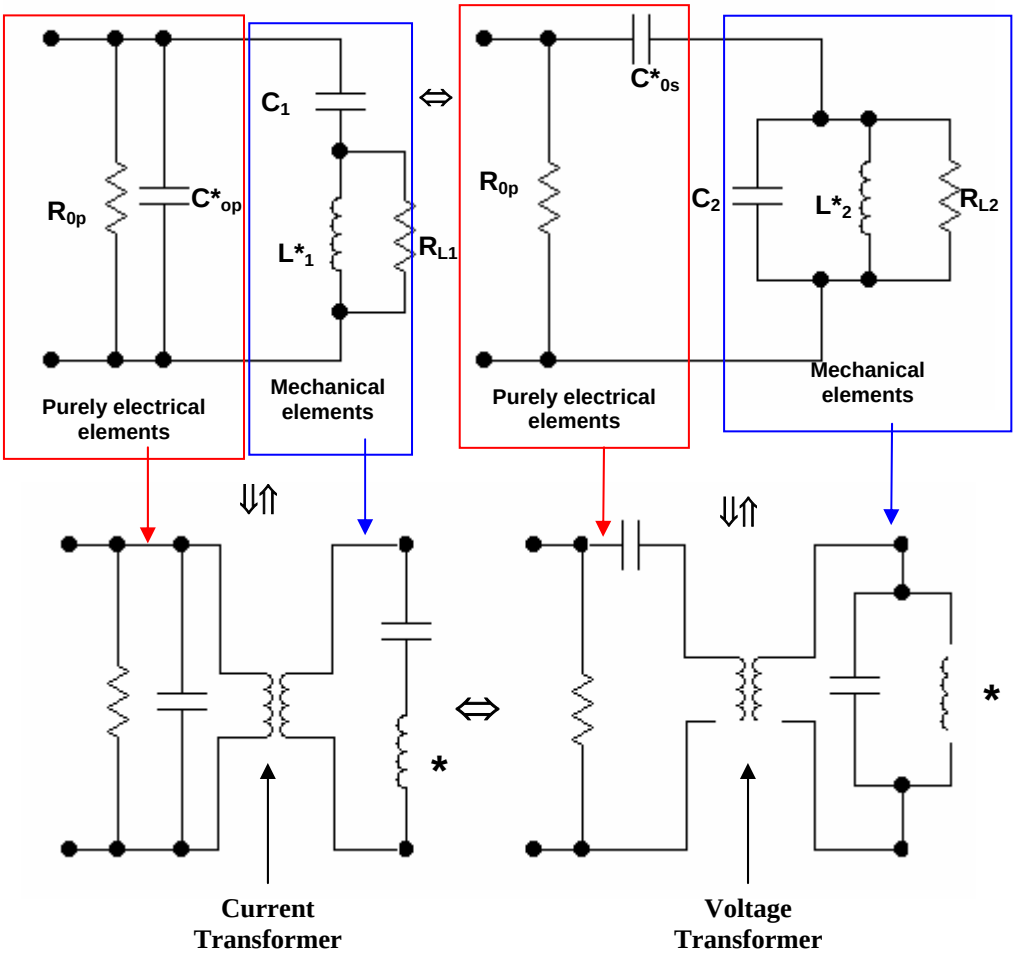

Fig. 6 Alternative BVD Models of Loaded Piezoelectric Converter with block separation of purely electrical and purely mechanical elements
Down: The same models with transformer-separation between electrical and mechanical circuits

Also in different literature regarding piezoelectric converters modeling, we can find very similar equivalent circuits (as previously presented on Figs. 1,2,3,5 & 6, all of them developed from Mason model), where some of circuit elements found in this paper are not present or have different topology. Here is accepted the strategy that all mutually equivalent piezoelectric models (Figs. 1,2,3,5 & 6) should mutually present 100% dual (equivalent) electric circuit-structures, having the same number of elements, and presenting the same (electrical) impedances for the same input DC and/or AC electrical currents and voltages, connected to their input terminals (regardless frequency).

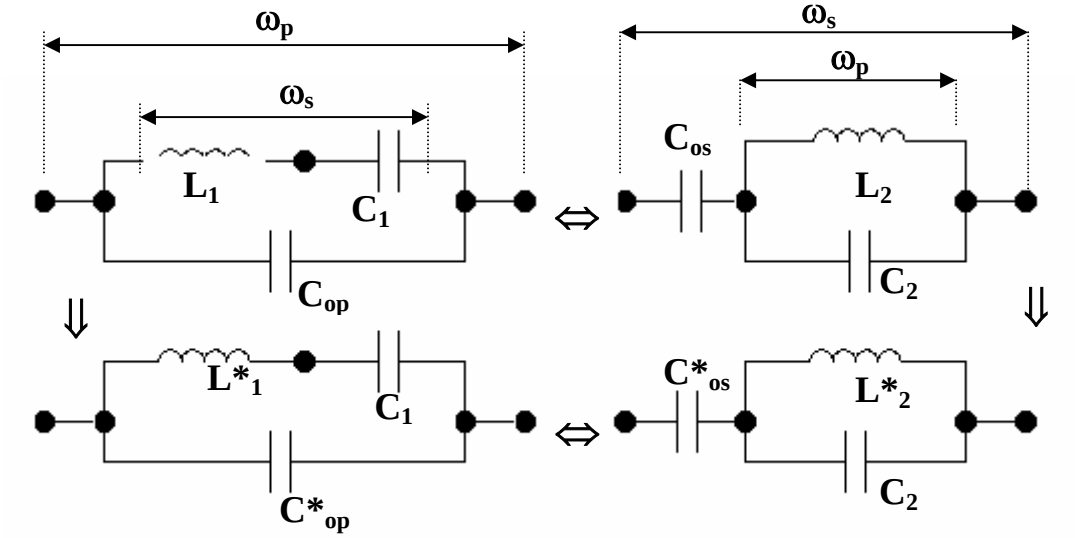

$$\omega_s = \omega_1 = 2\pi f_1 = \frac{1}{\sqrt{L_1 C_1}} = \frac{1}{\sqrt{L_2 (C_2 + C_{os})}}, C_{os} = C_1 \frac{f_2^{\,2}}{f_2^{\,2} - f_1^{\,2}}, \frac{C_{op}}{C_1} \approx \frac{C_2}{C_{os}},$$

$$\omega_p = \omega_2 = 2\pi f_2 = \frac{1}{\sqrt{L_2 C_2}} = \frac{1}{\sqrt{L_1 \frac{C_1 C_{op}}{C_2 + C_{os}}}}, C_{op} = \frac{C_2 C_{os}}{C_2 + C_{os}}, \frac{C_{op}}{C_1 + C_{op}} = \left(\frac{f_1}{f_2}\right)^2,$$

$$C_1 = C_{os} - C_{op}\ , C_2 = (C_1 + C_{op}) \frac{f_1^{\,2}}{f_2^{\,2} - f_1^{\,2}} = \frac{L_1 C_1 C_{op}}{L_2 C_{os}}\ ,$$

$$L_1 = \frac{L_2}{C_1}(C_2 + C_{os}),\ L_2 = \frac{L_1 C_1}{C_{os}}\left(1 - \frac{C_{op}}{C_{os}}\right),\ k^2 = \frac{C_1}{C_{op} + C_1} = \frac{C_{os}}{C_2} \cdot \frac{f_1^{\,2}}{f_2^{\,2}}.$$

Fig. 7 Simplified Evolution of BVD, Equivalent, Dual Circuits

Following this strategy, it was necessary to introduce certain electric elements that are not found in other literature sources regarding the same problematic in order to satisfy circuits symmetry and DC and AC current/s and voltage/s balance, when applying Kirchoff's, Ohm's and other Circuit Theory Laws.

Practically, as presented in a very simplified and condensed form on Fig. 7, we can easily see that all of above discussed equivalent electric circuits (Figs.1,2,3,5,6) are based (or established) on the evolution of mutually equivalent (or dual) electric circuits (known in modern filter design), combined with circuit equivalents from Fig. 4. Different relations between dual-model elements found on Fig. 7 are also applicable (as the best approximation for sufficiently high quality factor circuits) to all models presented on Figs. 1, 2, 3, 5, 6 and to other piezoelectric transducer models based on Mason model.

In order to give the full picture of the modeling strategy presented in this paper, it would be interesting to explain how model of a (single) piezoelectric converter transforms when we connect a horn or booster to it (of course, added horn or booster should have almost the same resonant frequency as a converter). Practically we should know where in the basic converter model we place one more equivalent

circuit-model presenting added horn. The most important background related to this situation is to know that added horn also presents one mechanical resonant structure that can be replaced with an electrical (equivalent) resonant circuit. In most of the literature regarding converters modeling, added horns are treated as converter loads, but here we shall (primarily) treat them as added resonant boxes, resonant circuits, or added filter circuits (all of them operating at the same resonance). Starting from evolution-equivalent circuits presented on Fig. 7, and from basic converter models presented on Fig. 3 we can illustrate what means "**converter+horn**" modeling with new step-by-step circuit-evolution models given in Fig. 8. We know that regardless how many boosters and horns we add to a converter (all of them having the same resonant frequency); -finally, after making impedance measurements (with HP 4194A, for instance) we get principally the same models as models on Fig. 3 (just particular circuit parameters and mechanical quality factor are changed). Of course this is a kind of over-simplified statement, since added sonotrodes with complex shapes can create new resonant frequencies, but here we accept (in advance) to limit our observations only to a well isolated and separated couple of series and parallel resonances. What is happening (Fig. 8) is that by adding horns to a converter we create higher-orders electrical and mechanical filter-circuits that can be again (going backwards and applying Electric Circuits Theory) transformed into basic converter models presented on Figs. 1,2,3,5,6. We also see that in simplified circuit evolution chart on Fig. 8, we deal with strongly mutually-coupled resonant-circuits (either the same current or the same voltage are coupling such circuits), operating on the same resonant frequency, and that we can place the Load where it would be physically (loading should again be treated on the same way as presented on Figs. 5 & 6). The internal losses of added horns are also not neglected, since we can find dissipative elements in added-horn-related resonant circuits.

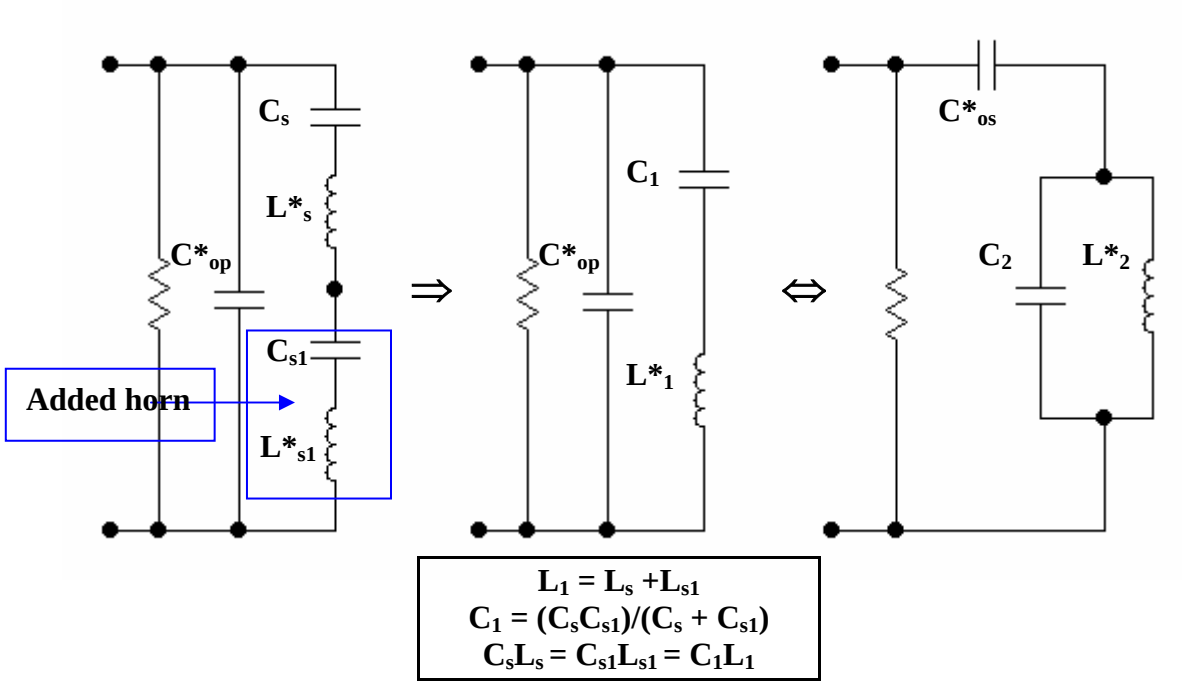

Fig. 8 Evolution of "Converter-Horn" BVD, Dual Circuits

We also know (from many years of experience in ultrasonic engineering) that when we add the horn, booster or some other (well designed) sonotrode to a converter, new, resulting mechanical quality factor of the combination "converter+horn" will

become much higher than it was in the case of a single converter, meaning that mechanical resonant circuits ("converter+horn") should be mutually connected in a connection that creates higher mechanical quality factors. This is in agreement with filter theory knowledge (regarding connecting multiple filter blocks in series (or sometimes parallel, or more complex) connection, having the same resonance/s), and also strongly supports the evolution chart on Figs. 8 & 9.

We can also create another simplified circuit evolution chart (see Fig. 9), equivalent to one of Fig. 8, in order to explain "**converter+horn**" modeling (when converter and horn operate on the same resonant frequency), starting from a dual circuit model where motional capacitance and inductance are in parallel connection. It is also important to underline that motional inductances of "**converter+horn**" combination, both given on Fig. 8 and Fig. 9 are strongly (acoustically, or mechanically) coupled, oscillating on the same resonant frequency, what makes presented circuit transformations easier to understand. From the point of view of Electric Circuit Theory, a strong "**converter+horn**" mechanical coupling on Figs. 8 & 9 can also be presented in the convenient equivalent form of coupled inductances (L^*_s coupled with L^*_{s1} and L^*_p coupled with L^*_{p1}), or in the form with ideal transformer/s coupling (where for Fig. 8, L^*_s is the primary transformer section and L^*_{s1} and C_{s1} are in the secondary transformer section, or where for Fig. 9, L^*_p is in the primary transformer section and L^*_{p1} and C_{p1} are in the secondary transformer section).

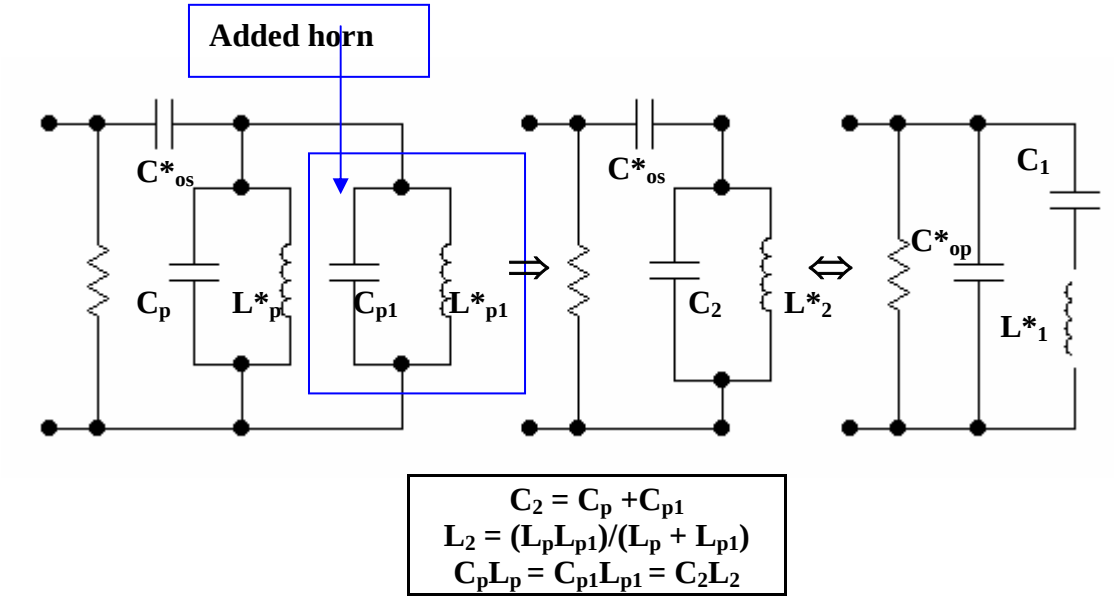

Fig. 9 Evolution of "Converter-Horn" BVD, Dual Circuits

It remains also to explain converter harmonics (higher frequency resonances) in the frame of already established lumped-parameters modeling. On the Fig. 10-a and Fig. 10-b are presented different circuit possibilities using series and parallel connection of basic resonant-circuit configurations. The cases on Fig. 10-a also present (simplified) direct resistive loading on the first resonant mode.

The single-resonant-mode loading (Fig. 10-a) can also be presented (using equivalent circuit transformations) in the form of inductive transformer coupling,

where R_L can be placed on the secondary side of the transformer, which primary side is the converter motional inductance, or we can make some other transformer and/or inductive-coupled (equivalent circuits) combinations in series with motional inductances. Most of above mentioned "inductive and transformer coupling options" we can implement in a certain (most convenient) form of equivalent circuit models to all of loading situations presented on Figs. 10-b until 10-e.

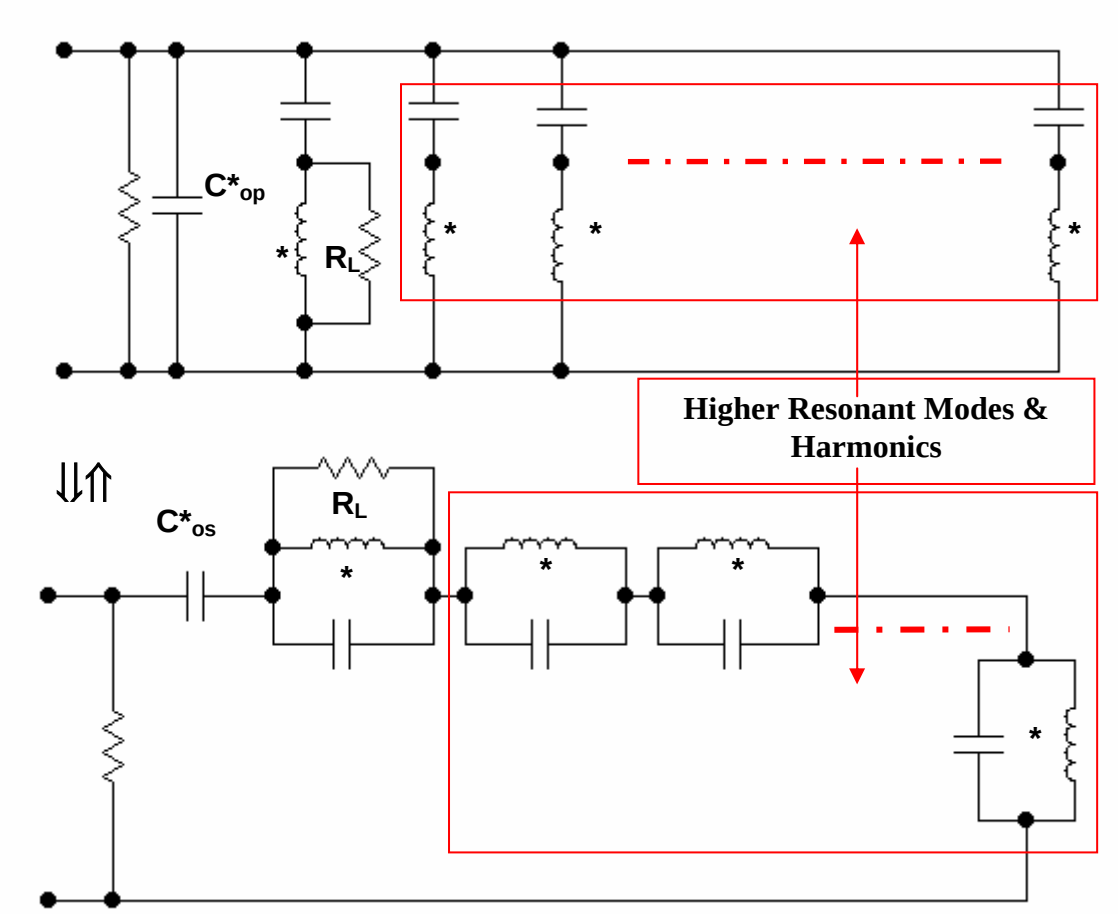

Fig. 10-a Dual-Circuits, Converter Modeling Including Harmonics, valid for acoustically or mechanically non-loaded converters

The much more general case of converter (dual) models with harmonics (than the case on Fig 10-a), including different loading situations (which are covering all previously discussed models), is presented on the Fig. 10-b. All possible mechanical loading situations (Fig. 10-b), are presented by (dual) load-impedances marked with **(1), (2), (3)** and **(4)**.

For instance, if we take only the upper converter model (Fig. 10-b), when load **(1)** is connected to mechanical output terminals (short-circuit connection), converter is operated in idle, or no-load condition, and it is called a piezoelectric resonator. If the load **(2)** is connected to mechanical output terminals, this is the case of resistive mechanical loading. If the load **(3)** is connected to mechanical output terminals, this is the case of a simple mechanical resonator similar to a single-resonant-frequency sonotrode or booster, or some other simple mechanical oscillating system. The load **(4)** presents the most general case of arbitrary and complex mechanical impedance.

For the lower converter model (Fig. 10-b) we again have the same (analogue and dual-models) situation, as already explained for the upper model. The only exception is that when load **(1)** is connected to mechanical output terminals (in fact nothing, or open-contacts are connected), converter is operated in idle, or no-load condition, and it is called a piezoelectric resonator. The loads **(2), (3)** and **(4)** have the same meaning as already explained for the upper model (but presented as dual circuits).

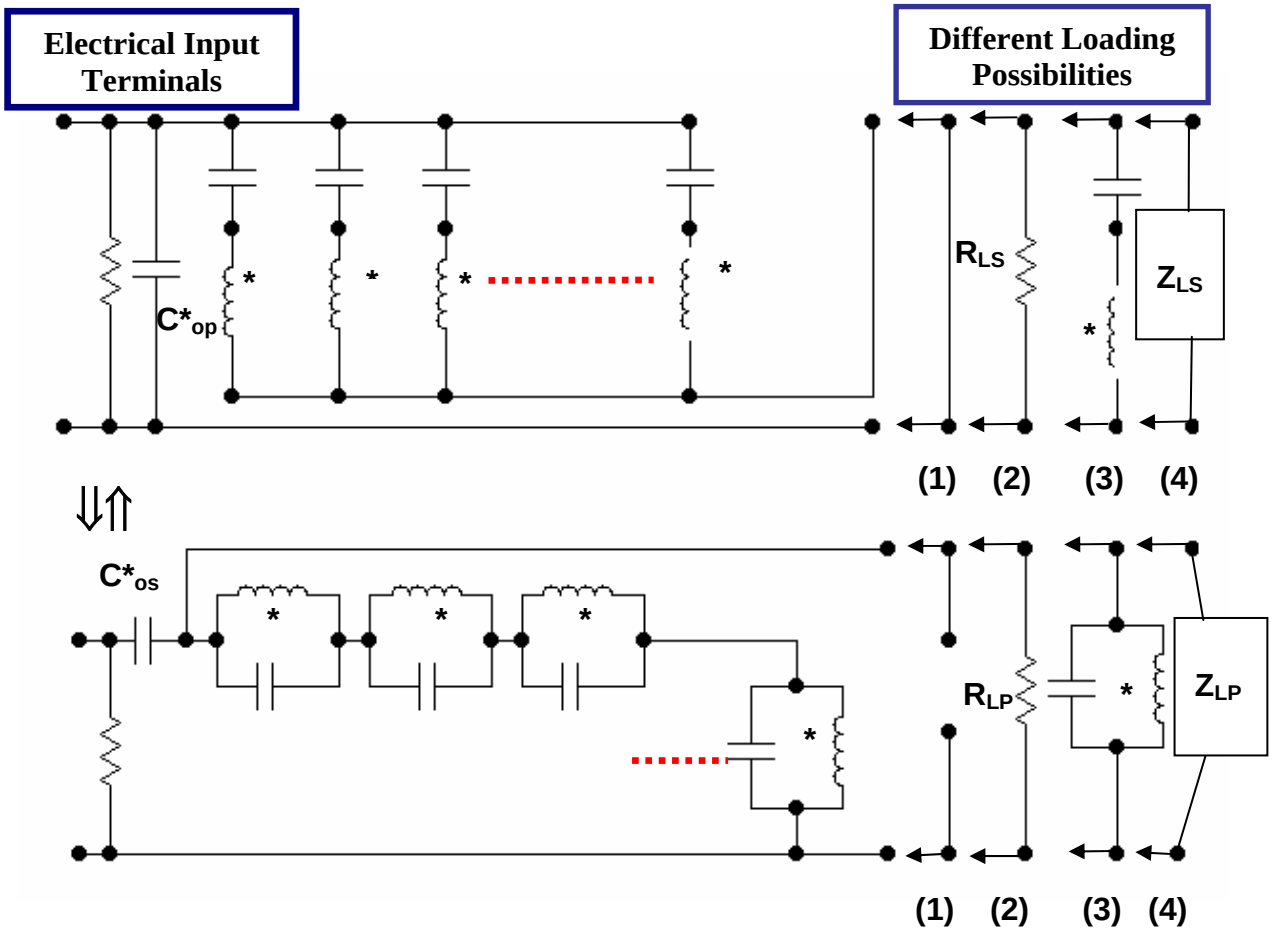

Fig. 10-b Dual-Circuits, Converter Modeling Including Harmonics and Different Loads (here marked by electric impedances (1), (2), (3) and (4))

In most of cases of practical interest (in ultrasonic technology), we use a single operating resonant mode, and operate converter in its series or parallel resonance, assuming that mechanical (or acoustic) load can be approximated or replaced by variable (load-dependant) resistance. For such simplified situations, instead of using loading models presented on Figs. 5, 6 … 10-b, we can standardize the use of the loading-models presented on the Fig. 10-c. All of models on Fig. 10-c are mutually equivalent (dual electric circuits), and can be mutually transformed using the generic equivalent circuits (and relations) presented on Fig. 7 and Fig. 4. Effectively, a resistive acoustic load (on Fig. 10-c) is presented either by series or parallel variable resistance ($\mathbf{R_{Ls1,2}}$ or $\mathbf{R_{Lp1,2}}$) placed (appropriately) in the motional part of the converter equivalent circuit/s. **If we apply the circuit options (Fig. 10-c) where we have only series load resistances, $R_{Ls1,2}$, by the acoustic load increase we shall have proportional increase of series load resistances. Also, if we apply the circuit options where we have only parallel load resistances, $R_{Lp1,2}$, by the**

acoustic load increase we shall have proportional reduction of parallel load resistances. Consequently series load resistances $R_{Ls1,2}$ should be directly proportional to the acoustic impedance ρvs (= density x sound speed x surface), and parallel load resistances $R_{Lp1,2}$ should be directly proportional to the acoustic admittance or mobility = 1/ρvs (of the media in contact with a piezoelectric converter). This situation is very important step in understanding and modeling of piezoelectric-converters loading, since (based on models on Fig. 10-c) we can establish generally valid platform for different analyses of optimal power transfer, impedance matching situations, reactive impedance compensation, mechanical output control etc.

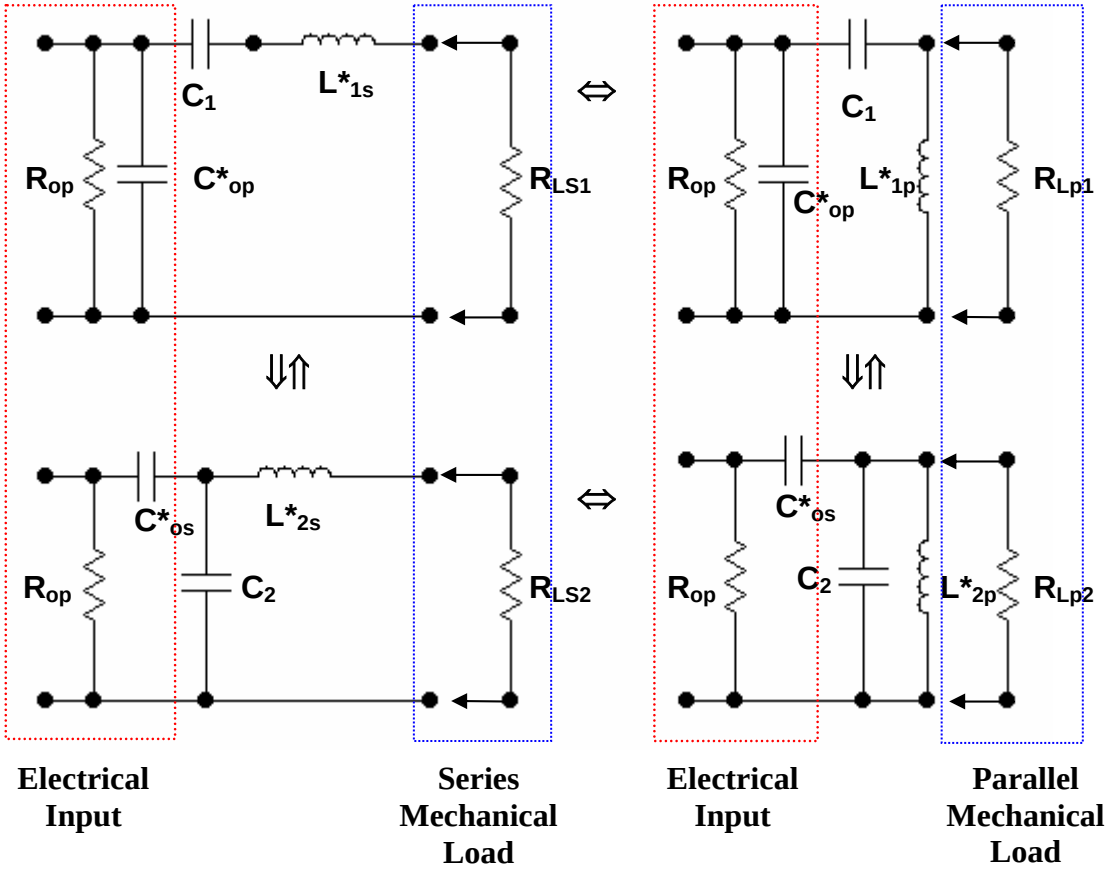

Fig. 10-c Single-Mode, Series and Parallel, Resistive Load-Impedance Models (Developed using equivalent circuits from Fig. 4)

Using similar equivalent-circuit idea, like presented on the lower part of the Fig. 3, we can also make transformer-separation between every converter and its load (applicable, for instance, to Fig. 10-b, Fig. 10-c…), by introducing voltage or current transformers (which will not change equivalent input impedance/s of the models where such separation would be applied).

Every piezoelectric converter is in the same time able to detect mechanical vibrations, serving as an accelerometer, microphone, receiver or sensor (producing an electrical output signal, proportional to its mechanical excitation). If we again consider only simplified converter models (without harmonics; Figs. 1, 2, 3, 5 and 6), we can present converter's mechanical excitation by dual models given on Fig. 10-d.

Later on, if we would like to include harmonics into Fig. 10-d, we can simply use the modeling structures presented on Fig. 10-b and keep the mechanical excitation in the same place/s as presented on the Fig. 10-d. It is important to have a feeling how external mechanical excitation influences converter's operation (and modeling) because in many situation of interest (like ultrasonic cleaning, welding, liquid processing…), when we drive a converter electrically in order to produce mechanical output, in the same time its load can produce (or reflect) mechanical excitation and generate additional charges, currents and voltages inside of a converter's structure. When piezoelectric converter is used only as the sensor of mechanical excitation, we also need to know what are its most convenient electrical models in order to qualify and quantify sensor parameters and sensor output signals. Models presented on the Fig. 10-d are also important if we would like to operate a piezoelectric converter as an (lock-in) active vibration source able in the same time to detect external mechanical excitation in the well-selected frequency zone (or using piezoelectric converters and sensors in interactive and impedance sensitive operating regimes).

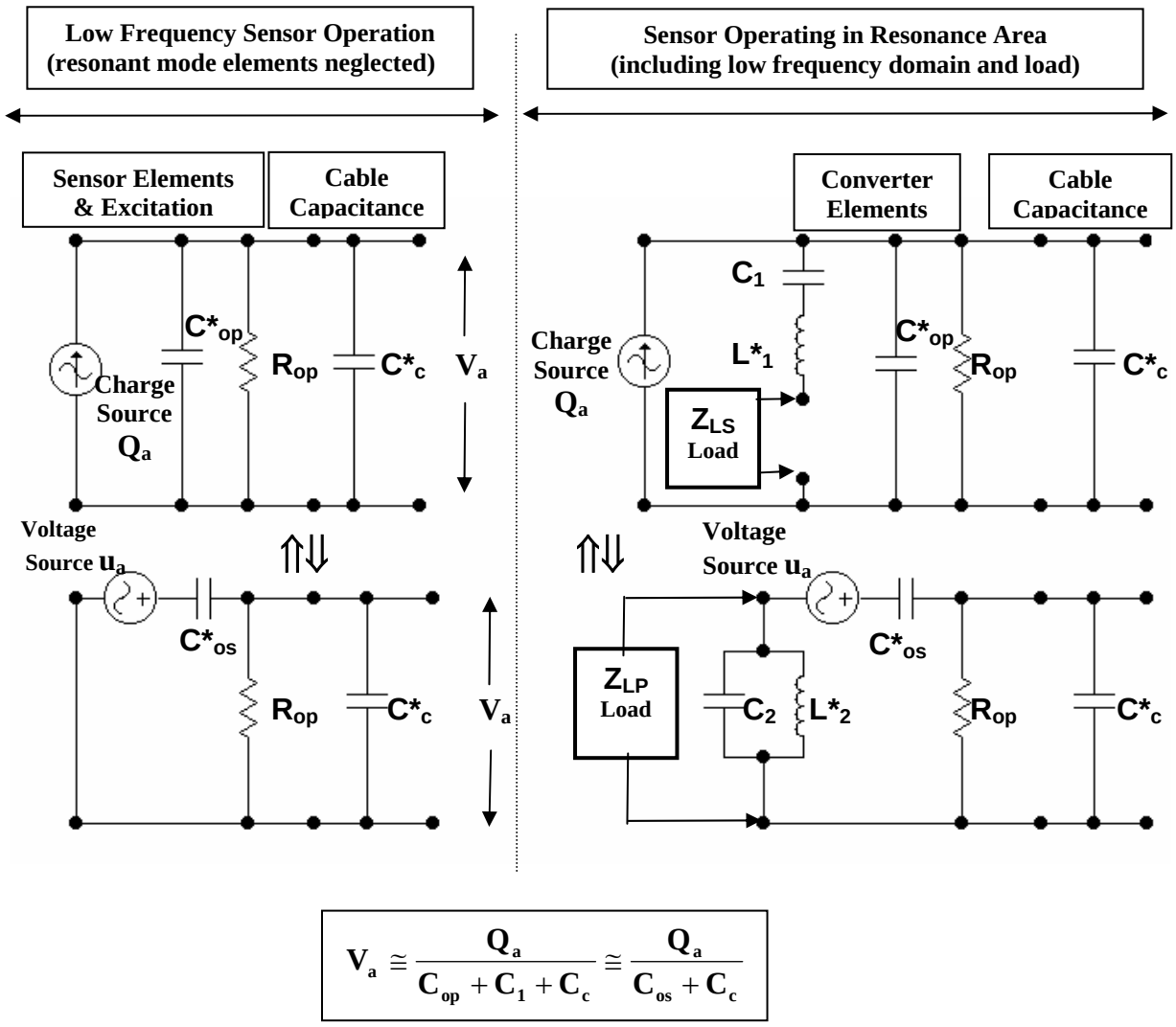

$$V_a \cong \frac{Q_a}{C_{op} + C_1 + C_c} \cong \frac{Q_a}{C_{os} + C_c}$$

Fig. 10-d Converter as a Receiver of Mechanical Excitation

Piezoelectric converters when operating as sensors are also able to detect static and constant mechanical excitation (external force), generating certain constant charge

and/or voltage, because of the presence of permanent (frozen) electrical field inside of the crystal structure of piezoelectric materials (created during production of that piezoelectric material by separating internal positive and negative electric charges in the form of oriented electrical dipoles). When external (static) force is applied on a piezoelectric sensor, internally separated electrical charges (belonging to polarized piezoelectric crystal structure) will slightly change their equilibrium position and release certain amount of free electrical charge (proportional to the applied force), which will appear on the external sensor electrodes. In cases when there is only a static, or low frequency mechanical excitation applied to a piezoelectric sensor, we can safely apply two sensor models presented on the left side of Fig. 10-d, and treat charge source $\mathbf{Q_a}$ and voltage source $\mathbf{u_a}$ as static electric sources.

The same situation becomes more interesting when external mechanical excitation is originated from a dynamical, high frequency vibration source, which is in the same frequency range where sensor has its resonant frequencies, because this type of excitation usually has very low, or close to zero average-level of amplitudes (regarding its average force or average velocity). Sensor will still remain able to react on constant external force, and in the same time be able to detect external dynamic excitation. For such situations we can create models where static and dynamic (or variable) excitation sources are separated, as presented on Fig. 10-e (or we could also separate them in the same positions where they are already placed on Fig. 10-d). Dynamic external excitation (Fig. 10-e) is introduced in the form of inductive coupled voltage sources with motional inductances.

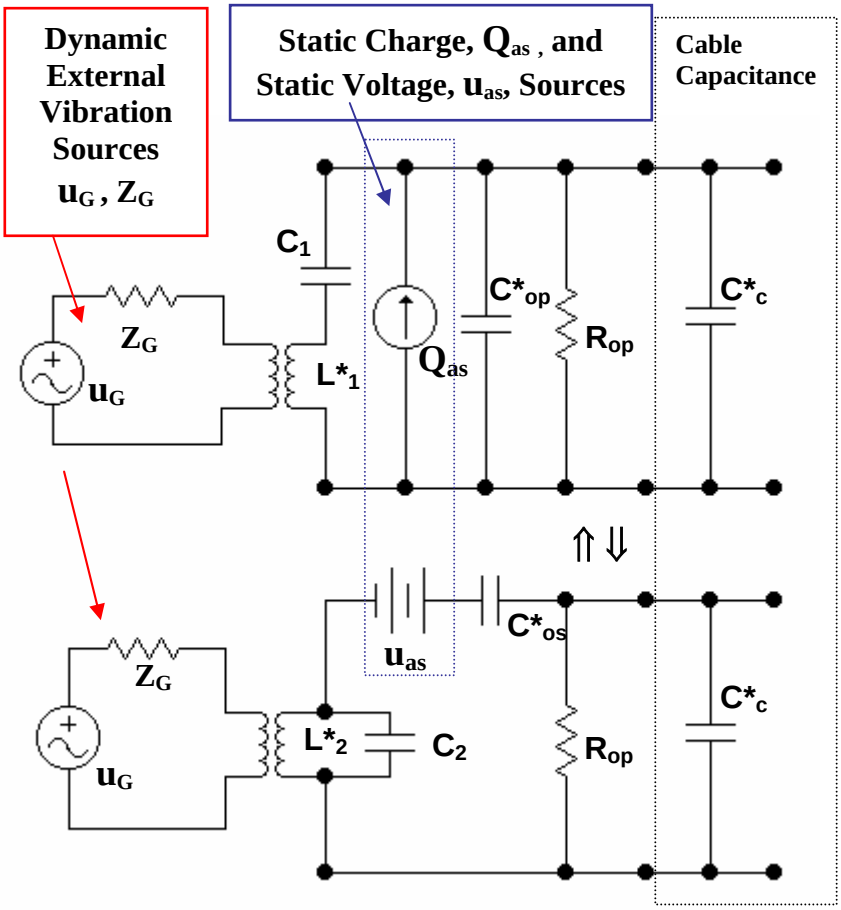

Fig. 10-e Converter as a Receiver of Mechanical Excitation where static and dynamic excitation are separated

Using Circuit Theory, we could create many of equivalent models, similar to models presented on Fig. 10-d and Fig. 10-e, "playing" with equivalent and/or dual circuits, with transformations between voltage and current/charge generators, etc.

Let us go back to converter models with isolated or single resonant mode presented on Fig. 1 until Fig. 6. It is obvious that we can drive piezoelectric converter in any of its characteristic resonant frequencies (series or parallel) exercising different advantages and disadvantages, depending on application and on converter's operating regime. Also, it is very important to know that in any of the resonant-frequency zones (in series and/or parallel resonance) we could create either maximal converter amplitude, or maximal velocity or maximal force, depending how we control the resonant output circuit and compensate the piezoelectric converter, and what we prefer to maximize as the mechanical output. For instance, in series resonance zone we shall have maximal motional current and maximal motional force mutually in phase (presenting natural, series mechanical resonance), but maximal velocity and maximal displacement (in the same zone) would be realized on two other resonant frequencies (and all of them would be relatively close to each other). The same is valid for parallel resonance zone where we shall have maximal motional voltage and maximal motional velocity mutually in phase (presenting natural, parallel mechanical resonance), but maximal force and maximal amplitude (in the same zone) would be realized on two other resonant frequencies (and again, all of them would be relatively

close to each other). When we create electrical resonance on the converter input terminals, maximizing either converter's input-current or input-voltage, such electrical resonance/s will not present in the same time the best (particular) mechanical resonance (or saying differently, converter's input-current resonance will be only close to converter's series mechanical-resonance (but not identical to it), and converter's input-voltage resonance will be close to converter's parallel-mechanical resonance, too).

Such finesses, regarding differences between electrical and mechanical resonance operating areas usually pass unrecognized by majority of people active in ultrasonic design and engineering. In this paper the frequency zone of converter series resonance and minimal impedance will be simply characterized by frequency f_1 *(or expressed as the frequency interval [*f_1*]), and frequency zone of converter parallel resonance and maximal impedance will be characterized by frequency* f_2 *(or expressed as the frequency interval [*f_2*]), since for high mechanical-quality-factor power converters, all electrical and mechanical resonances in the zone [*f_1*] are very close to each other, and the same is valid for zone [*f_2*]. The more detailed analyze of the piezoelectric converter impedance (of an isolated resonant mode: Figs. 1- 6) will show that the typical impedance-frequency curve (as well as other impedance parameters in the function of frequency) are similar as presented on the Fig. 11-a.*

In order to give precise mathematical expressions for all possible converter resonances (valid for single resonance; -models from Figs. 1,2,3,5,6), let us present converter complex impedance as two electrical parts in series connection, or as a connection between resistive impedance $\mathbf{R_e}$ and reactive impedance $\mathbf{Xe}$ (Fig. 11-a).

$$\mathbf{Z} = \mathbf{R_e} + \mathbf{jX_e} = \sqrt{\mathbf{R^2_e} + \mathbf{X^2_e}} \cdot \mathbf{e}^{\mathbf{j}\arctan\frac{\mathbf{X_e}}{\mathbf{R_e}}} = |\mathbf{Z}| \cdot \mathbf{e}^{\mathbf{j}\arctan\frac{\mathbf{X_e}}{\mathbf{R_e}}} = |\mathbf{Z}| \cdot \mathbf{e}^{\mathbf{j}\theta},$$

$$\theta = \arctan\frac{\mathbf{X_e}}{\mathbf{R_e}}.$$

It will also be very much useful to present reactive parts of converter's motional impedances (see dual electrical circuits: Figs. 1,2,3,5,6 & Fig. 11-a) as $\mathbf{X_1}$ and $\mathbf{X_2}$,

$$\mathbf{X_1} = \mathbf{X_{L1}} + \mathbf{X_{C1}} = \omega\mathbf{L_1} - \frac{\mathbf{1}}{\omega\mathbf{C_1}} \quad \textbf{(= motional inductance \& capacitance in series)},$$

$$\mathbf{X_2} = \mathbf{X_{L2}} \Big\| \mathbf{X_{C2}} = \frac{\omega\mathbf{L_2}}{\mathbf{1} - \omega^2\mathbf{L_2C_2}} \quad \textbf{(= motional inductance \& capacitance in parallel)}$$

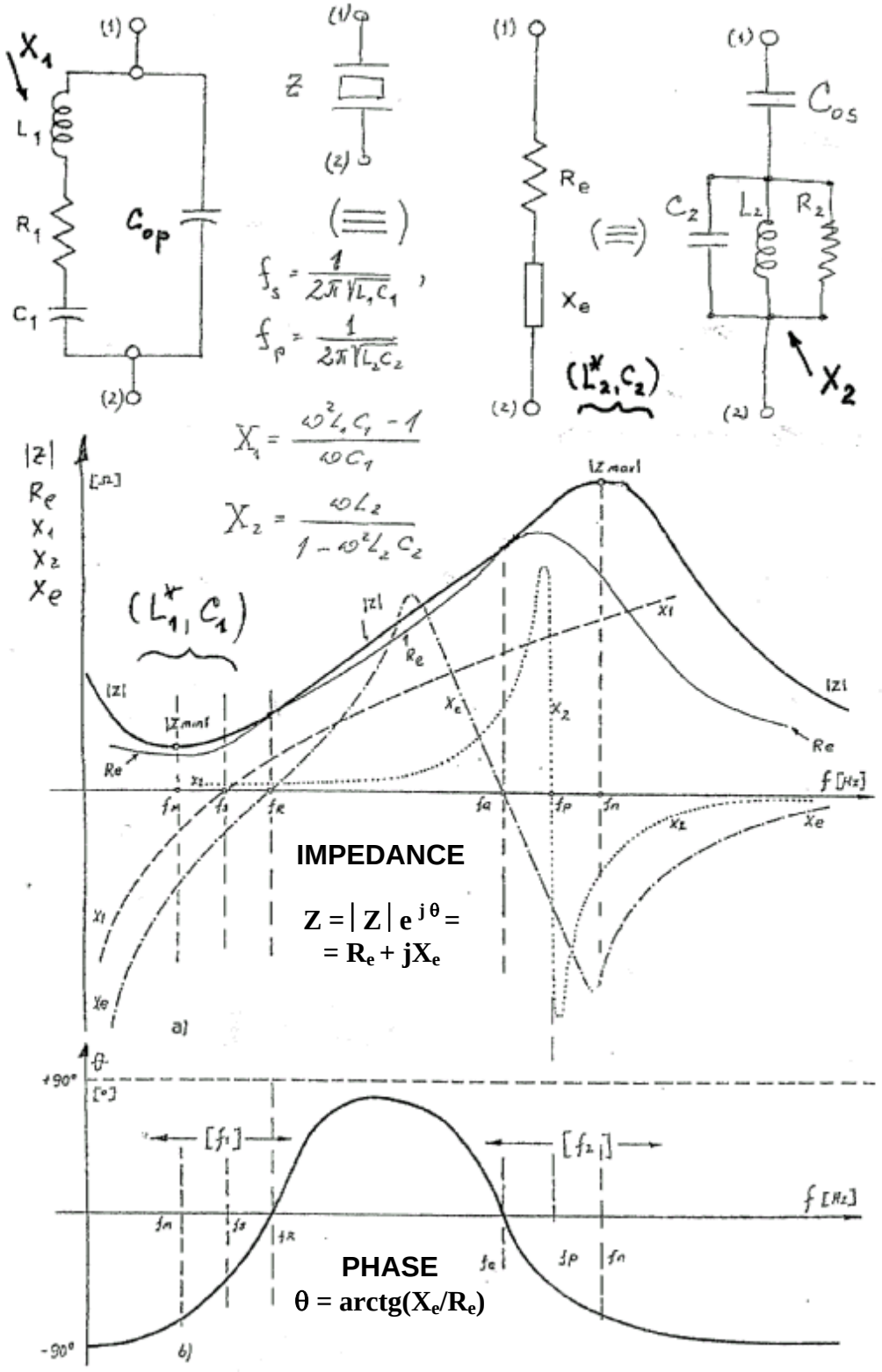

Fig. 11-a Impedance Functions vs. Frequency

The meaning of characteristic resonant frequencies (on Fig. 11-a) is as follows:

RESONANCES	CONDITIONS	EQUATION
$\mathbf{f_m}$ – frequency where absolute value of impedance reaches its minimum	$\lvert\mathbf{Z}\rvert = \lvert\mathbf{Z}_{\min.}\rvert$	$\mathbf{f_m} = \mathbf{f_s}(\mathbf{1} - \frac{\alpha^2}{\mathbf{2r}})$
$\mathbf{f_s}$ – series motional current-force, mechanical resonant frequency	$\mathbf{X_1} = \mathbf{X_{L1}} + \mathbf{X_{C1}} = \omega\mathbf{L_1} - \frac{\mathbf{1}}{\omega\mathbf{C_1}} = \mathbf{0}$	$\mathbf{f_s} = \frac{\mathbf{1}}{\mathbf{2}\pi\sqrt{\mathbf{L_1C_1}}}$
$\mathbf{f_r}$ – series electrical, input-current resonance, where phase pass zero line	$\theta = \arctan\frac{\mathbf{X_e}}{\mathbf{R_e}} = \mathbf{0},\ \mathbf{X_e} = \mathbf{0}$	$\mathbf{f_r} = \mathbf{f_s}(\mathbf{1} + \frac{\alpha^2}{\mathbf{2r}})$
$\mathbf{f_a}$ – parallel, electrical, input-voltage resonance, where phase pass zero line	$\theta = \arctan\frac{\mathbf{X_e}}{\mathbf{R_e}} = \mathbf{0},\ \mathbf{X_e} = \mathbf{0}$	$\mathbf{f_a} = \mathbf{f_s}(\mathbf{1} + \frac{\mathbf{1}-\alpha^2}{\mathbf{2r}})$
$\mathbf{f_p}$ – parallel motional voltage-velocity, mechanical resonant frequency	$\mathbf{X_2} = \frac{\omega\mathbf{L_2}}{\mathbf{1} - \omega^2\mathbf{L_2C_2}} \to \infty$	$\mathbf{f_p} = \frac{\mathbf{1}}{\mathbf{2}\pi\sqrt{\mathbf{L_2C_2}}}$
$\mathbf{f_n}$ – frequency where absolute value of impedance reaches its maximum	$\lvert\mathbf{Z}\rvert = \lvert\mathbf{Z}_{\max.}\rvert$	$\mathbf{f_n} = \mathbf{f_s}(\mathbf{1} + \frac{\mathbf{1}+\alpha^2}{\mathbf{2r}})$
Abbreviated symbols	$\mathbf{r} = \frac{\mathbf{C_{op}}}{\mathbf{C_1}} = \frac{\mathbf{f_1}^2}{\mathbf{f_2}^2 - \mathbf{f_1}^2}$, $\alpha = \frac{\mathbf{r}}{\mathbf{Q_{m1}}} = \frac{\mathbf{C_{op}R_1}}{\mathbf{2}\pi\mathbf{f_sL_1C_1}}$	

A piezoelectric converter when operating at $\mathbf{f_s}$, presents the source of high motional force and relatively low motional velocity (comparing it with the same converter operating in $\mathbf{f_p}$ and producing the same power). If we operate the same converter slightly increasing its operating frequency towards $\mathbf{f_r}$, the converter would start decreasing its motional force and increasing its motional velocity. Since all of the frequencies, $\mathbf{f_m}$, $\mathbf{f_s}$ and $\mathbf{f_r}$ are mutually very close (for high mechanical quality-factor converters), in most of analyzes here we shall replace all of them with $\mathbf{f_1} \approx (\mathbf{f_m} < \mathbf{f_s} < \mathbf{f_r})$. Something similar (but in much wider frequency range) would also happen if we start operating converter (high power) from $\mathbf{f_s}$, decreasing its operating frequency towards lower frequencies.

Also, a piezoelectric converter when operating at $\mathbf{f_p}$, presents the source of high motional velocity and relatively low motional force (comparing it with the same converter operating in $\mathbf{f_s}$ and producing the same power). If we operate the same converter slightly decreasing its operating frequency towards $\mathbf{f_a}$, the converter would start decreasing its motional velocity and increasing its motional force. Since all of the frequencies, $\mathbf{f_a}$, $\mathbf{f_p}$ and $\mathbf{f_n}$ are mutually very close (for high mechanical quality-factor converters), in most of analyzes here we shall replace all of them with $\mathbf{f_2} \approx (\mathbf{f_a} < \mathbf{f_p} < \mathbf{f_n})$. Operating in the vicinity of $\mathbf{f_2}$ towards higher frequencies is not beneficial

regarding producing high power, since the amount of accumulated elastomechanical (potential) energy in that frequency area is on the very low level.

The converter output mechanical power is equal to the product between its motional velocity and motional force, or to the product between its motional voltage and motional current. An optimal power transfer (from electrical to oscillatory, mechanical power) is achieved when motional current and motional voltage are mutually in phase, producing only the active or real output power (and consequently converter should operate either in $\mathbf{f_s}$ or in $\mathbf{f_p}$). Some ultrasonic companies are also operating their converters in the frequency area between $\mathbf{f_1}$ and $\mathbf{f_2}$, this way realizing the output power regulation by moving the impedance-frequency operating point (or effectively controlling the phase difference between motional current and motional voltage). The same phase-impedance regulation concept (moving the impedance-frequency operating point) can also be realized for the frequency area in close vicinity to $\mathbf{f_1}$ and left from $\mathbf{f_1}$, towards lower frequencies.

The simplest circuit replacements (equivalent circuits) for complex impedance of a piezoelectric converter, in the function of operating frequency interval/s, are presented on Fig. 11-b. For the most of design needs regarding electronics where piezoelectric converters and sensors are involved, it is very important to know the parameters of the circuits presented on Fig. 11-b in order to select the proper converter or sensor regime.

Obviously the piezoelectric converter impedance is complex and changing its character (depending on frequency), being dominantly capacitive, or dominantly inductive and/or certain combination of capacitive, resistive and inductive elements. On the Fig. 11-c are presented different aspects of converter impedance vs. frequency that can be measured using Network Impedance Analyzer (programmed to detect only particular impedance element, such as input converter capacitance, or input inductance or input resistance).

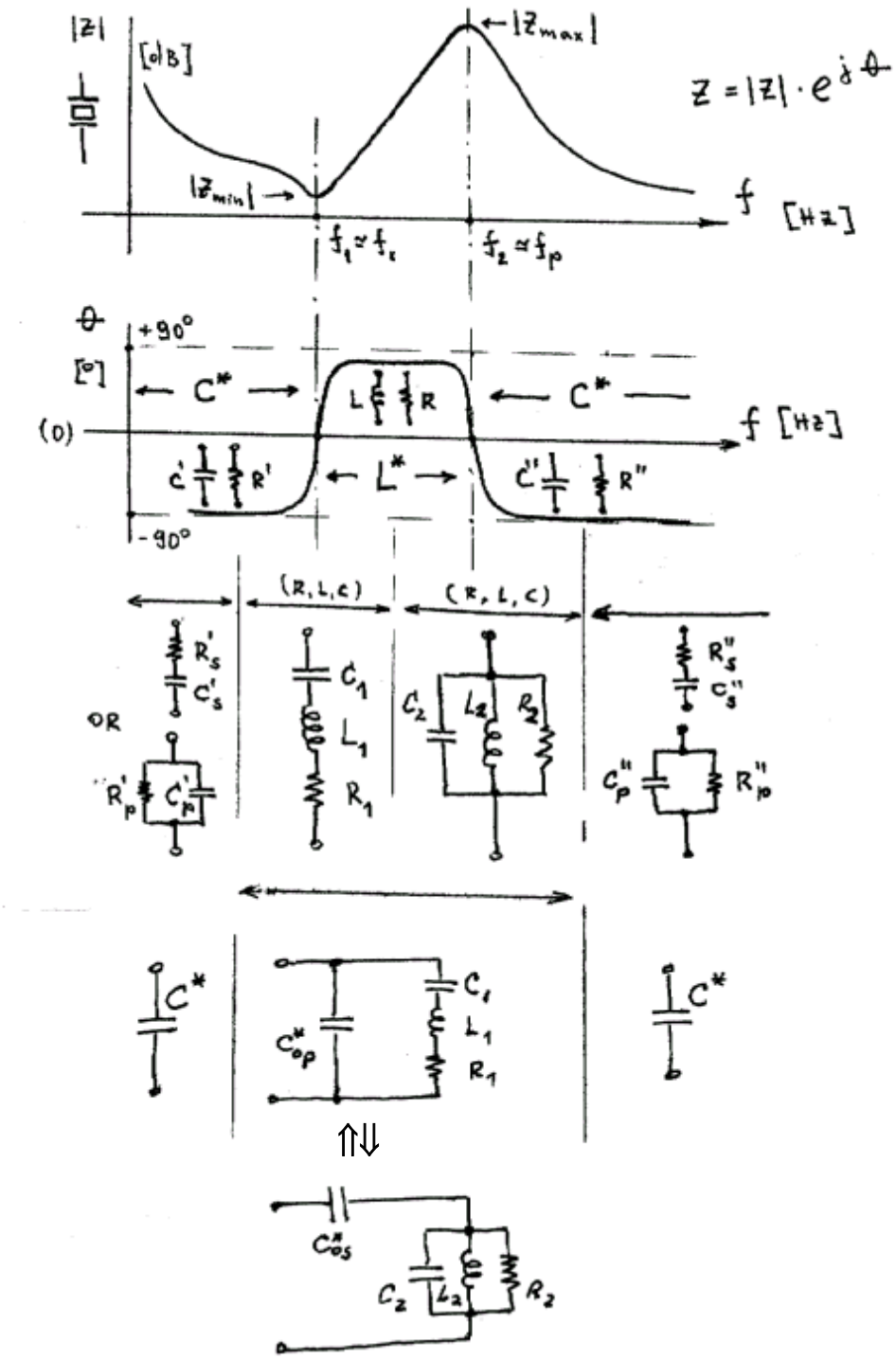

Fig. 11-b Simplified Piezoelectric-Impedance Models vs. Frequency

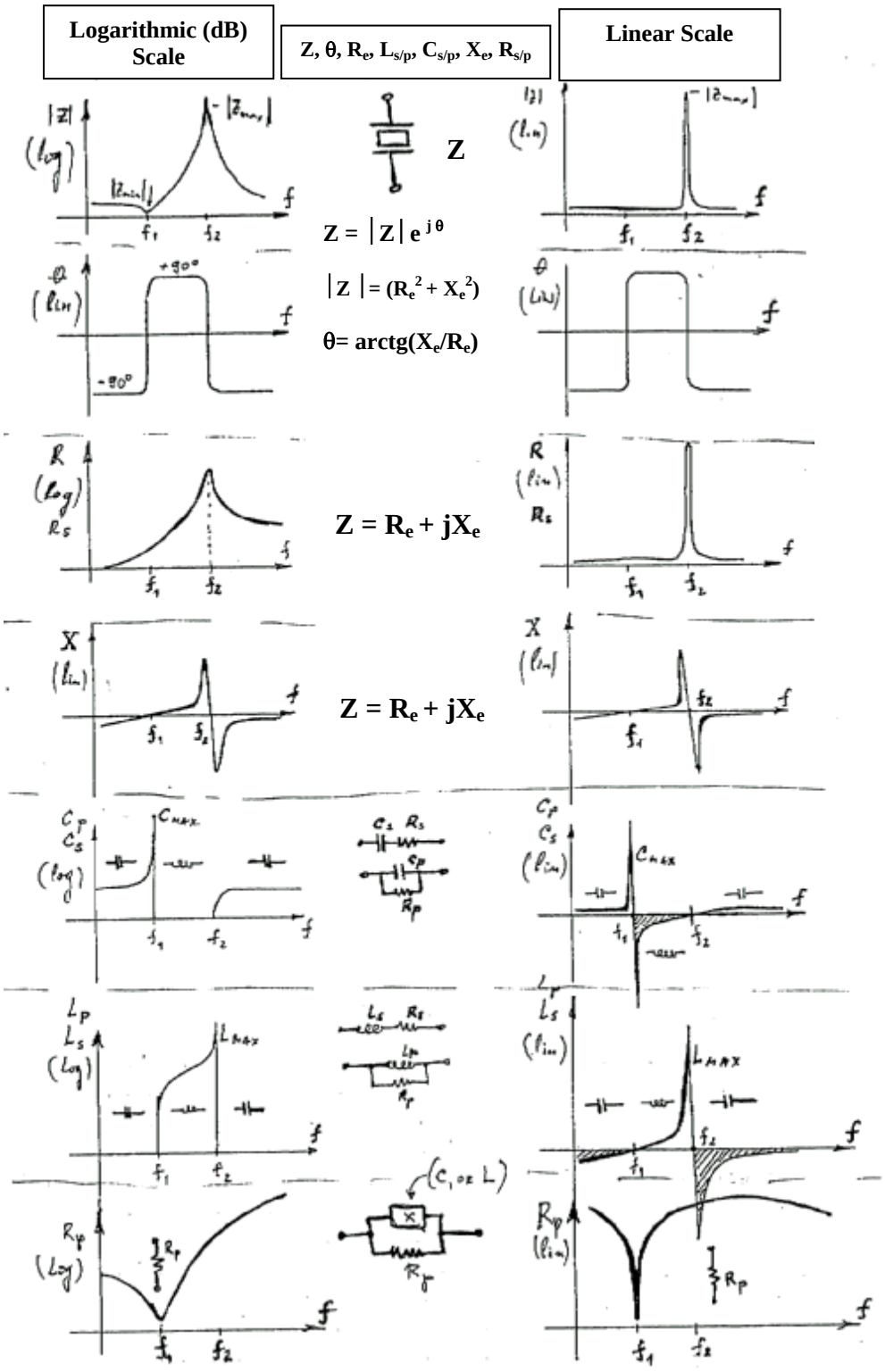

Fig. 11-c Different Converter-Impedance Elements vs. Frequency

Based on Mobility system of electromechanical analogies (Current = Force, Voltage = Velocity), electrical equivalent circuits and particular electrical impedance curves presented on Fig. 11-b and Fig. 11-c can be directly transformed into corresponding mechanical equivalents, as given on Fig. 11-d.

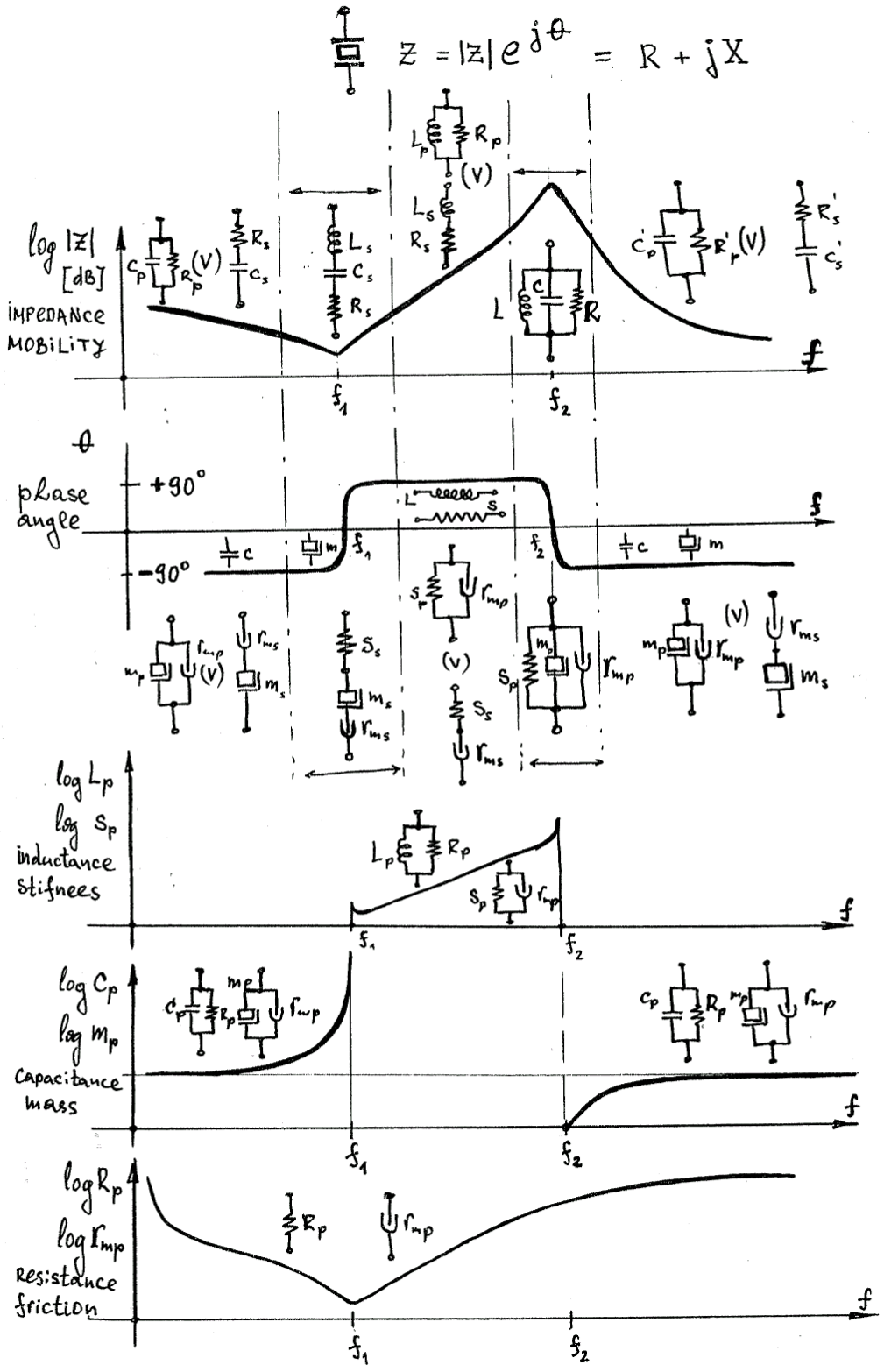

Fig. 11-d Simplified Piezoelectric-Impedance Electrical and Mechanical Models vs. Frequency (based on Mobility type of Analogies).

In ultrasonic engineering, regarding (isolated) resonant operating regimes of piezoelectric converters (and sensors), the most interesting is to determine the simplest and sufficiently applicable equivalent circuit models in order to realize

optimal converter driving, optimal power transfer, the best signal reception and proper electrical and mechanical converter impedance matching. Let us take the most widely used converter (dual) models presented on Fig. 1 (used later on, too). If we now imagine that converter is operating precisely in its series resonance, the corresponding motional reactive-impedance part would be equal zero, $\mathbf{X_1} = \omega \mathbf{L_1} - \frac{\mathbf{1}}{\omega \mathbf{C_1}} = \mathbf{0}$. In case if converter would operate exactly in its parallel resonance, the corresponding motional reactive-impedance part would disappear becoming extremely high impedance, $\mathbf{X_2} = \frac{\omega \mathbf{L_2}}{\mathbf{1} - \omega^2 \mathbf{L_2 C_2}} \to \infty$. Now, for resonant operating regimes of sufficiently high mechanical quality factor converters (where we can apply all reasonable approximations and circuit simplifications, as already explained in this chapter), the models presented on Fig. 1 can be even more simplified, as presented on Fig. 11-d.

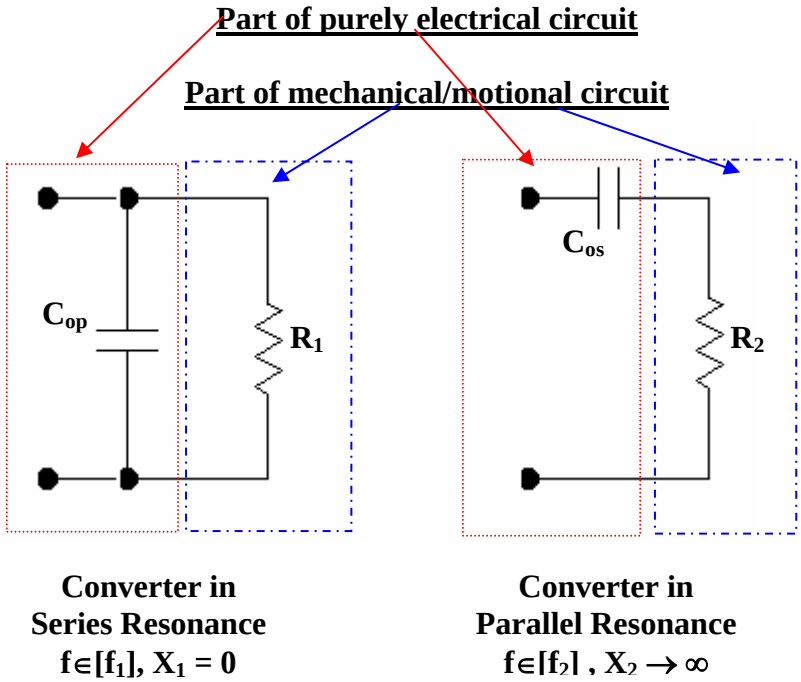

Fig. 11-d Approximated Converter Models in Series and Parallel Resonance in free, no-load conditions

If we apply equivalent circuit transformations as presented on Fig. 4, it will be possible to additionally transform both models from Fig. 11-d into two more of mutually corresponding series and parallel connection/s between equivalent resistance/s and capacitance/s. It is also important to underline that two circuit models presented on Fig. 11-d are no more mutually equivalent (as their predecessors), since each of them is previously simplified for different operating frequency. In order to maximize real (or active) output power of a piezoelectric converter operating in one of its resonances it would be necessary to neutralize the capacitive components belonging to circuits on Fig. 11-d, by connecting externally one inductance in parallel or series connection (respectively). In reality, when we analyze the optimal power conversion, we should upgrade models on Fig. 11-d with other circuit-elements visible on Figs. 2,3,5,6…that are presently neglected. We

should also know that for non-loaded piezoelectric converters, in most cases of practical interests (Fig. 11-d, Figs. 1,2,3,5,6…), $\mathbf{R_1}$ is in the range between 5 Ω and 100 Ω, and $\mathbf{R_2}$ is in the range between 10 kΩ and 100 kΩ (or higher than 100 kΩ). Coincidently with converter load increase we can find that, $\mathbf{R_1}$ would also proportionally increase (typically until approx. 10 times higher value), and $\mathbf{R_2}$ would proportionally decrease (typically until approx. 10 times lower value).

In certain circuit configurations, piezoelectric converter can be conveniently compensated (by adding external inductive and capacitive components to its input electric terminals) to become pure resistive impedance in relatively large frequency intervals, and still be able to operate high power inside of such frequency intervals.

2. Converters Measurements and Characterization

Let us now start using converters modeling (based on previously established equivalent models) for the purpose of converters characterization, optimization and defining converters quality parameters (using only electrical measurements data).

For the purpose of illustrating measured and calculated converters' quality parameters, in the table T 1.1 are given (low-signal) measurement data of BRANSON's converter, model 502/932R, max. 3000 Watts, 20 kHz (see also Fig. 12 and Fig. 13 with impedance-phase curves of the same, non-loaded and fully-loaded 502/932R converter), measured using HP 4194A Network Impedance Analyzer. The converter example chosen here is neither the best nor the worst case of 502/932 BRANSON converters, and it is only taken for the purpose of having numerical illustration/s following converters modeling presented in this paper.

Converter loading (regarding data in T 1.1) is realized by placing its front emitting surface on a thick rubber-foam full with water (with wooden-plate backing), and by pressing the converter towards its load (applying a force of about 20 kg, on the converter housing). Practically, this kind of load simulation is measured by HP 4194A under low current and voltage signals (sweeping frequency signal of 1 v, rms, produced internally in HP 4194A). In reality loading measurements should be made with operating converter driven high power, but from long experience in this field, we know that it is sufficiently representative to make low-signal measurements (similar to above explained situation) in order to get useful results that would be in the error-limits of max. 10%, compared to a situation if measurements were made operating converter full power. Here we shall follow the strategy to explain qualitative changes during converters (mechanical or acoustical) loading, and until standardized loading situations are not specified, loading would stay application-dependant and descriptively explained process.

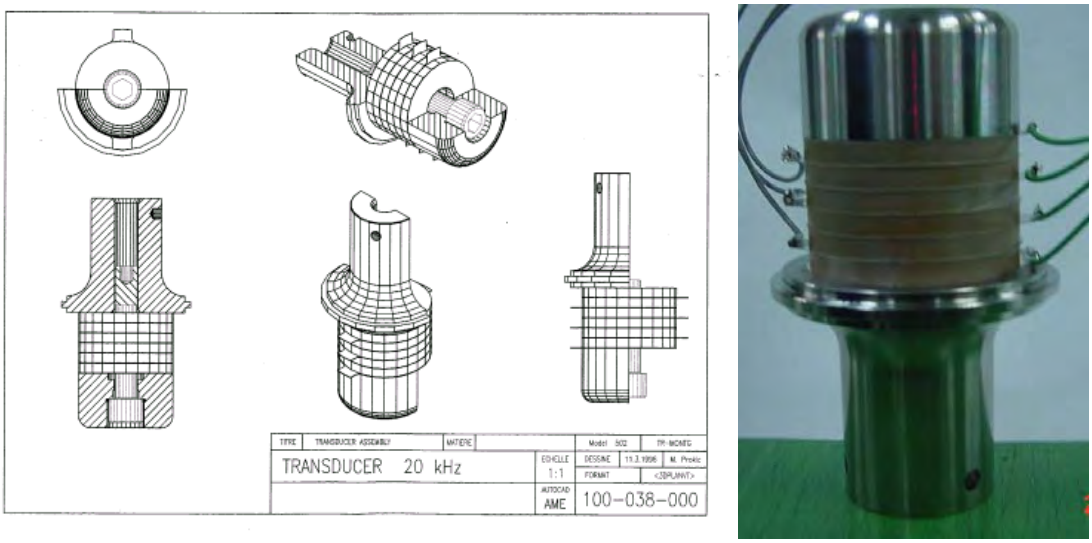

502/932R converter

T 1.1 (BRANSON 502/932R, 3000 Watts, 20 kHz converter; measurement data)

Assembled Converter	In Series Resonance	In Parallel Resonance
Non-Loaded (modest quality) Converter Fig. 12	$C_{op} = 18.1\,nF$, $C_1 = 4.046\,nF$, $L_1 = 17.534\,mH$, $R_1 = 4.6\,\Omega$, $\lvert Z_{min}\rvert = 4.66\,\Omega$, $f_1 = 18900\,Hz$, $Q_{m01} = 453.73$	$C_{os} = 22.05\,nF$, $C_2 = 101.53\,nF$, $L_2 = 570.50\,\mu H$, $R_2 = 94.20\ K\Omega$, $\lvert Z_{max}\rvert = 96\,K\Omega$, $f_2 = 20912\,Hz$, $Q_{m02} = 1256.7$
	$\frac{\lvert Z_{max}\rvert}{1000\lvert Z_{min}\rvert} \cong \frac{R_2}{1000R_1} \cong 20.54$	
	Coupling factor of the fully assembled, converter (PZT8, k_{33}=0.64) $k_c^2 = \frac{\text{Energy stored in mechanical form}}{\text{Total input energy}} = \frac{C_1}{C_{op}+C_1} \cong \frac{C_{os}}{C_2}\cdot\frac{f_1^2}{f_2^2} \cong 0.18,\ k_c \cong 0.4243$ $\frac{k_c^2}{k_{33}^2} \cong \frac{\text{Mechanical energy stored by (assembled) converter}}{\text{Mechanical energy that can be stored (only) in piezoceramics}} \cong (\frac{0.4243}{0.640})^2 \cong 0.44.$ (the ideal converter design would be when $(k_c / k_{33})^2 \cong 1$)	

Fully-Loaded (modest quality) Converter (still well operational and able to deliver maximal output power), Fig. 13	$C_{op} = 18.78\,nF$, $C_1 = 3.80\,nF$, $L_1 = 19.37\,mH$, $R_1 = 57.574\,\Omega$, $\lvert Z_{min}\rvert = 56.24\,\Omega$, $f_1 = 18525\,Hz$, $Q_{mL1} = 39.205$	$C_{os} = 22.58\,nF$, $C_2 = 96.74\,nF$, $L_2 = 631.23\,\mu H$, $R_2 = 1.50\ K\Omega$, $\lvert Z_{max}\rvert = 1.879\,K\Omega$, $f_2 = 20387\,Hz$, $Q_{mL2} = 18.63$
	$\frac{\lvert Z_{max}\rvert}{1000\lvert Z_{min}\rvert} \cong \frac{R_2}{1000R_1} \cong 0.03$	
	$k_c^2 = \frac{\text{Energy stored in mechanical form}}{\text{Total input energy}} = \frac{C_1}{C_{op}+C_1} \cong \frac{C_{os}}{C_2}\cdot\frac{f_1^2}{f_2^2} \cong 0.18,\ k_c \cong 0.425$ $\frac{k_c^2}{k_{33}^2} \cong \frac{\text{Mechanical energy stored by (assembled) converter}}{\text{Mechanical energy that can be stored (only) in piezoceramics}} \cong (\frac{0.425}{0.640})^2 \cong 0.441.$ (the ideal converter design would be when $(k_c / k_{33})^2 \cong 1$)	

Assembled Converter	In Series Resonance	In Parallel Resonance
Non-Loaded, High Quality 502/932R Converter (well selected, just for comparison with modest quality converter)	$C_{0p} = 17.32401\,nF$, $C_1 = 3.9044\ nF$, $L_1 = 18.3335\ mH$, $R_1 = 1.87\,\Omega$, $\lvert Z_{min}\rvert = 1.98\ \Omega$, $f_1 = 18815\ Hz$, $Q_{m01} = 1139$	$C_{0s} = 21.228\,nF$, $C_2 = 97.08423\,nF$, $L_2 = 595.6\,\mu H$, $R_2 = 216\ K\Omega$, $\lvert Z_{max}\rvert = 191\,K\Omega$, $f_2 = 20828\,Hz$, $Q_{m02} = 2485$
	$\frac{\lvert Z_{max}\rvert}{1000\lvert Z_{min}\rvert} \cong \frac{R_2}{1000R_1} \cong 106$	
	Coupling factor of the fully assembled, converter (PZT8, k_{33}=0.64) $k_c^2 = \frac{\text{Energy stored in mechanical form}}{\text{Total input energy}} = \frac{C_1}{C_{0p}+C_1} \cong \frac{C_{0s}}{C_2}\cdot\frac{f_1^2}{f_2^2} \cong 0.1811,\ k_c \cong 0.4256,$ $\frac{k_c^2}{k_{33}^2} \cong \frac{\text{Mechanical energy stored by (assembled) converter}}{\text{Mechanical energy that can be stored (only) in piezoceramics}} \cong (\frac{0.4256}{0.640})^2 = 0.442,$ (The ideal converter design would be when $(k_c / k_{33})^2 \cong 1$).	

Only piezoceramics	In Series Resonance	In Parallel Resonance
Parameters of Non-Loaded, single, PZT8 piezoceramic ring/s, used for assembling BRANSON 502/932R (first, natural, radial resonance mode/s)	PZT-8, Vernitron – Morgan-Matroc, USA n = 6 piezoceramic rings: ≅ ϕ50 x ϕ20 x 5 mm $d_{33} = 245 \times 10^{-12}$ [v/m] ± 10% , $k_{33} = 0.640$, $C_{inp.}$(1 kHz) = 19.55 nF, tan δ (1 kHz) = 0.000279, R_s(1 kHz) = 56 Ω, R_p(1 kHz) = 52 MΩ	
	$C_{op} = 2.68554\ nF$, $C_1 = 336.552\ pF$, $L_1 = 69.6164\ mH$, $R_1 = 12.741\ \Omega$, $\lvert Z\,min.\rvert = 12.8724\,\Omega$, $f_1 = 32880\ Hz$, $Q_{m10} = 1129$	$C_{os} = 3.0221\ nF$, $C_2 = 24.26\ nF$, $L_2 = 857.9\ \mu H$, $R_2 = 260.045\ k\Omega$, $\lvert Z\,max.\rvert = 256.861$, $f_2 = 34880\ Hz$, $Q_{m20} = 1385$
	$\frac{\lvert Z_{max}\rvert}{1000\lvert Z_{min}\rvert} \cong \frac{R_2}{1000R_1} \cong 20.18$	
	$k_c^2 = k_{eff.}^2 = \frac{f_2^2 - f_1^2}{f_2^2} \cong \frac{C_1}{C_{op}+C_1} \cong \frac{C_{os}}{C_2}\cdot\frac{f_1^2}{f_2^2} \cong 0.1110,\ \sqrt{0.1110} \cong 0.3332.$ (numerical values relevant only for the first radial mode)	

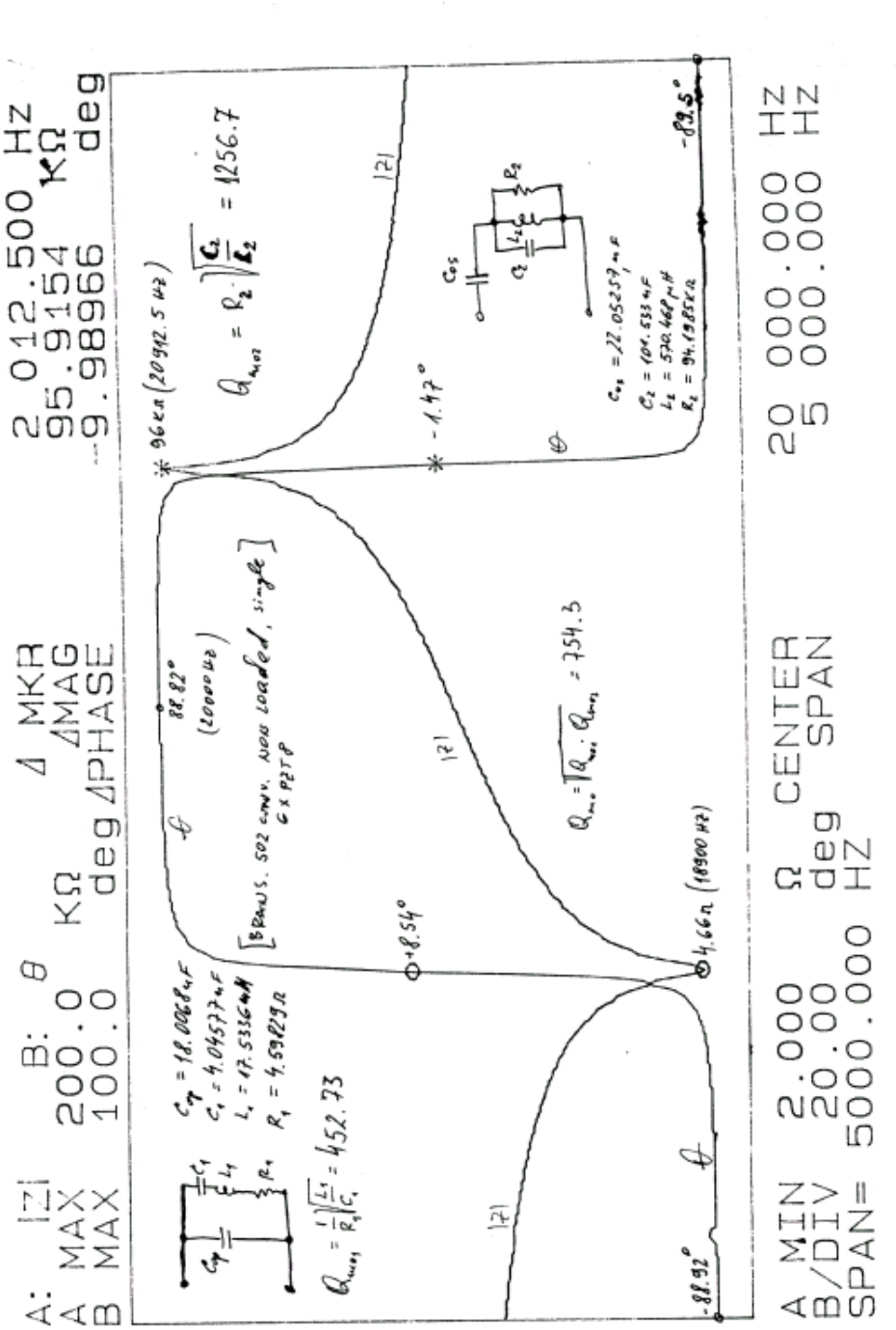

Fig. 12 Impedance curve of non-loaded BRANSON 502, 932R converter

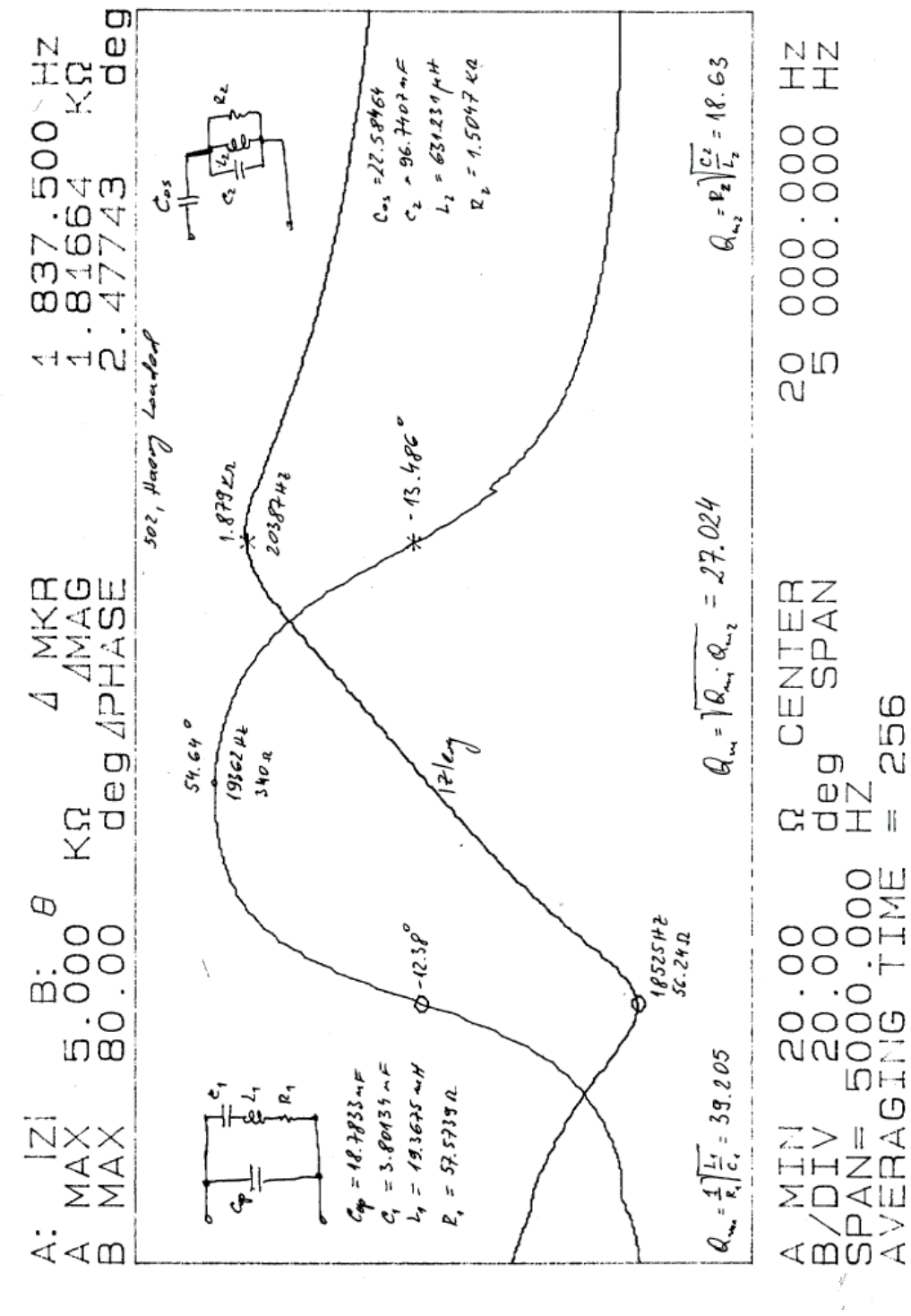

Fig. 13 Impedance curve of fully-loaded BRANSON 502, 932R converter

Converters Quality Parameters

The most important quality quantifications of a high power ultrasonic converter (operating in certain selected resonant mode) are its mechanical quality factors (related and found only for the mechanical oscillatory circuit-part/s of the equivalent converter models, Fig. 6), equal to,

$$\mathbf{Q_m} = 2\pi \frac{\textbf{Energy stored in the transducer during one full periode}}{\textbf{Energy dissipated in the transducer during one full periode}} = 2\pi \frac{\mathbf{E_s}}{\mathbf{E_d}}, \qquad (1.1)$$

and can be expressed (similar as in Electric Circuit Theory) for series resonance and for non-loaded piezoelectric converter (hanging in air) as,

$$\mathbf{Q_{mo1}} = \frac{\mathbf{Z_{cm01}}}{\mathbf{R_1}} = \frac{\mathbf{1}}{\mathbf{R_1}}\sqrt{\frac{\mathbf{L_1}}{\mathbf{C_1}}} \ (= \mathbf{452.73 \ \ for\ BRANSON\ 502\,/\,932R,\ \ from\ T\ 1.1)}, \qquad (1.2)$$

and for parallel resonance (for non-loaded piezoelectric converter, hanging in air) as,

$$\mathbf{Q_{mo2}} = \frac{\mathbf{R_2}}{\mathbf{Z_{cm02}}} = \mathbf{R_2}\sqrt{\frac{\mathbf{C_2}}{\mathbf{L_2}}} \ (= \mathbf{1256.7 \ \ for\ BRANSON\ 502\,/\,932R,\ \ from\ T\ 1.1)}. \qquad (1.3)$$

When we are talking about converters' mechanical quality factors, this is usually related to non-loaded (fully free) converters, hanging in air, and in all above given expressions (as well as in other parts of this paper) every indexing with "**o**" indicates this situation ("**o**" = non-loaded). Index "**m**" indicates that we are talking about mechanical-circuit related parameter/s, and indexing with "**1**" and "**2**" is related to series and parallel resonances. Since the same parameters can be found for loaded converters, indexing "**L**" is reserved for loading and/or load-influenced parameters.

A well operating and highly efficient (high power) converter, operating in a continuous regime should be designed to have as higher as possible mechanical quality factors (either being non-loaded, or fully loaded), and in this paper we shall mostly address only such kind of converters (what will significantly simplify different mathematical expressions and formulas related to such converters).

In (1.2) and (1.3) we can see two of unusual mechanical parameters (not found in literature), which are here addressed as "characteristic mechanical impedances of series and parallel resonance, of non-loaded converters", defined as,

$$\mathbf{Z_{cm01}} = \sqrt{\frac{\mathbf{L_1}}{\mathbf{C_1}}} = \frac{\mathbf{1}}{\mathbf{2\pi f_1 C_1}} \ (= \mathbf{2081.745\ \Omega\ ,for\ BRANSON\ 502\,/\,932R}) >> \mathbf{Z_{cm02}}$$

$$\mathbf{Z_{cm02}} = \sqrt{\frac{\mathbf{L_2}}{\mathbf{C_2}}} = \frac{\mathbf{1}}{\mathbf{2\pi f_1 (C_{0p} + C_1)}} \cdot \frac{\mathbf{f_2}^2 - \mathbf{f_1}^2}{\mathbf{f_1 f_2}} = \mathbf{Z_{cm01}} \cdot \frac{\mathbf{C_1}}{\mathbf{C_{0p} + C_1}} \cdot \frac{\mathbf{f_2}^2 - \mathbf{f_1}^2}{\mathbf{f_1 f_2}} \qquad (1.4)$$

$(\mathbf{Z_{cm02}} = \mathbf{74.96\ \Omega,\ for\ BRANSON\ 502\,/\,932R})$.

Another couple of unusual mechanical parameters (invented in this paper for the purpose of converters characterization and comparison), are "*characteristic average, axial wave-velocities of non-loaded half-wavelength converters, operating in series and/or parallel resonance*", defined as,

$$\mathbf{v_{cm01}} = \lambda \cdot \mathbf{f_{01}} = \mathbf{2H} \cdot \frac{\mathbf{1}}{\mathbf{2\pi\sqrt{L_1C_1}}} = \frac{\mathbf{H}}{\mathbf{\pi\sqrt{L_1C_1}}} = \mathbf{2Hf_{01}} = \frac{\mathbf{f_{01}}}{\mathbf{f_{02}}}\mathbf{v_{cm02}}\ ,$$

$$\mathbf{(v_{cm01} = 4611.6\left[\frac{m}{s}\right], H = 122\,mm, for\ BRANSON\ 502/932R, from\ T\ 1.1),}$$

$$\mathbf{v_{cm02}} = \lambda \cdot \mathbf{f_{02}} = \mathbf{2H} \cdot \frac{\mathbf{1}}{\mathbf{2\pi\sqrt{L_2C_2}}} = \frac{\mathbf{H}}{\mathbf{\pi\sqrt{L_2C_2}}} = \mathbf{2Hf_{02}} > \mathbf{v_{cm01}}\ \mathbf{,\ (f_{02} > f_{01})} \qquad (1.5)$$

$$\mathbf{(v_{cm02} = 5102.528\left[\frac{m}{s}\right], H = 122\,mm, for\ BRANSON\ 502/932R, from\ T\ 1.1),}$$

$$\mathbf{H\ (=)\ Effective\ Axial\ Transducer\ Length} = \frac{\lambda}{\mathbf{2}}\mathbf{.}$$

In all previously given expressions, it is obvious that we are talking about series and parallel resonant impedance characteristics, where series and parallel resonant frequencies can be approximated (in the case of high quality converters) as,

$$\mathbf{f_{01}} = \frac{\mathbf{1}}{\mathbf{2\pi\sqrt{L_1C_1}}} \cong \mathbf{f_{0s}} < \mathbf{f_{02}}\ \mathbf{,\ (series\ resonance,\ |Z_{01}| = |Z_{0-min.}|)},$$
$$\mathbf{f_{02}} = \frac{\mathbf{1}}{\mathbf{2\pi\sqrt{L_2C_2}}} \cong \mathbf{f_{01}}\sqrt{\mathbf{1} + \frac{\mathbf{C_1}}{\mathbf{C_{0p}}}} \cong \mathbf{f_{0p}} > \mathbf{f_{01}}\ \ \mathbf{(series\ resonance,\ |Z_{02}| = |Z_{0-max.}|)}\ . \qquad (1.6)$$

Also, the absolute values of converter's impedance in its series and parallel resonance (for non-loaded converter) are,

$$\mathbf{|Z_{01}| = |Z_{0s}| = |Z_{0-min.}| \approx R_1\ ,\ (Series\ resonance,\ f_{01})},$$
$$\mathbf{|Z_{02}| = |Z_{0p}| = |Z_{0-max.}| \approx R_2\ \ (Parallel\ resonance,\ f_{02})}. \qquad (1.7)$$

High quality converters usually have very low series impedance ($|\mathbf{Z_{01}}| = |\mathbf{Z_{0s}}| = |\mathbf{Z_{0-min.}}| \approx \mathbf{R_1} \approx 10\ \Omega$ range, and lower values), and very high parallel impedance ($|\mathbf{Z_{02}}| = |\mathbf{Z_{0p}}| = |\mathbf{Z_{0-max.}}| \approx \mathbf{R_2} \approx$ 100 KΩ range, and higher values).

Now, after introducing definitions and symbolic related to most important converter "static" parameters, we can address the other very-important, dynamic (loading) parameters of high power piezoelectric converters. Converters loading process is changing its electrical impedance on the way that (under loading) minimal series impedance is increasing, and that maximal parallel impedance is decreasing (coincidently). Both mechanical quality factors ((1.2) & (1.3)) of series and parallel resonance mechanical-circuits are also dropping down coincidently following mechanical load increase.

It will be shown that the mechanical quality-factors ratio, between the state of non-loaded and fully-loaded converter, is one of the best measure of converter's dynamic (loading) performances (see T 1.2). Let us establish the following convention and symbolic regarding converters mechanical quality factors (in non-loaded and loaded conditions):

$$\left\{\begin{array}{l} \mathbf{Q_{mo1}=\dfrac{Z_{cm01}}{R_{01}}=\dfrac{1}{R_{01}}\sqrt{\dfrac{L_{01}}{C_{01}}}\ (=)\ Non-loaded\ converter} \\ \mathbf{Quality\ Factor\ at\ f_{01},\ |Z_{01}|\approx R_{01}} \\ \mathbf{(=452.73\ \ for\ BRANSON\ 502/932R,\ T\ 1.1)} \end{array}\right\},$$

$$\left\{\begin{array}{l} \mathbf{Q_{mL1}<<Q_{mo1}\ (=)\ Fully-loaded\ converter} \\ \mathbf{Quality\ Factor\ at\ f_{L1},|Z_{L1}|\approx R_{L1}} \\ \mathbf{(=39.205\ \ for\ BRANSON\ 502/932R,\ T\ 1.1)} \end{array}\right\}$$

(1.8)

$$\left\{\begin{array}{l} \mathbf{Q_{mo2}=\dfrac{R_{02}}{Z_{cm02}}=R_{02}\sqrt{\dfrac{C_{02}}{L_{02}}}\ (=)\ Non-loaded\ converter} \\ \mathbf{Quality\ Factor\ at\ f_{02},|Z_{02}|\approx R_{02}} \\ \mathbf{(=1256.7\ \ for\ BRANSON\ 502/932R,\ T.1.1)} \end{array}\right\},$$

$$\left\{\begin{array}{l} \mathbf{Q_{mL2}<<Q_{mo2}\ (=)\ Fully-loaded\ converter} \\ \mathbf{Quality\ Factor\ at\ f_{L2},|Z_{L2}|\approx R_{L2}} \\ \mathbf{(=18.63\ \ for\ BRANSON\ 502/932R,\ T\ 1.1)} \end{array}\right\}$$

Under fully-loaded converter's quality factors, (1.8), we shall understand that converter is measured when heavily (maximally) loaded, but being still well operational and able to deliver (safely) 100% of its maximal operating power. This time we shall not describe what means heavy-loaded converter, since this is an application-dependent situation, but generally, certain loading situations could be standardized, such as process of immersing the front emitting face of the converter in water, or contacting and pressing converter's front emitting face to some other material (until it properly operates full-power). In reality, we should first test the chosen maximal load situation, by operating converter full-power (to see where is maximal loading level, when converter delivers its maximal output power), and then we should keep the same loading (the same kind of contact between converter and its load), and make low-signal impedance measurements using Impedance Analyzer (this time converter is only connected to Impedance Analyzer). Of course, the best would be to have an impedance analyzer able to operate in high power conditions, measuring high voltage and high current values, and to avoid load simulation, until all loading standards and correlations between Low-signal and High-signal measurements become well known (but such instruments are still not available).

Using symbolic from (1.8) we can formulate the following, most important dynamic loading parameters of ultrasonic high power converters, related separately to converters' efficiency (η in %) in series and parallel resonance operation/s:

$$\left\{\begin{array}{l} \dfrac{\mathbf{Q_{mo1}}}{\mathbf{Q_{mL1}}} \cong \left|\dfrac{\mathbf{Z_{L1}}}{\mathbf{Z_{01}}}\right| \cong \dfrac{\mathbf{R_{L1}}}{\mathbf{R_{01}}}\textbf{, measured at series resonance / s } \ \mathbf{f_{01}} \textbf{ and } \mathbf{f_{L1}} \\ \textbf{(} = \mathbf{11.57} \cong \mathbf{12.07} \cong \mathbf{12.52} \textbf{ for BRANSON 502 / 932R, T 1.1)} \\ \eta_1 \approx \dfrac{\mathbf{Q_{mo1}} - \mathbf{Q_{mL1}}}{\mathbf{Q_{mo1}}}\mathbf{x100\%} = [\mathbf{1} - \dfrac{\mathbf{Q_{mL1}}}{\mathbf{Q_{mo1}}}]\% \textbf{ (} \cong \mathbf{91.36\%} \textbf{ for BRANSON 502 / 932R)} \end{array}\right\}$$

$$\left\{\begin{array}{l} \dfrac{\mathbf{Q_{mo2}}}{\mathbf{Q_{mL2}}} \cong \left|\dfrac{\mathbf{Z_{02}}}{\mathbf{Z_{L2}}}\right| \cong \dfrac{\mathbf{R_{02}}}{\mathbf{R_{L2}}}\textbf{, measured at parallel resonance / s } \ \mathbf{f_{02}} \textbf{ and } \mathbf{f_{L2}} \\ \textbf{(} = \mathbf{67.45} \cong \mathbf{51.09} \cong \mathbf{62.60} \textbf{ for BRANSON 502 / 932R, T 1.1)} \\ \eta_2 \approx \dfrac{\mathbf{Q_{mo2}} - \mathbf{Q_{mL2}}}{\mathbf{Q_{mo2}}}\mathbf{x100\%} = [\mathbf{1} - \dfrac{\mathbf{Q_{mL2}}}{\mathbf{Q_{mo2}}}]\% \textbf{ (} = \mathbf{98.52\%} \textbf{ for BRANSON 502 / 932R)} \end{array}\right\} \quad (1.9)$$

Practically, the higher the ratio between non-loaded and fully-loaded mechanical quality factors (1.9) is, the higher efficiency η, and better dynamic (loading) converter performances are (respecting that fully-loaded converter is still well operational and able to deliver its maximal power). The ratio/s (1.9) also present the measure/s of converters capacity to accumulate and exchange potential elastomechanical energy with input electric energy (when converter operates in resonance and when electrical and elastomechanical energy are mutually transforming, producing converter oscillations).

In the close relation with converters dynamic performances are relations presenting resonant frequency shift (or frequency deviation) from non-loaded until fully-loaded situation, expressed as,

$$\left\{\begin{array}{l} \dfrac{\mathbf{f_{L2}} - \mathbf{f_{L1}}}{\mathbf{f_{02}} - \mathbf{f_{01}}} = \dfrac{\Delta \mathbf{f_L}}{\Delta \mathbf{f_0}} \ (=) \textbf{ resonant frequency intervals ratio} \\ \textbf{(} \dfrac{\Delta \mathbf{f_L}}{\Delta \mathbf{f_0}} = \dfrac{\mathbf{1862}}{\mathbf{2012}} = \mathbf{0.92545} \textbf{ for BRANSON 502 / 932R, T 1.1)} \end{array}\right\}$$

$$\left\{\begin{array}{l} \dfrac{\mathbf{f_{L1}} + \mathbf{f_{L2}}}{\mathbf{f_{01}} + \mathbf{f_{02}}} = \dfrac{\mathbf{f_{LC}}}{\mathbf{f_{0C}}} = \dfrac{\langle \mathbf{f_L} \rangle}{\langle \mathbf{f_0} \rangle} \ (=) \textbf{ central frequencies ratio} \\ \textbf{(} \dfrac{\langle \mathbf{f_L} \rangle}{\langle \mathbf{f_0} \rangle} = \mathbf{1.02313}; \dfrac{\Delta \mathbf{f_0}}{\langle \mathbf{f_0} \rangle} = \mathbf{0.1011}, \dfrac{\Delta \mathbf{f_L}}{\langle \mathbf{f_L} \rangle} = \mathbf{0.0957}, \textbf{ for BRANSON 502 / 932R)} \end{array}\right\} \quad (1.10)$$

High quality converters should have frequency intervals and central frequencies ratios (1.10) close to 1 (or saying differently, as this ratio is closer to 1, the converter is more stable and performing better).

Regarding frequency stability between loaded and non-loaded converter states we can also calculate the central frequency-shift ratios on the following way,

$$\frac{\mathbf{f_{0C}-f_{LC}}}{\mathbf{f_{L2}-f_{L1}}}=\frac{\mathbf{\Delta f_C}}{\mathbf{\Delta f_L}}\ \left(=\frac{\mathbf{450}}{\mathbf{1862}}=\mathbf{0.242}\ \ \mathbf{for\ BRANSON\ 502/932R,\ T\ 1.1)}\right.$$

$$\frac{\mathbf{f_{0C}-f_{LC}}}{\mathbf{f_{02}-f_{01}}}=\frac{\mathbf{\Delta f_C}}{\mathbf{\Delta f_0}}\ \left(=\frac{\mathbf{450}}{\mathbf{2012}}=\mathbf{0.2236}\ \ \mathbf{for\ BRANSON\ 502/932R,\ T\ 1.1)}\right., \qquad (1.11)$$

$$\mathbf{f_{0C}=0.5(f_{01}+f_{02})},\ \mathbf{f_{LC}=0.5(f_{L1}+f_{L2})},\ \mathbf{\langle f_C\rangle=0.5(f_{0C}+f_{LC})}.$$

High quality converters should have all central frequency shifts (1.11) as lower as possible. Relations given in (1.10) and (1.11) are also useful for designing ultrasonic power supplies and circuits for automatic, PLL resonant frequency tracking.

Since **in certain operating regimes converters can operate between series and parallel resonant frequency**, and in any case series and parallel resonance (of the same converter) are mutually coupled and dependant (both, minimal and maximal converter's impedances are coincidently changing under loading), we can also define "***mixed-mode, static and low signal quality parameters***", formulating a kind of effective parameters, practically creating average value/s between every quality parameter defined for series and for parallel resonance (see the last column in T 1.2). The table T 1.2 is presenting an overview of converters quality parameters (as already introduced above), and all numerical values in T 1.2 are calculated for Branson 502/932R converter (see measured impedance-phase curves and model parameters presented on Fig. 12 & Fig. 13 and in T 1.1).

There is another important quality parameter of a piezoelectric converter, dominantly related to its mechanical design, and to elastomechanical material properties of all components and parts of that converter, known as Converter's Electromechanical Coupling Factor, $\mathbf{k_c}$. If we take converter/s from T 1.1 (either modest or high quality, non-loaded and/or loaded, one), we shall see that effective Coupling Factor in all mentioned cases remains almost unchanged,

$$\mathbf{k_c}^2=\frac{\mathbf{Energy\ stored\ in\ mechanical\ form}}{\mathbf{Total\ input\ energy}}=\mathbf{k_{eff.}^2}=\frac{\mathbf{f_2^2-f_1^2}}{\mathbf{f_2^2}}\cong\frac{\mathbf{C_1}}{\mathbf{C_{op}+C_1}}\cong\frac{\mathbf{C_{os}}}{\mathbf{C_2}}\cdot\frac{\mathbf{f_1}^2}{\mathbf{f_2}^2}\cong\mathbf{0.18},\quad . \qquad (1.12)$$

$$\mathbf{k_c\cong 0.4243}$$

If we now compare the Converter Coupling factor $\mathbf{k_c}$ with the Coupling Factor, $\mathbf{k_{33}}$ of the single and load-free piezoceramics (that is the part of the same converter), we shall see how good (or optimal) the mechanical design of that converter is,

$$\left(\frac{\mathbf{k_c}}{\mathbf{k_{33}}}\right)^2\cong\frac{\mathbf{Mechanical\ energy\ stored\ by\ (assembled)\ converter}}{\mathbf{Mechanical\ energy\ that\ can\ be\ stored\ (only)\ in\ piezoceramics}}\cong\left(\frac{\mathbf{0.4243}}{\mathbf{0.640}}\right)^2\cong\mathbf{0.44}\,. \qquad (1.13)$$

since the ideal mechanical converter design would be when converter is not changing the initial Coupling Factor of its piezoceramics, $(\mathbf{k_c}/\mathbf{k_{33}})^2\cong\mathbf{1}$, meaning that elastomechanical properties of converter metal parts would perfectly match such properties of piezoceramics.

T 1.2 **(All numerical values in this table are related to BRANSON 502/932R converter: see T 1.1 & Figs. 12,13)**

Parameter ⇓	Series Resonance ⇓	Parallel Resonance ⇓	Mixed-mode ⇓
Mechanical Quality Factors ⇒ (non-loaded converter)	$Q_{mo1} = \frac{Z_{cm01}}{R_{01}} = \frac{1}{R_{01}}\sqrt{\frac{L_{01}}{C_{01}}} = 453.73$	$Q_{mo2} = \frac{R_{02}}{Z_{cm02}} = R_{02}\sqrt{\frac{C_{02}}{L_{02}}} = 1256.7$	$Q^*_{m0} = \sqrt{Q_{mo1}\cdot Q_{mo2}} = \sqrt{\frac{R_{02}}{R_{01}}\cdot\frac{Z_{cm01}}{Z_{cm02}}} = \sqrt{\frac{R_{02}}{R_{01}}\sqrt{\frac{L_{01}}{L_{02}}\cdot\frac{C_{02}}{C_{01}}}} = \sqrt{\frac{R_{02}}{R_{01}}\frac{C_{0p}+C_1}{C_1}\frac{f_{01}f_{02}}{f_{02}^2-f_{01}^2}} = 755.12$
Mechanical Quality Factors ⇒ (fully-loaded converter)	$Q_{mL1} = 39.205$	$Q_{mL2} = 18.63$	$Q^*_{mL} = \sqrt{Q_{mL1}\cdot Q_{mL2}} = 27.0257$
Ratio of Mechanical Quality Factors ⇒ & Efficiency (non-loaded): (fully-loaded converter)	$\frac{Q_{mo1}}{Q_{mL1}} = \frac{Z_{cm01}R_{L1}}{Z_{cmL1}R_{01}} = \frac{R_{L1}}{R_{01}}\sqrt{\frac{L_{01}C_{L1}}{L_{L1}C_{01}}} \cong \cong \left\lvert\frac{Z_{L1}}{Z_{01}}\right\rvert \cong \frac{R_{L1}}{R_{01}}$ (= 11.57 ≅ 12.07 ≅ ≅ 12.52) $\eta_1 \approx \frac{Q_{mo1}-Q_{mL1}}{Q_{mo1}}100 \cong 91.36\%$	$\frac{Q_{mo2}}{Q_{mL2}} = \frac{Z_{cmL2}R_{02}}{Z_{cm02}R_{L2}} = \frac{R_{02}}{R_{L2}}\sqrt{\frac{L_{L2}C_{02}}{L_{02}C_{L2}}} \cong \cong \left\lvert\frac{Z_{02}}{Z_{L2}}\right\rvert \cong \frac{R_{02}}{R_{L2}}$ (= 67.45 ≅ 51.09 ≅ ≅ 62.8) $\eta_2 \approx \frac{Q_{mo2}-Q_{mL2}}{Q_{mo2}}100 \cong 98.52\%$	$\sqrt{\frac{Q_{m01}}{Q_{mL1}}\frac{Q_{m02}}{Q_{mL2}}} = \frac{Q^*_{m0}}{Q^*_{mL}} = \sqrt{\frac{Z_{cm01}Z_{cmL2}}{Z_{cmL1}Z_{cm02}}\frac{R_{L1}R_{02}}{R_{L2}R_{01}}} = \sqrt{\frac{R_{L1}R_{02}}{R_{L2}R_{01}}\sqrt{\frac{L_{01}L_{L2}}{L_{L1}L_{02}}\frac{C_{L1}C_{02}}{C_{L2}C_{01}}}} \cong \sqrt{\left\lvert\frac{Z_{L1}}{Z_{L2}}\frac{Z_{02}}{Z_{01}}\right\rvert} \cong \sqrt{\frac{R_{L1}}{R_{L2}}\frac{R_{02}}{R_{01}}}$ (= 27.94 ≅ 24.83 ≅ 28.04)
Characteristic Mechanical Impedance ⇒ (non-loaded converter)	$Z_{cm01} = \sqrt{\frac{L_1}{C_1}} = \frac{1}{2\pi f_1 C_1} = 2081.745\ \Omega$	$Z_{cm02} = \sqrt{\frac{L_2}{C_2}} = 74.96\ \Omega$	$Z^*_{cm0} = \sqrt{Z_{cm01}Z_{cm02}} = \sqrt{\frac{L_1}{C_1}\cdot\frac{L_2}{C_2}} = \sqrt{R_{01}R_{02}\cdot\frac{Q_{m01}}{Q_{m02}}} = 395.029\ \Omega$
Characteristic Mechanical Impedance ⇒ (fully-loaded converter)	$Z_{cm1} = \sqrt{\frac{L_1}{C_1}} = 2257.73\ \Omega$	$Z_{cm2} = \sqrt{\frac{L_2}{C_2}} = 80.77\ \Omega$	$Z^*_{cm} = \sqrt{Z_{cm1}Z_{cm2}} = 427.033\ \Omega$

Characteristic Axial Wave Velocity ⇒ (non-loaded converter)	$v_{cm01} = \lambda \cdot f_{01} = 2H \cdot \frac{1}{2\pi\sqrt{L_1 C_1}} = \frac{H}{\pi\sqrt{L_1 C_1}} = 2Hf_{01} = 4611.6\left[\frac{m}{s}\right]$, $H = 122\,mm$	$v_{cm02} = \lambda \cdot f_{02} = 2H \cdot \frac{1}{2\pi\sqrt{L_2 C_2}} = \frac{H}{\pi\sqrt{L_2 C_2}} = 2Hf_{02} = 5102.528\left[\frac{m}{s}\right]$, $H = 122\,mm$	$v^*_{cm0} = \sqrt{v_{cm01} v_{cm02}} = 2Hf^*_C = \frac{H}{\pi\sqrt{L_1 C_1 L_2 C_2}} = 4850.86\left[\frac{m}{s}\right]$, $H = 122\,mm$
Characteristic Axial Wave Velocity ⇒ (fully-loaded converter)	$v_{cm1} = \lambda \cdot f_1 = 2Hf_1 = 4520.1\left[\frac{m}{s}\right]$, $H = 122\,mm$	$v_{cm2} = \lambda \cdot f_2 = 2Hf_2 = 4974.43\left[\frac{m}{s}\right]$, $H = 122\,mm$	$v^*_{cm} = \sqrt{v_{cm1} v_{cm2}} = 2Hf^*_C = 4741.73\left[\frac{m}{s}\right]$, $H = 122\,mm$
Resonant Frequency ⇒ (non-loaded converter)	$f_{01} = \frac{1}{2\pi\sqrt{L_1 C_1}} \cong f_{0s} = 18900\ Hz$	$f_{02} = \frac{1}{2\pi\sqrt{L_2 C_2}} \cong f_{0p} = 20912\ Hz$	$f^*_{0C} = \sqrt{f_{01} f_{02}} = 19880.56\ Hz$
Resonant Frequency ⇒ (fully-loaded converter)	$f_1 = \frac{1}{2\pi\sqrt{L_1 C_1}} \cong f_s = 18525\ Hz$	$f_2 = \frac{1}{2\pi\sqrt{L_2 C_2}} \cong f_p = 20387\ Hz$	$f^*_C = \sqrt{f_1 f_2} = 19433.71\ Hz$
Converter's Resonant Frequency Stability Parameters	$\frac{f_{L2} - f_{L1}}{f_{02} - f_{01}} = \frac{\Delta f_L}{\Delta f_0} = \frac{1862}{2012} = 0.92545$, $\frac{f_{L1} + f_{L2}}{f_{01} + f_{02}} = \frac{f_{LC}}{f_{0C}} = \frac{\langle f_L \rangle}{\langle f_0 \rangle} = 1.02313$; $\frac{\Delta f_0}{\langle f_0 \rangle} = 0.1011$, $\frac{\Delta f_L}{\langle f_L \rangle} = 0.0957$ $\frac{f_{0C} - f_{LC}}{f_{L2} - f_{L1}} = \frac{\Delta f_C}{\Delta f_L} = \frac{450}{1862} = 0.242$, $\frac{f_{0C} - f_{LC}}{f_{02} - f_{01}} = \frac{\Delta f_C}{\Delta f_0} = \frac{450}{2012} = 0.2236$, $f_{0C} = 0.5(f_{01} + f_{02}) = 19906\,Hz$, $f_{LC} = 0.5(f_{L1} + f_{L2}) = 19456\ Hz$, $\langle f_C \rangle = 0.5(f_{0C} + f_{LC}) = 19681\,Hz$.		
Coupling factor of the assembled converter from T 1.1 (PZT8, k_{33}=0.64)	$k_c^2 = \frac{\text{Energy stored in mechanical form}}{\text{Total input energy}} = \frac{C_1}{C_{op} + C_1} \cong \frac{C_{os}}{C_2} \cdot \frac{f_1^2}{f_2^2} \cong 0.18$, $k_c \cong 0.4243$ $(\frac{k_c}{k_{33}})^2 \cong \frac{\text{Mechanical energy stored by (assembled) converter}}{\text{Mechanical energy that can be stored (only) in piezoceramics}} \cong (\frac{0.4243}{0.640})^2 \cong 0.44$. (the ideal converter design would be when $(k_c / k_{33})^2 \cong 1$)		

Empirical and other important quality parameters and figure of merits of ultrasonic converters, good for fast selection of high power converters. Static & Low-signal parameters (converter is operating in air = no-load)	
$C_{inp.}\,(\text{at } 1\text{kHz}) \rightarrow \text{High enough}\ [\text{nF}]$	**Total input capacitance**
$E \rightarrow \text{max.}\ [N/m^2]$	**Piezoceramics Young modulus**
$T_c \rightarrow \text{High enough (max.} > 300),\ [^\circ C]$	**Curie temperature**
$\tan\delta\,(\text{at } 1\text{kHz}) = \dfrac{1}{Q_e} \rightarrow \text{minimum}$	**Dielectric loss factor** **Q_e = Dielectric quality factor**
$d_{33} \rightarrow \text{High enough, } 10^{-12} \cdot \left[\dfrac{m}{V} = \dfrac{C}{N}\right]$	**Piezoelectric charge constant**
$Q_{mo1,2}\,(\text{of assembled, non-loaded converter}) \geq$ $\geq Q_{mo1,2}\,(\text{of single, non-loaded piezoceramics}) \rightarrow \text{max.}$	**Relations between Mechanical Quality Factors of assembled, non-loaded converter and Quality factor of piezoceramics (that is the part of the same converter)**
$Q^*_{mo} = \sqrt{Q_{mo1} \cdot Q_{mo2}} \rightarrow \text{max.},$ $(\geq 1000, \text{for instance})$	**Effective mechanical quality factor (here invented parameter)**
$Q^*_{emo} = \sqrt{Q^*_{mo} \cdot Q_e} \rightarrow \text{max.},$ $(\geq 1000, \text{for instance})$	**Effective electromechanical quality factor (here invented parameter)**
$\left\lvert\dfrac{Z_{max.}}{1000 \cdot Z_{min.}}\right\rvert \cong \left\lvert\dfrac{R_2}{1000 \cdot R_1}\right\rvert \rightarrow \text{max.},$ $(\geq 100, \text{ for example})$	**Maximum to minimum impedance ratio (here invented parameter)**
$\Delta f = (f_2 - f_1) \rightarrow \text{max.}$ $\text{for ex.: } 100 \cdot \dfrac{\Delta f}{\langle f \rangle} \geq 10\%$	**Frequency gap between series and parallel resonant frequency**
$\left\{\begin{matrix}\theta \rightarrow \max. \\ \lvert\theta\rvert \leq 90^\circ\end{matrix}\right\} \Rightarrow \dfrac{\theta}{90} \rightarrow \max.(\leq 1)$	**Positive phase angle between series and parallel resonant frequency**
$\dfrac{R_2}{R_1} \cdot \dfrac{\Delta f}{\langle f \rangle} \cdot \dfrac{\theta}{90} \cong \dfrac{\lvert Z_{max.}\rvert}{\lvert Z_{min.}\rvert} \cdot \dfrac{\Delta f}{\langle f \rangle} \cdot \dfrac{\theta}{90} \rightarrow \max.$ $\langle f \rangle = 0.5(f_1 + f_2)$	**Combined figure of merit (empirical quality factor; -here invented parameter)**

3.0 Loading of piezoelectric transducers

Field(s) of Application:

In applications such as Ultrasonic Welding, single operating, well-defined, resonant frequency transducers are usually used (operating often on 20, 40 and sometimes around 100 kHz and higher). In recent time, some new transducer designs can be driven on sweeping frequency intervals (applied to a single transducer).

In Sonochemistry and Ultrasonic Cleaning we use single or multiple ultrasonic transducers (operating in parallel), with single resonant frequency, two operating frequencies, multi-frequency regime, and all of the previously mentioned options combined with frequency sweeping. Frequency sweeping is related to the vicinity of the best operating (central) resonant frequency of transducer group. Frequency sweeping can also be applied in a low frequency (PWM, ON-OFF) group modulation (producing pulse-repetitive ultrasonic train, sometimes-called digital modulation).

Also, multi-frequency concept is used in Sonochemistry and Ultrasonic Cleaning when we can drive a single transducer on its ground (basic, natural) frequency and on several higher frequency harmonics (jumping from one frequency to another, without changing transducer/s).

Real time and fast automatic resonant (or optimal operating frequency) control/tuning of ultrasonic transducers is one of the most important tasks in producing (useful) ultrasonic energy for different technological applications, because in every application we should realize/find/control:

1° The best operating frequency regime in order to stimulate only desirable vibrating modes.
2° To deliver a maximum of real or active power to the load (in a given/found operating frequency domain/s).
3° To keep ultrasonic transducers in a pulse-by-pulse, real time, safe operating area regarding all critical overload/overpower situations, or to protect them against: overvoltage, overcurrent, overheating, etc.

All of the previously mentioned (control and protecting) aspects are so interconnected, that none of them can be realized independently, without the other two. All of them also have two levels of control and internal structure:

a) Up to a certain (first) level, with the design and hardware, we try to insure/incorporate the most important controls and protecting, (automatic) functions.
b) At the second level we include certain logic and decision-making algorithm (software) which takes care of real-time and dynamic changes and interconnections between them.

It is necessary to have in mind that in certain applications (such as ultrasonic welding), operating and loading regime of ultrasonic transducer changes drastically in relatively short time intervals, starting from a very regular and no-load situation (which is easy to control), going to a full-load situation, which changes all parameters of ultrasonic system (impedance parameters, resonant frequencies...). In a no-load and/or low power operation, ultrasonic system behaves as a typically linear system; however, in high power operation the system becomes more and more non-linear (depending on the applied mechanical load). The presence of dynamic and fast changing, transient situations is creating the absolute need to have one frequency auto tuning control block, which will always keep ultrasonic drive (generator) in its best operating regime (tracking the best operating frequency).

The meaning of mechanical loading of ultrasonic transducers:

Mechanical loading of the transducer means realizing contact/coupling of the transducer with a fluid, solid or some other media (in order to transfer ultrasonic vibrations into loading media). All mechanical parameters/properties (of the load media) regarding such contact area (during energy transfer) are important, such as: contact surface, pressure, sound velocity, temperature, density, mechanical impedance, ... Mechanical load (similar to electrical load) can have resistive or frictional character (as an active load), can be reactive/imaginary impedance (such as masses and springs are), or it can be presented as a complex mechanical impedance (any combination of masses, springs and frictional elements). In fact, direct mechanical analogue to electric impedance is the value that is called Mobility in mechanics, but this will not influence further explanation. Instead of measuring complex mechanical impedance (or mobility) of an ultrasonic transducer, we can easily find its complex electrical impedance (and later on, make important conclusions regarding mechanical impedance). Mechanical loading of a piezoceramic transducer is transforming its starting impedance characteristic (in a no-load situation in air) into similar new impedance that has lower mechanical quality factor in characteristic resonant area/s. There are many

electrical impedance meters and network impedance analyzers to determine/measure full (electrical) impedance-phase-frequency characteristic/s of certain ultrasonic transducers on a low sinus-sweeping signal (up to 5 V rms.). However, the basic problem is in the fact that impedance-phase-frequency characteristics of the same transducer are not the same when transducer is driven on higher voltages (say 200 Volts/mm on piezoceramics). Also, impedance-phase-frequency characteristics of one transducer are dependent on transducer's (body) operating temperature, as well as on its mechanical loading. It is necessary to mention that measuring electrical Impedance-Phase-Frequency characteristic of one ultrasonic transducer immediately gives almost full qualitative picture about its mechanical Impedance-Phase-Frequency characteristic (by applying a certain system of electromechanical analogies). We should not forget that ultrasonic, piezoelectric transducer is almost equally good as a source/emitter of ultrasonic vibrations and as a receiver of such externally present vibrations. While it is emitting vibrations, the transducer is receiving its own reflected (and other) waves/vibrations and different mechanical excitation from its loading environment. It is not easy to organize such impedance measurements (when transducer is driven full power) due to high voltages and high currents during high power driving under variable mechanical loading. Since we know that the transducer driven full power (high voltages) will not considerably change its resonant points (not more than ±5% from previous value), we rely on low signal impedance measurements (because we do not have any better and quicker option). Also, power measurements of input electrical power into transducer, measured directly on its input electrical terminals (in a high-power loading situation) are not a simple task, because we should measure RMS active and reactive power in a very wide frequency band in order to be sure what is really happening. During those measurements we should not forget that we have principal power delivered on a natural resonant frequency (or band) of one transducer, as well as power components on many of its higher and lower frequency harmonics. There are only a few available electrical power meters able to perform such selective and complex measurements (say on voltages up to 5000 Volts, currents up to 100 Amps, and frequencies up to 1 MHz, just for measuring transducers that are operating below 100 kHz).

Optimal driving of ultrasonic transducers:

For optimal transducer efficiency, the best situation is if/when transducer is driven in one of its mechanical resonant frequencies, delivering high active power (and very low reactive power) to the loading media. Since usually resonant frequency of loaded transducer is not stable (because of dynamical change of many mechanical, electrical and temperature parameters), a PLL resonant frequency (in real-time) tracking system has to be applied. When we drive transducer on its resonant frequency, we are sure that the transducer presents dominantly resistive load. That means that maximum power is delivered from ultrasonic power supply (or ultrasonic generator) to the transducer and later on to its mechanical load. If we have a reactive power on the transducer, this can present a problem for transducer and ultrasonic generator and cause overheating, or the ultrasonic energy may not be transferred (efficiently) to its mechanical load. Usually, the presence of reactive power means that this part of power is going back to its source. The next condition that is necessary to satisfy (for optimal power transfer) is the impedance matching between ultrasonic generator and ultrasonic transducer, as well as between ultrasonic transducer and loading media. If optimal resonant frequency control is realized, but impedance/s matching is/are not optimal, this will again cause transducer and generator overheating, or ultrasonic energy won't be transferred (efficiently) to its mechanical load. Impedance matching is an extremely important objective for realizing a maximum efficiency of an ultrasonic transducer (for good impedance matching it is necessary to adjust ferrite transformer ratio and inductive compensation of piezoelectric transducer, operating on a properly controlled resonant frequency). Output (vibration) amplitude adjustments, using boosters or amplitude amplifiers (or attenuators) usually adjust mechanical impedance matching conditions. Recently, some ultrasonic companies (Herman, for instance) used only electrical adjustments of output mechanical amplitude (for mechanical load matching), avoiding any use of static mechanical amplitude transformers such as boosters (this way, ultrasonic configuration becomes much shorter and much more load-adaptable/flexible, but its electric control becomes more complex). By the way, we can say that previously given conditions for optimal power transfer are equally valid for any situation/system where we have energy/power source and its load (To understand this problem easily, the best will be to apply some of the convenient systems of electromechanical analogies).

It is important to know that Impedance-Phase-Frequency characteristics of one transducer (measured on a low sinus-sweeping signal) are giving indicative and important information for basic quality parameters of one transducer, but not sufficient information for high power loaded conditions of the same transducer. Every new loading situation should be rigorously tested, measured and optimized to produce optimal ultrasonic effects in a certain mechanical load.

It is also very important to know that safe operating limits of heavy-loaded ultrasonic transducers have to be controlled/guaranteed/maintained by hardware and software of ultrasonic generator. The usual limits are maximal operating temperature, maximal-operating voltage, maximal operating current, maximal operating power, operating frequency band, and maximum acceptable stress. All of the previously mentioned parameters should be

controlled by means of convenient sensors, and protected/limited in real time by means of special protecting components and special software/logical instructions in the control circuits of ultrasonic generator. A mechanism of very fast overpower/overload protection should be intrinsically incorporated/included in every ultrasonic generator for technologically complex tasks. Operating/resonant frequency regulation should work in parallel with overpower/overload protection. Also, power regulation and control (within safe operating limits) is an additional system, which should be synchronized with operating frequency control in order to isolate and select only desirable resonances that are producing desirable mechanical output.

Electronically, we can organize extremely fast signal processing and controls (several orders of magnitude faster than the mechanical system, such as ultrasonic transducer, is able to handle/accept). The problem appears when we drive ultrasonic configuration that has high mechanical quality factor and therefore long response time, which is when mechanical inertia of ultrasonic configuration becomes a limiting factor. Also, complex mechanical shapes of the elements of ultrasonic configuration are creating many frequency harmonics, and low frequency (amplitude) modulation of ultrasonic system influencing system instability that should be permanently monitored and controlled. We cannot go against physic and mechanical limitations of a complex mechanical system (such as ultrasonic transducer and its surrounding elements are), but in order to keep ultrasonic transducer in a stable (and most preferable) regime we should have absolute control over all transducer loading factors and its vital functions (current, voltage, frequency...). This is very important in case of applications like ultrasonic welding, where ultrasonic system is permanently commuting between no-load and full load situation. In a traditional concept of ultrasonic welding control we can often find that no-load situation is followed by the absence of frequency and power control (because system is not operational), and when start (switch-on) signal is produced, ultrasonic generator initiates all frequency and power controls. Some more modern ultrasonic generators memorize the last (and the best found) operating frequency (from the previous operating stage), and if control system is unable to find the proper operating frequency, the previously memorized frequency is taken as the new operating frequency. Usually this is sufficiently good for periodically repetitive technological operations of ultrasonic welding, but this situation is still far from the optimal power and frequency control. In fact, the best operating regime tuning/tracking/control should mean a 100% system control during the totality of ON and OFF regime, or during full-load and no-load conditions. Previously described situation can be guaranteed when Power-Off (=) no-load situation is programmed to be (also) one transducer-operating regime which consumes very low power compared to Power-ON (=) full-load situation. This way, transducer is always operational and we can always have the necessary information for controlling all transducer parameters. Response time of permanently controlled/driven ultrasonic transducers can be significantly faster than in the case when we start tracking and control from the beginning of new Power-ON period.

When transducers are driven full power, it happens in the process of harmonic oscillation, so input electrical energy is permanently transformed to mechanical oscillations. What happens when we stop or break the electrical input to the transducer? - The generator no longer drives the transducer, and/or they effectively separate. The transducer still continues to oscillate certain time, because of its elastomechanical properties, relatively high electro-mechanical Q-factor, and residual potential (mechanical) energy. Of course, the simplest analogy for an ultrasonic transducer is a certain combination of Spring-Mass oscillating system. Any piezoelectric or magnetostrictive transducer is a very good energy transformer. It means that if the input is electrical, the transducer will react by giving mechanical output; but, if the active, electrical input is absent (generator is not giving any driving signal to the transducer) and the transducer is still mechanically oscillating (for a certain time), residual electrical back-output will be (simultaneously) generated. It will go back to the ultrasonic generator through the transducer's electrical terminals (which are permanently connected to the US generator output). Usually, this residual transducer response is a kind of reactive electrical power, sometimes dangerous to ultrasonic generator and to the power and frequency control. It will not be synchronized with the next generator driving train, or it could damage generator's output switching components.

Most existing ultrasonic generator designs do not take into account this residual (accumulated) and reversed power. In practice, we find different protection circuits (on the output transistors) to suppress self-generated transients. Obviously, this is not a satisfactory solution. The best would be never to leave the transducers in free-running oscillations (without the input electrical drive, or with "open" input-electrical terminals on the primary transformer side). Also, it is necessary to give certain time to the transducers for the electrical discharging of their accumulated elasto-mechanic energy.

Resonant frequency control under load:

Frequency control of high power ultrasonic converters (piezoelectric transducers) under mechanical loading conditions is a very complex situation. The problem is in the following: when the transducer is operating in air, its resonant frequency control is easily realizable because the transducer has equivalent circuit (in the vicinity of this frequency) which is similar to some (resonant) configuration of oscillating R-L-C circuits. When the transducer is

under heavy mechanical load (in contact with some other mass, liquid, plastic under welding...), its equivalent electrical circuit loses (the previous) typical oscillating configuration of R-L-C circuit and becomes much more closer to some (parallel or series) combination of R and C. Using the impedance-phase-network analyzer (for transducer characterization), we can still recognize the typical impedance phase characteristic of piezo transducer. However, it is considerably modified, degraded, deformed, shifted to a lower frequency range, and its phase characteristic goes below zero-phase line (meaning the transducer becomes dominantly capacitive under very heavy mechanical loading). If we do not have the transducer phase characteristic that is crossing zero line (between negative and positive values, or from capacitive to inductive character of impedance) we cannot find its resonant frequency (there is no resonance), because electrically we do not see which one is the best mechanical resonant frequency.

Active and Reactive Power and Optimal Operating Frequency:

The most important thing is to understand that ultrasonic transducers that are used for ultrasonic equipment (piezoelectric or sometimes magnetostrictive) have complex electrical impedance and strong coupling between their electrical inputs and relevant mechanical structure (to understand this we have to discuss all relevant electromechanical, equivalent models of transducers, but not at this time). This is the reason why parallel or serial (inductive for piezoelectric, or capacitive for magnetostrictive transducers) compensation has to be applied on the transducer, to make the transducer closer to resistive (active-real) electrical impedance in the operating frequency range. The reactive compensation is often combined with electrical filtering of the output, transducers driving signals. Universal reactive compensation of transducers is not possible, meaning that the transducers can be tuned as resistive impedance only within certain frequencies (or at maximum in band-limited frequency intervals). Most designers think that this is enough (good electrical compensation of the transducers), but, in fact, this is only the necessary first step.

This time we are coming to the necessity of making the difference between electrical resonant frequency and mechanical resonant frequency of an ultrasonic converter. In air (non-loaded) conditions, both electrical and mechanical resonant frequencies of one transducer are in the same frequency point/s and are well and precisely defined. However, under mechanical loading this is not always correct (sometimes it is approximately correct, or it can be the question of appearance of some different frequencies, or of something else like very complicated impedance characteristic). From the mechanical point of view, there is still (under heavy mechanical load) one optimal mechanical resonant frequency, but somehow it is covered (screened, shielded, mixed) by other dominant electrical parameters, and by surrounding electrical impedances belonging to ultrasonic generator. To better understand this phenomenon, we can imagine that we start driving one ultrasonic transducer (under heavy loading conditions), using forced (variable frequency), high power sinus generator, without taking into account any PLL, or automatic resonant frequency tuning. Manually (and visually) we can find an operating frequency producing high power ultrasonic (mechanical) vibrations on the transducer. As we know, heavy loaded transducer presents kind of dominantly capacitive electrical impedance (R-C), but it is still able to produce visible ultrasonic/mechanical output (and we know that we cannot find any electrical pure resonant frequency in it, because there is no such frequency). In fact, what we see, and what we can measure is how much of active and reactive power circulates from ultrasonic generator to piezoelectric transducer (and back from transducer to generator). When we say that we can see/detect a kind of strong ultrasonic activity, it means most probably that we are transferring significant amount of active/real electrical power to the transducer, and that much smaller amount of reactive/imaginary power is present, but we cannot be absolutely sure that such loaded transducer has proper resonant frequency (it could still be dominantly capacitive type of impedance, or some other complex impedance). In fact, in any situation, the best we can achieve is to maximize active/real power transfer, and to minimize reactive/imaginary power circulation (between ultrasonic generator and piezoelectric ultrasonic transducer). If/when our (manually controlled) sinus generator produces/supplies low electrical power, the efficiency of loaded ultrasonic conversion is also very low, because there is a lot of reactive power circulating inside of loaded transducer (and back to the generator).

Here is the most interesting part of this situation: if we intentionally increase the electrical power that drives the loaded transducer (keeping manually its best operating frequency, or maximizing real/active power transfer), the transducer becomes more and more electro-acoustically efficient, producing more and more mechanical output, and less and less reactive power. Also, thermal dissipation (on the transducer) percentage-wise (compared to the total input energy) becomes lower. What is really happening: under heavy mechanical loading and high power electrical driving (on the manually/visually found, best operating frequency, when real power reaches its maximum) the transducer is again recreating/regaining (or reconstructing) its typical piezoelectric impedance-phase

characteristic which, now, has new phase characteristic passing zero line, again (like in real, oscillatory R-L-C circuits). Somehow, high mechanical strain and elasto-mechanical properties of total mechanical system (under high power driving) are accumulating enough (electrical and mechanical) potential energy, and the system is again coming back, mechanically decoupling itself from its load (for instance from liquid) and/or starting to present typical R-L-C structure that is easy for any PLL resonant frequency control (having, again, real/recognizable resonant frequency).

Of course, loaded ultrasonic transducer (optimally) driven by high power will have some other resonant frequency, different than the frequency when it was driven by low power, and also different than its resonant frequency (or frequencies) in non-loaded conditions (in air), because resonant frequency is moving/changing according to time-dependant loading situation (in the range of ±5% around previously found resonant frequency).

To better understand the importance of active power maximization, we know that when we have optimal power transfer (from the energy source to its load), the current and the voltage time-dependant shapes/functions (on the load) have to be in phase. This means that in this situation electrical load is behaving as pure resistive, or active load. (Electrically reactive loads are capacitive and inductive impedances). The next condition (for optimal power transfer) is that load impedance has to be equal to the internal impedance of its energy source (meaning the generator). In mechanical systems, this situation is analogous or equivalent to the previously explained electrical situation, but this time force and velocity time-dependant shapes/functions (on the mechanical load) have to be in phase, which means that in such situations mechanical load is behaving as pure (mechanically) resistive, or active load. Active mechanical loads are basically frictional loads (and mechanically reactive loads/impedances are masses and springs in any combination). We usually do not know/see exactly (and clearly) if we are producing active mechanical power, but by following/monitoring/controlling electrical power, we know that when we succeed in producing/transferring certain amount of active electrical power to one ultrasonic transducer, that corresponds, at the same time, to one directly proportional amount of active mechanical power (dissipated in mechanical load). Delivering active power to some load usually means producing heat on active/resistive elements of this load. We also know that productivity, efficiency and quality of ultrasonic action (in Sonochemistry, plastic welding, ultrasonic cleaning...) strongly and directly depend on how much active mechanical power we are able to transfer to a certain mechanical load (say to a liquid or plastic, or something else). When we have visually strong ultrasonic activity, but without transferring significant amount of active power to the load, we can only be confused in thinking (feeling) that our ultrasonic system is operating well, but in reality, we do not have big efficiency of such system. Users and engineers working in/with ultrasonic cleaning know this situation well. Sometimes, we can see very strong ultrasonic waving in one ultrasonic cleaner (on its liquid surface), but there is no ultrasonic activity and cleaning effects are missing.

In conclusion, it is correct to say that: *active electrical power & active mechanical power*, for an electromechanical system where we transfer electrical energy to the mechanical load. Another conclusion is that we also need to install convenient mechanical/acoustical/ultrasonic sensors which are able to detect, follow, monitor and/or measure resulting ultrasonic/acoustical/mechanical activity (in real-time) on the mechanical load, in order to be 100% sure that we are transferring active mechanical power to certain mechanical load, and to be able to have a closed feedback loop for automatic (mechanical, ultrasonic) power regulation. For instance, in liquids (Sonochemistry and ultrasonic cleaning applications), the appearance of cavitation is the principal sign of producing active ultrasonic power. To control this we need sensors of ultrasonic cavitation. Also, we know that the last step in any energy chain (during electromechanical energy transfer) is heat energy. By supplying electrical resistive load with electrical energy we produce heat. The same is valid for supplying mechanical resistive/frictional load with ultrasonic energy, when the last step in this process is again heat energy (but, again, force and velocity wave shapes of delivered ultrasonic waves have to be in phase, measured on its load). From the previous commentary we can conclude that the best sensors for measuring active/resistive ultrasonic energy transfer in liquids are real-time, very fast responding temperature sensors (or some extremely sensitive thermocouples, and/or thermopiles).

There can be a practical problem (for resonant frequency tracking) if we start driving certain transducer full power, under load, if we are not sure that we know its best operating mechanical resonant frequency (because we can destroy the transducer and output transistors if we start with a wrong frequency). In real life, every well designed PLL starts with a kind of low power sweep frequency test (say giving 10% of total power to the transducer), around its known best operating frequency taking/accepting one frequency interval that is given in advance. When the best operating resonant frequency is confirmed/found, PLL system tracks this frequency, and at the same time the power regulation (PWM) increases output power (of ultrasonic generator) to the desired maximum. Of course, when the transducer is in air (mechanically non-loaded), previous explanation is readily applicable because we can easily find its best resonant frequency, and later on we can start gradually increasing the power on the transducer. If starting and operating situation is with already heavy loaded transducer (which can be represented by

dominantly R-C impedance), the problem is much more serious, because we should know how to recognize (automatically) the optimal mechanical resonant frequency (without the possibility of using phase characteristic that is crossing zero line). There are some tricks, which may help us realize such control. Of course, before driving one transducer in automatic PLL regime, we should know its impedance-phase vs. frequency properties (and limits) in non-loaded and fully loaded situations. In order to master previous complexity of driving ultrasonic transducers (and to explain this situation) we should know all possible and necessary equivalent (electrical) circuits of non loaded and loaded ultrasonic transducers, where we can see/discuss/adjust different methods of possible PLL control/s. Since ultrasonic transducer is always driven by using ultrasonic generator which has output ferrite transformer, inductive compensation and other filtering elements, it is necessary to know the relevant (and equivalent) impedance-phase characteristics in all of such situations in order to take the most convenient and proper current and voltage signals for PLL.

All previous comments are relevant when driving (input) signal is either sinusoidal or square shaped, but always with a (symmetrical, internal) duty cycle of 1:1 (T_{on}: T_{off} = 1:1), meaning being a regular sinusoidal or square shaped wave train. There is a special interest in finding a way/method/circuit capable of driving ultrasonic transducers directly using high power (and high ultrasonic frequency), PWM electrical (input) signals, because of the enormous advantages of PWM regulating philosophy. Applying special filtering networks in front of an ultrasonic transducer can be very useful when we want to drive ultrasonic transducer with PWM signals.

Influence of External Mechanical Excitation:

One of the biggest problems for PLL frequency tracking is when ultrasonic (piezoelectric) transducer under mechanical load, driven by ultrasonic generator, produces mechanical oscillations, but also receives mechanical response from its environment (receiving reflected waves). Sometimes, received mechanical signals are so strong, irregular and strangely shaped that equivalent impedance characteristic of loaded transducer becomes very variable, losing any controllable (typical impedance) shape. It looks like all the parameters of equivalent electrical circuit of loaded transducer are becoming non-linear, variable and like transients signals. There is no PLL good enough to track the resonant frequency of such transducer, but luckily, we can introduce certain filtering configuration in the (electrical) front of transducer and make this situation much more convenient and controllable (meaning that external mechanical influences can be attenuated/minimized).

Sometimes loaded ultrasonic transducer (in high power operation) behaves as multi-resonant electrical and mechanical impedance, with its entire equivalent-model parameters variable and irregular. Optimal driving of such transducer, either on constant or sweeping frequency, becomes uncontrollable without applying a kind of filtering and attenuation of external vibrations and signals received by the same transducer. In fact, the transducer produces/emits vibrations and at the same time receives its own vibrations, reflected from the load. There is a relatively simple protection against such situation by adding a parallel capacitance to the output piezoelectric transducer. Added capacitance should be of the same order as input capacitance of the transducer. This way, ultrasonic generator (frequency control circuit) will be able to continue controlling such transducer, because parallel added capacitance cannot be changed by transducer parameters variation. In case of large band frequency sweeping, we can also add to the input transducer terminals certain serial resistive impedance (or some additional L-R-C filtering network). This way we avoid overloading the transducer by smoothly passing trough its critical impedance-frequency points (present along the sweeping interval).

In any situation we can combine some successful, useful and convenient PLL procedures with a real/active power maximizing procedure incorporated in an automatic, closed feedback loop regulation (of course, trying in the same time to minimize the reactive/imaginary power).

Objectives and new R&D tasks:

Traditional ultrasonic equipment exploits mainly single resonant frequency sources, but it becomes increasingly important to introduce/use different levels of frequency and amplitude modulating signals, as well as low frequency (ON – OFF) group PWM digital-modulation in low and high frequency domains. Several modulation levels and techniques could be applied to maximize the power and frequency range delivered to heavily loaded ultrasonic transducers (and, this way, many of the above-mentioned loading problems could be avoided or handled in a more efficient way). Discussing such situations can be a subject of a special chapter.

As we can see from the previous explanation, it is not so simple and easy to explain all the aspects of future ultrasonic generators, but it is already a big advantage to understand the basic principles and principal targets. The question is: how is it possible that a number of producers in the ultrasonic field are working/ producing

relatively good ultrasonic equipment, if we take into account all previous design problems and tasks. The answer is that probably almost none of them has neither in practice nor in R&D all of the previously mentioned activities. Possibly, at least some of them understand the existence of such problems, and during a long experimental practice (or sometimes by luck and copying from the others), they have found and optimized some particular situations (designs), which are operating satisfactorily in certain conditions. Each proposal, without the exact knowledge of what has to be done, is an expensive R&D and technological excursion. When possible, it is reasonable to avoid this kind of adventure. It is sure that all traditional applications that can tolerate old design philosophy are already obsolete; for the new generation of Ultrasonic Generators, we have to take a new approach in R&D and strategic planning.

CONCLUSION:

Digital-Phase-Frequency-Locked-Loop, combined with a convenient frequency counting /searching algorithm, and real/active power tracking, with a programmable mono-frequency, multi-frequency and frequency sweeping concept/s can be included/combined in one FPGA microchip. Of course, resonant frequency control has to be simultaneously linked to (automatic) output power regulation and multilevel overload protection. This could be a powerful (multifunction) controller for today's technologies of different ultrasonic processing and similar applications.

Today, the most demanding digital PLL (resonant frequency) control of industrial, high power ultrasonic transducers (operating between 20 and 100 kHz) is connected to the following set of parameters/characteristics:

1. Master clock 100 MHz, in order to derive the frequency resolution better than 0.5 Hz.
2. Frequency band for automatic PLL regulation ($\in$) **[**$f_{oper.} - 10\% f_{oper.}$ to $f_{oper.} + 10\% f_{oper.}$**]**.
3. Searching for sgn (PHI) i.e. abs (PHI) is the best way to identify a singular resonant system, which is capable of oscillating.
4. Over-damped/overloaded systems are too broad for any accurate identification.
5. A/D capability and embedded micro-controller conditions for different calculations and synchronous output power regulation are necessary.

M. Prokic **MPI, Marais 36, 2400, Le Locle, Switzerland,** **E-mail: mpi@bluewin.ch**

PLL FLOW CHART (example)

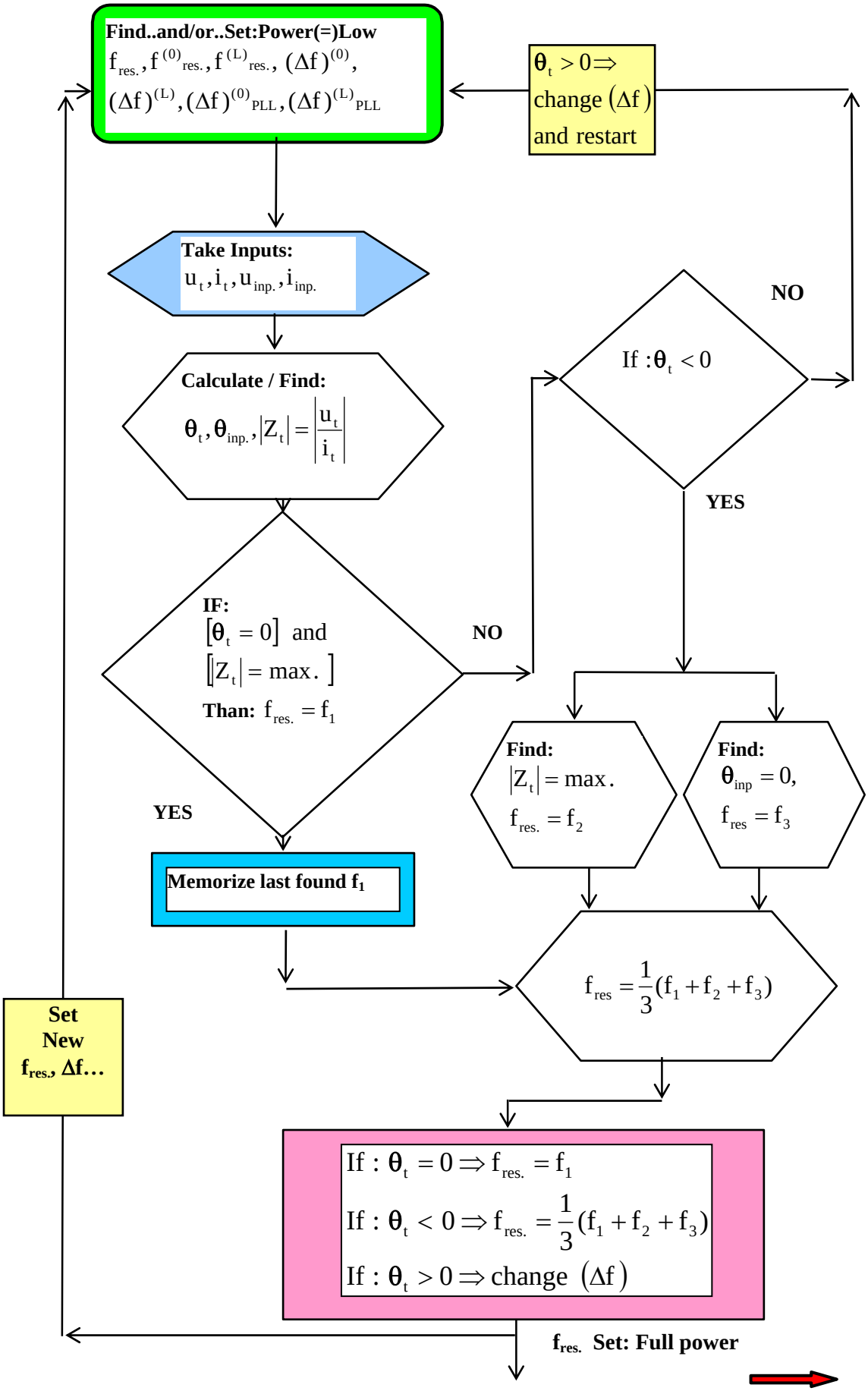

M. Prokic MPI, Marais 36, 2400, Le Locle, Switzerland, E-mail: mpi@bluewin.ch

3.1 Converters Loading and Associated Losses

Let us try to understand converters loading process, converters internal losses and the meaning of the mechanical quality factors ratio (referring to numerical results for Branson converter 502/932R; -see T 1.1 and T 1.2). We know that mechanical quality factor presents the ratio of stored and dissipated energy per one oscillation of a converter,

$$\mathbf{Q_m} = 2\pi \frac{\textbf{Energy stored in the transducer during one full periode}}{\textbf{Energy dissipated in the transducer during one full periode}} = 2\pi \frac{\mathbf{E_s}}{\mathbf{E_d}}$$

$$\mathbf{Q_{m01}} = 2\pi \frac{\mathbf{E_{s01}}}{\mathbf{E_{d01}}} = \mathbf{453.73},\ \mathbf{Q_{m02}} = 2\pi \frac{\mathbf{E_{s02}}}{\mathbf{E_{d02}}} = \mathbf{1256.70},$$

$$\mathbf{Q_{mL1}} = 2\pi \frac{\mathbf{E_{sL1}}}{\mathbf{E_{dL1}}} = \mathbf{39.205},\ \mathbf{Q_{mL2}} = 2\pi \frac{\mathbf{E_{sL2}}}{\mathbf{E_{dL2}}} = \mathbf{18.63}$$

$$\frac{\mathbf{Q_{m01}}}{\mathbf{Q_{mL1}}} = \frac{\mathbf{E_{s01}}}{\mathbf{E_{sL1}}} \frac{\mathbf{E_{dL1}}}{\mathbf{E_{d01}}} \cong \frac{\mathbf{E_{dL1}}}{\mathbf{E_{d01}}}\ \mathbf{(=11.57)},$$

$$\eta_1 \approx \frac{\mathbf{Q_{mo1}} - \mathbf{Q_{mL1}}}{\mathbf{Q_{mo1}}} \mathbf{x100\%} = [\mathbf{1} - \frac{\mathbf{Q_{mL1}}}{\mathbf{Q_{mo1}}}]\% \ \mathbf{(\cong 91.36\%)}$$

$$\frac{\mathbf{Q_{m02}}}{\mathbf{Q_{mL2}}} = \frac{\mathbf{E_{s02}}}{\mathbf{E_{sL2}}} \frac{\mathbf{E_{dL2}}}{\mathbf{E_{d02}}} \cong \frac{\mathbf{E_{dL2}}}{\mathbf{E_{d02}}}\ \mathbf{(=67.45)},$$

$$\eta_2 \approx \frac{\mathbf{Q_{mo2}} - \mathbf{Q_{mL2}}}{\mathbf{Q_{mo2}}} \mathbf{x100\%} = [\mathbf{1} - \frac{\mathbf{Q_{mL2}}}{\mathbf{Q_{mo2}}}]\% \ \mathbf{(\cong 98.52\%)} \qquad (1.12)$$

$$\frac{\mathbf{Q^*_{m0}}}{\mathbf{Q^*_{mL}}} = \sqrt{\frac{\mathbf{Q_{m01}}}{\mathbf{Q_{mL1}}} \frac{\mathbf{Q_{m02}}}{\mathbf{Q_{mL2}}}} = \sqrt{\frac{\mathbf{E_{s01}}}{\mathbf{E_{sL1}}} \frac{\mathbf{E_{s02}}}{\mathbf{E_{sL2}}} \frac{\mathbf{E_{dL1}}}{\mathbf{E_{d01}}} \frac{\mathbf{E_{dL2}}}{\mathbf{E_{d02}}}} \cong \sqrt{\frac{\mathbf{E_{dL1}}}{\mathbf{E_{d01}}} \frac{\mathbf{E_{dL2}}}{\mathbf{E_{d02}}}}\ \mathbf{(=27.93)}$$

For instance, in case of BRANSON 502/932R converter (data given in T 1.1, Figs. 12 & 13), we know (based on measurements) that average power dissipation in series resonance (in air = non-loaded converter) is $\mathbf{P_{d01} \approx 60 \div 65\ W}$, and in parallel resonance $\mathbf{P_{d02} \approx 10 \div 32\,W}$, while converter is producing the same output amplitude of 20 μm-pp (in both resonant regimes). We can also notice that converter's efficiency is higher in parallel resonance than in series resonance (98.52% > 91.36%, for BRANSON 503/932R and for many other power converters, too).

Thermal power dissipation of non-loaded 502/932R converter was measured using Clarke-Hess power meter connected just before converter (keeping converters current and driving voltage in phase). The converter output amplitude in series resonance, was stabilized to 20 micrometers (peak-to-peak), the voltage on the converter necessary to produce that amplitude was found to be in the range of 21.6 V, rms, and the converter input current was 2.98 A, rms. Of course, the input current into converter was many times higher comparing it to the converter current when operating in parallel resonance. Measured total power consumption (in series resonance) was in the range of 60 to 65 Watts (and this is the thermal dissipation, since converter was operating load-free in air). In order to avoid high internal power dissipation, when converter is operating non-loaded in series resonance, most of

modern designs of ultrasonic power supplies are implementing PWM, load-current control, reducing automatically converter's current, and shifting a little bit converter operating frequency towards higher impedance, when converter is not delivering power to its load. Series resonance regimes of piezoelectric converters should be permanently loaded in order to produce minimal or acceptable internal power dissipation.

We also know that series resonance is current-resonance (high current & limited voltage), and that parallel resonance is voltage-resonance (high voltage & limited current). Converter operating in series resonance is able to produce high output force (or pressure) and relatively low output velocity (proportional to its high driving, motional-current and relatively low input-voltage), and converter operating in parallel resonance is able to produce high output velocity and relatively low output force (proportional to its high driving, motional-voltage and relatively low input-current consumption). Here we should pay attention on the fact/s that motional current in series resonance is a bit smaller than converter input current, and that motional voltage in parallel resonance is also smaller than input converter voltage, since equivalent, motional converter circuit/s is/are separated from converter input by the presence of reactive, capacitive elements C_{op} and C_{os}.

For parallel-resonance dissipation-measurements Branson is testing converters the same way as in series resonance (the input converter electrical-field, directly on piezoceramics, is in the range between 186 and 300 V-rms/mm, and the motional converter voltage is stabilized on 930 V-rms for piezoceramics thick 5 millimeters = 930/5 = 186 V-rms/mm), while converter is producing 20 micrometers, peak-to-peak amplitude (keeping the same amplitude as in the case of series resonance measurements). The best what was possible to find in parallel resonance regime (but seldom and for well selected, excellent quality converters), regarding 502/932R, non-loaded converters operating in air, was between 5 and 10 Watts of total internal power dissipation, or total power consumption, and in larger number of measurements the consumption was between 15 and 32 Watts. For standard quality of 502/932R converters Branson is specifying allowed power dissipation (for parallel resonance of non-loaded converter) to be between 10 and 20 Watts.

Since when we make a ratio between two mechanical quality factors, we shall get the ratio of corresponding energies, and this is in the same time the ratio between corresponding powers, consequently, based on (1.12), we can roughly estimate how much would be the (worst case scenario of) power dissipation, $\mathbf{P_{dL1}}$ **and** $\mathbf{P_{dL2}}$, of fully-loaded (and still acceptable quality: T 1.1, Figs. 12 & 13) converter in its series and parallel resonance,

$$\mathbf{P_{dL1} \cong P_{d01} \cdot 11.57 = 60 \cdot 11.57 = 694.20\ W}$$
$$\mathbf{P_{dL2} \cong P_{d02} \cdot 67.45 = 10 \cdot 67.45 = 674.5\ W} \qquad (1.13)$$
$$\mathbf{P^*_{dL} = \sqrt{P_{dL1} P_{dL2}} = 684.28\ W}\ .$$

As we can see from (1.13), estimated thermal power dissipation in the case of fully-loaded high-power converter delivering its maximal output power (here is selected one of modest but still acceptable-quality, BRANSON 502/932R converters, T 1.1, Figs. 12 & 13, which is also able to perform much better in cases of well selected

converters), would be too high (close to 700 Watts), meaning that we should try to design and/or select only converters that already have extremely low power dissipation in non-loaded conditions. The second conclusion is that we should not operate high-power converters in long-time, continuous (full-power) regime/s; -it is always better to have certain pulse-repetitive, ON-OFF regime (for instance 1:1), allowing to a converter's forced-cooling eliminating excessive heat.

Until present we were only taking opposite extremes in analyzing converters performances, such as non-loaded and fully-loaded situations. Loading process between no-load and maximal-load (when converter still operates well) is continuously influencing converter's performances, and for the purpose of better converters characterization it would be meaningful to create the functional diagram (based on measurements), as presented in the table, T 1.3 (numerically illustrated again for the same BRANSON 502/932R converter, Figs. 12, 13 & 14, T 1.1).

T 1.3 Loading of BRANSON 502/932R converter (data from T 1.1, Figs. 12 & 13)

Effective Mechanical Quality Factors Ratio, (1.11)	**Non-Loaded Converter** $(Q^*_{mL-x} = Q^*_{m0})$	**Load increase** $(Q^*_{m0} < Q^*_{mL-x} < Q^*_{mL})$	**Fully-Loaded Converter** $(Q^*_{mL-x} = Q^*_{mL} = \max.)$
$\alpha = \frac{Q^*_{mL-x}}{Q^*_{mo}}$	$\alpha = 1$	$1 > \alpha > 0.0358$	$\alpha = 0.0358$

Of course, the table T 1.3 can be extended to have separate values for series and parallel resonance, or some other loading function can be created (tracing, under loading: output converter amplitude, velocity, force, different model parameters…).

Until present, under converter loading (in this paper) we are only simulating real load conditions (by immersing converter in water, or some other similar method), and making low-signal impedance measurements. In reality, for exact and correct converters characterization we need a kind of instrument similar to Network Impedance Analyzer (for instance similar to HP 4194A), able to perform frequency sweeping, power, impedance, and spectral measurements, using high voltage and high current signals (still not available in one compact and sophisticated instrument).

In order to simplify understanding of internal power losses, we can go back to a basic knowledge from elementary electro-technique. Power losses inside of a converter are losses on its equivalent resistive components. When converter is not loaded, the most significant resistive components able to dissipate power are: in series resonance $\mathbf{R_1}$ (at $\mathbf{f_1}$), and in parallel resonance $\mathbf{R_2}$ (at $\mathbf{f_2}$). For Branson non-loaded converter presented on Figs. 12 & 13, T 1.1, R_1 = 4.6 Ω and R_2 = 94.20 kΩ (f_1 = 18900 Hz, f_2 = 20912 Hz). Since experimentally we already know that for reaching converter amplitude of 20 μm-pp in series-resonance, we need 21.6 V-rms and 2.98 A-rms at the converter input terminals, we can (approximately) calculate the power internally dissipated in the converter as $\approx R_1 \times I^2 = 4.6 \times 2.98^2 = 41$ W, that is close to the experimentally measured range of 60 – 65 W. Also, we know (based on measurements) that for reaching converter amplitude of 20 μm-pp in parallel-resonance, we need approximately 1000 V-rms at the converter input terminals, and

we can (approximately) calculate the power internally dissipated in the converter as ≈ $U^2 / R_2 = 1000^2 / 94200 = 10.62$ W, that is also close to the experimentally measured values. When the same converter is fully-loaded, $R_{1L} = 57.574\ \Omega$ and $R_{2L} = 1.50\ k\Omega$ ($f_1 = 18525$ Hz, $f_2 = 20387$ Hz), the same approximate calculation would produce results similar to results already predicted in (1.13), as for instance: $P_{dL1} \approx R_{1L} \times I^2 \approx 57.574 \times 2.98^2 = 511$ W, and $P_{dL2} \approx U^2 / R_{2L} \approx 1000^2 / 1500 = 667$ W.

In order to present another view of the same situation (regarding power losses), let us consider an ultrasonic converter as simple combination/s of equivalent capacitive, inductive and resistive elements. If we program an Impedance Analyzer to measure converter (in its resonant area) as a series connection between an equivalent resistance and an equivalent inductance, and if we again take the same Branson converter (Figs. 12 & 13, T 1.1), we shall get inductance-resistance plots presented on Figs. 14.1 – 14.2.

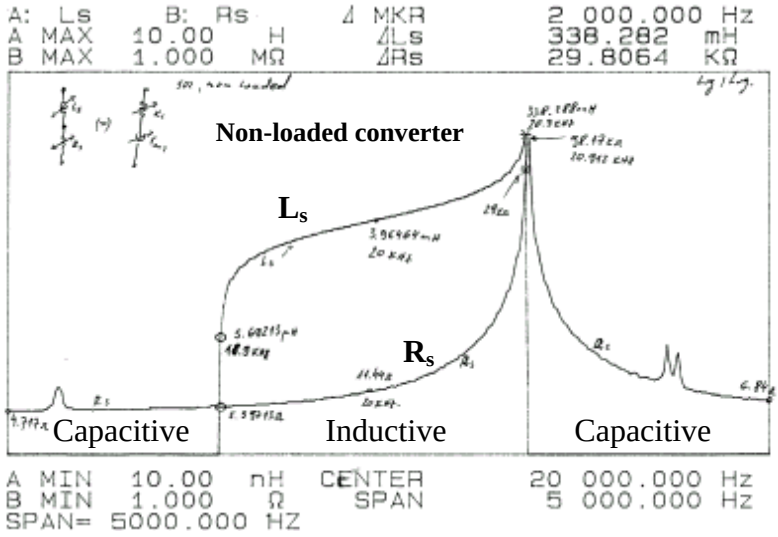

f_1: R_s= 5.597 Ω, L_s= 5.69 μH, f_2: R_s= 98.17 kΩ, L_s= 338.288 mH

Fig. 14.1 Non-loaded converter as the series Inductance-Resistance

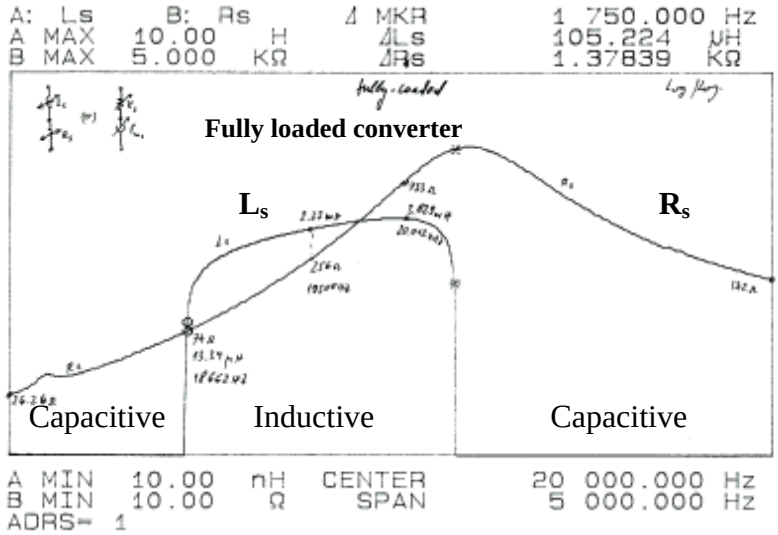

f_1: R_s= 74 Ω, L_s= 13.34 μH, f_2: R_s= 1.378 kΩ, L_s= 105.224 mH

Fig. 14.2 Fully-loaded converter as the series Inductance-Resistance

If we again program an Impedance Analyzer to measure converter (in its resonant area) as a parallel connection between an equivalent resistance and an equivalent inductance, and if we again take the same Branson converter (Figs. 12 & 13, T 1.1), we shall get inductance-resistance plots presented on Figs. 14.3 – 14.4.

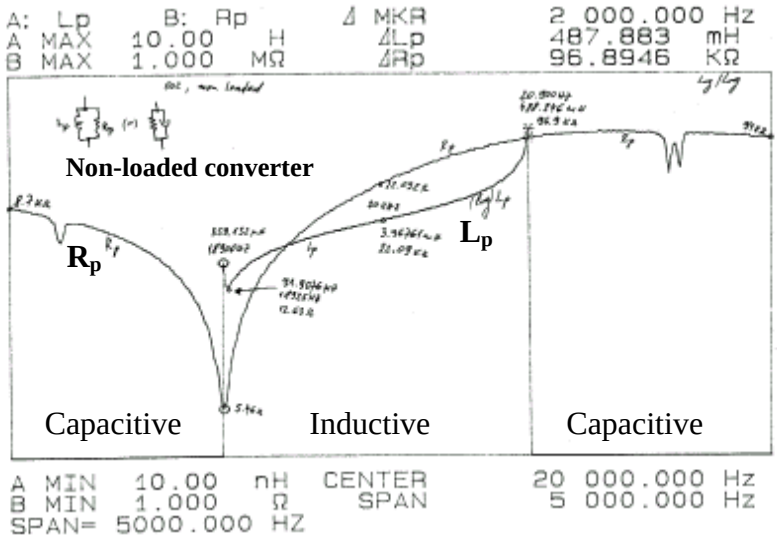

f_1: R_p= 5.46 Ω, L_p= 359.132 μH, f_2: R_p= 96.9 kΩ, L_p= 488.246 mH

Fig. 14.3 Non-loaded converter as the parallel Inductance-Resistance

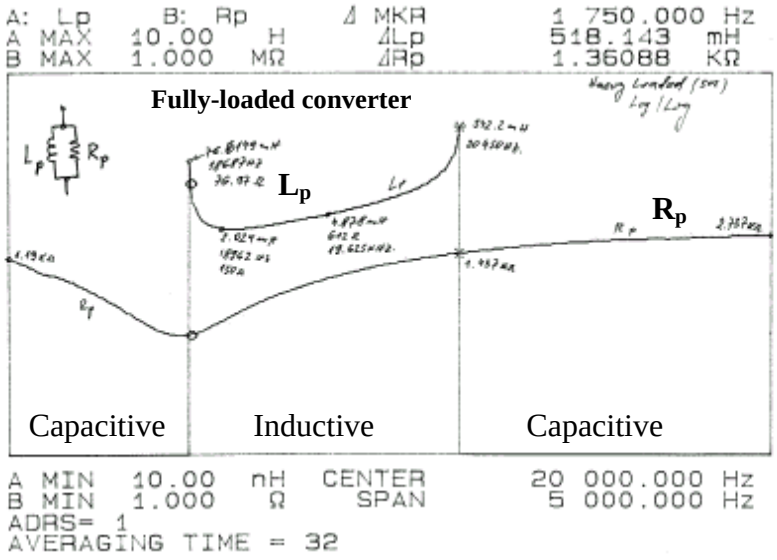

f_1: R_p= 76.97 Ω, L_p= 76.615 mH, f_2: R_p= 1.437 kΩ, L_p= 542.2 mH

Fig. 14.4 Fully-loaded converter as the parallel Inductance-Resistance

If we now program an Impedance Analyzer to measure converter (in its resonant area) as a series connection between an equivalent resistance and an equivalent capacitance, for the same Branson converter (Figs. 12 & 13, T 1.1), we shall get capacitance-resistance plots presented on Figs. 14.5 – 14.6.

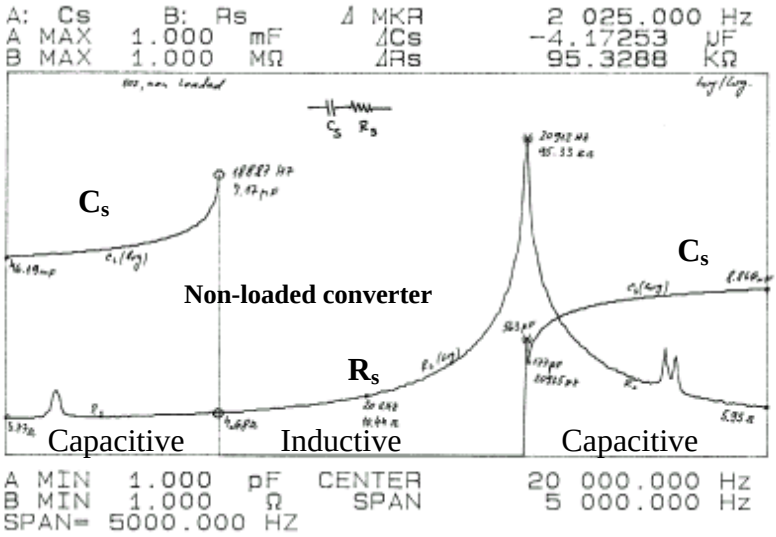

f_1: R_s = 4.68 Ω, C_s = 4.17 μF, f_2: R_s = 95.33 kΩ, C_s= 563 pF

Fig. 14.5 Non-loaded converter as the series Capacitance-Resistance

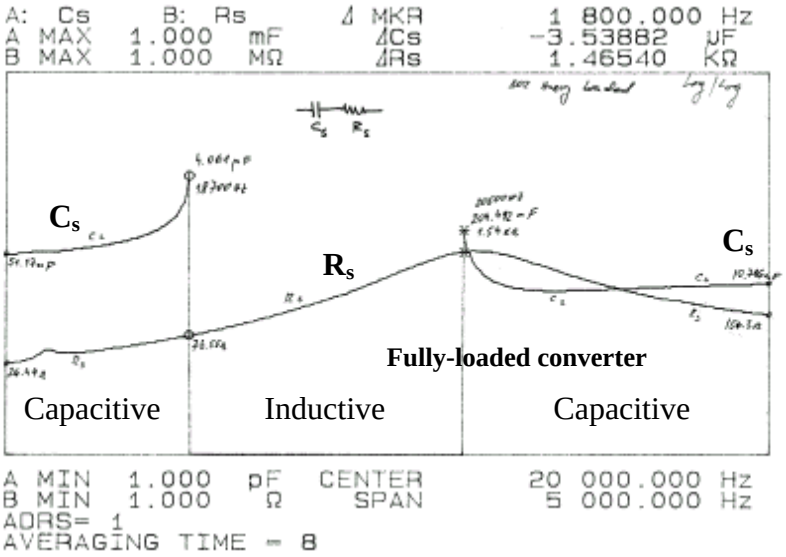

f_1: R_s = 73.55 Ω, C_s = 4.061 μF, f_2: R_s = 1.54 kΩ, C_s= 204.492 nF

Fig. 14.6 Fully-loaded converter as the series Capacitance-Resistance

If we now program an Impedance Analyzer to measure converter (in its resonant area) as a parallel connection between an equivalent resistance and an equivalent capacitance, for the same Branson converter (Figs. 12 & 13, T 1.1), we shall get capacitance-resistance plots presented on Figs. 14.7 – 14.8.

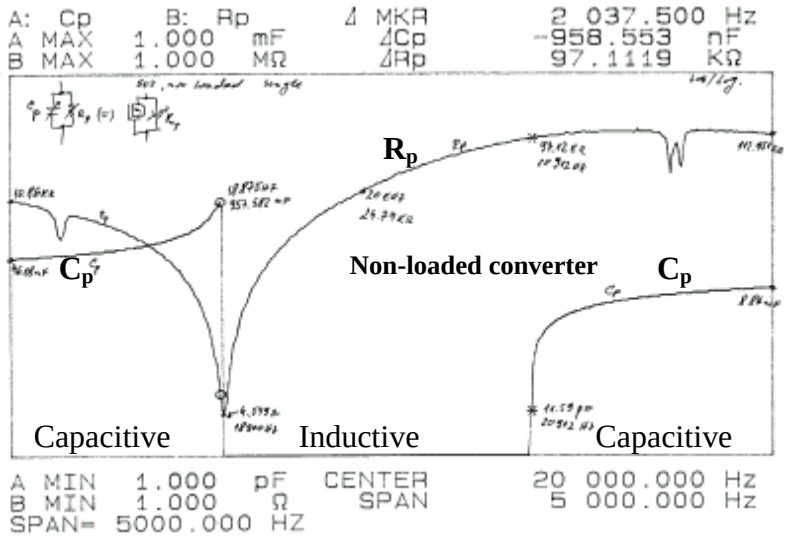

f_1: R_p= 4.549 Ω, C_p= 957.582 nF, f_2: R_p= 97.12 kΩ, C_p= 11.59 pF

Fig. 14.7 Non-loaded converter as the parallel Capacitance-Resistance

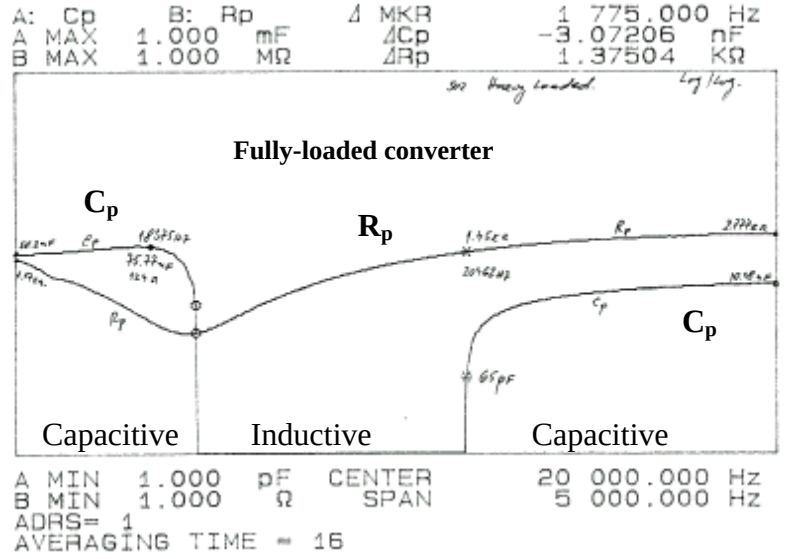

f_1: R_p= 76 Ω, C_p= 8 nF, f_2: R_p= 1.45 kΩ, C_p= 65 pF

Fig. 14.8 Fully-loaded converter as the parallel Capacitance-Resistance

In all of here presented Inductance, Capacitance vs. Resistance plots Figs. 14.1 – 14.8) we can find that equivalent non-loaded converter resistance in its series resonance is always in the range between 4.549Ω and 5.597Ω, and in fully loaded situation between 73.55Ω and 76.97Ω (similar to model parameters from T 1.1). Also in parallel resonance, resistance of non-loaded converter is in the range between 95.33kΩ and 98.17kΩ, and in fully loaded situation between 1.3kΩ and 1.54kΩ (again close to model parameters from T 1.1). Simply considering that in series resonance converter current is producing power dissipation on its series resistance, and that in parallel resonance converter voltage is responsible for power dissipation on its parallel resistance, we shall again get similar results as already estimated in (1.13), as for instance: $P_{do1} \approx R_1 \times I^2 \approx 45$ W, $P_{dL1} \approx R_{1L} \times I^2 \approx 668$ W, $P_{do2} \approx U^2 / R_2 \approx 10$ W, and $P_{dL2} \approx U^2 / R_{2L} \approx 704$ W.

The meaning of here presented analysis of converter power losses is to give us estimation tools to qualify converters (in order to optimize them), and to (roughly) quantify their losses, using low-signal impedance measurements, while having enough prediction-security to say that what we are predicting is approximately and sufficiently valid (and applicable) to conditions when converter is operating full-power (driven either with high input current or high input voltage, depending on its operating resonant regime).

Another platform for analyzing (or understanding) converter power losses in resonance is to measure its effective tangent delta, or dissipation factor (in resonant operating area), as presented on Figs. 14.9 – 14.10.

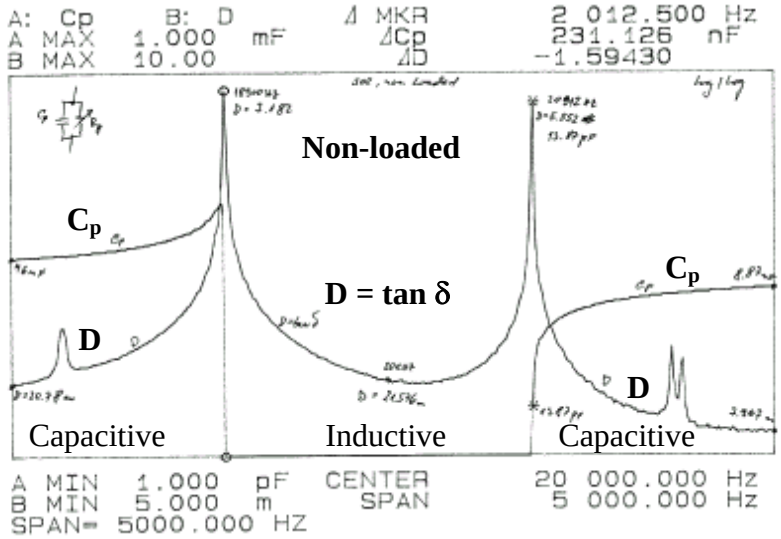

f_1 = 18900 Hz, D = 7.182; f_2 = 20912 Hz, D = 5.552

Fig. 14.9 Non-loaded converter, Dissipation Factor

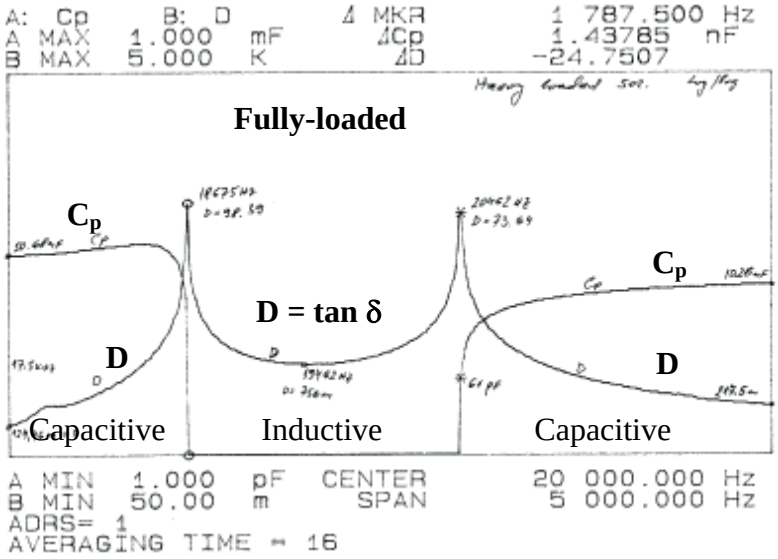

f_1 = 18675 Hz, D = 98.39; f_2 = 20462 Hz, D = 73.64

Fig. 14.10 Fully-loaded converter, Dissipation Factor

From Figs. 14.9 -14.10 we can see that dissipation factor in series resonance is always a little bit higher than in parallel resonance (7.182 > 5.552; 98.39 > 73.64), but they are approximately close to each other, too. We can also see that the ratio between fully-loaded converter's dissipation factor/s to non-loaded converter's dissipation factor/s, in this example (for Branson converter Figs. 12 & 13, T 1.1), is close to 13 (98.39/7.182 = 12.58, 73.64/5.552 = 13.264), meaning that converter internal losses would also rise approximately 13 times, comparing non-loaded and fully-loaded situation (similar to results of mechanical quality ratio/s found in (1.12)).

Another important conclusion is that maximal power performances (and efficiency) of a piezoelectric converter are approximately the same, either converter is operating in its series or parallel resonance, but converter loading nature and electrical driving configurations are very much different regarding series and parallel resonance. Also, converter mechanical output in series resonance presents dominant force or pressure source, and converter output in parallel resonance presents dominant velocity source.

We can also see that dissipation factors are reaching maximal values in converter's electrical resonant points (Impedance zero-phase points), meaning that in real operating conditions, in order to avoid high internal dissipation, we should operate converter either in its motional (mechanical) series resonance, or in its motional (mechanical) parallel resonance, or in the frequency zone between them (also in the frequency interval towards lower frequencies).

In order to analyze converter losses and thermal dissipation it is important to have convenient converter models that are applicable for low and high signal driving conditions. There is a kind of understanding in modern ultrasonic technology that simplified, lumped parameters, piezo-converter models (described in the first chapter) are only well applicable for very low signal measurements and converter characterization (for instance, when we use Network Impedance Analyzer that produces 1 V sinusoidal frequency sweeping signal). Since still we are not able to make full-scale impedance measurements when converter is operating full power (on high driving voltages and high input currents), because for such situations we do not have high-power Network Impedance Analyzers, based on particular measurements in high power and heavy loading driving conditions, we can conclude that low-signal lumped parameters models are not applicable. Generally, this is not correct. If converter is operating in piezoceramics' safe operating area, and in any of its linear regimes, or steady, stationary and stable oscillatory (sinusoidal) regimes, and if converter is not overloaded, models are well applicable (for low and high driving signals). Of course, under higher voltage (or high power) driving we can have certain resonant frequency shifts, which are never higher than 10% comparing them to low signal converter parameters. In Branson case (converter analyzed here: 502/932R), since converters are sufficiently well optimized, resonant frequency shifts (in high power driving conditions) are in the range of 1% or less (depending on piezoceramics choice, central bolt choice, static pressure on ceramics, surface finishing...). Also, if we know what are essential signal-feedback values for controlling mechanical output parameters of converters (motional voltage and motional current), and if we know how to extract such signals from our power circuits, we would conclude that lumped parameters models are very much applicable for low and high signal driving conditions, as long we stay in the safe operating limits of

piezoceramics (for instance not to apply more than 200V-rms. per millimeter of piezoceramic thickness, directly on piezoceramics, etc.).

It is another problem (regarding modeling) when we go to converter overload situations. Most of lumped parameter models are significantly evolving and degrading because of load contribution/s. Some of the lumped circuit model parameters will significantly degenerate, and a few of them will stay relatively stable under heavy loading conditions, and we should profit exploiting this knowledge in order to design proper external matching electronics. It would be too easy to conclude that in high power (usually under overloading) our simple converter models are not valid. In reality, this could be conditionally correct, because our simple models (under heavy loading) are progressively evolving and becoming even simpler models (becoming dominantly a combination of R and C components), or saying differently, our models are still valid, but our knowledge of models evolution under loading is most probably missing. In the next part of this chapter we shall analyze some experimental loading situations in order to give deeper insight in this situation.

3.2 Model Parameters Evolution Under Water Loading

Let us now take as an example, the water loading of the particular bell-shaped titanium sonotrode connected to titanium booster (1:1), and to Sonics & Materials ultrasonic converter type CV-154 (similar to Branson high power converters), where we shall trace the changes in converter impedance parameters caused by load increase.

T 1.4.1	Piezoelectric Converter Impedance Parameters in Series Resonance (CV-154)							
Water Loading in %	Cop [nF]	C_1 [pF]	L_1 [mH]	R_1 [Ω]	f_1 [kHz]	Q_{m1} [1]	α (1.11) T 1.3	$\sqrt{L_1/C_1}$ [kΩ] (1.4)
0.00	14.6487	158.360	402.506	14.960	19.934	3370	1	50.415
0.80	14.7020	164.165	389.809	17.820	19.895	2734	0.8113	48.720
8.33	14.8980	167.179	386.398	19.536	19.802	2461	0.7303	48.078
25.0	15.1125	160.505	404.183	22.760	19.760	2205	0.6543	50.186
36.0	15.1504	146.329	447.355	95.050	19.673	582	0.1727	55.319
42.0	15.5491	107.887	617.514	164.83	19.506	459	0.1362	75.657

T 1.4.2	Piezoelectric Converter Impedance Parameters in Parallel Resonance (CV-154)							
Water Loading in %	Cos [nF]	C_2 [μF]	L_2 [μH]	R_2 [kΩ]	f_2 [kHz]	Q_{m2} [1]	α (1.11) T 1.3	$\sqrt{L_2/C_2}$ [Ω] (1.4)
0.00	14.80706	1.38004	45.6939	29.880	20.042	5193	1	5.7539
0.80	14.86617	1.37674	45.9680	20.729	20.005	3587	0.6907	5.7789
8.33	14.87437	1.36744	46.7808	17.650	19.912	3018	0.5812	5.8482
25.0	15.27301	1.39914	45.8797	12.780	19.864	2232	0.4298	5.7258
36.0	15.29673	1.31706	49.2255	2.1500	19.763	352	0.0678	6.1079
42.0	15.65699	1.25125	52.9027	1.2000	19.559	184	0.03543	6.5217

T 1.4.3	Coupling factor ($k_c = k \cong k' \cong k''$) under loading (for CV-154)			
Water Loading in %	$k' = \sqrt{\frac{C_1}{C_{op}+C_1}}$	$k'' = \sqrt{\frac{C_{os}}{C_2}\cdot\frac{f_1^2}{f_2^2}}$	$\sqrt{k'k''}$	$0.5(k'+k'')$
0.00	0.103416	0.103027	0.1032213	0.1032215
0.80	0.100850	0.103342	0.1020884	0.1020960
8.33	0.105342	0.104903	0.1051223	0.1051225
25.0	0.102514	0.103932	0.1032206	0.1032230
36.0	0.097806	0.107279	0.1024330	0.1025425
42.0	0.083010	0.111559	0.0962316	0.0972845

The loading level will be quantified as the percentage of the bell-shaped-sonotrode axial-length immersed in water. All low-signal impedance measurements data are related to models presented on Figs. 1-6 and summarized in the tables T 1.4.1, T 1.4.2 and T 1.4.3. Impedance-Phase measurements-data from T 1.4.1 and T 1.4.2 can be found on the Figs. 15.1 – 15.6, and curve-fitting plots of all model parameters (from T 1.4.1 and T 1.4.2) are given on Figs. 16.1 –16.6.

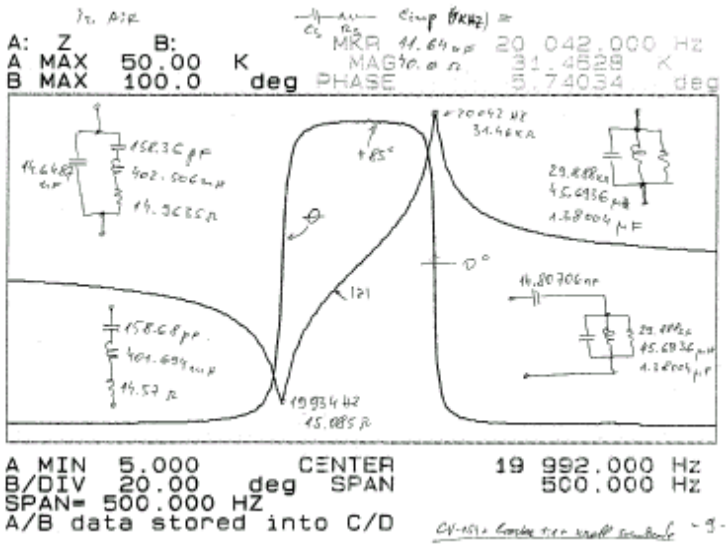

Fig. 15.1 Non-loaded Converter Impedance (CV-154 + Booster + Sonotrode)

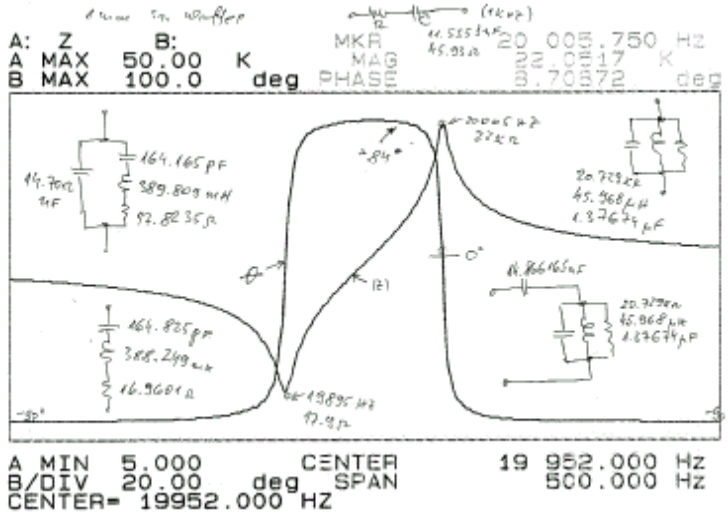

Fig. 15.2 Water-loaded Converter Impedance (Loading = 0.80%)

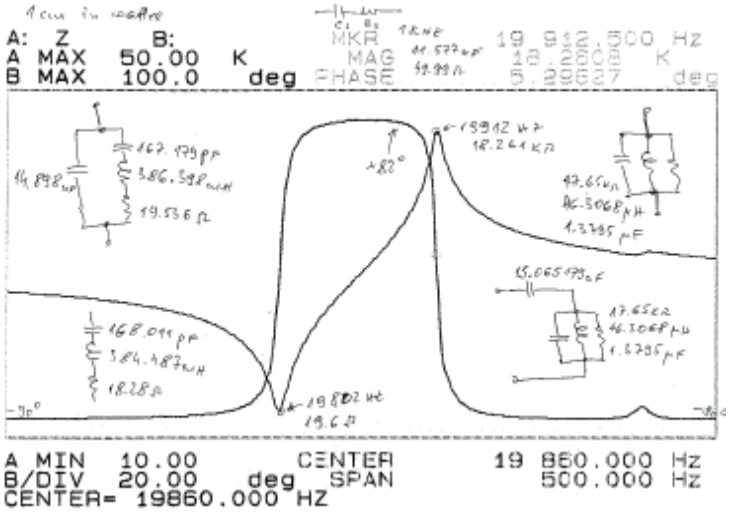

Fig. 15.3 Water-loaded Converter Impedance (Loading = 8.33%)

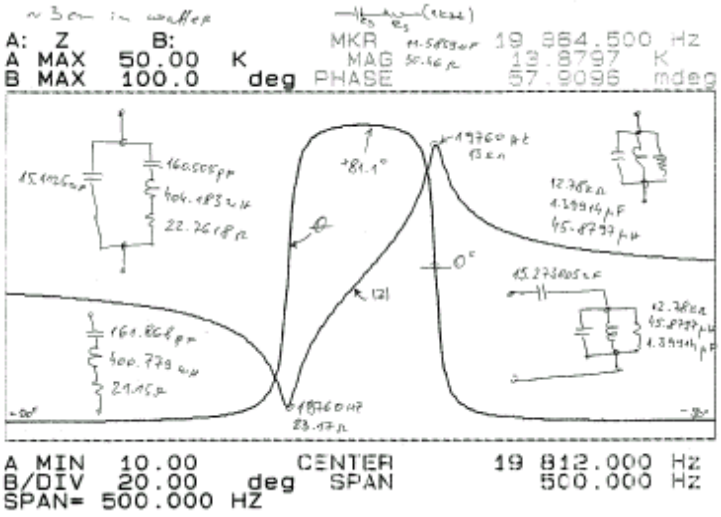

Fig. 15.4 Water-loaded Converter Impedance (Loading = 25%)

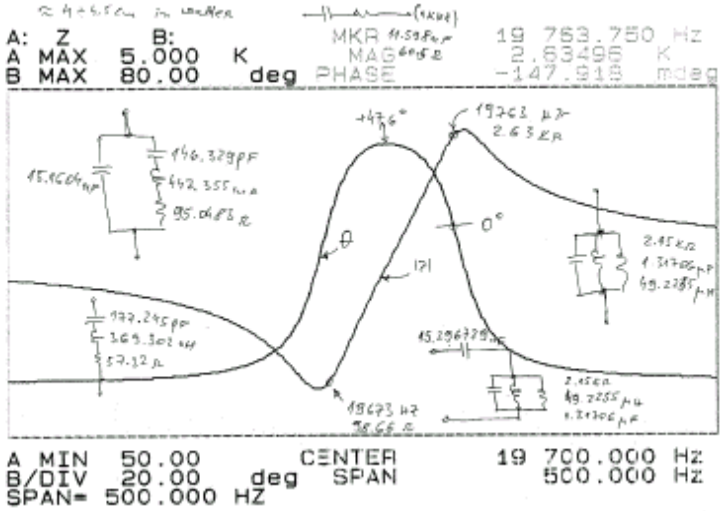

Fig. 15.5 Water-loaded Converter Impedance (Loading = 36%)

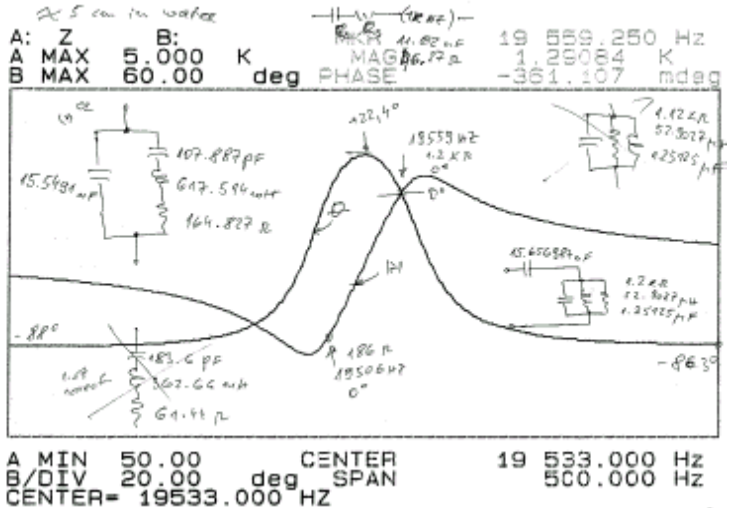

Fig. 15.6 Water-loaded Converter Impedance (Loading = 42%)

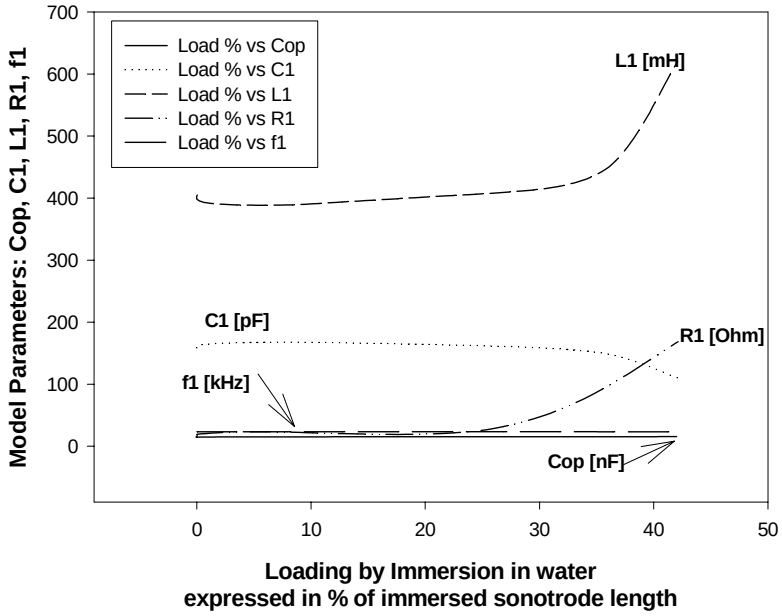

Fig. 16.1 Series Resonance, Model Parameters from T 1.4.1 vs Load %

Piezoelectric Converter Impedance Parameters
In Parallel Resonance (CV-154)

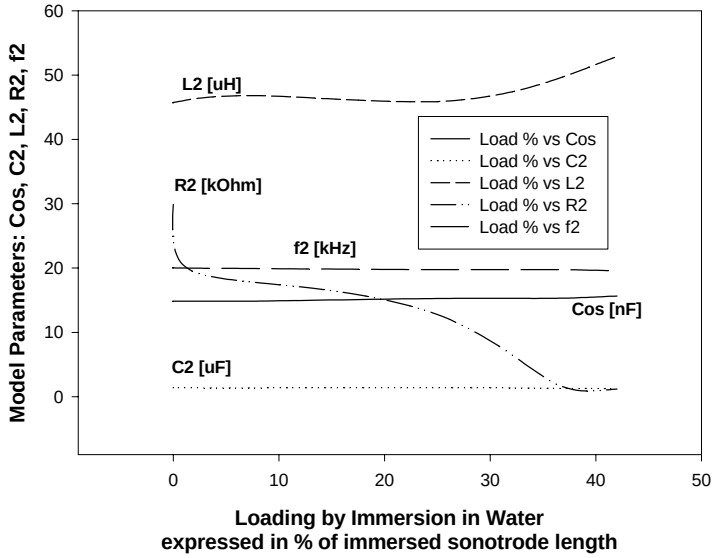

Fig. 16.2 Model Parameters from T 1.4.2 vs Load %

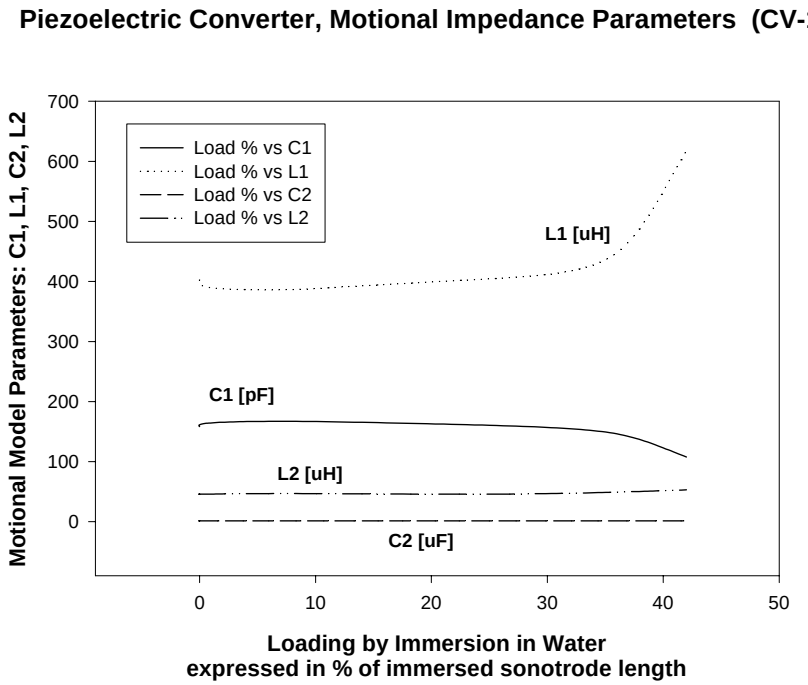

Fig. 16.3 Motional Model Parameters from T 1.4.1 & T 4.1.2 vs Load %

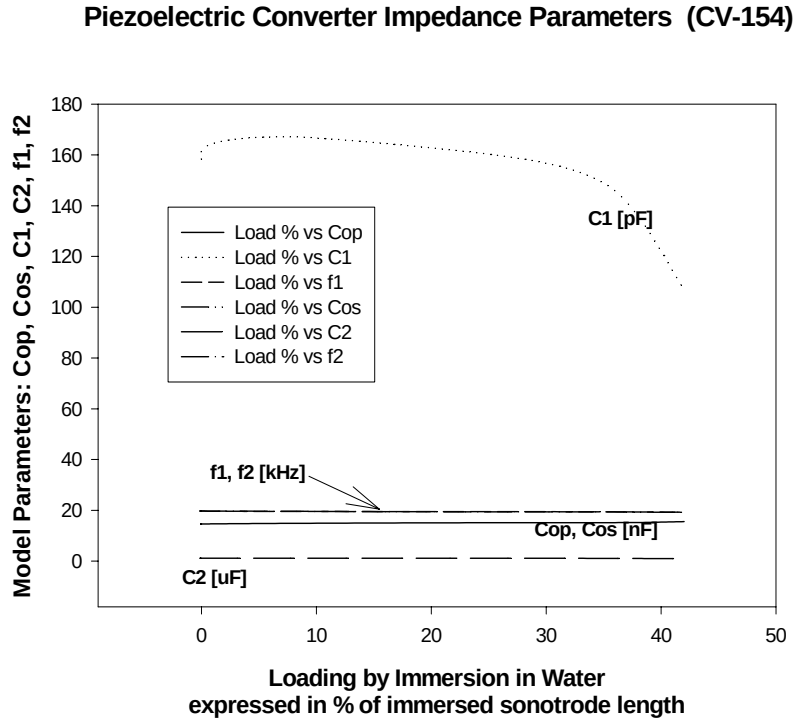

Fig. 16.4 Capacitive Parameters from T 1.4.1 & T 1.4.2 vs Load %

For the regular and acceptable loading interval in this example (and generally) is taken the situation when $\mathbf{f_1}$ and $\mathbf{f_2}$ and mechanical coupling factor $\mathbf{k}$ (from T 1.4.3) under loading are remaining very stable (almost constant), and when electrical

complex impedance-phase-angle between $\mathbf{f_1}$ and $\mathbf{f_2}$ remains positive. We can also see from Figs. 16.1 – 16.6 that the most-stable model parameters (vs Water-Load) are capacitances **Cop** and **Cos**.

Converter loading would become unacceptably too high (or start going to overloading) when $\mathbf{f_1}$, $\mathbf{f_2}$, **Cop**, **Cos** and mechanical coupling factor **k** start changing drastically (irregularly and in a non-linear fashion), compared to values under low and moderate loading.

Motional capacitance and inductance C_2 and L_2 are also sufficiently stable parameters (vs Water-Load) in comparison with Cop and Cos, but motional capacitance and inductance C_1 and L_1 are obviously much less stable (vs Water-Load). We can also see that resistive motional model-parameters R_1 and R_2 are behaving very much non-linear in the function of water-loading.

The reason of relative "instability" of motional parameters C_1 and L_1 is in the character of a loading process associated to series and/or parallel resonance, or saying differently, the loading interval of a converter operating in parallel resonance is much wider (and acoustically much different) than the loading interval of a converter operating in series resonance. From mechanical quality factors changes in the function of water loading (Fig. 16.5) we can conclude that for low and moderate loads, it is more convenient to operate converter in parallel resonance (since $Q_{m2} > Q_{m1}$), and for heavy mechanical-load situations, series resonance becomes more favorable operating regime (since $Q_{m1} > Q_{m2}$).

This example will only serve to initiate possible ideas and conclusions regarding future and more rigorous analyses regarding power conversion in piezoelectric converters. For instance, we can conclude that certain converter parameters are remaining almost unchanged under load and use them in realizing converter reactive (inductive) compensation, optimal power transfer, resonant frequency control, choice of series or parallel resonance, etc.

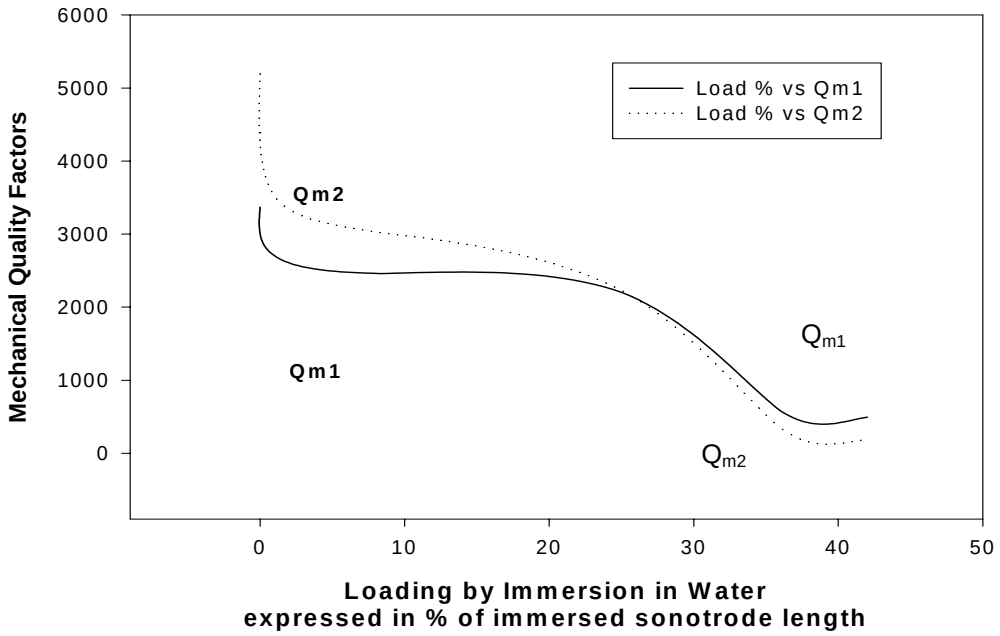

Fig. 16.5 Mechanical Quality Factors from T 1.4.1 & T 1.4.2 vs Load %

Characteristic Mechanical Impedances (see eqs. (1.4) and T 1.2, Fig. 16.6), are also interesting for qualification of a piezoelectric converter loading process. For instance, on the Fig. 16.6 we can find that Characteristic Mechanical Impedance in parallel resonance, Z_{cm2}, remains relatively stable (constant) for wide loading interval that is not the case with Characteristic Mechanical Impedance of series resonance, Z_{cm1}. This is only confirming that the nature of piezoelectric converter loading is very much different between converter operating in series and parallel resonance.

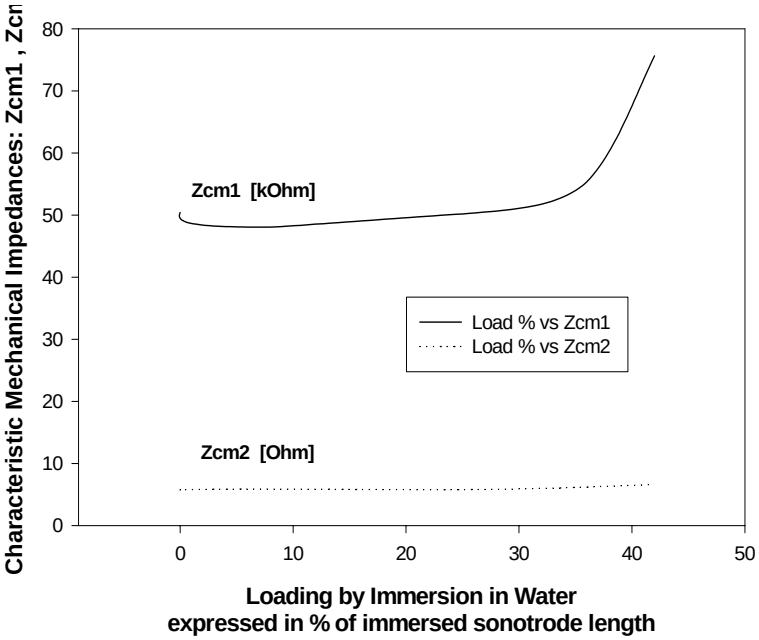

Fig. 16.6 Characteristic Mechanical Impedances from T 1.4.1 & T 1.4.2 vs Load %

3.3 Evolution of Model Parameters When Connecting Boosters and Sonotrodes

Here are pictures of typical converter-booster-sonotrode configurations.

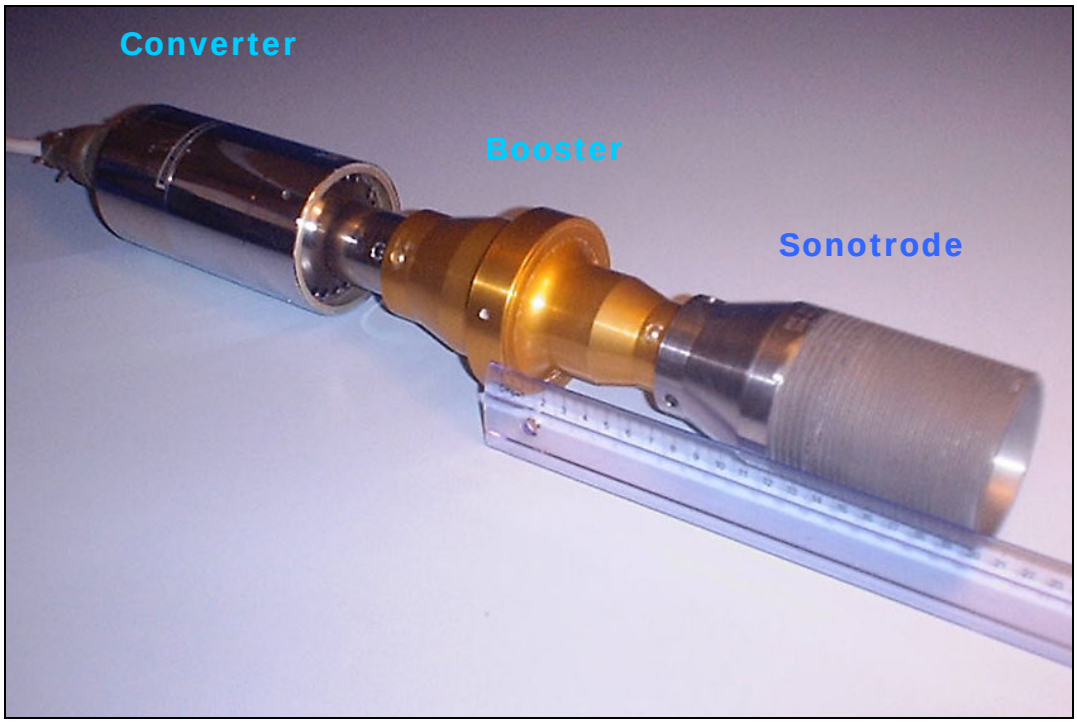

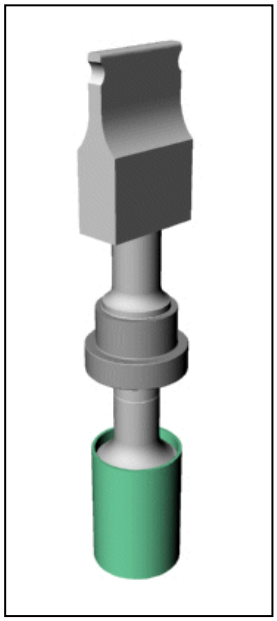

Different Boosters and Sonotrodes

In literature, it is habitual to find that adding boosters and sonotrodes to a converter is addressed as the case of converter loading. Here we can simply name the same situation as: “assembling” a complex transducer structure (see Figs. 8, 9, 10). By adding new resonant elements to a converter we are simply creating a chain of mechanical filters (or chain of strongly coupled resonators), where every new resonant element is contributing by increasing the total mechanical quality factor of the complex transducer structure (if all resonant elements are mutually tuned to operate in the same frequency range). This fact is also supported by the measurement results presented in T 1.5.1 – T 1.5.4, given below.

We should also make the difference between converters low frequency (1 kHz), input, static, clamped capacitance (C_{inp}.), and model parameters C_{op} and C_{os}, valid (or fitted) for certain high frequency resonant mode (for an isolated couple of resonances in f_1 and f_2). Usually, the low frequency (1 kHz) input capacitance of a converter will always stay the same (constant), regardless how many boosters and sonotrodes we attach to the same converter, but particular model parameters C_{op} and C_{os} would increase significantly when adding boosters and sonotrodes to a converter (of course we should add only compatible boosters and sonotrodes, operating in the same frequency range as the basic converter). If there is a case of a single converter (without attached boosters and sonotrodes), its low frequency input capacitance would be approximately equal to model parameter clamped capacitances, C_{inp}.(1kHz) $\leq C_{os} \cong C_{op} + C_1$, but when we start attaching boosters and sonotrodes to it, Cop and Cos would start increasing significantly (with every added booster or horn), comparing them to the low frequency input capacitance (C_{inp}. at 1 kHz) that will not change.

For the same example as already introduced by T 1.4.1, T 1.4.2 and Figs. 15.1 – 16.6, which presents the combination of: Conics & Materials converter (CV-154) + Titanium Booster (1:1) + Bell Sonotrode, we can trace (in no-load conditions) the changes of C_{op} and C_{os}, starting from the situation when (**1°**) there is only the single converter (CV-154), Fig. 17.1, then (**2°**) Converter + Booster, Fig. 17.2, and finally (**3°**) Converter + Booster + Bell-Sonotrode (Fig. 15.1). The measurement data for cases (**1°**), (**2°**) and (**3°**) are summarized in the tables T 1.5.1 and T 1.5.2.

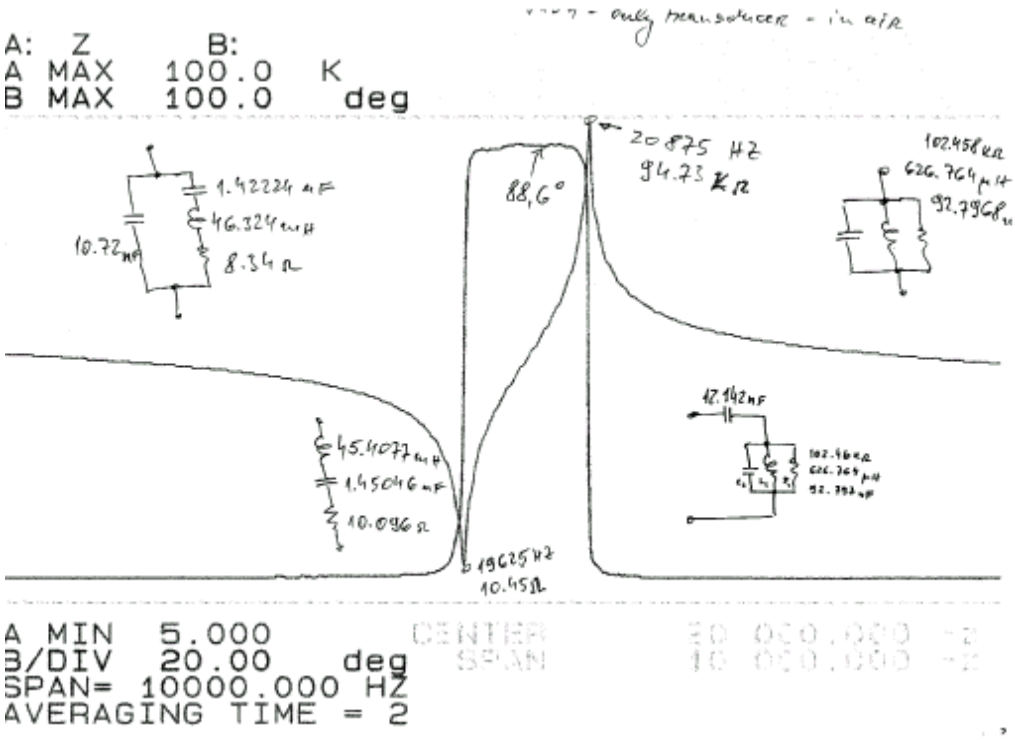

Fig. 17.1 Non-loaded Converter Impedance (single CV-154)

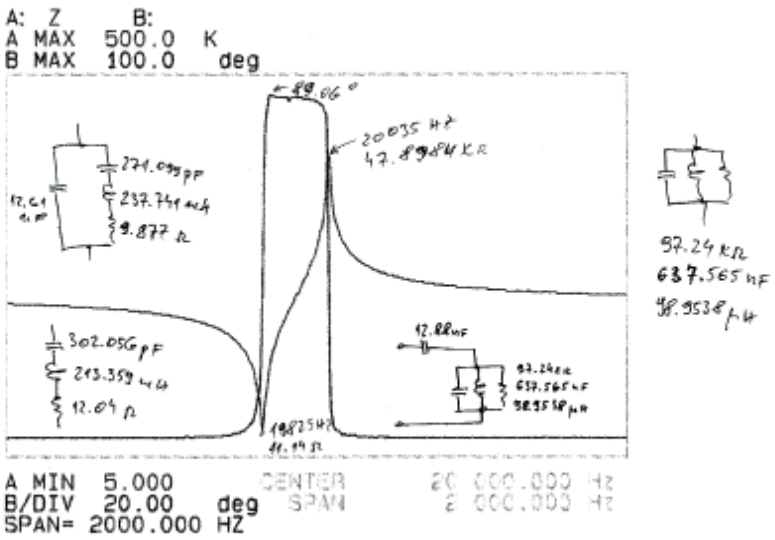

Fig. 17.2 Non-loaded Converter Impedance (CV-154 + Booster)

It is important to notice that if we create a chain of ultrasonic resonators connected axially to each other, such as: converter + booster + sonotrode(1) + sonotrode(2) +… the resulting impedance-phase characteristic, after adding every new element, will become more and more narrow and sharp, making the difference between parallel and series resonance/s gradually smaller, and creating gradually higher mechanical

quality factors, as presented on the Fig. 17.3. The best frequency matching criteria in such situations (between all resonators in the chain) is to keep the central frequency (a middle point between any couple of series and parallel resonant frequency), $\mathbf{f_0 \approx 0.5(f_{11} + f_{21}) \approx 0.5(f_{12} + f_{22}) \approx 0.5(f_{13} + f_{23}) \approx Constant.}$ approximately constant. The resonant frequency control (PLL) also becomes gradually more and more difficult because the difference between parallel and series resonant frequency becomes increasingly smaller and mechanical quality factors are significantly increasing.

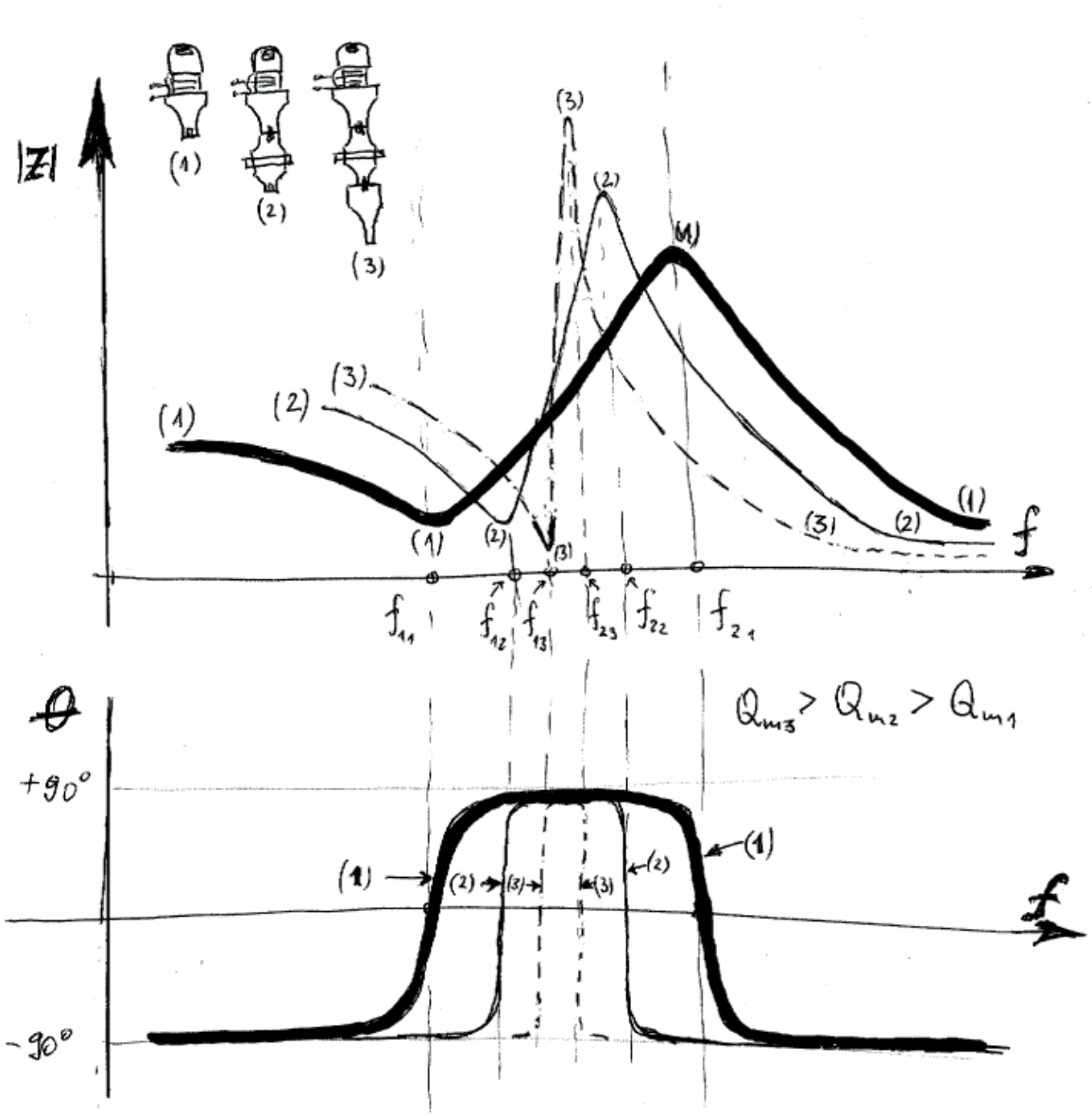

$$\mathbf{f_0 \approx 0.5(f_{11} + f_{21}) \approx 0.5(f_{12} + f_{22}) \approx 0.5(f_{13} + f_{23}),}$$
$$\mathbf{f_{21} - f_{11} > f_{22} - f_{12} > f_{23} - f_{13},\ Q_{m3} > Q_{m2} > Q_{m1}}$$

Fig. 17.3 Impedance Evolution of Non-loaded Converter
(1)- only converter, (2)- converter + booster,
(3)- converter + booster + sonotrode

Generally (see the picture below, Fig. 17.3-1), in ultrasonic engineering, depending of chosen resonant operating regime, we can make frequency-matching between certain converter and sonotrode taking as an objective that new configuration (converter-sonotrode) would operate either in series $|\mathbf{Z}_1|$, $\mathbf{f}_1$, or in parallel $|\mathbf{Z}_2|$, $\mathbf{f}_2$ resonant frequency of the single converter $|\mathbf{Z}|$, or as the optimal-case scenario between series and parallel resonant frequency (case $|\mathbf{Z}_3|$) , as already presented on Fig. 17.3.

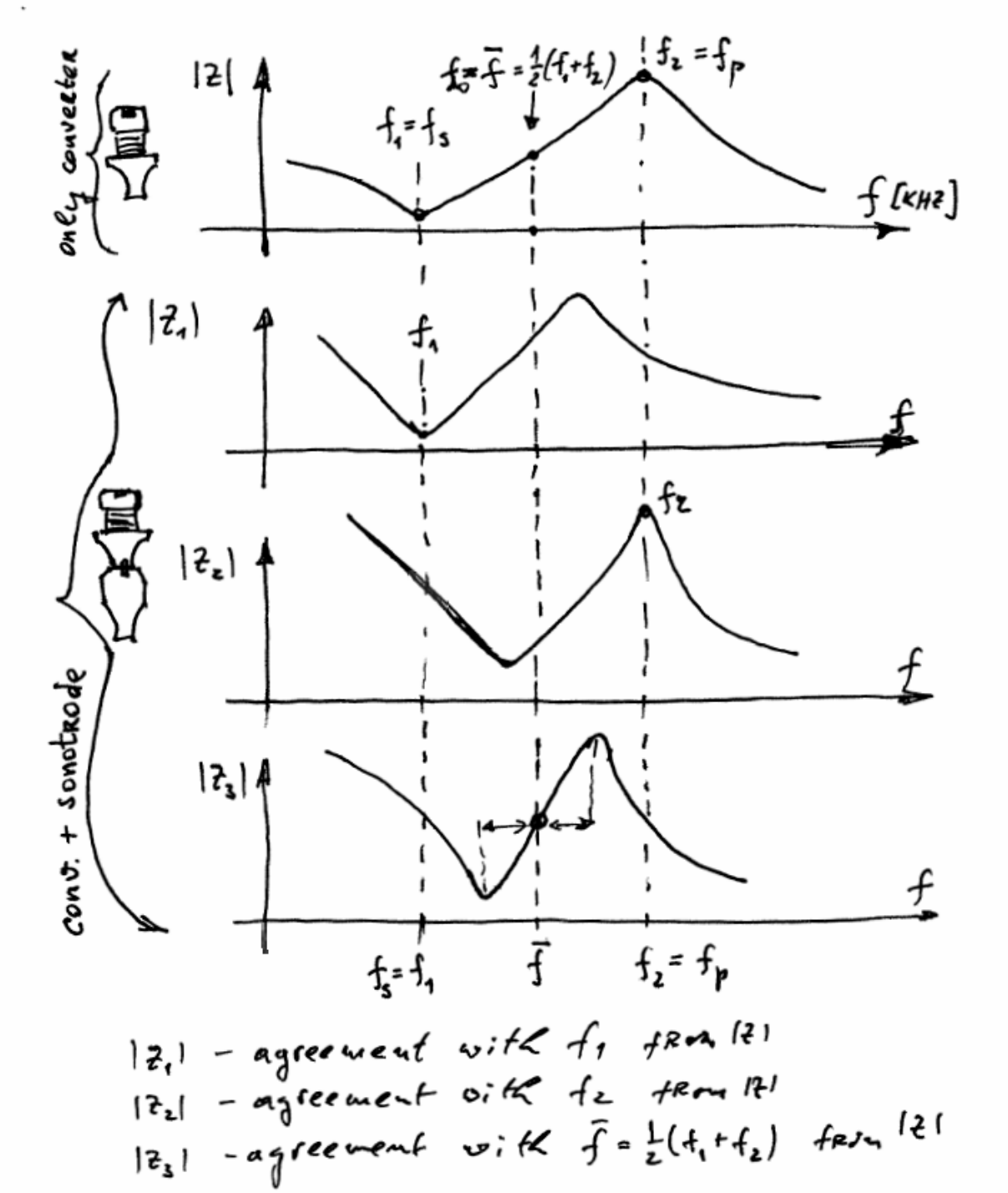

Fig. 17.3-1 Different possibilities for converter-sonotrode frequency-matching

T 1.5.1	Piezoelectric Converter Impedance Parameters in Series Resonance (CV-154…)							
No-Load C(1kHz) =11.12nF	C_{op} [nF]	C_1 [pF]	L_1 [mH]	R_1 [Ω]	f_1 [kHz]	Q_{m1} [1]	Δf [Hz]	$\sqrt{L_1/C_1}$ [kΩ] equat. (1.4)
(1°)	10.72	1422.24	46.324	8.34	19.625	684	1250	5.7071
(2°)	12.61	271.099	237.741	9.877	19.825	2998	210	29.6134
(3°)	14.6487	158.360	402.506	14.960	19.934	3370	108	50.415

T 1.5.2	Piezoelectric Converter Impedance Parameters in Parallel Resonance (CV-154…)							
No-Load C(1kHz) =11.12nF	C_{os} [nF]	C_2 [μF]	L_2 [μH]	R_2 [kΩ]	f_2 [kHz]	Q_{m2} [1]	Δf [Hz]	$\sqrt{L_2/C_2}$ [Ω] equat. (1.4)
(1°)	12.142	0.092797	626.764	102.46	20.875	1247	1250	82.1836
(2°)	12.88	0.637556	98.9538	97.24	20.035	7805	210	12.4582
(3°)	14.80706	1.38004	45.6939	29.880	20.042	5193	108	5.7539

From results in T 1.5.1 and T 1.5.2 we can easily calculate that (in this specific configuration; -converter CV-154) C_{op} is increasing for 31% and C_{os} is increasing for 19.8% (comparing single converter and Converter+Booster+Bell-Horn). Of course, C_{op} and C_{os} will not endlessly increase if we continue adding boosters and sonotrodes to a converter (the experimentally known limit seems to be less than +50%). For the same example we can also see that C_1 is decreasing, L_1 increasing, Z_{cm1} increasing, C_2 increasing, L_2 decreasing, Z_{cm2} decreasing, and that in almost all cases mechanical quality factors are increasing (while difference between parallel and series resonant frequencies is decreasing, also when comparing single converter and Converter+Booster+Bell-Horn). The input, low frequency, clamped (and static) capacitance of the same single converter (CV-154) is C_{inp}.(1kHz) = 11.12 nF, and it is not changing when we add Booster + Bell-Horn to the converter.

The above-described situation (regarding mainstream tendency of model parameters evolution) is typical and generally valid for all complex converter-booster-sonotrode structures. For instance, if we again take Branson 502/932R converter (data for single converter are given in T 1.1, T 1.2, Figs. 12 & 13) and summarize the same situation as already presented in T 1.5.1 and T 1.5.2 (starting from single converter (**1°**), then Converter + Booster (**2°**), and finally Converter + Booster + Large Sonotrode (**3°**)), we will get results presented in T 1.5.3 and T 1.5.4 (which are qualitatively equal or similar to results from T 1.5.1 and T 1.5.2).

T 1.5.3	Piezoelectric Converter Impedance Parameters in Series Resonance (502/932R…)							
No-Load C(1kHz) =19.55nF	C_{op} [nF]	C_1 [pF]	L_1 [mH]	R_1 [Ω]	f_1 [kHz]	Q_{m1} [1]	Δf [Hz]	$\sqrt{L_1/C_1}$ [kΩ] equat. (1.4)
(1°)	18.1	4046	17.534	4.6	18.900	454	2012	2.0817
(2°)	26.6025	958.442	66.0934	4.724	20.000	1758	350	8.304
(3°)	26.5929	63.8892	981.240	34.4779	20.101	3594	24	123.9291

T 1.5.4	Piezoelectric Converter Impedance Parameters in Parallel Resonance (502/932…)							
No-Load C(1kHz) =19.55nF	C_{os} [nF]	C_2 [μF]	L_2 [μH]	R_2 [kΩ]	f_2 [kHz]	Q_{m2} [1]	Δf [Hz]	$\sqrt{\frac{L_2}{C_2}}$ [Ω] equat. (1.4)
(1°)	22.05	0.10153	570.50	94.20	20.912	1257	2012	80.77
(2°)	27.56094	0.82906	73.7318	29.2549	20.350	3102	350	9.430
(3°)	26.65678	16.8820	3.70444	5.68529	20.125	12137	24	0.468437

In reality, looks logical that the low frequency input capacitance C_{inp}.(1 kHz), and model-parameter capacitance C_{os} should always stay constant, mutually equal, static capacitance of a converter. The reason why we are getting the difference (between C_{inp}. and C_{os}), when making impedance measurements with Network Impedance Analyzer, is just in fact that we measure C_{inp} in one discrete frequency point (at 1 kHz), and C_{os} is found after best curve fitting, respecting piezoelectric converter models, on a limited frequency interval that captures only the close vicinity of a series and parallel resonant frequency couple f_1 and f_2. Since we give the limited data-input to the Network Impedance Analyzer (taking into account the frequency interval only a bit larger than $\Delta f = f_2 - f_1$), neglecting enormously large interval of impedance values between very low frequency (say 1 kHz) and first resonant mode (and also neglecting frequencies higher than f_2), results of best curve fitting are creating the value of C_{os} that seems different (higher) than C_{inp}. Since in resonant operating conditions we usually care only about converter characteristics in the close vicinity of certain resonance, it is obvious that we need to know the model parameters C_{os} and C_{op} valid for the same operating frequency interval. This is also confirming that lumped parameters models, we usually use for describing piezoelectric impedance, are only locally valid (for a close vicinity of a well-isolated, single resonant mode). In ultrasonic applications, when making inductive converter compensation (to eliminate C_{os} or C_{op}), we can often notice that calculated inductance in reality is different than the value we really need to apply (to make converter to become resistive load), because in converter resonant area (for frequencies lower than f_1 and higher than f_2), effective converter (total input) capacitance is very mach frequency-dependant. For instance, in ultrasonic cleaning applications, when many single converters are operating as a group (in parallel connection), series compensating-inductance is often significantly lower than calculated-value based on C_{inp}. or C_{os} (because cleaning converters, as a group, usually operate in the area just below series resonance, where effective converters capacitance is significantly higher than C_{inp}.(1 kHz)). In order to graphically visualize this situation (regarding capacitive and inductive character of a piezoelectric converter vs. frequency), on the Fig. 18 are qualitatively improvised equivalent converter capacitance and inductance in the area of a selected resonant mode (only showing their typical tendency, without any precise and quantitative significance). It is also known that single piezoelectric converters can easily be forced to operate high power on frequencies lower than f_1, since in this area converter has significantly high effective capacitance (higher than C_{inp}.(1 kHz)), but the same is not valid for frequency area higher than f_2, since in that frequency interval converter has relatively low effective capacitance (much lower than C_{inp}.(1 kHz), which is increasing slowly and exponentially towards C_{inp}.). Obviously we can conclude that sufficiently high effective converter capacitance is enabling converter to accumulate proportionally high potential energy, necessary for continuous and high power oscillating regime. Analogous logic (regarding inductive

potential energy accumulation) should be applicable to converters operation below f_2 (between f_1 and f_2). Differently formulating the same conclusion we can say that natural and highly efficient converters oscillating regimes (for producing high power) are in frequency areas left from f_2 (or between f_1 and f_2: $\mathbf{L_{MAX.}}$), and left from f_1 (towards lower frequencies: $\mathbf{C_{MAX.}}$). The same situation (regarding best operating-power frequency areas) would be only slightly changed when we make piezoelectric converter inductive compensation/s, but again it will be valid that best operating areas will stay below converter's parallel resonance, between series and parallel resonance, and below series resonance, in the frequency areas where converter's effective capacitance and/or effective inductance are significantly elevated.

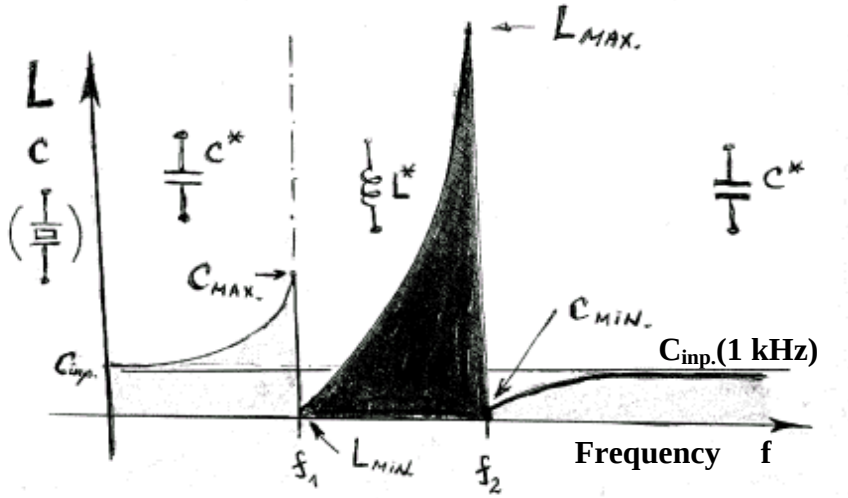

$$\mathbf{f_1 \cong \frac{1}{2\pi\sqrt{L_{MIN}C_{MAX}}}\ ,\ f_2 \cong \frac{1}{2\pi\sqrt{L_{MAX}C_{MIN}}}}$$

Fig. 18 Piezoelectric Converter Effective Capacitance & Inductance

In order to make a piezoelectric converter operating as a resistive load (to produce real power), we should know the dominant static converter capacitance and compensate it by adding certain series or parallel inductance that will neutralize converter's static capacitance. Here we shall explain the procedure how we can find dominant, static converter capacitance (valid for wide frequency interval).

We know that all piezoelectric converters as electrical components (characterized in a large frequency interval) are dominantly capacitive components, except in a certain number of limited frequency intervals where converters could have inductive and/or complex impedance character (in converters resonance zones). Let us first establish the normalized impedance concept for an ideal capacitor $\mathbf{C_o}$ in order to compare it (later on) with a normalized impedance of the converter that would have the same (dominant) static capacitance (as being an ideal capacitor):

$$\mathbf{Z = \frac{1}{j\omega C_0} = \frac{1}{j2\pi fC_0} \Rightarrow |Z| = \frac{1}{2\pi fC_0}\ ,\ |Z_0| = \frac{1}{2\pi f_0 C_0} = Const.,\ f_0 = const.,}$$

$$\mathbf{\frac{|Z|}{|Z_0|} = \frac{1}{2\pi fC_0}\cdot\frac{1}{|Z_0|} = \frac{1}{2\pi f_0 C_0 |Z_0|\cdot(f/f_0)}\ (=\frac{f_0}{f})\ \Rightarrow}$$

$$\Rightarrow \mathbf{log}\left(\frac{|\mathbf{Z}|}{|\mathbf{Z_0}|}\right) = \mathbf{-log}(2\pi \mathbf{f_0 C_0 |Z_0|}) - \mathbf{log}\left(\frac{\mathbf{f}}{\mathbf{f_0}}\right),$$

$$\mathbf{Y} = \mathbf{log}\left(\frac{|\mathbf{Z}|}{|\mathbf{Z_0}|}\right),\ \mathbf{X} = \mathbf{log}\left(\frac{\mathbf{f}}{\mathbf{f_0}}\right),\ \mathbf{A} = \mathbf{-log}(2\pi \mathbf{f_0 C_0 |Z_0|}) = \overline{\mathbf{Const.}} \Rightarrow$$

$$\Rightarrow \mathbf{Y + X = A}$$

From the equation of line, $\mathbf{Y + X = A}$, we can see that normalized impedance of an ideal capacitor $\mathbf{C_o}$, $\mathbf{Y} = \mathbf{log}\left(\frac{|\mathbf{Z}|}{|\mathbf{Z_0}|}\right)$, can be presented in the function of a normalized frequency, $\mathbf{X} = \mathbf{log}\left(\frac{\mathbf{f}}{\mathbf{f_0}}\right)$, similar to the curve on the left side of Fig. 19.

If we now take a piezoelectric converter (which should have the same dominant capacitance $\mathbf{C_o}$), and using Impedance Analyzer measure its normalized impedance, $\mathbf{Y} = \mathbf{log}\left(\frac{|\mathbf{Z}|}{|\mathbf{Z_0}|}\right)$, in the function of normalized frequency, $\mathbf{X} = \mathbf{log}\left(\frac{\mathbf{f}}{\mathbf{f_0}}\right)$, (setting horizontal and vertical axes, $\mathbf{X}$ and $\mathbf{Y}$, to have logarithmic divisions), we shall get the $\mathbf{Y}$ **vs** $\mathbf{X}$ curve, as presented on the right side of Fig. 19.

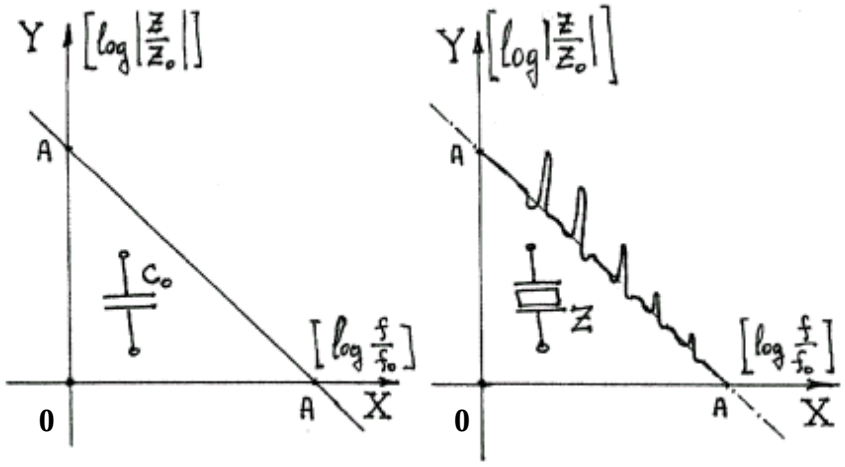

Fig. 19 Normalized Impedance of an Ideal Capacitor (left), and of a Piezoelectric Converter (right)

When using Network Impedance Analyzer, we should be able to find experimentally the value of the constant $\mathbf{A} = \mathbf{-log}(2\pi \mathbf{f_0 C_0 |Z_0|})$, by simple linear extrapolation of the normalized piezoelectric impedance curve (right side of Fig. 19), passing the middle asymptotic line that would cross the X and Y axis in two points: (0, A) and (A, 0). This way, we shall be in a position to calculate the dominant (static) converter capacitance $\mathbf{C_0}$ that should satisfy the equation:

$$\mathbf{C_0} = \frac{\mathbf{1}}{2\pi \mathbf{f_0 C_0 |Z_0|} \cdot \mathbf{10^A}} .$$

If we make the comparison between $\mathbf{C_o}$, low frequency capacitance $\mathbf{C_{inp.}}$(1 kHz) and model capacitance $\mathbf{C_{os}}$ of the same piezoelectric converter, we shall again find that all of them are only approximately equal, $\mathbf{C_o} \cong \mathbf{C_{inp.}}$(1 kHz) $\cong \mathbf{C_{os}}$. As the conclusion regarding static converter capacitances, we can say that when converter is operating on a very low frequency or in a constant driving-voltage regime, the most important should be $\mathbf{C_{inp.}}$(1 kHz), and when converter is operating in a very large frequency interval, then $\mathbf{C_o}$ becomes important static capacitance parameter. In other situations when we drive converter in a single resonance point, then $\mathbf{C_{os}}$ should be considered as the most important static capacitance.

Impedance Changes in Case of Converters Bonded to Thin-Walls Vessels

In many applications like ultrasonic cleaning and ultrasonic liquid processing, ultrasonic converters are bonded or glued to (thin walls) cleaning or reactor vessels. For the purpose of electrical and mechanical impedance matching and optimal power conversion (from an ultrasonic power supply, or ultrasonic generator to ultrasonic converters) it is important to know the range of possible impedance changes, comparing the impedance-characteristics of non-loaded (free in air) converters, and characteristics of the same converters after bonding and after water loading. Generally valid situation (see Fig. 20) is that converter after bonding or gluing to a cleaning vessel has a bit lower series and parallel resonant frequencies (than non-loaded converter), and that every additional loading is reducing converter's maximal (parallel-resonance) impedance, and increasing minimal (series-resonance) impedance. Fig. 20 presents (qualitatively) a typical loading situation regarding impedance changes, when single piezoelectric converter is: in the case (0), non-loaded and non-bonded, in air; -the case (1), when the same converter is bonded to an empty and thin-walls vessel or ultrasonic cleaning tank; -and case (2), when the same vessel (or ultrasonic cleaning tank) is full with water. There are many bonding and gluing techniques, and many different adhesives for fixing piezoelectric converters to ultrasonic cleaning vessels or liquid processing reactors. Depending on bonding technology and used adhesives, piezoelectric converter would change its impedance parameters in the frames given numerically in T 1.6 (of course, all data in T 1.6 are presenting approximate values, typical for ultrasonic cleaning converters).

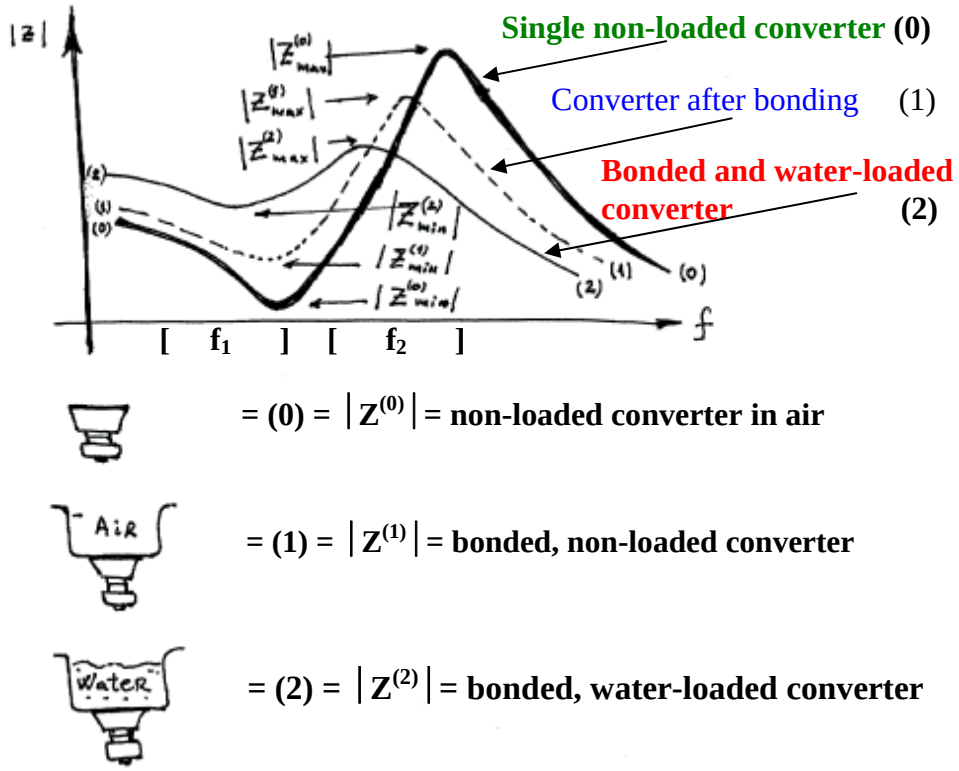

Fig. 20 Piezoelectric Converter Impedance after Bonding & Water Loading

T 1.6 Typical impedance limits in cases of bonding & water loading (see Fig. 20)

$\lvert Z_{min}\rvert$, $[f_1]$	$\lvert Z_{max}\rvert$, $[f_2]$
$\left\lvert \frac{Z^{(1)}_{min}}{Z^{(0)}_{min}} \right\rvert \in (5, 15)$, $\left\lvert \frac{f_1^{(1)}}{f_1^{(0)}} \right\rvert \approx 0.96$	$\left\lvert \frac{Z^{(0)}_{max}}{Z^{(1)}_{max}} \right\rvert \in (4, 9)$, $\left\lvert \frac{f_2^{(1)}}{f_2^{(0)}} \right\rvert \approx 0.94$
$Z^{(0)}_{min} = 15\,\Omega \Rightarrow 75\,\Omega \le Z^{(1)}_{min} \le 225\,\Omega$	$Z^{(0)}_{max} = 60\,k\,\Omega \Rightarrow 6.67k\Omega \le Z^{(1)}_{max} \le 15\,k\Omega$
$\left\lvert \frac{Z^{(2)}_{min}}{Z^{(1)}_{min}} \right\rvert \in (2, 7)$, $\left\lvert \frac{f_1^{(2)}}{f_1^{(1)}} \right\rvert \approx (0.96, 0.99)$	$\left\lvert \frac{Z^{(1)}_{max}}{Z^{(2)}_{max}} \right\rvert \in (2, 6)$, $\left\lvert \frac{f_2^{(2)}}{f_2^{(1)}} \right\rvert \approx (0.98, 1.05)$
$Z^{(1)}_{min} = 150\,\Omega \Rightarrow 300\Omega \le Z^{(2)}_{min} \le 1050\Omega$	$Z^{(1)}_{max} = 10\,k\,\Omega \Rightarrow 1.67k\Omega \le Z^{(2)}_{max} \le 5\,k\Omega$
$10 \le \left\lvert \frac{Z^{(2)}_{min}}{Z^{(0)}_{min}} \right\rvert \le 100$, $\left\lvert \frac{f_1^{(2)}}{f_1^{(0)}} \right\rvert \approx (0.92, 0.95)$	$6 \le \left\lvert \frac{Z^{(0)}_{max}}{Z^{(2)}_{max}} \right\rvert \le 60$, $\left\lvert \frac{f_2^{(2)}}{f_2^{(0)}} \right\rvert \approx (0.92, 0.99)$
if $Z^{(0)}_{min} = 15\,\Omega \Rightarrow 150\,\Omega \le Z^{(2)}_{min} \le 1500\,\Omega$	**if** $Z^{(0)}_{max} = 60\,k\,\Omega \Rightarrow 1k\Omega \le Z^{(2)}_{max} \le 10k\Omega$

Ultrasonic cleaning and liquid processing systems are usually driven by arrays of many similar converters, connected electrically in parallel, and glued to the same surface. If all converters in parallel connection are identical, or very similar to each other, we can approximately estimate the resulting impedances of certain converters group, just by dividing all impedance values valid for a single transducer (found in Fig. 20 and T 1.6) by the number of transducers in a group (like having identical resistances in parallel connection), and doing this way we shall stay in the error limit of ±10%. When we know the absolute limits of impedance variations of a converter group in parallel connection, we shall be able to design optimal power supplies for them, to calculate optimal driving current and voltages, to calculate transformer ratio for optimal load-impedance matching (to ultrasonic generator), and to implement proper power control strategy. In all other cases, when converters are mutually dissimilar, we should experimentally and by (Impedance-Phase) measurements determine equivalent impedance parameters and frequency areas of high converters efficiency.

4.0 Converter Electric Impedance Modifications and Mechanical Resonances

In this chapter we shall describe several experiments where converter electrical impedance is externally changed by adding to it in series and/or parallel connection passive electric components (adding resistances, capacitances and inductances). The resulting converter resonances are measured using electrical means (Impedance Network Analyzer), and mechanical means (mechanical vibrating platform with variable frequency, and wide-frequency-band mechanical amplitude sensor). For this situation it was chosen a very simple cylindrical, bolted, Langevin, sandwich converter (back mass: stainless steel, front mass: aluminum 7075, and 2 of PZT8 piezoceramic rings in the middle area). The choice of the converter was made to satisfy the criteria that its first resonance-couple (natural series and parallel resonance) is sufficiently isolated on the frequency axis (or that all higher harmonics are placed very far from the first resonance couple), and to have regular and typical piezoelectric impedance shape (see Fig. 1).

In many situations of practical interest, when driving piezoelectric converters, ultrasonic generators or electric power supply units are used, where different R, L and C elements are effectively placed in parallel or series connection to a converter (for the purpose of impedance and power matching, and for converter reactive impedance compensation). Consequently, it is clear that in any case converter impedance characteristics and resonant operating zones are affected by the presence of surrounding electronics (as well as by converters mechanical loading conditions). In order to establish the correlation between converter electrical and mechanical resonant zones, converter was placed (vertically or axially) on the mechanical vibrating platform, **VP** (made for measuring axial, resonant, half-wave lengths of ultrasonic sonotrodes). This way, converter was considered as a solid cylinder (rod), and it was possible to measure its half-wave mechanical resonances ($\lambda/2$ – resonant frequencies). On the opposite converter face, the wide-band (piezoelectric) displacement-sensor was placed (touching converter vertically, only in one point), in order to detect the $\lambda/2$ – axial resonances of such (composite) solid rod. The vibrating platform **VP** was equipped with variable frequency (sinusoidal signal-shape) generator and frequency meter, and this frequency (produced by **VP**) was considered as a converter mechanical frequency f_m (see Fig. 2, d)).

Electrical converter impedance was (first) externally modified (by adding different electrical components to converter's input terminals) and resulting converter (equivalent) impedance was measured with Impedance Network Analyzer, and then the same converter (including all external electrical modifications) was moved to vibration platform **VP**, and resulting mechanical $\lambda/2$ – axial-resonances were measured. This way (for a non-loaded converter) it was possible to establish relations between typically electrical resonances (measured only using electrical means), and typically mechanical resonances (measured using mechanical means). Mechanical vibrating platform **VP** (used here) was able to measure very precisely the resonant frequency f_m and to give sufficiently good information about mechanical amplitude of an oscillating $\lambda/2$ –rod, on its opposite side (in relative units from 1 to 10). When resonant $\lambda/2$-mechanical frequency was found, the amplitude sensor **S** was generating a high electrical signal.

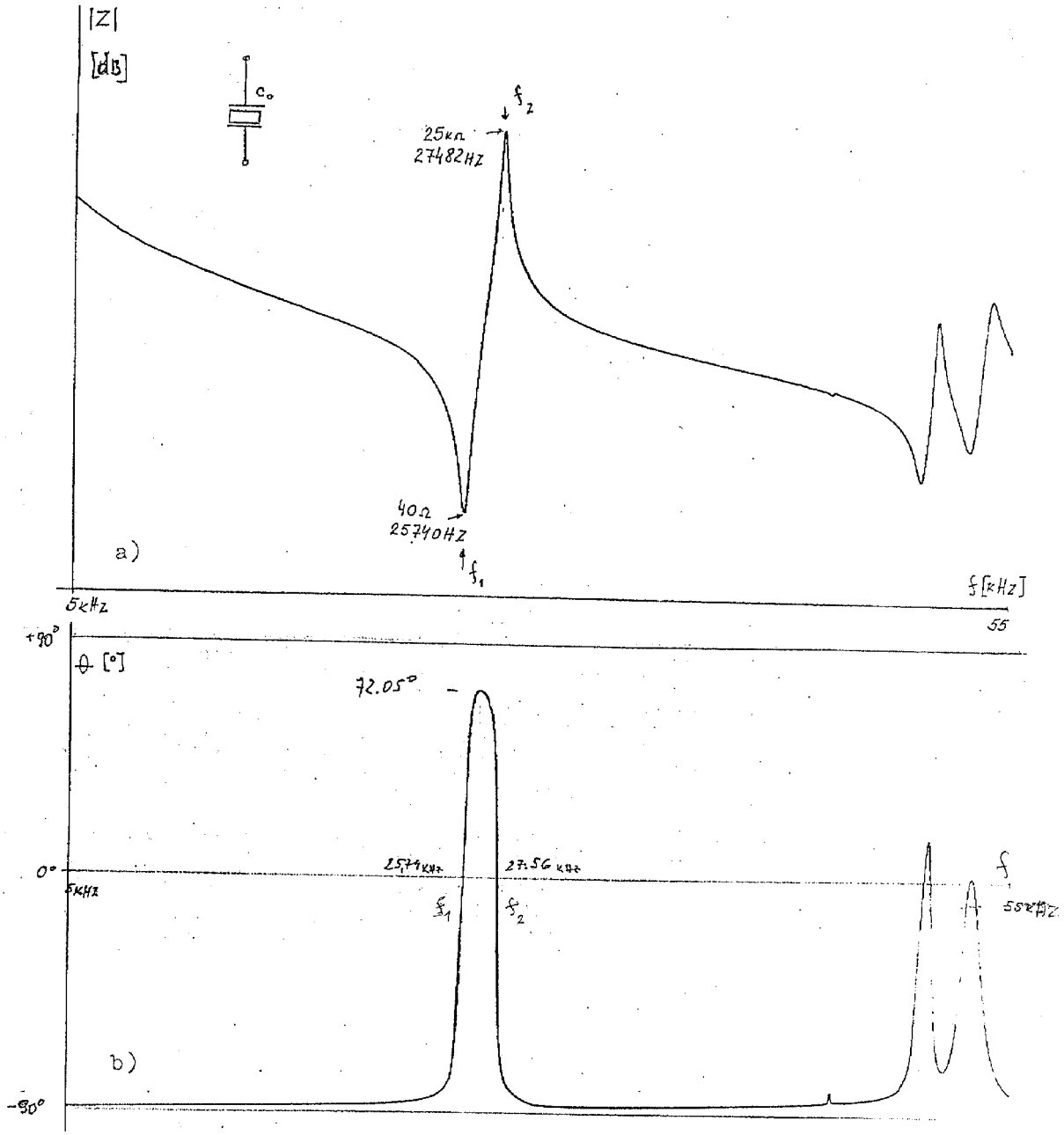

Fig. 1 Typical Non-loaded Converter Impedance-Phase Characteristics

The next, more profound benefit of such impedance modifications is to become able to compare the same converter-characteristics electrically modified (with passive electric components connected externally), and the converter characteristics under different mechanical loading situations (without any external, electrical impedance modification). This way, indirectly, we can conclude that certain types of mechanical loads are modifying converter equivalent impedance on the similar way as connecting resistance or capacitance or inductance… to the same (non-loaded) converter. Consequently, we can get a feeling about modeling of different mechanical loads (or we can give the answers to what means mechanical resistive, capacitive, inductive and/or some other complex loading, applying analogies).

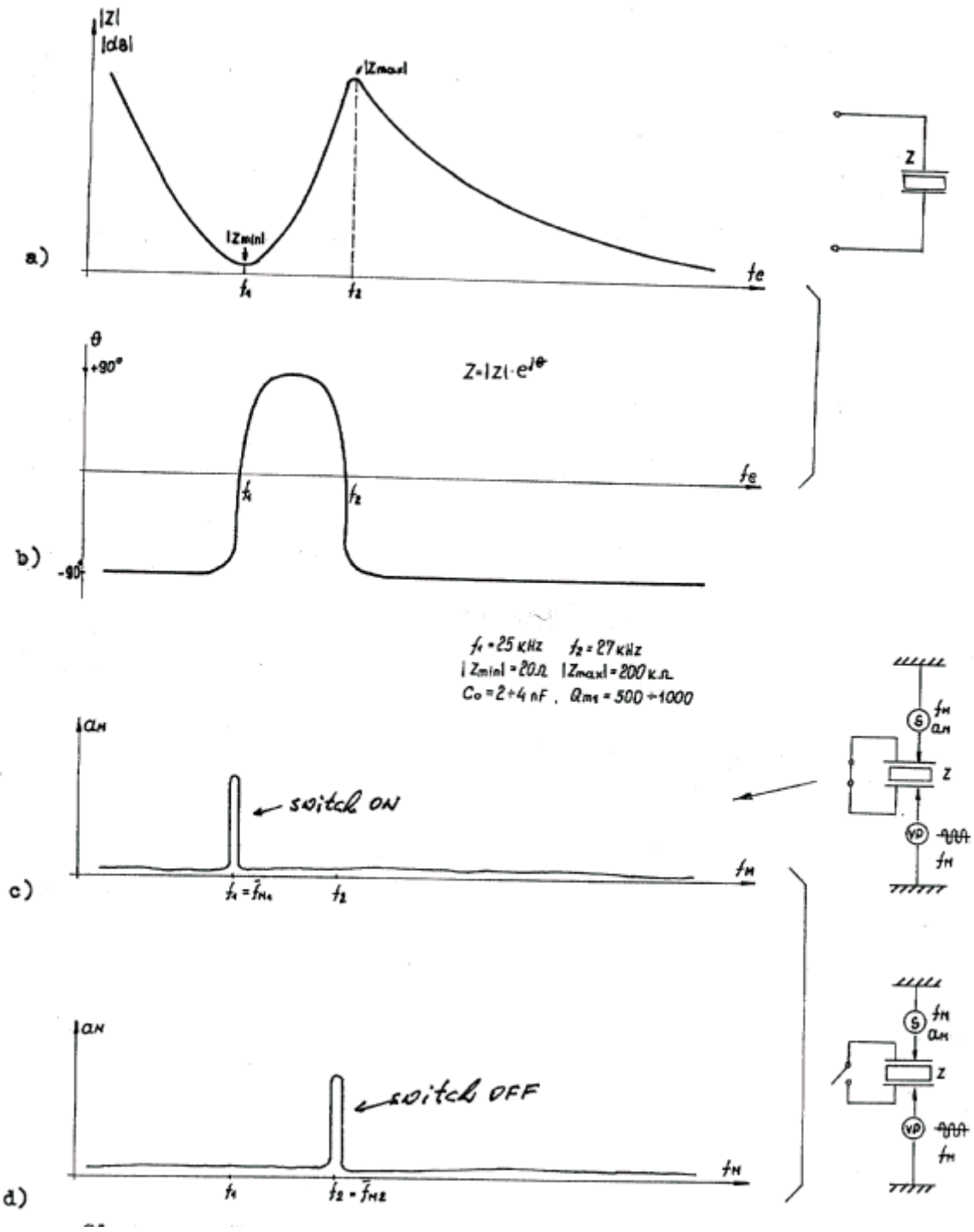

Fig. 2 Electrical and Mechanical, Non-loaded Converter Characteristics
a) & b) Typical Electric Impedance-Phase Curves
c) λ/2 – axial mechanical resonance with shortened input terminals
d) λ/2 – axial mechanical resonance with open input terminals

On the Fig. 2 are presented (in a simplified, summary form) almost the same facts found on Fig. 1 (such as electrical impedance and phase, Fig. 1, a) & b)), and two more measurements when the same converter is placed on the vibrating platform **VP** (Fig. 2, c) & d)). Fig. 2, c) presents converter mechanical amplitude and mechanical

resonant frequency when its input electrical terminals are in a short circuit: switch = ON. Fig. 2, d) presents converter mechanical amplitude and mechanical resonant frequency when its input electrical terminals are open: switch = OFF. We can immediately conclude that series electrical resonance corresponds to the high-current driven converter, when electrical driving circuit has very low internal impedance (input terminals in a short circuit), and that parallel electrical resonance corresponds to the high-voltage driven converter, when electrical driving circuit has very high internal impedance (input terminals open).

We can also (indirectly) conclude that if a converter should dominantly operate under heavy mechanical loading, it should be operated in its series resonance, and if a converter should dominantly operate under low and moderate mechanical loading conditions, it should be operated in its parallel resonance.

We can also find out that electrical and mechanical series and/or parallel resonance/s are (approximately) in the same frequency zone/s (almost mutually equal for high mechanical quality-factor converters).

Since parallel resonance is higher than series resonance, and because, when making mechanical resonance measurements, we do not change converter's axial length (it is always the same converter), it looks that a short-circuited converter has lower effective (or resulting) sound speed than open-terminals converter (because in the case of here described mechanical measurements, using **VP**, we treat converter only as a solid, elastic rod).

Let us now generalize the measurements presented on the Fig. 2, by connecting in parallel to the same converter input-terminals a variable resistance ($R_p \in 10\ \Omega$ until 500 kΩ), as shown on the Fig. 3. When parallel resistance is very high, this corresponds to open converter terminals (Fig. 2, d)), and when parallel resistance is very low, this corresponds to converter terminals in a short circuit (Fig. 2, c)). Fig. 3 presents electrical Impedance-Phase characteristics (measured by Network Impedance Analyzer) when parallel resistance is taking different values. We can easily notice (on the Fig. 3) that parallel resistance will not change series and parallel converter resonant frequencies. The much more interesting situation is to find out what is happening with mechanical resonant frequencies when we use mechanical vibrating platform **VP** (as previously explained), Fig. 4.

Fig. 4 a) & b) presents in a simplified form the same electric Impedance-Phase curves, as already seen on the Fig. 3. Fig. 4, c) is just underlining where are electrical resonant frequencies (in order to compare them with mechanical resonant frequencies), Fig. 4, d) presents mechanical resonances measured on the **VP**, and Fig.4, e) presents positions and relative amplitudes of $\lambda/2$–axial-mechanical resonances. The basic and most important conclusions relevant for Fig. 4 are practically (almost) the same as all conclusions relevant for Fig. 2.

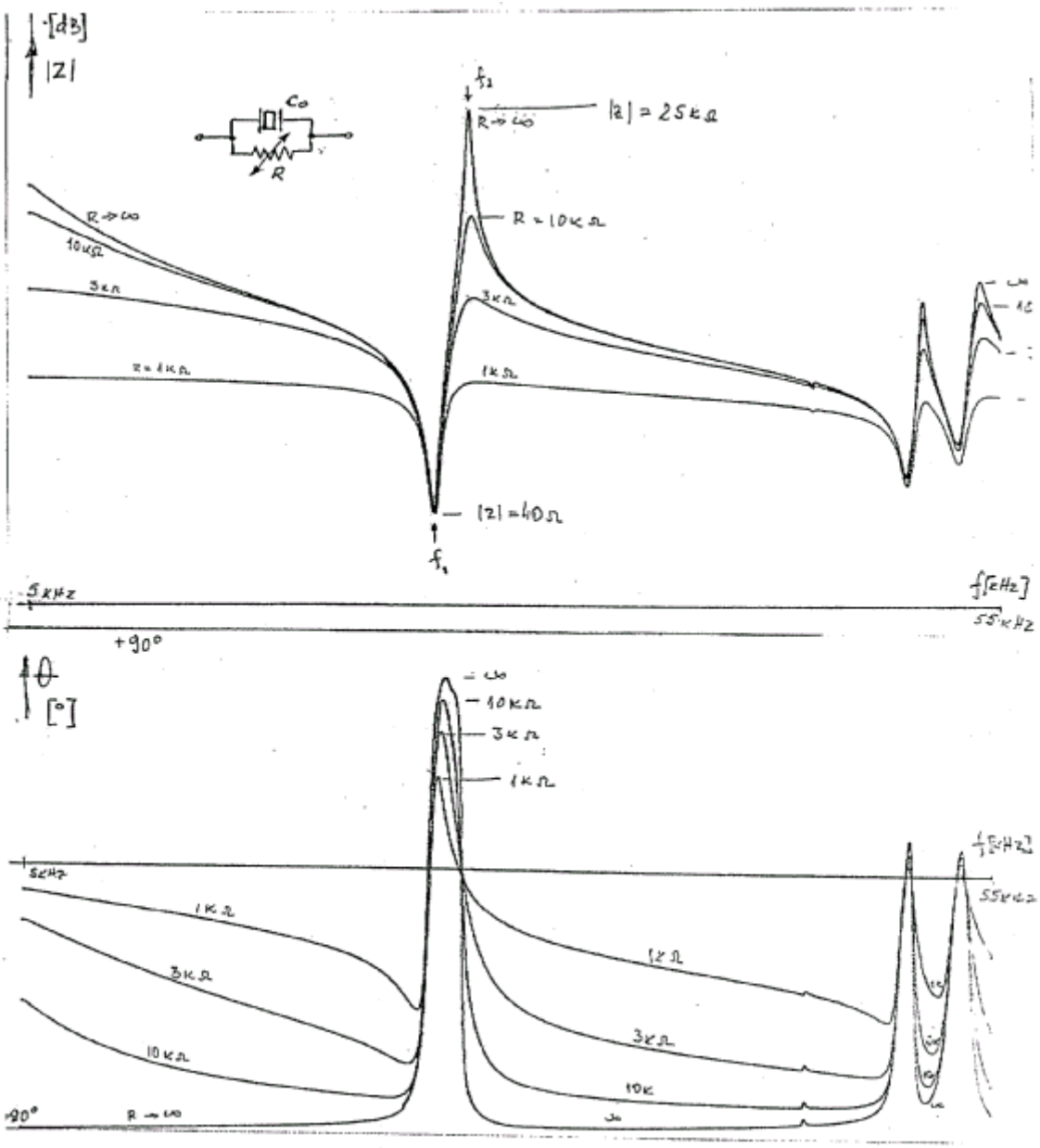

Fig. 3 Converter Impedance-Phase Characteristics with Parallel Resistance

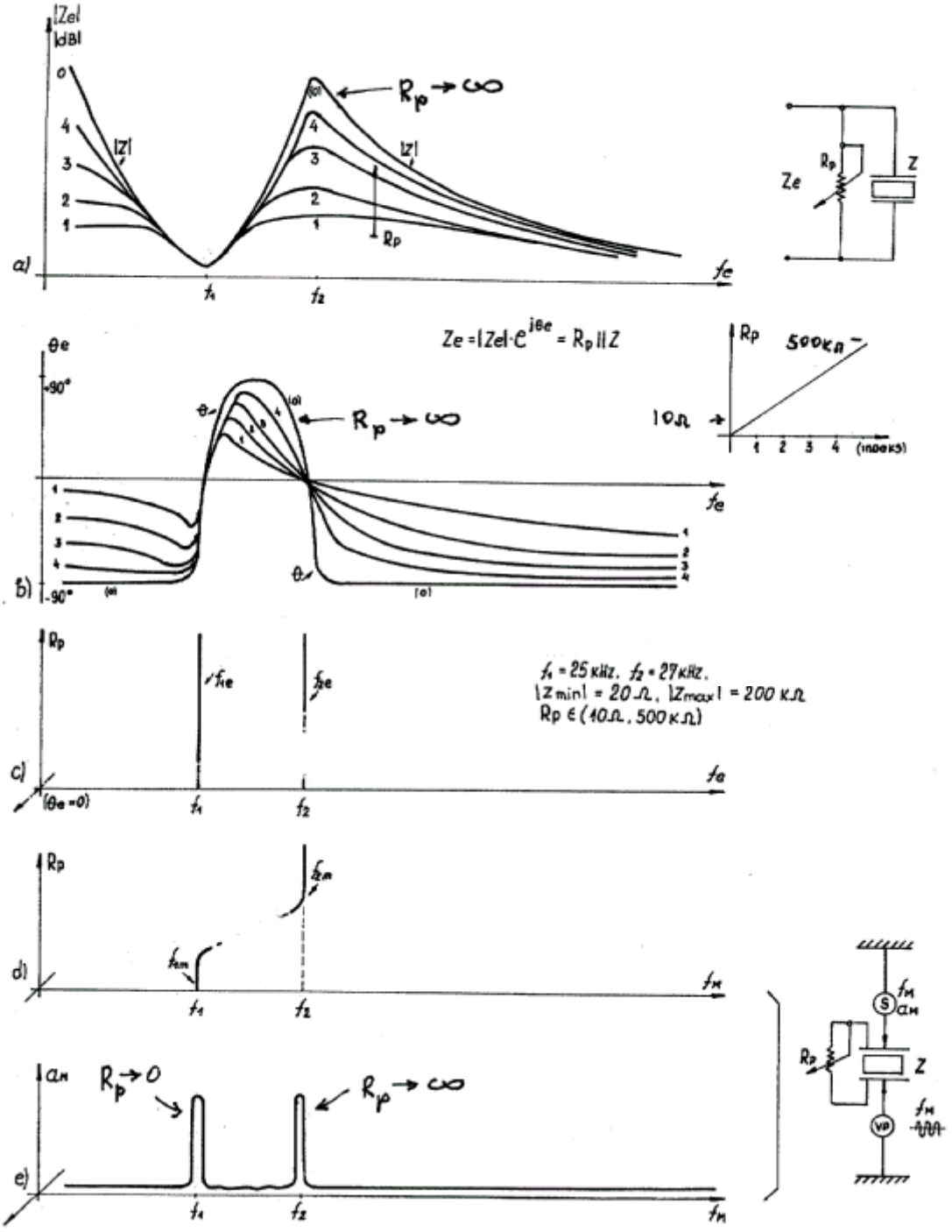

Fig. 4 Converter Characteristics with Parallel Resistance (see Fig. 3)
a) & b) Electric Impedance-Phase Curves
c) Electrical resonances
d) Mechanical resonances
e) λ/2 – axial-mechanical resonances

We can now connect variable resistance ($R_S \in 10\ \Omega$ until 100 kΩ) in series with converter input terminals, and trace the equivalent impedance changes, as presented on the Fig. 5. When series resistance is very low, this situation electrically corresponds to a free converter from the Fig. 1. If series resistance increases,

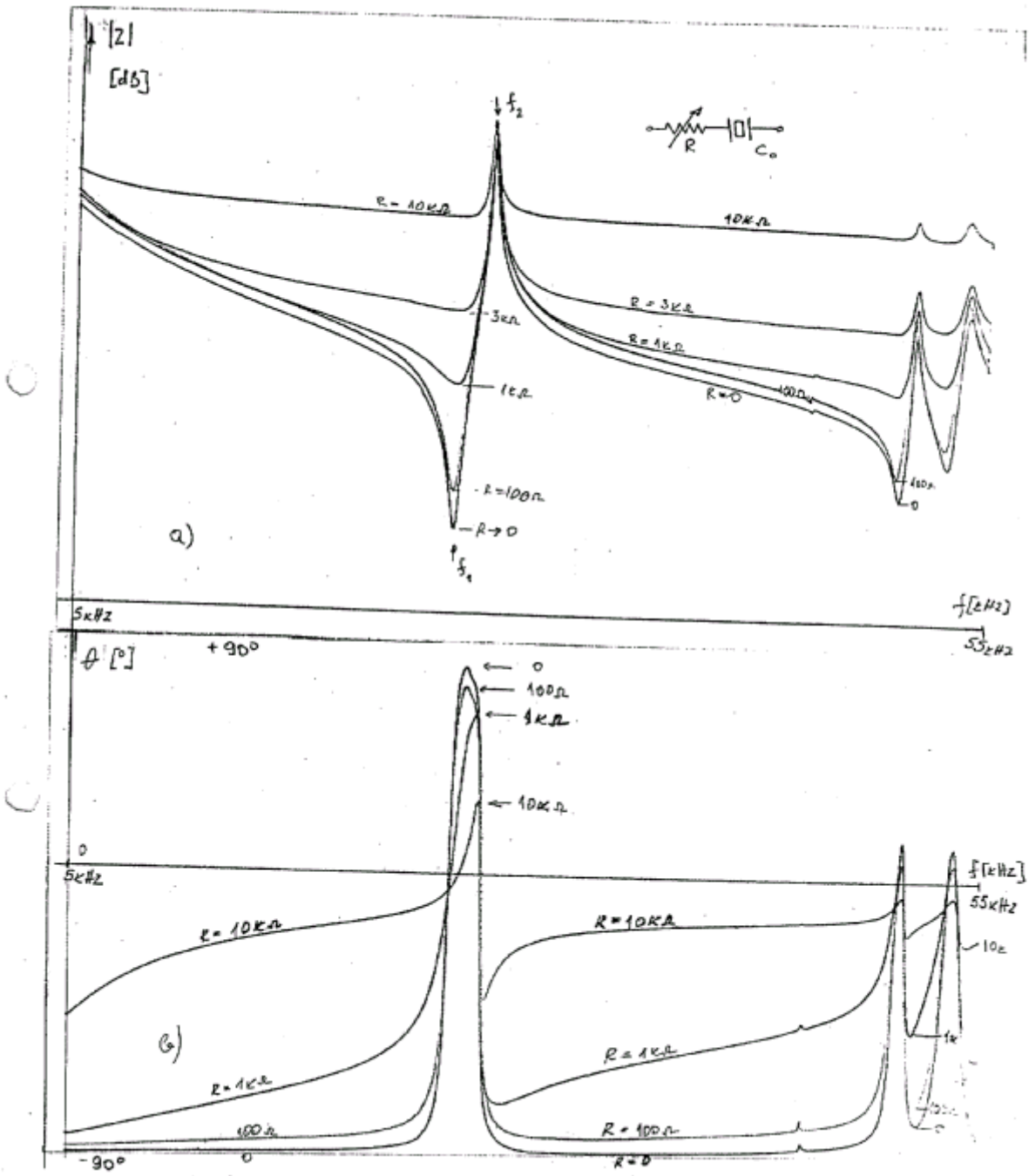

Fig. 5 Converter Impedance-Phase Characteristics with Series Resistance

converter series resonance will simply disappear, becoming weaker and weaker (by amplitude), and moving a little bit towards parallel resonance, until completely becomes undetectable for sufficiently high values of R_s. It only remains a well detectable converter's parallel resonance (for high values of R_s). On the Fig. 6, a), b) & c) is presented the same situation in a simplified summary form, in order to make more clear conclusions that can be drawn from the Fig. 5.

When we place the same converter (see Fig. 5 d) & e)) on the mechanical vibrating platform **VP** (as before), we shall have exactly the same mechanical-situation (λ/2 –

axial mechanical resonance with converter's open input terminals) as already explained for the Fig. 2, d).

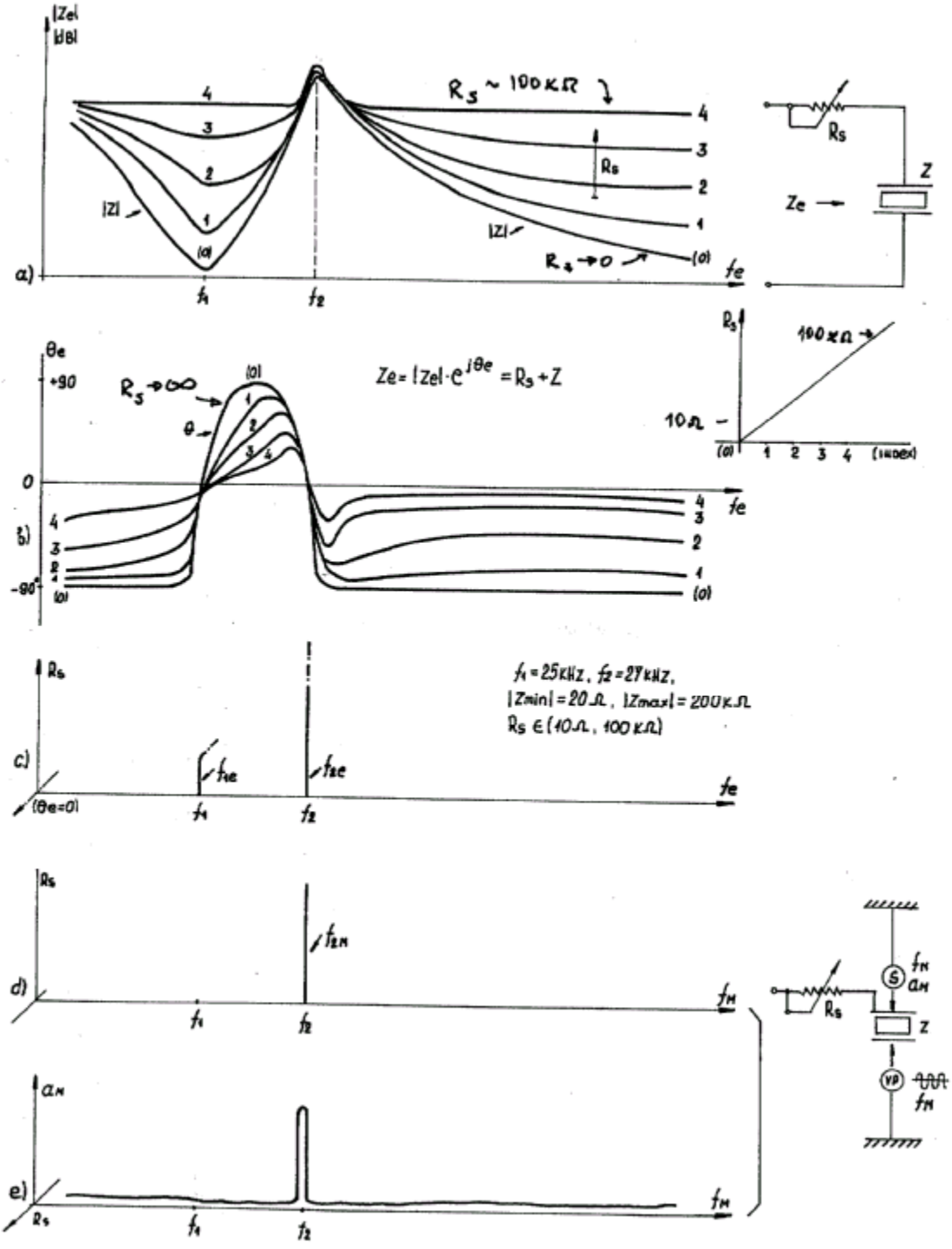

Fig. 6 Converter Characteristics with Series Resistance (see Fig. 5)
a) & b) Electric Impedance-Phase Curves
c) Electrical resonances
d) Mechanical resonances
e) λ/2 – axial-mechanical resonances

The next example presented on the Fig. 7 and Fig. 8, is a variable capacitance connected in parallel to the same converter ($C_p \in$ 0.1 nF until 100 nF). When parallel capacitance C_p is very low (close to zero), this corresponds (electrically and mechanically) to open converter terminals (see Fig. 2, d)), and when parallel capacitance is very high (much higher than converter static capacitance), this situation corresponds (only) mechanically to converter terminals in a short circuit (see Fig. 2, c)).

Fig. 7 and Fig. 8, a) & b) present electrical Impedance-Phase characteristics (measured by Network Impedance Analyzer) when parallel capacitance is taking different values. We can easily notice (on the Fig. 7) that parallel capacitance will not change (electrically or mechanically) converter series resonant frequency. Electrically, increase of parallel capacitance is only reducing and destroying natural parallel resonance of the converter, making converter to become dominantly a capacitive component, and moving its parallel resonance (electrically and mechanically) towards converter series resonance (see also Fig. 8, where the same situation is simplified and presented in a summary form, convenient for comparison between electrical and mechanical resonance measurements, as shown before). Fig. 8, c) is just qualitatively underlining where are electrical resonant frequencies (in order to compare them with mechanical resonant frequencies), Fig. 8, d) gives a rough idea about evolution of mechanical resonances measured on the **VP**, and Fig.8, e) presents positions and relative amplitudes of $\lambda/2$–axial-mechanical resonances.

Effectively, piezoelectric converter with parallel capacitance becomes (using only electrical means) variable-sound-speed solid-rod (in the frequency area between its series and parallel resonance), since resulting sound speed will depend on connected capacitance (see Fig. 8, e)). We can easily imagine producing different semi-active ultrasonic tools such as boosters, sonotrodes and solid-wave-guides with possibility for easy external sound speed tuning and resonance adjustment (installing one piezoceramic, sandwiched layer inside of such tools, and adding variable parallel capacitance to it). Also a number of electromechanical band-limited filters, selective acoustic receivers, and frequency and amplitude modulators can be designed based on variable-sound-speed solid-rod (operating as $\lambda/2$–axial-mechanical resonator).

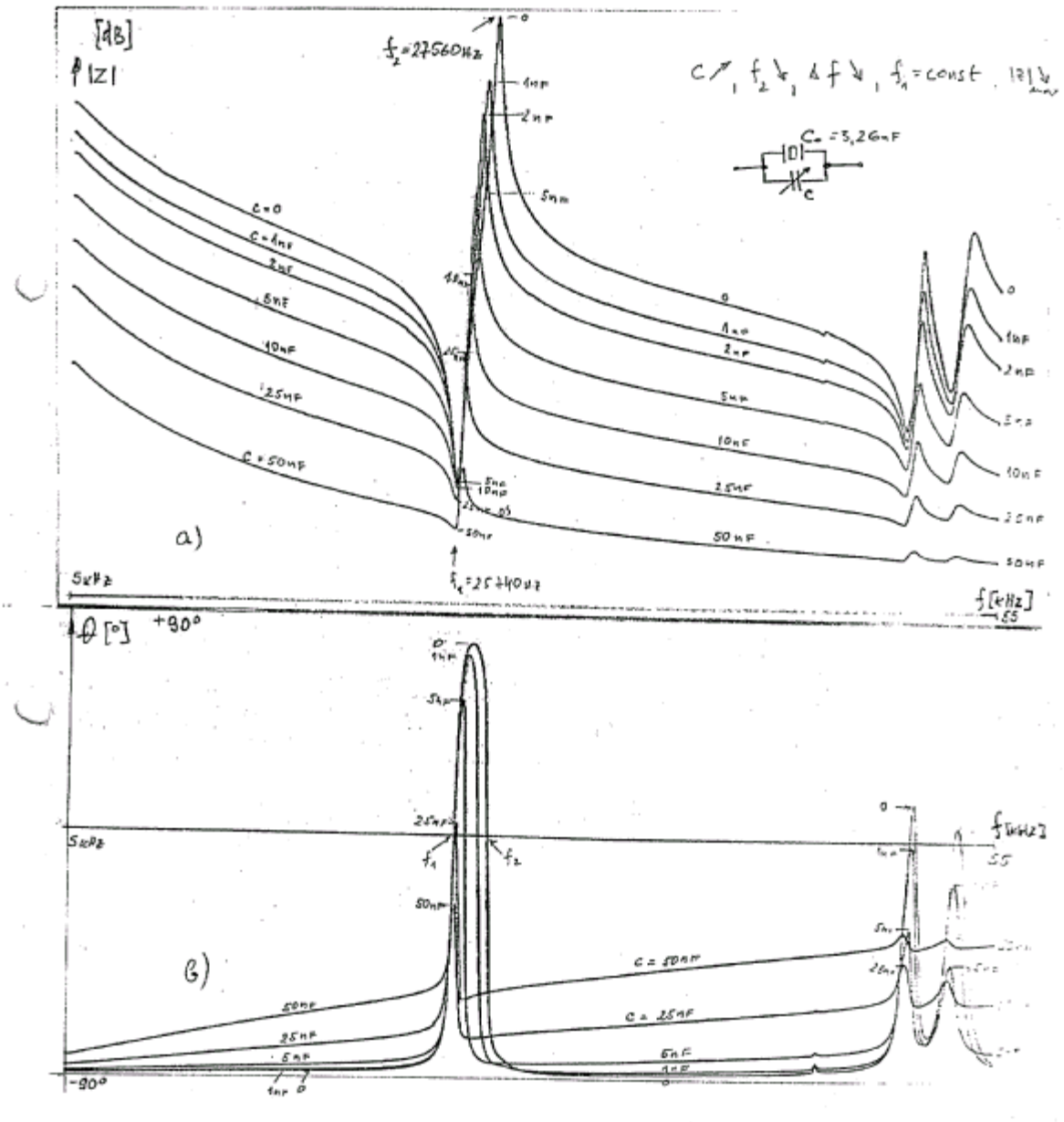

Fig. 7 Converter Impedance-Phase Characteristics with Parallel Capacitance

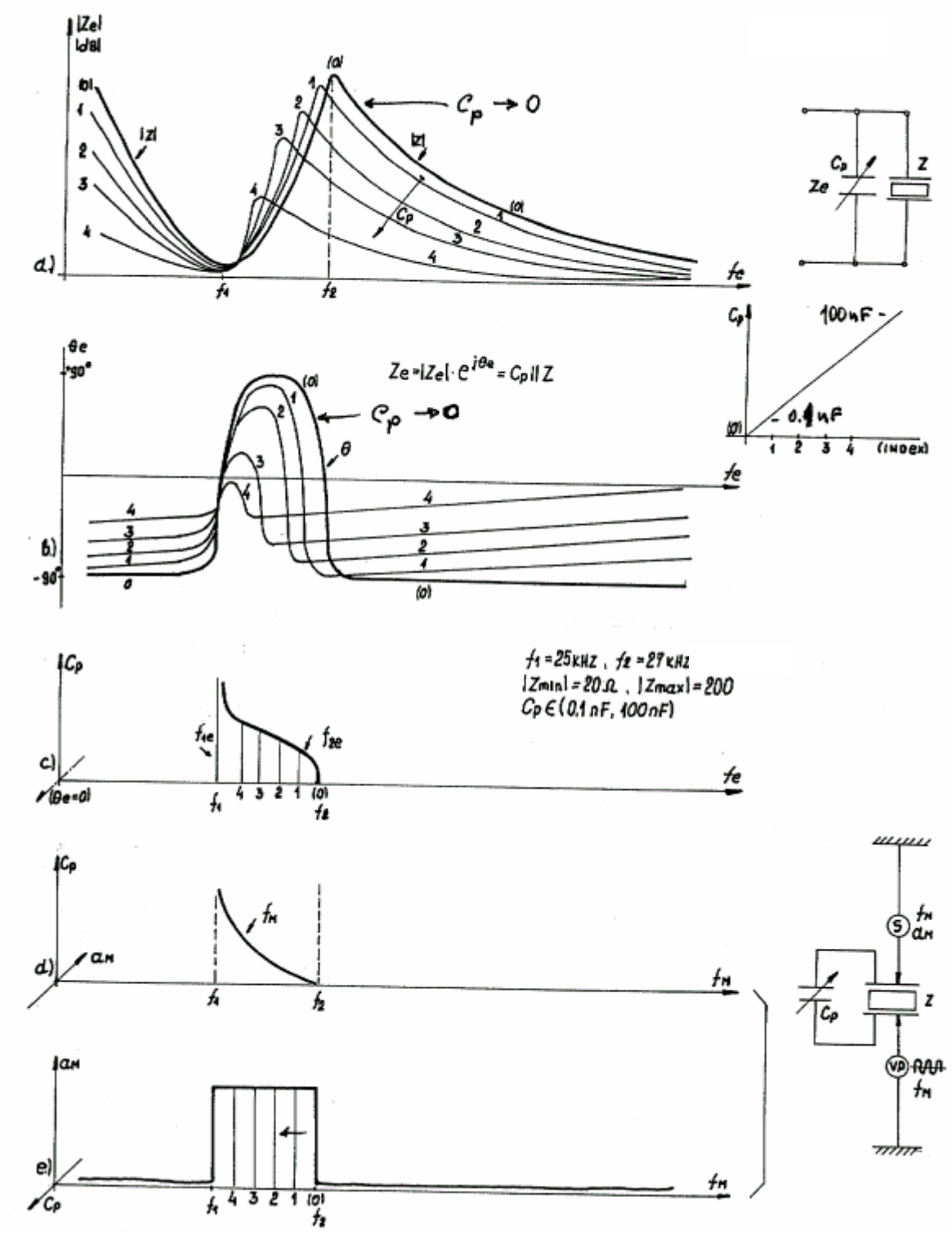

Fig. 8 Converter Characteristics with Parallel Capacitance (see Fig. 7)
a) & b) Electric Impedance-Phase Curves
c) Electrical resonances
d) Mechanical resonances
e) λ/2 – axial-mechanical resonances

The next example presented on the Fig. 9 and Fig. 10, is a variable capacitance connected in series to the same converter ($C_s \in$ 0.1 nF until 10 nF). When series capacitance C_s is very high (much higher than converter static capacitance), this corresponds (electrically and mechanically) to an open converter terminals (see Fig. 1 and Fig. 2, d)), and when series capacitance is decreasing towards very low values, series converter resonance is mowing closer to parallel resonance and progressively disappearing (see Fig. 9 and Fig. 10, a), b) and c)).

Fig. 9 and Fig. 10, a) & b) present electrical Impedance-Phase characteristics (measured by Network Impedance Analyzer) when series capacitance is taking different values. We can easily notice (on the Fig. 9 and Fig. 10) that series capacitance will not change (electrically or mechanically) converter parallel resonant frequency. Electrically, a decrease of series capacitance is only reducing and destroying natural series resonance of the converter. Fig. 10, c) is just qualitatively underlining where are electrical resonant frequencies (in order to compare them with mechanical resonant frequencies), Fig. 10, d) shows where converter will resonate mechanically measured on the **VP**, and Fig. 10, e) presents relative mechanical amplitude of converter's $\lambda/2$–axial-mechanical resonance.

Here described situation with series capacitance is showing us how (in certain applications) we can eliminate undesirable series resonant frequencies and make a piezoelectric converter operating only on its (high impedance) parallel resonance, where converter becomes extremely sensitive as a sensor of mechanical vibrations, as a hydrophone, or sensitive microphone, since mechanical and electrical parallel resonance will stay unchanged, and only series resonance would disappear.

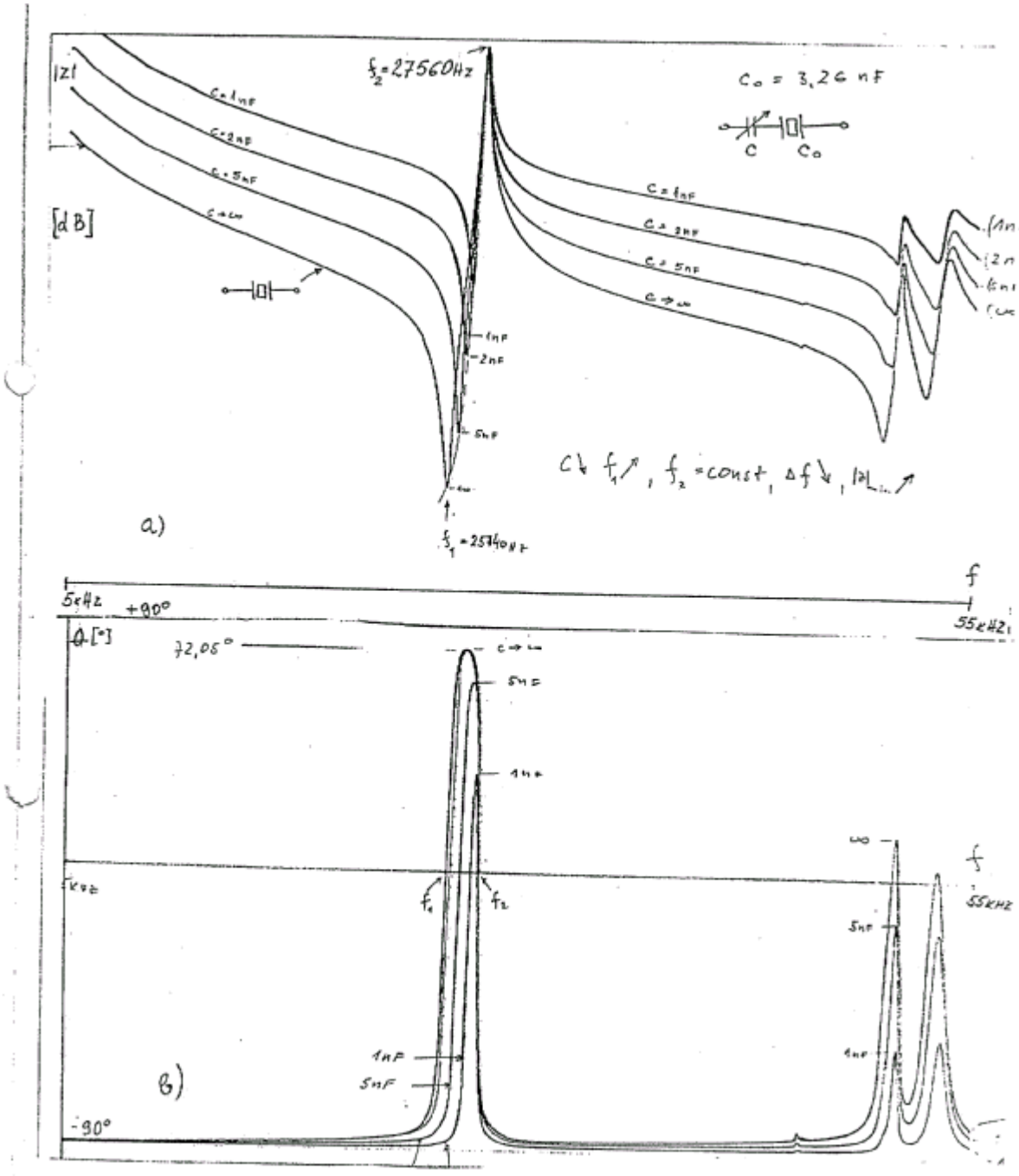

Fig. 9 Converter Impedance-Phase Characteristics with Series Capacitance

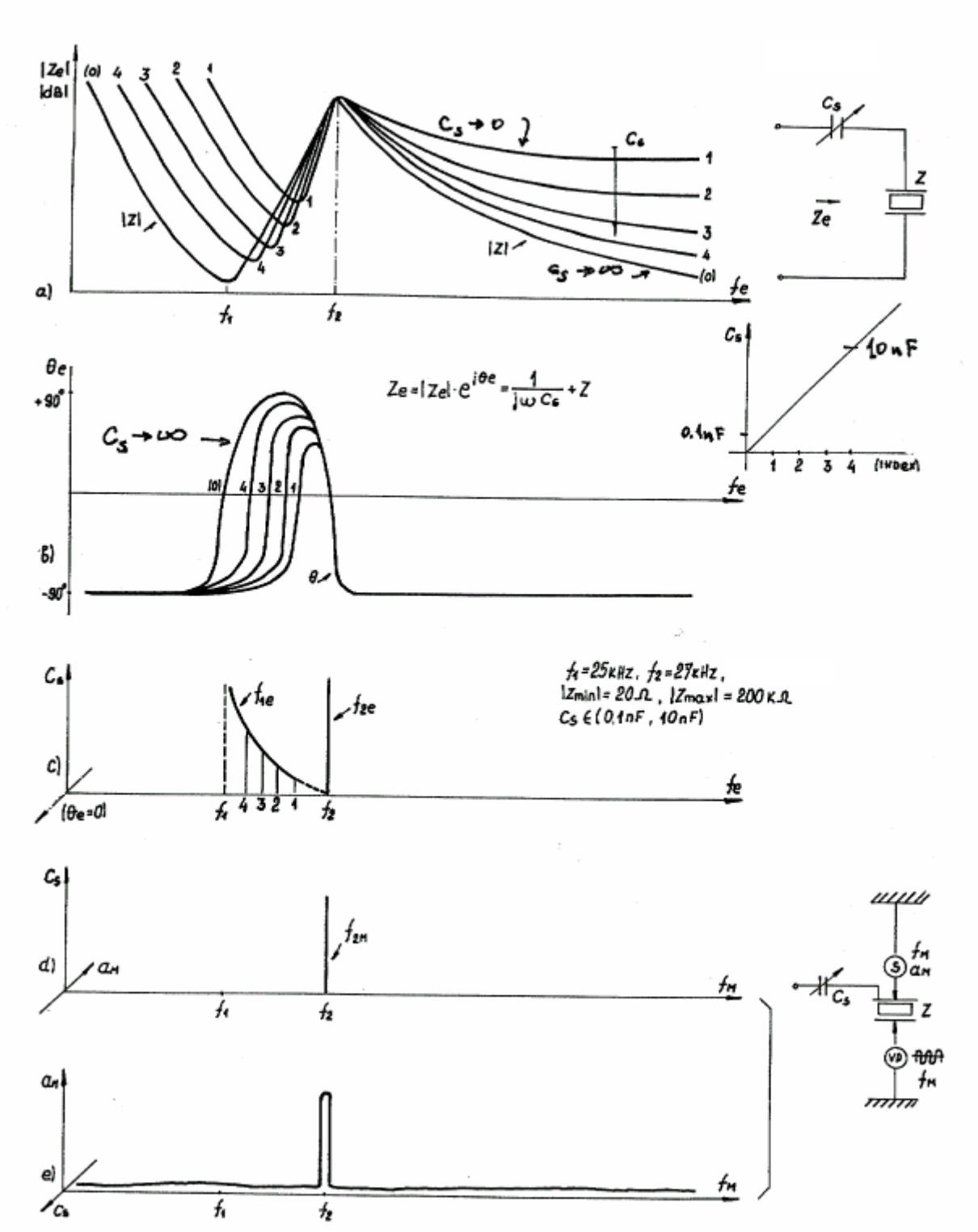

Fig. 10 Converter Characteristics with Series Capacitance (see Fig. 9)

a) & b) Electric Impedance-Phase Curves

c) Electrical resonances

d) Mechanical resonance

e) λ/2 – axial-mechanical resonance

The next example presented on the Fig. 11 and Fig. 12, is a variable inductance connected in parallel to the same converter ($L_p \in 60\ \mu$ until 35 mH). When parallel inductance L_p is very high, this approximately corresponds (electrically and mechanically, but only in oscillatory operating conditions) to open converter terminals (see Fig. 1 and Fig. 2, d)), except that booth series and parallel electrical and mechanical resonances would be easy detectable (and operational) by electrical and/or mechanical means. When parallel inductance is very low, this situation approximately corresponds (only mechanically) to converter terminals in a short circuit (see Fig. 2, c)). Based only on electrical impedance measurements (Fig. 11 and Fig. 12, a) & b)), we can also notice that variable parallel inductance generates two (frequency and inductance dependant) high impedance zones (lower and higher parallel resonance zones), and keeps relatively stable converter's series resonance.

Fig. 11 and Fig. 12, a) & b) present electrical Impedance-Phase characteristics (measured by Network Impedance Analyzer) when parallel inductance is taking different values. We can easily notice (on the Fig. 11) that parallel inductance will change (electrically and mechanically) booth of converter's parallel resonant frequencies. Electrically, starting from very high parallel inductance and then decreasing will shift lower (first) parallel resonance of the converter towards higher frequencies (until its series resonance), and it will also shift the higher (second) parallel resonance towards higher frequencies, while keeping series resonance in a stable position.

Fig. 12, c) is just qualitatively underlining the evolution of electrical resonant frequencies (in order to compare them with mechanical resonant frequencies). Fig. 12, d) gives a rough idea about evolution of mechanical resonances measured on the **VP**, and Fig.12, e) presents positions and relative amplitudes of $\lambda/2$–axial-mechanical resonances.

*Effectively, piezoelectric converter with parallel inductance becomes (using only electrical means) variable-sound-speed solid-rod, since resulting sound speed (and converter's parallel resonances) will depend on connected inductance (see Fig. 12, e)). What is very interesting is that electrically we can notice existence of movable, lower and higher parallel-resonant-zone (see Fig. 11, Fig. 12, a), b) and c)), but in reality, after making measurements using vibrating platform **VP**, we will find that converter operating as $\lambda/2$–axial-mechanical resonator is inefficient in the higher (or second) parallel-resonant-zone, since it will have relatively low mechanical amplitudes in such resonant states (see Fig. 12, e)). Contrary, the lower (movable) parallel resonant zone will be mechanically fully efficient in a large frequency interval, starting from series resonance towards lower frequencies, since $\lambda/2$–axial-mechanical resonant amplitudes will be relatively high (Fig. 12, e)).*

Again, similar to parallel capacitance option (Fig. 7 and Fig. 8), we can easily imagine making different semi-active ultrasonic tools such as boosters, sonotrodes and solid-wave-guides with possibility for easy external sound speed tuning and resonance adjustment (installing one piezoceramic, sandwiched layer inside of such tools, and adding variable parallel inductance to it). Also a number of electromechanical filters, selective acoustic receivers, and frequency and amplitude modulators can be designed based on variable-sound-speed solid-rod (operating as $\lambda/2$–axial-mechanical resonator).

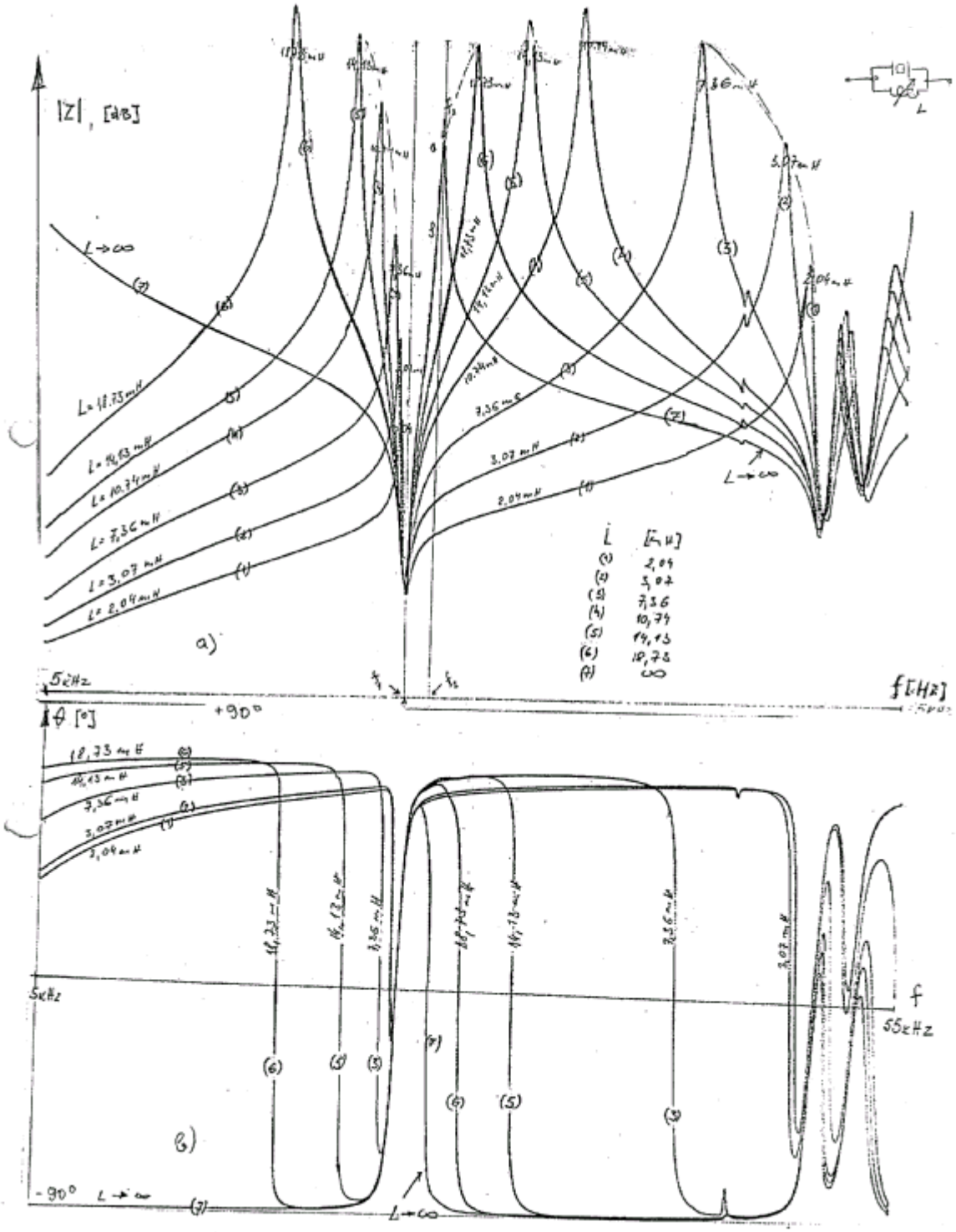

Fig. 11 Converter Impedance-Phase Characteristics with Parallel Inductance

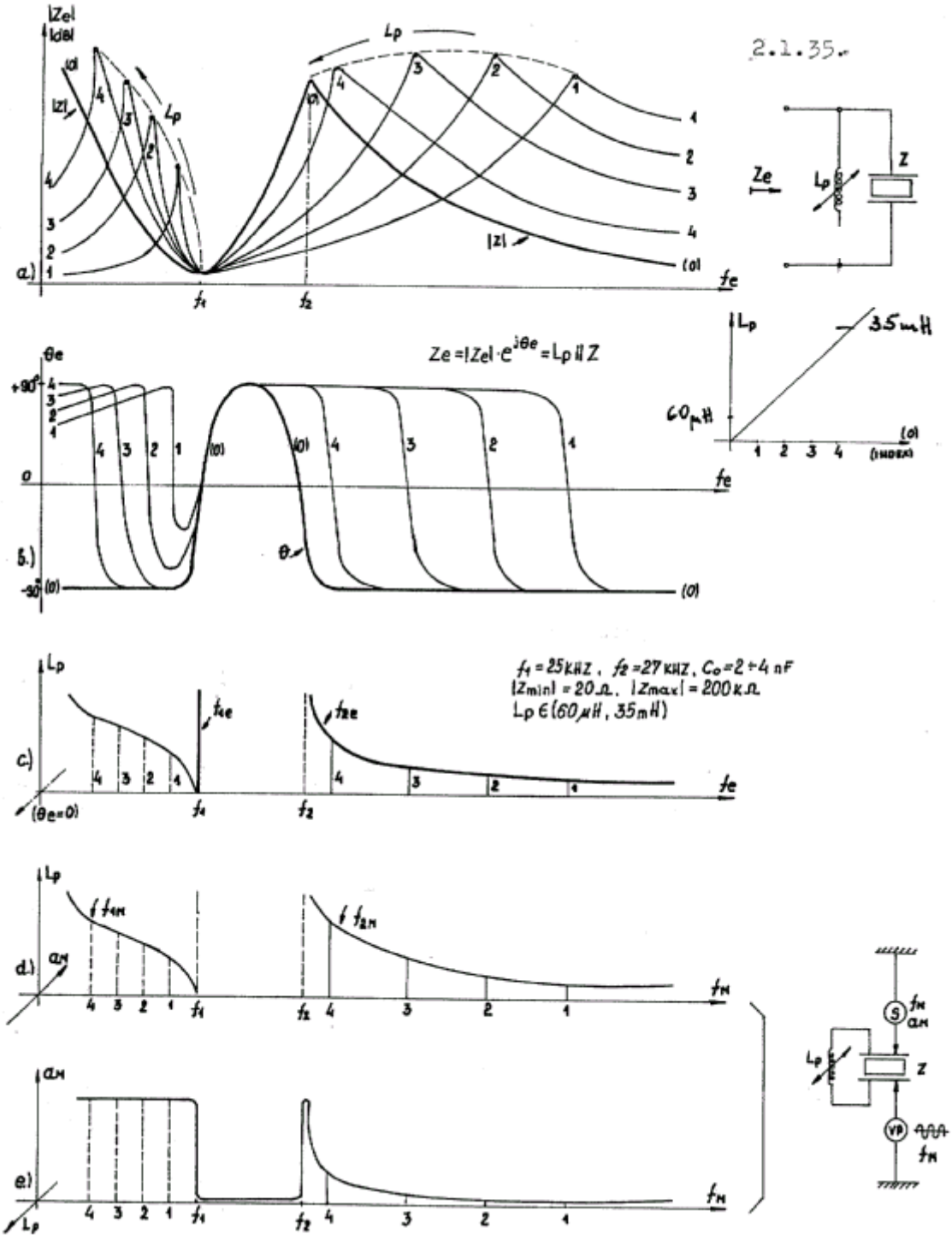

Fig. 12 Converter Characteristics with Parallel Inductance (see Fig. 11)

a) & b) Electric Impedance-Phase Curves

c) Electrical resonances

d) Mechanical resonances

e) λ/2 – axial-mechanical resonances

The next example presented on the Fig. 13 and Fig. 14, is a variable inductance connected in series to the same converter ($L_s \in 10\ \mu H$ until 10 mH). When series inductance L_s is very low (or zero), this corresponds (electrically and mechanically) to an open single converter terminals (see Fig. 1 and Fig. 2, d)). Based only on electrical impedance measurements (Fig. 13 and Fig. 14, a) & b)), we can also notice that variable series inductance generates two (frequency and inductance dependant) low impedance zones (lower and higher series resonance zones), and keeps relatively stable converter's parallel resonance.

When series inductance start increasing its value, electrical, lower series converter resonance starts mowing towards lower frequencies, and higher series resonance also moves towards converter's parallel resonance or effectively also decreasing (see Fig. 13 and Fig. 14, a), b) and c)).

Fig. 13 and Fig. 14, a) & b) present electrical Impedance-Phase characteristics (measured by Network Impedance Analyzer), when series inductance is taking different values. We can easily notice (on the Fig. 13 and Fig. 14) that series inductance will not change (electrically or mechanically) converter's parallel resonant frequency. Fig. 14, c) is just qualitatively underlining where are electrical resonant frequencies (in order to compare them with mechanical resonant frequencies), Fig. 14, d) shows where converter will resonate mechanically measured on the **VP**, and Fig. 14, e) presents relative mechanical amplitude of converter's $\lambda/2$–axial-mechanical resonance.

Now, based on all above described experimental situations, we can generalize the following conclusions:

a) **By connecting in series any of passive R, L and C components to a single piezoelectric converter we shall be able to modify, and/or move, or attenuate series resonance zone/s of the converter (impedance minimum zone/s), while its parallel resonance zone remains in a stable position.**

b) **By connecting in parallel any of passive R, L and C components to a single piezoelectric converter we shall be able to modify, and/or move, or attenuate parallel resonance zone/s of the converter (impedance maximum zone/s), while its series resonance zone remains in a stable position.**

c) **In any case of practical interest, piezoelectric converter can be efficiently driven in its low frequency area, below its series resonant frequency, then in certain situations the frequency interval between converter's series and parallel resonant frequencies can also be efficiently activated (including operations in series and parallel resonances), and in a remaining frequency area, higher than converter's parallel resonant frequency, converter becomes electromechanically inefficient (regardless of possible presence of different electrical resonant zones).**

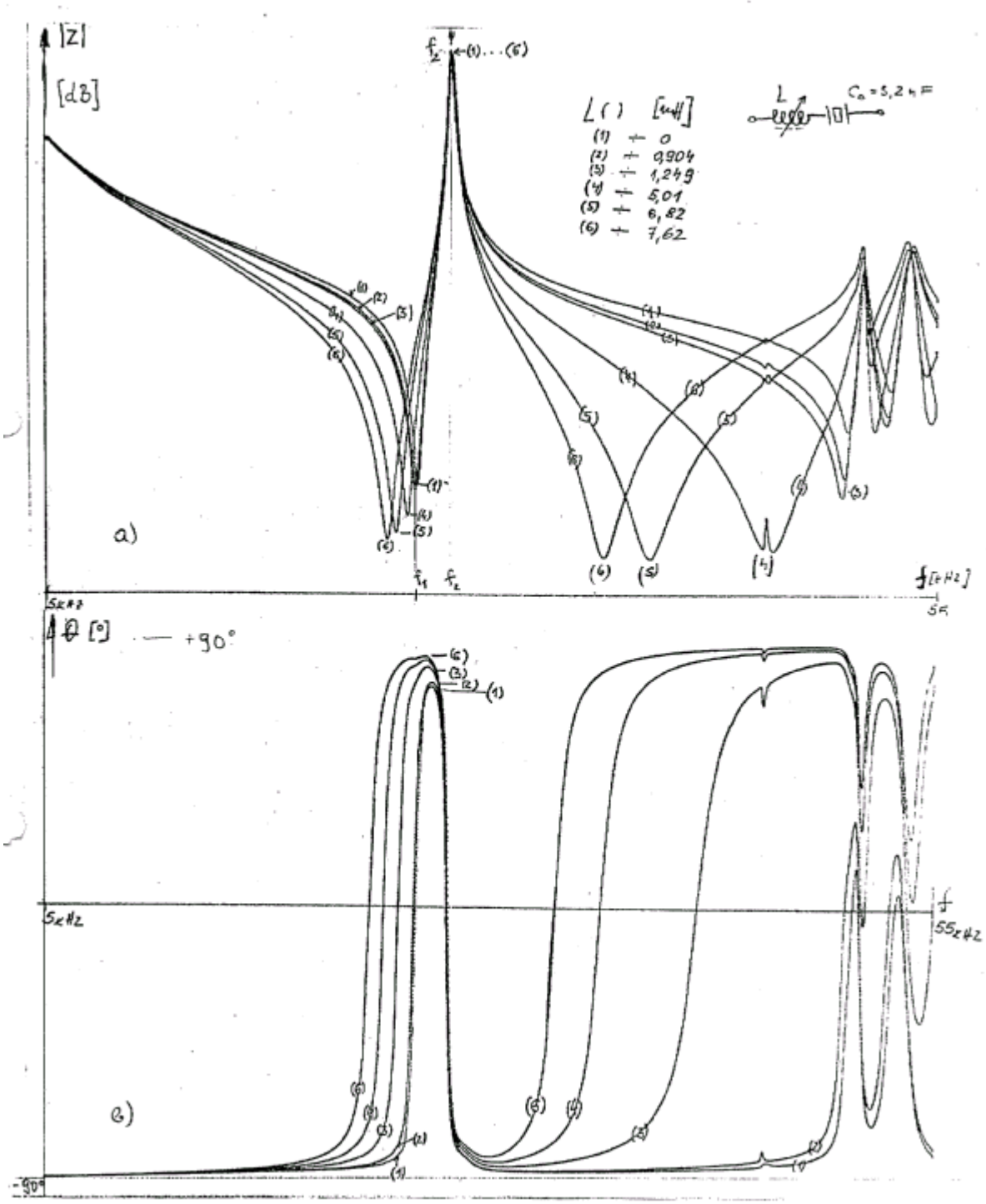

Fig. 13 Converter Impedance-Phase Characteristics with Series Inductance

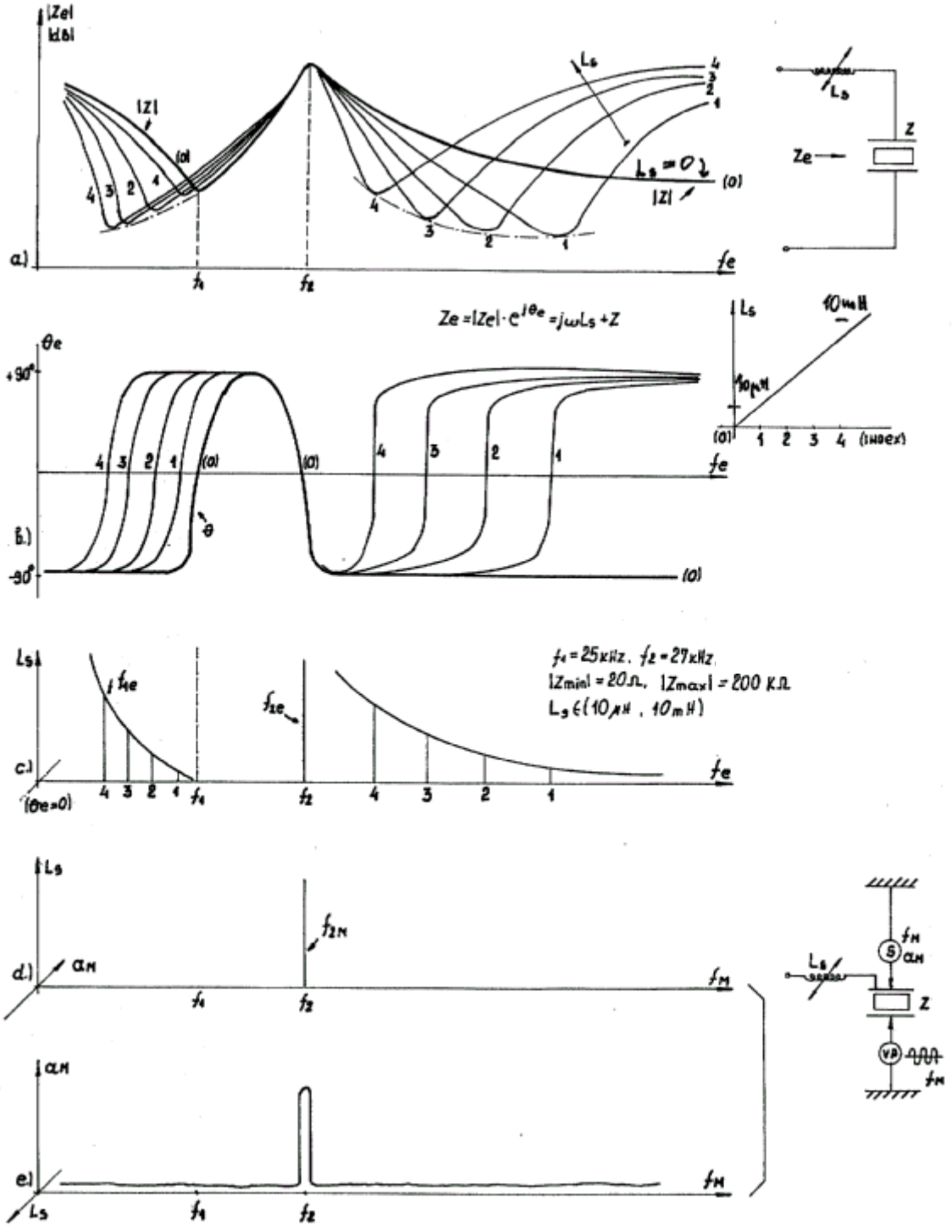

Fig. 14 Converter Characteristics with Series Inductance (see Fig. 13)

a) & b) Electric Impedance-Phase Curves

c) Electrical resonances

d) Mechanical resonance

e) λ/2 – axial-mechanical resonance

4.1 Inductive Compensation and Sensitivity of Piezoelectric Converters

On the Fig. 4.1-1 are presented series and parallel inductive compensations of a piezoelectric converter (L_s = series inductance, L_p = parallel inductance). All circuits on the left side of the Fig. 4.1-1 are mutually equivalent, and the same is valid for the circuits on the right side (but there is no equivalence between left and right side circuits). We can also notice on the Fig. 4.1-1 that most significant elements responsible for creating different resonant zones are encircled in order to visualize the appearance of three different resonant frequencies in each case.

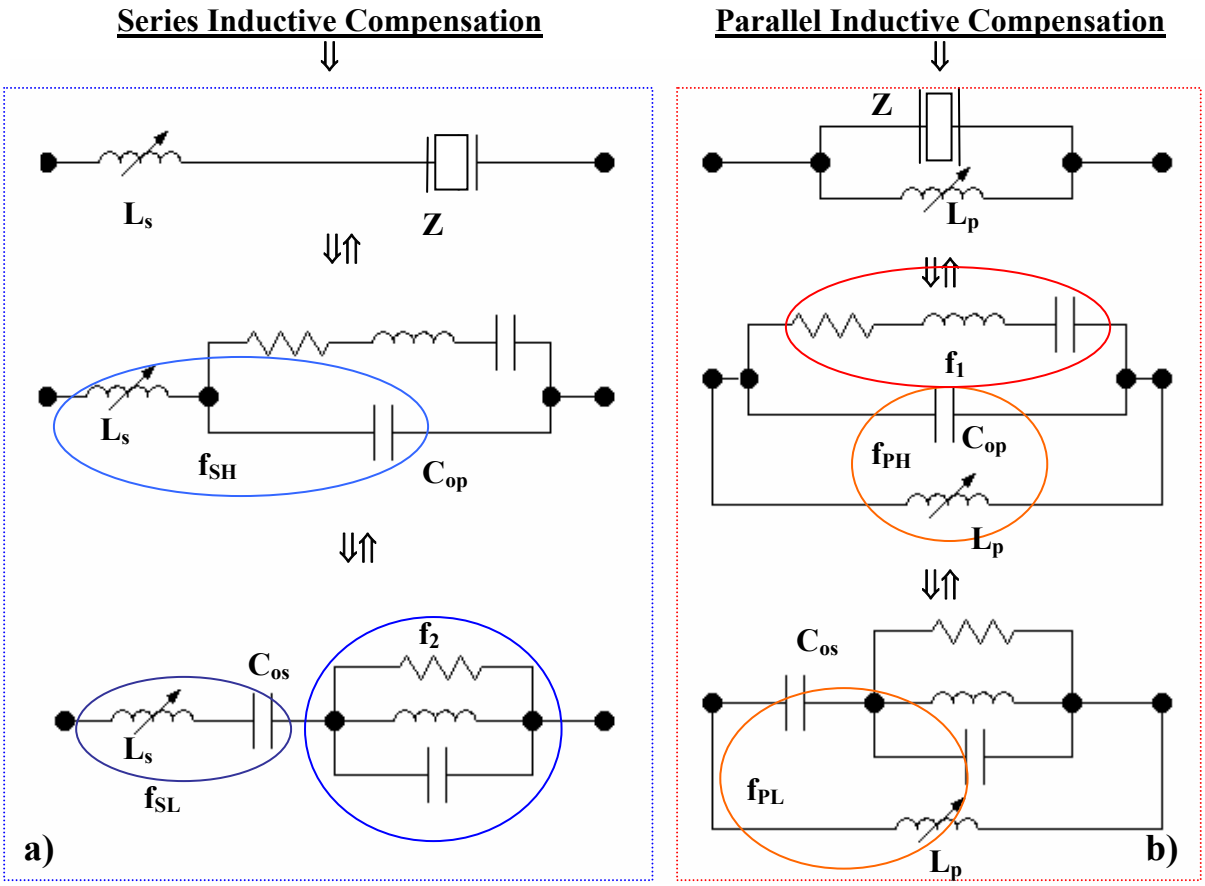

Fig. 4.1-1 Series, a), and Parallel, b), Inductive Compensation

Series inductive compensation is naturally enabling converter to produce real (active) power in its parallel mechanical-resonance $f_p \approx f_2$, and parallel inductive compensation is naturally enabling converter to produce real power in its series mechanical-resonance $f_s \approx f_1$. One of the problems for designers in this field is that both, series and parallel inductive compensations are creating two more side-band resonant zones. For instance, when we use series inductive compensation to stimulate parallel mechanical-resonance f_2, we also create, left and right from f_2, the low-impedance resonant zones with frequencies f_{SL} and f_{SH} (respectively), Fig. 4.1-3.1. Also, when we use parallel inductive compensation to stimulate series mechanical-resonance f_1, we also create, left and right from f_1, the high-impedance resonant zones with frequencies f_{PL} and f_{PH} (respectively), Fig. 4.1-3.2. It is the fact that piezoelectric converter can also operate in all resonant zones created by series

and/or parallel inductive compensation (in $\mathbf{f_{PL}}$, $\mathbf{f_1}$, $\mathbf{f_{PH}}$, $\mathbf{f_{SL}}$, $\mathbf{f_2}$, $\mathbf{f_{SH}}$), but not all of them are equally efficient (regarding power conversion). The objective in optimal inductive compensation (in most of cases) is to make $\mathbf{f_1}$ to be in the middle point between $\mathbf{f_{PL}}$, and $\mathbf{f_{PH}}$, and $\mathbf{f_2}$ to be in the middle point between $\mathbf{f_{SL}}$, and $\mathbf{f_{SH}}$. Another objective (in most of cases) is to create maximal possible difference between $\mathbf{f_{PL}}$, and $\mathbf{f_{PH}}$, and between $\mathbf{f_{SL}}$, and $\mathbf{f_{SH}}$, in order to make a safe operating frequency band larger (placed symmetrically around chosen resonant frequency: see Fig. 4.1-3.1 and Fig. 4.1-3.2).

It is also easy, by changing the value of series or parallel inductance, to create unsymmetrical positioning of $\mathbf{fx_L}$, and $\mathbf{fx_H}$ around series or parallel resonance point/s. This option can be useful in cases when we intend to apply series inductive compensation in order to drive converter in its series mechanical resonant frequency (by making $\mathbf{f_{SL}} \approx \mathbf{f_1}$), or when we intend to apply parallel inductive compensation and drive converter in its parallel mechanical resonant frequency (by making $\mathbf{f_{PH}} \approx \mathbf{f_2}$). In reality, by adding external inductances (in series or in parallel to a converter), we are modifying the effective sound speed inside the structure of certain converter, effectively modifying its piezo-properties.

In most of literature explaining inductive compensation of piezoelectric converters and sensors (operating in resonance), above described situation is oversimplified suggesting that for operating in parallel mechanical resonance we should apply series inductance that satisfies the expression: $\mathbf{f_2} = \dfrac{\mathbf{1}}{\mathbf{2\pi\sqrt{L_s C_{os}}}}$, and in cases when operating in series mechanical resonant frequency we should apply parallel inductance that satisfies the expression: $\mathbf{f_1} = \dfrac{\mathbf{1}}{\mathbf{2\pi\sqrt{L_p C_{op}}}}$. In reality, calculating the necessary inductance values that way, we are making certain errors (for instance, actual and the best experimentally found inductance, for single converter compensation, could be approximately +10% higher than calculated values, but this statement cannot be generalized for all piezoelectric converters). Since the differences between calculated and experimentally found inductance values are not too high, for the sake of simplicity, we are using above mentioned expressions for calculating inductive compensation, and later on, experimentally we should make necessary corrections.

Let us give a couple of practical examples regarding series inductive compensation,

A) When transducer will operate in its parallel mechanical resonance $\mathbf{f_m} \cong \mathbf{f_2}$, and
B) When transducer will operate in equivalent electrical series resonance $\mathbf{f_m = f'_{SL} \leq f_1}$

Without entering into any formula-development, we can present the table of best empirically-found and approximated results regarding how to calculate series inductance (see the following picture and table).

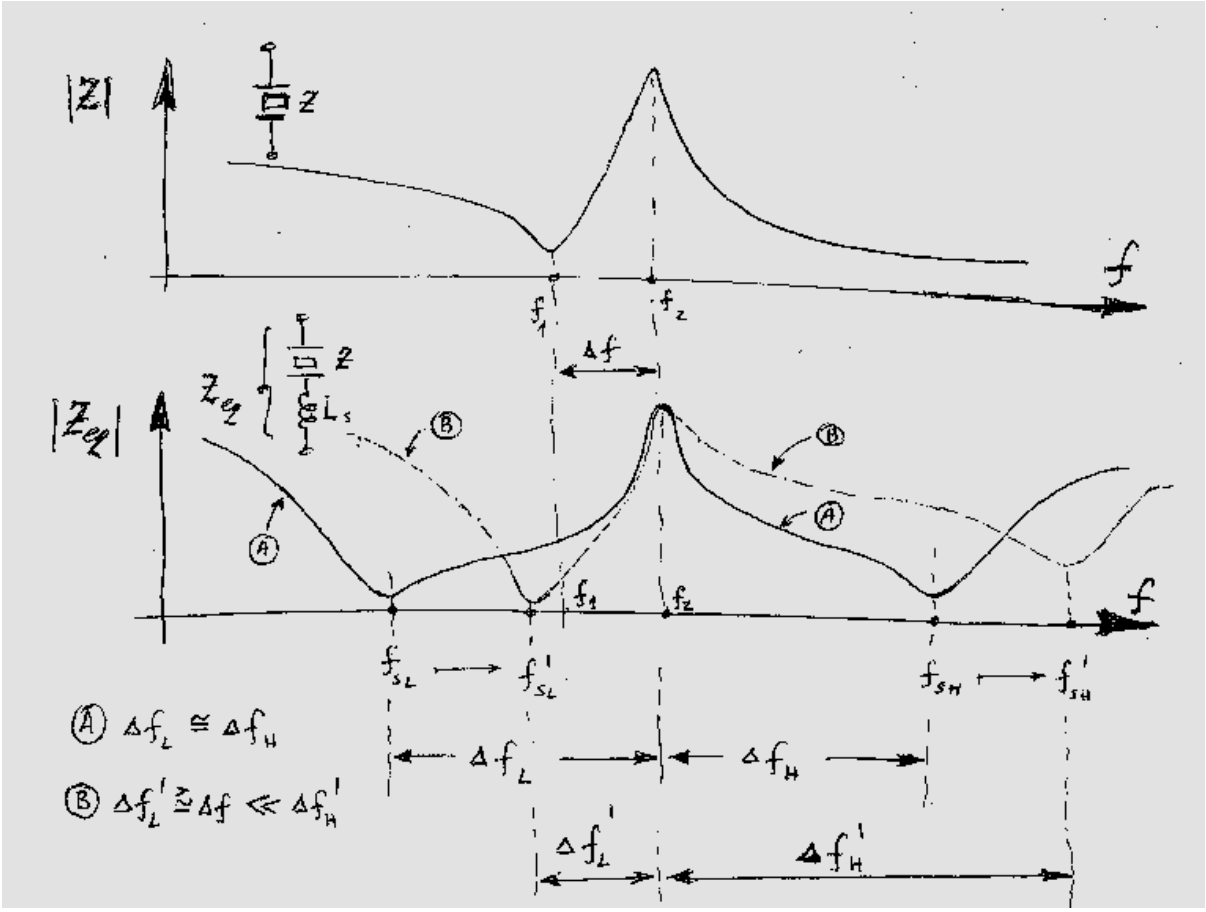

Resonant Regime	Values of series inductive compensation
Case A) Series inductive compensation $(\mathbf{L_s = L_{sA} = High}) \Rightarrow$ Transducer is operating in its parallel mechanical, or voltage resonance: $\mathbf{f_m = f_2 \cong const.}$. $\mathbf{\Delta f_L \cong \Delta f_H \approx 3\,\Delta f}$ $\mathbf{\Delta f_L + \Delta f_H \approx 6\,\Delta f}$	$$\frac{1}{4\pi^2 f_2^2 C_0} < \left\{ \begin{array}{l} L_s \approx \dfrac{1}{4\pi^2 f_2^2 C_0 (1 - \dfrac{\Delta f}{2 f_2})} \approx \\ \\ \approx \dfrac{1}{4\pi^2 f_1 f_2 C_0} \end{array} \right\} < \frac{1}{4\pi^2 f_1^2 C_0}$$
Case B) Series inductive compensation $(\mathbf{L_s = L_{sB} \approx \frac{1}{2} L_{sA} = Low}) \Rightarrow$ Transducer is operating in equivalent series or current resonance: $\mathbf{(f_m = f'_{sL} \le f_1) = Load - dependent}$ $\mathbf{(\Delta f'_L \approx \Delta f) < \Delta f'_H}$ $\mathbf{\Delta f'_L + \Delta f'_H \approx 6\,\Delta f}$	$$\frac{1}{8\pi^2 f_2^2 C_0} < \left\{ \begin{array}{l} L_s \approx \dfrac{1}{8\pi^2 f_2^2 C_0 (1 - \dfrac{\Delta f}{2 f_2})} \approx \\ \\ \approx \dfrac{1}{8\pi^2 f_1 f_2 C_0} \end{array} \right\} < \frac{1}{8\pi^2 f_1^2 C_0}$$

We can also give a couple of practical examples regarding parallel inductive compensation,

C) When transducer will operate in its series mechanical resonance $\mathbf{f_m \cong f_1}$, and
D) When transducer will operate in equivalent electrical parallel resonance $\mathbf{f_m = f'_{PH} \geq f_2}$

Without entering into any formula-development, we can present the table of best empirically-found and approximated results regarding how to calculate parallel inductance (see the following picture and table).

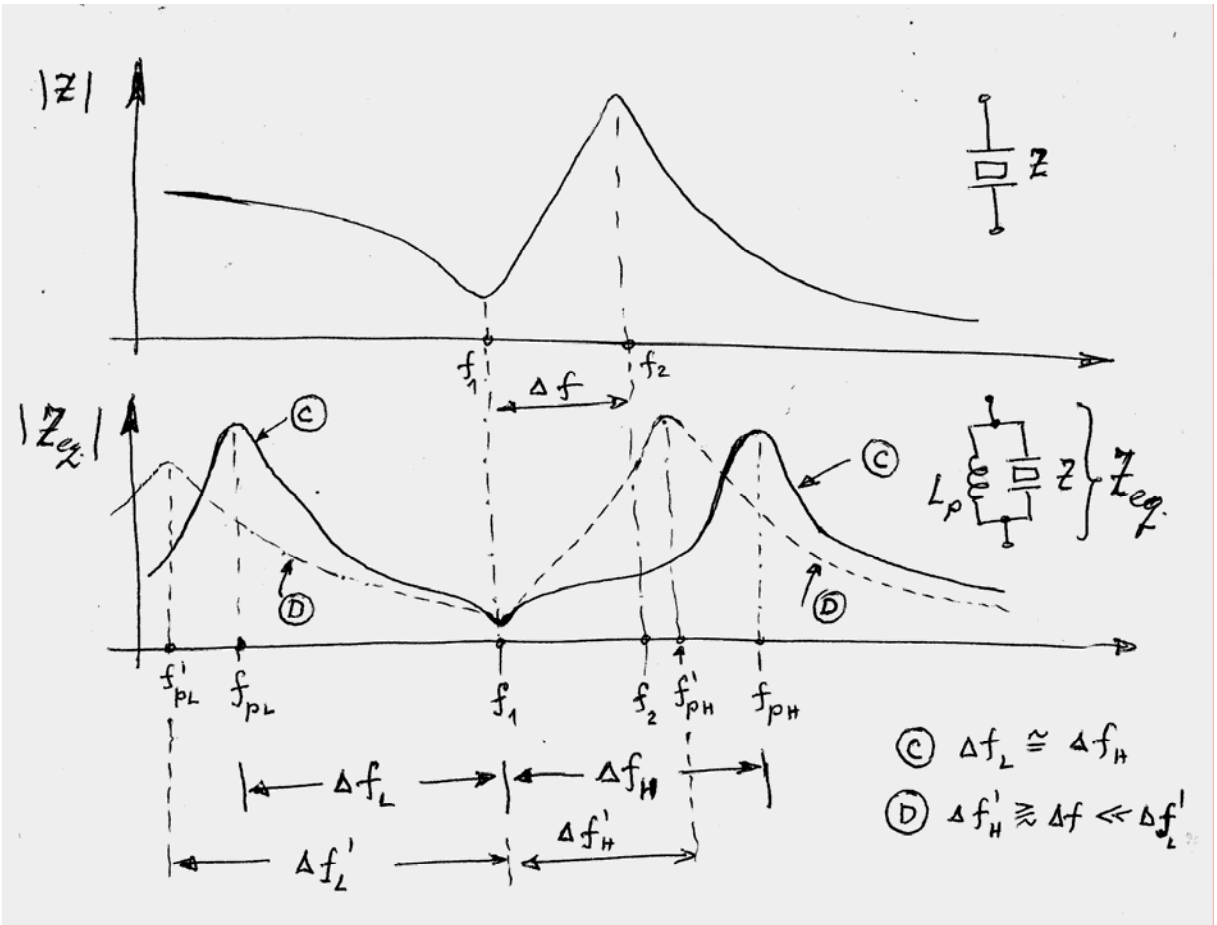

Resonant Regime	Value of parallel inductive compensation
Case C) Parallel inductive compensation $(\mathbf{L_p = L_{pC} = Low}) \Rightarrow$ Transducer is operating in its series mechanical, or current resonance: $\mathbf{f_m = f_1 \cong const.}$. $\mathbf{\Delta f_L \cong \Delta f_H \approx 3\,\Delta f}$ $\mathbf{\Delta f_L + \Delta f_H \approx 6\,\Delta f}$	$$\frac{1}{4\pi^2 f_1^2 C_0} < \left\{ L_p \approx \frac{1}{4\pi^2 f_1^2 C_0 (1 - \frac{2\Delta f}{f_1})} \right\}$$

Case D) Series inductive compensation $(\mathbf{L_p = L_{pD} \approx 2L_{pC} = High}) \Rightarrow$ Transducer is operating in equivalent parallel or voltage resonance: $(\mathbf{f_m = f'_{pL} \geq f_2}) = \mathbf{Load-dependent}$ $(\mathbf{\Delta f'_H \approx \Delta f}) < \mathbf{\Delta f'_L}$ $\mathbf{\Delta f'_L + \Delta f'_H \approx 6\,\Delta f}$	$$\frac{1}{2\pi^2 f_1^2 C_0} < \left\{ L_p \approx \frac{1}{2\pi^2 f_1^2 C_0 (1 - \frac{2\Delta f}{f_1})} \right\}$$

Only resonant regimes in mechanical parallel and series resonances (case A) and case C)) are able to keep stable and almost-constant operating frequency, $\mathbf{f_2}$ or $\mathbf{f_1}$). Most of ultrasonic plastic welding applications are covered by cases A) and C), combined with a convenient PLL resonance-control circuit (but there are some other regimes where combined series + parallel inductive compensation is very successfully used, as kind of high power filtering). We can notice that changing series or parallel (compensating) inductances in very large intervals is not significantly changing $\mathbf{f_2}$ or $\mathbf{f_1}$, but it is changing very much all values for $\mathbf{f_L}$ and $\mathbf{f_H}$**.**

When operating in electrically-created, equivalent series and/or parallel resonance/s (case B) and case D)), mechanical resonant frequency is very much load-dependent (meaning moderately-variable), since all electrical and mechanical parameters are slightly changing in the function of the acoustic load (load current and voltage are changing, equivalent impedance is changing, ferrite core properties are current dependent…). Cases B) and D) are very good for ultrasonic cleaning, Sonochemistry and other liquid processing applications, as well as for wide band and multifrequency, large sweeping operating regimes. Transducers operating in regimes described by B) and D) are often producing extraordinary effects, which can not be produced by regimes A) and C).

Because of security and circuit-simplicity reasons (such as short circuit protection, load current limiting etc.), the most-widely used is series inductive compensation described by cases A) and B).

If the objective is to make an ideal series and/or parallel inductive compensation applied on the same piezoelectric converter (of course, not in the same time), in order to get the widest possible bandwidth and symmetrical distribution of Low and High electrical resonant points (cases A and C), we will notice that (experimentally found) series and parallel inductances are mutually different, and that always a parallel inductance will be higher than series inductance, while relevant and mutually corresponding frequency intervals (between characteristic resonant points) would stay approximately equal. Just to get a rough idea about what means such Ideal and Symmetrical piezoelectric impedance matching in both resonances see the picture below.

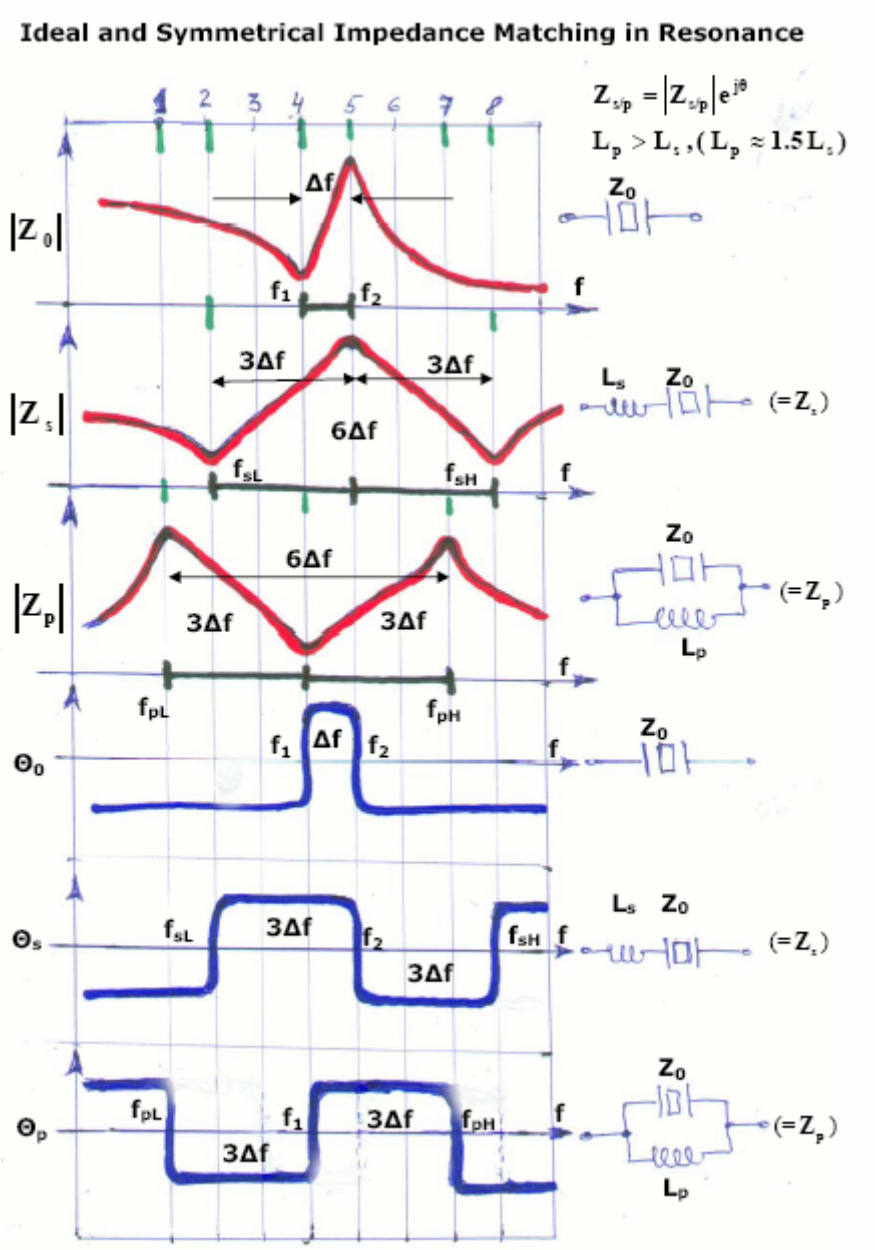

The purpose of making inductive compensation of piezoelectric converters is not only to enable them operating efficiently on a stable (constant) resonant frequency. Applying proper inductive compensation (or combined parallel and series inductive compensation) we can also make converter operating efficiently in a relatively large frequency interval (for instance in the interval between series and parallel resonant frequency), maximize active (or real) output converter-power, and control particular mechanical output/s such as: output oscillatory speed, acceleration and amplitude. In cases when making acoustically well-matched emitter-receiver transducers (or coupled sensors), we will try to realize that $\mathbf{f_{sL} \cong f_{pL}}$, $\mathbf{f_{sH} \cong f_{pH}}$ (see later **Fig. 4.1-3.3**).

Let us take as an example a single (non-loaded) piezoceramic, PZT8 ring. All equivalent-models data (regarding its first, radial resonant mode) are given in T. 4.1-1 (measured using Network Impedance Analyzer HP4194A). For such (and any other) piezoelectric converter we can find many different equivalent-models, depending how large frequency interval we consider as relevant for our modeling.

T. 4.1-1 Piezoelectric Converter Models (Ultrasonic Welding Piezoceramics)

Piezoceramic Ring: Vernitron, PZT8, 45 / 89, ∅2" x ∅0.8" x 0.2"

First Radial Resonance Parameters

$f_1 = 32880$ Hz
$f_2 = 34880$ Hz
$|Z\,\text{min.}| = 12.8724\,\Omega$
$|Z\,\text{max.}| = 256.861\,\text{k}\Omega$
$Q_{m10} = 1129$
$Q_{m20} = 1385$

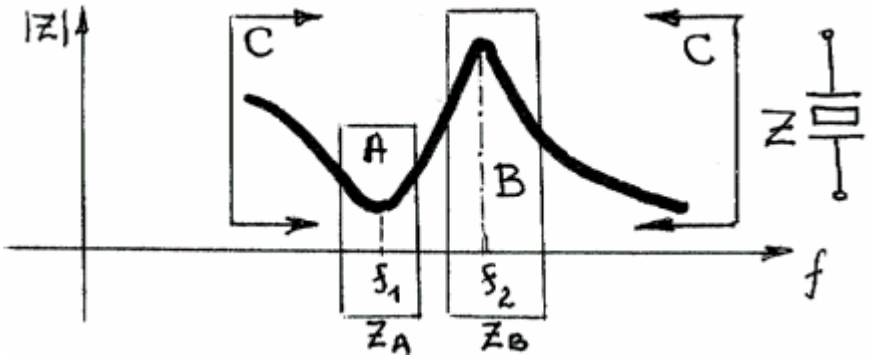

A

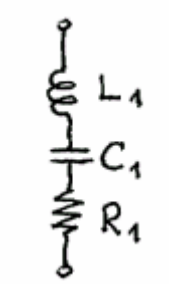

Z_A

$C_1 = 336.812$ pF
$L_1 = 69.5565$ mH
$R_1 = 12.6210\ \Omega$

⇔

A

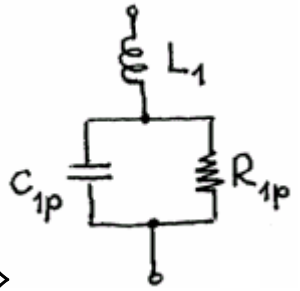

Z_A

$C_{1p} = 336.812$ pF
$L_1 = 69.5565$ mH
$R_{1p} = 16.8762\ \text{M}\Omega$

B

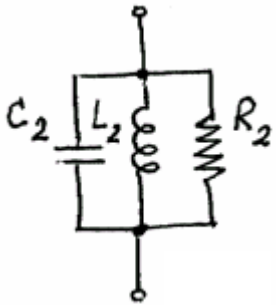

Z_B

$C_2 = 24.2667$ nF
$L_2 = 857.904\ \mu$H
$R_2 = 260.045\ \text{k}\Omega$

⇔

B

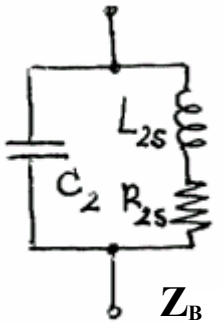

Z_B

$C_2 = 24.2667$ nF
$L_{2s} = 857.903\ \mu$H
$R_{2s} = 142.611\ \text{m}\Omega$

C

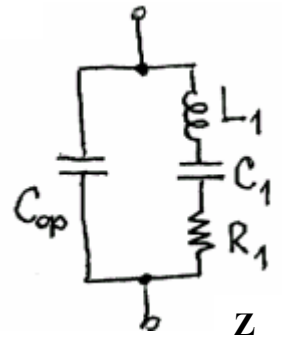

Z

$C_{op} = 2.68554$ nF
$C_1 = 336.552$ pF
$L_1 = 69.6164$ mH
$R_1 = 12.741\ \Omega$

⇔

C

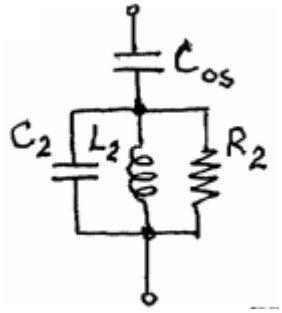

Z

$C_{os} = C_{op} + C_1 =$
$= 3.0221$ nF
$C_2 = 24.26$ nF
$L_2 = 857.9\ \mu$H
$R_2 = 260.045\ \text{k}\Omega$

We can now, experimentally, make the perfect inductive matching (inductive compensation) using the same piezoceramic ring (or piezoelectric converter) presented in T. 4.1-1, and find the best values for series and parallel compensating inductances.

Let us create the equivalent circuit, Fig. 4.1-2, a) that corresponds to series inductive compensation (see Fig. 4.1-1, a) and Fig. 4.1-3.1), and equivalent circuit, Fig. 4.1-2, b) that corresponds to parallel inductive compensation (see Fig. 4.1-1, b), and Fig. 4.1-3.2). The series and parallel compensating inductances are experimentally found by satisfying the criteria of optimal inductive matching, creating large and symmetrically shaped impedance curve around parallel and/or series resonant frequency (or making that: $\mathbf{L_s \Rightarrow (f_{SH} - f_2 \cong f_2 - f_{SL})}$, $\mathbf{L_p \Rightarrow (f_{PH} - f_1 \cong f_1 - f_{PL})}$, see Fig. 4.1-3.1 and Fig. 4.1-3.2). All measurements and model data are also presented on the Fig. 4.1-2.

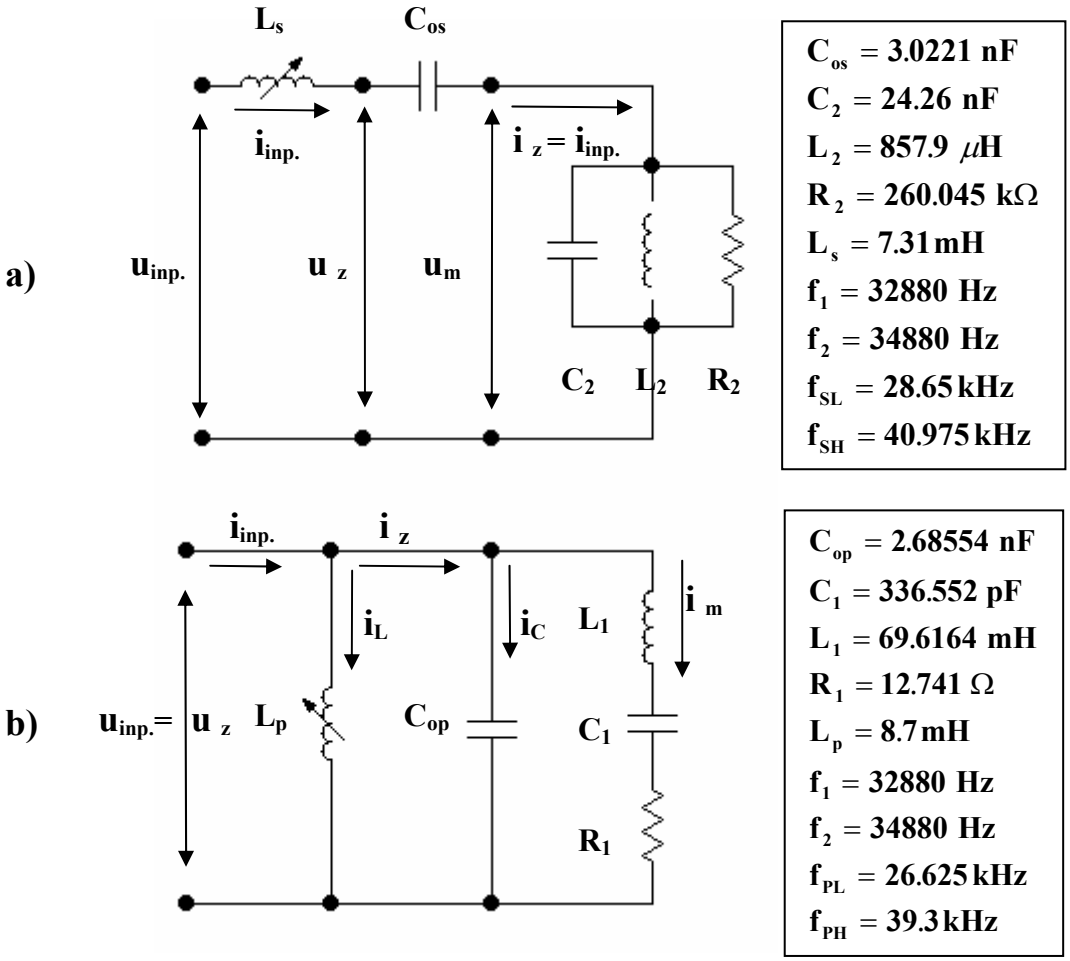

Fig. 4.1-2 Series, a), and Parallel, b), Inductive Compensation Equivalent circuits for the converter from T. 4.1-1.

We shall, first, analyze interesting aspects of series inductive compensation, when converter (from T. 4.1-1) operates in its parallel mechanical resonance f_2 (Fig. 4.1-1, a), Fig. 4.1-2, a) and Fig. 4.1-3.1). The input driving-signal in this case is input voltage $\mathbf{u_{inp.}}$ and mechanical output is represented by motional voltage $\mathbf{u_m}$, effectively

representing converter's output velocity (Fig. 4.1-2, a)). The objective of optimal power and frequency control (and best inductive matching) in this case is to realize linear dependence between $\mathbf{u_{inp.}}$ and $\mathbf{u_m}$, or to make them mutually equal and in phase (see Fig. 4.1-3.1, e) and f)), in the largest possible frequency interval ($\Delta\mathbf{f} = (\mathbf{f_{SH}} - \mathbf{f_2}) \cong (\mathbf{f_2} - \mathbf{f_{SL}}) \approx \mathbf{6.15\,kHz}$, $\Delta\mathbf{f_0} = (\mathbf{f_2} - \mathbf{f_1}) = \mathbf{2\,kHz}$, $\mathbf{f_{SH}} - \mathbf{f_{SL}} = \mathbf{2}\Delta\mathbf{f} \approx \mathbf{6}\Delta\mathbf{f_0} \cong \mathbf{12.3\,kHz}$), while having parallel mechanical resonance $\mathbf{f_2}$ in the middle point of that interval ($\mathbf{f_2} \approx \mathbf{0.5}(\mathbf{f_{SH}} + \mathbf{f_{SL}})$). This way, by controlling the input voltage we are effectively controlling the output velocity. Of course, in order to control the input voltage $\mathbf{u_{inp.}}$ we need to detect converter motional voltage $\mathbf{u_m}$, and to use it as the feedback information for automatic, closed-loop regulation. In high power ultrasonics world is more commonly found the explanation that when keeping $\mathbf{u_m}$ constant we are keeping the converter output (displacement) amplitude constant. In reality, since (usually) high power converters operate on a constant resonant frequency ($\mathbf{f_2}$ = const., PLL controlled), this is the same because if peak velocity-amplitude is $\mathbf{v_p}$ = const., then the peak converter displacement will be $\mathbf{a_p = v_p / 2\pi f_2}$ = Const.

Now, we can analyze interesting aspects of parallel inductive compensation, when converter (from T. 4.1-1) operates in its series mechanical resonance $\mathbf{f_1}$ (Fig. 4.1-1, a), Fig. 4.1-2, b) and Fig. 4.1-3.2). The input driving-signal in this case is input current $\mathbf{i_{inp.}}$ and mechanical output is represented by motional current $\mathbf{i_m}$, effectively representing converter's output force (Fig. 4.1-2, b)). The objective of optimal power and frequency control (and best inductive matching) in this case is to realize linear dependence between $\mathbf{i_{inp.}}$ and $\mathbf{i_m}$, or to make them mutually equal and in phase (see Fig. 4.1-3.2, e) and f)), in the largest possible frequency interval ($\Delta\mathbf{f} = (\mathbf{f_{PH}} - \mathbf{f_1}) \approx (\mathbf{f_1} - \mathbf{f_{PL}}) \approx \mathbf{6.3\,kHz}$, $\Delta\mathbf{f_0} = (\mathbf{f_2} - \mathbf{f_1}) = \mathbf{2\,kHz}$, $\mathbf{f_{PH}} - \mathbf{f_{PL}} = \mathbf{2}\Delta\mathbf{f} \approx \mathbf{6}\Delta\mathbf{f_0} \cong \mathbf{12.6\,kHz}$), while having series mechanical resonance $\mathbf{f_1}$ in the middle point of that interval ($\mathbf{f_1} \approx \mathbf{0.5}(\mathbf{f_{PH}} + \mathbf{f_{PL}})$). This way, by controlling the input current we are effectively controlling the output force. Of course, in order to control the input current $\mathbf{i_{inp.}}$ we need to detect converter motional current $\mathbf{i_m}$, and to use it as the feedback information for automatic, closed-loop regulation. In high power ultrasonics world is more commonly found the explanation that when keeping $\mathbf{i_m}$ constant we are keeping the converter output (displacement) amplitude constant. In reality, since (usually) high power converters operate on a constant resonant frequency ($\mathbf{f_1}$ = const., PLL controlled), this is the same because if peak force-amplitude is $\mathbf{F_p}$ = const., then the peak converter displacement will be $\mathbf{a_p = F_p / (2\pi f_1)^2}$ = Const..

All Impedance-Phase and Transfer function plots on Fig. 4.1-3.1 and Fig. 4.1-3.2 are realized exactly for the same converter from T. 4.1-1, using models and data given on Fig. 4.1-2, a) and b). Measurements (and inductive tuning) are originally made using Network Impedance Analyzer HP 4194A, and in order to present them in a very systematic and summary form, all model data and component values are introduced in the corresponding P-Spice (and Orcad) models, resulting with Fig. 4.1-3.1 and Fig. 4.1-3.2. Doing this way (using P-Spice models) we are able to reconstruct electromechanical transfer functions (Fig. 4.1-3.1, e), f) and Fig. 4.1-3.2, e), f)), because **otherwise we can not directly measure such transfer functions**. We also see that in the area of series and/or parallel resonant frequency, transfer functions are almost flat ($A_{tr.}$ (=) Gain (=) 1 (=) 0 dB), and phase of the transfer

function/s is equal zero, in a large frequency interval (almost between $\mathbf{f_L}$ and $\mathbf{f_H}$), what makes motional voltage and motional current to be ideal parameters for mechanical output control (or for converter output power control).

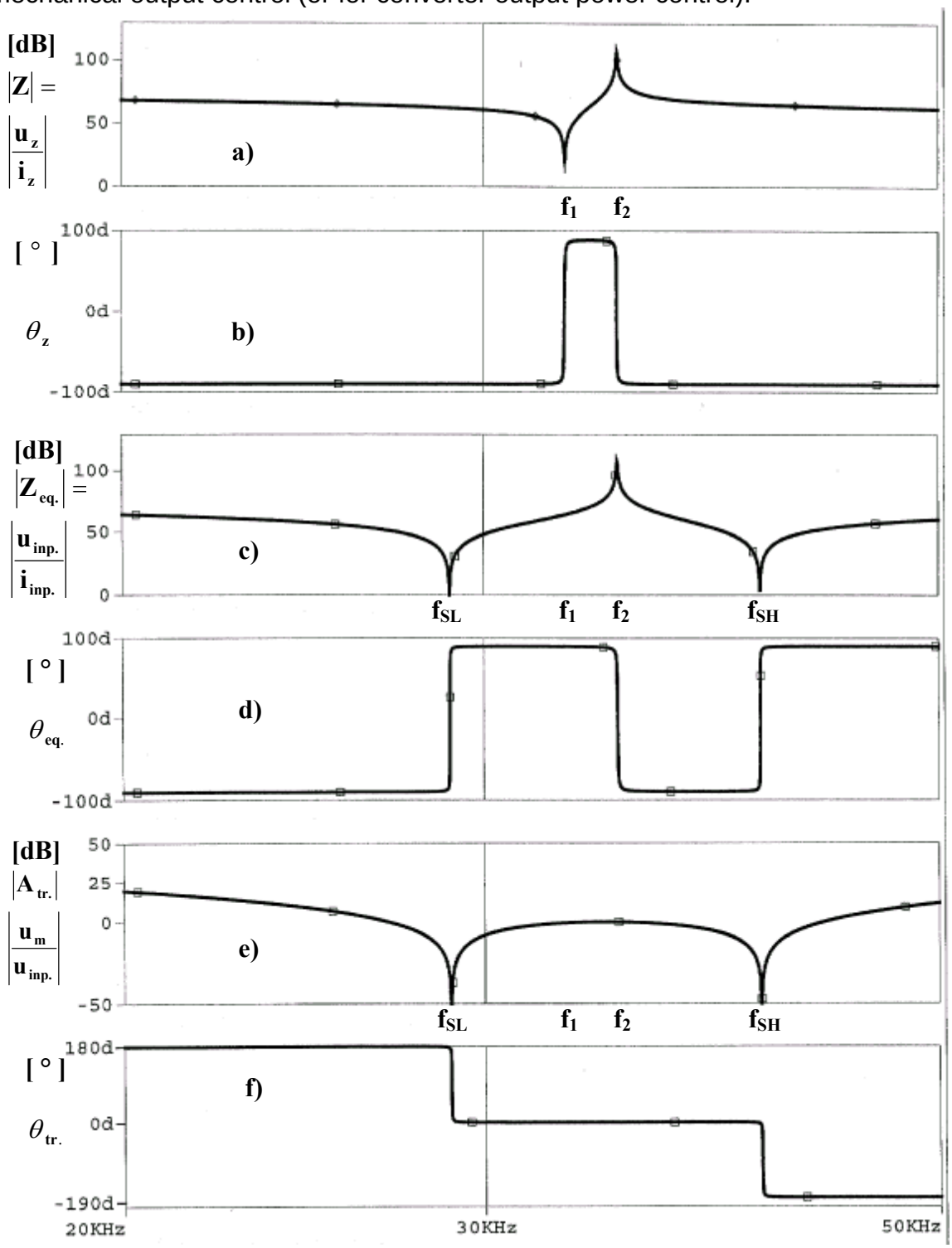

Fig. 4.1-3.1 Series Inductive Compensation Impedance-Phase Curves (corresponds to converter data from T. 4.1-1 and Fig. 4.1-2, a))

a) Converter Impedance vs. Frequency, b) Converter Phase vs. Frequency, c) Equivalent Input Impedance vs. Frequency, d) Equivalent Input Phase vs. Frequency, e) Motional Transfer Function vs. Frequency, f) Phase of the Motional Transfer Function vs. Frequency.

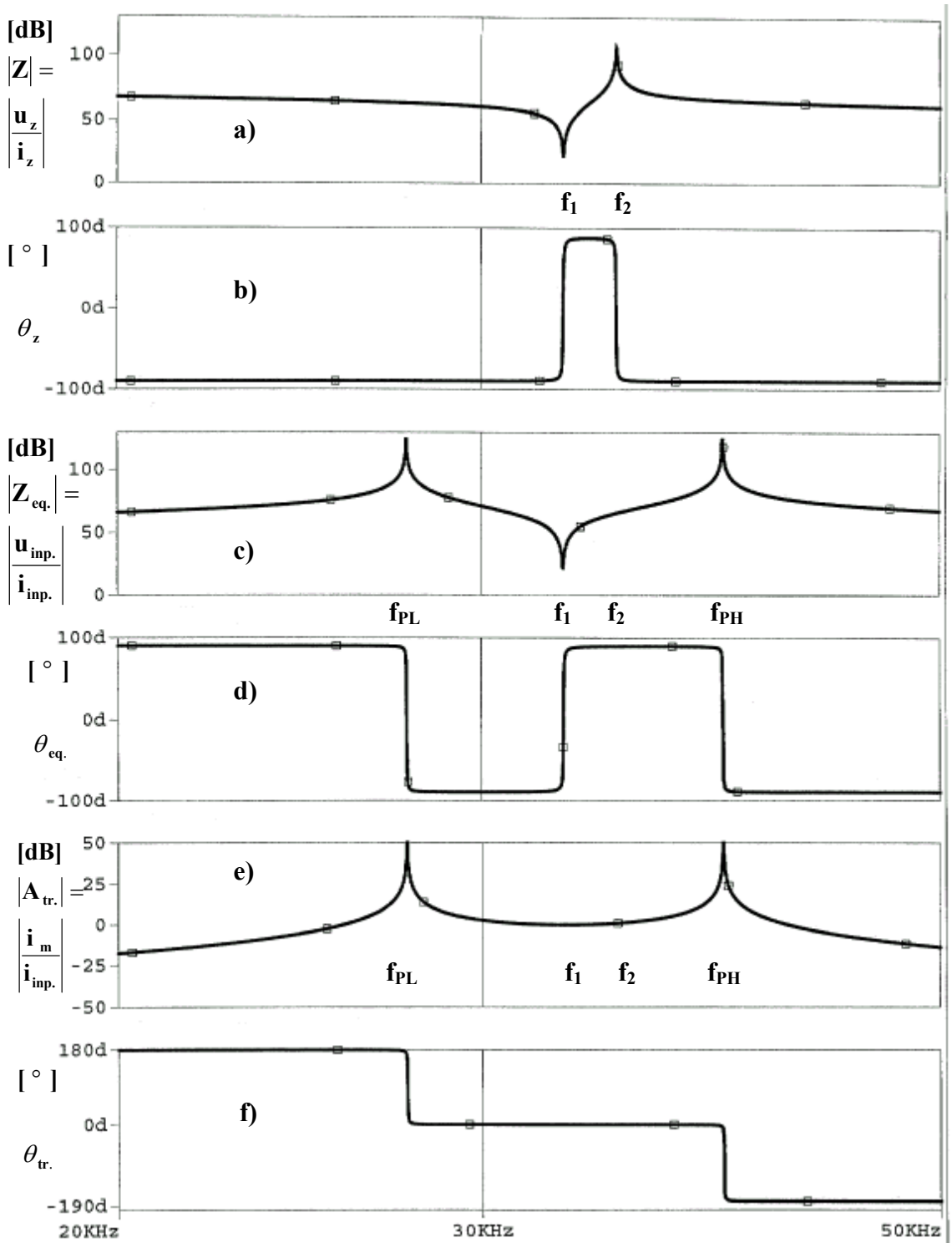

Fig. 4.1-3.2 Parallel Inductive Compensation Impedance-Phase Curves (corresponds to converter data from T. 4.1-1and Fig. 4.1-2, b))
a) Converter Impedance vs. Frequency, b) Converter Phase vs. Frequency, c) Equivalent Input Impedance vs. Frequency, d) Equivalent Input Phase vs. Frequency, e) Motional Transfer Function vs. Frequency, f) Phase of the Motional Transfer Function vs. Frequency.

Piezoelectric Converters Operating as Sensors

From flat and zero-phase transfer-functions (Fig. 4.1-3.1, e), f) and Fig. 4.1-3.2, e), f)), we also see that efficient and large frequency sweeping (between $\mathbf{f_L}$ **and** $\mathbf{f_H}$) can be applied when converter operates in any of its resonance area. This is particularly interesting situation for acoustic or ultrasonic sensors design, since we can extend operating sensor/s bandwidth, booth in the transmitting and receiving mode. When we design well-matched sensors (transmitter-receiver couple), we usually search to find series and parallel inductive compensation that makes: $(\mathbf{f_{SH}} - \mathbf{f_{SL}}) \cong (\mathbf{f_{PH}} - \mathbf{f_{PL}})$, $(\mathbf{f_{SL}} \cong \mathbf{f_{PL}}) = \mathbf{f_L}$, $(\mathbf{f_{SH}} \cong \mathbf{f_{PH}}) = \mathbf{f_H}$, $(\mathbf{f_H} - \mathbf{f_1}) \cong (\mathbf{f_2} - \mathbf{f_L})$. One of excellent examples regarding piezoelectric transmitter-receiver matching and tuning (in air), Fig. 4.1-3.3, can be found in the catalogue of Massa Products Corporation, company specialized in producing different piezoelectric sensors and transducers (Massa Products Corporation, 280 Lincoln Street, Hingham, MA 02043, USA).

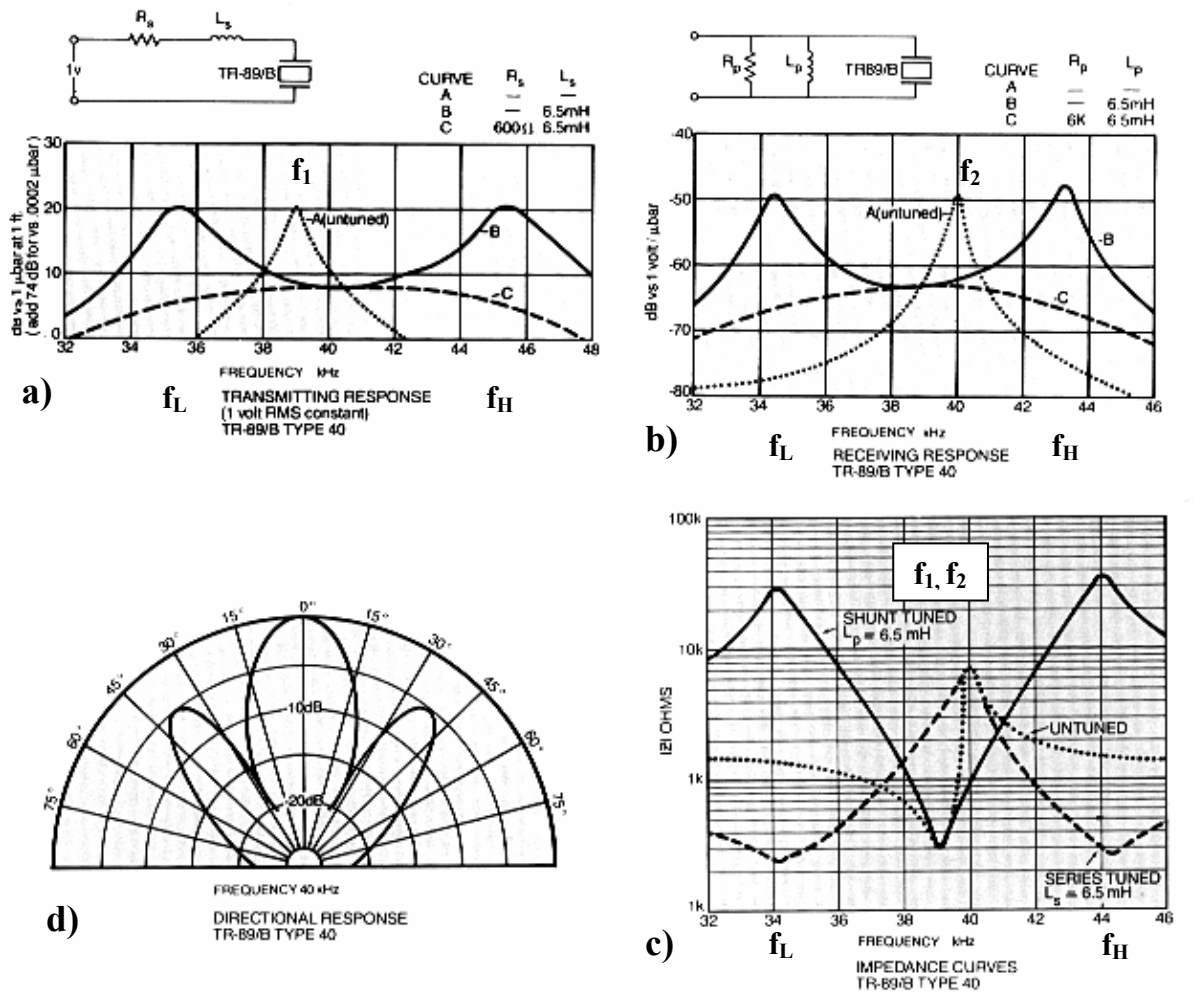

Fig. 4.1-3.3 Series and Parallel Inductive Compensation Applied for Tuning Transmitter-Receiver Sensor-Couple TR-89/B, Produced by Massa

a) Transmitting Sensor Response with Series Tuning
b) Receiving Response with Parallel Tuning
c) Equivalent Impedance Curves (untuned sensor, series-tuned sensor, and parallel or shunt-tuned sensor)
d) Sensor's Directional Response

Series Compensation

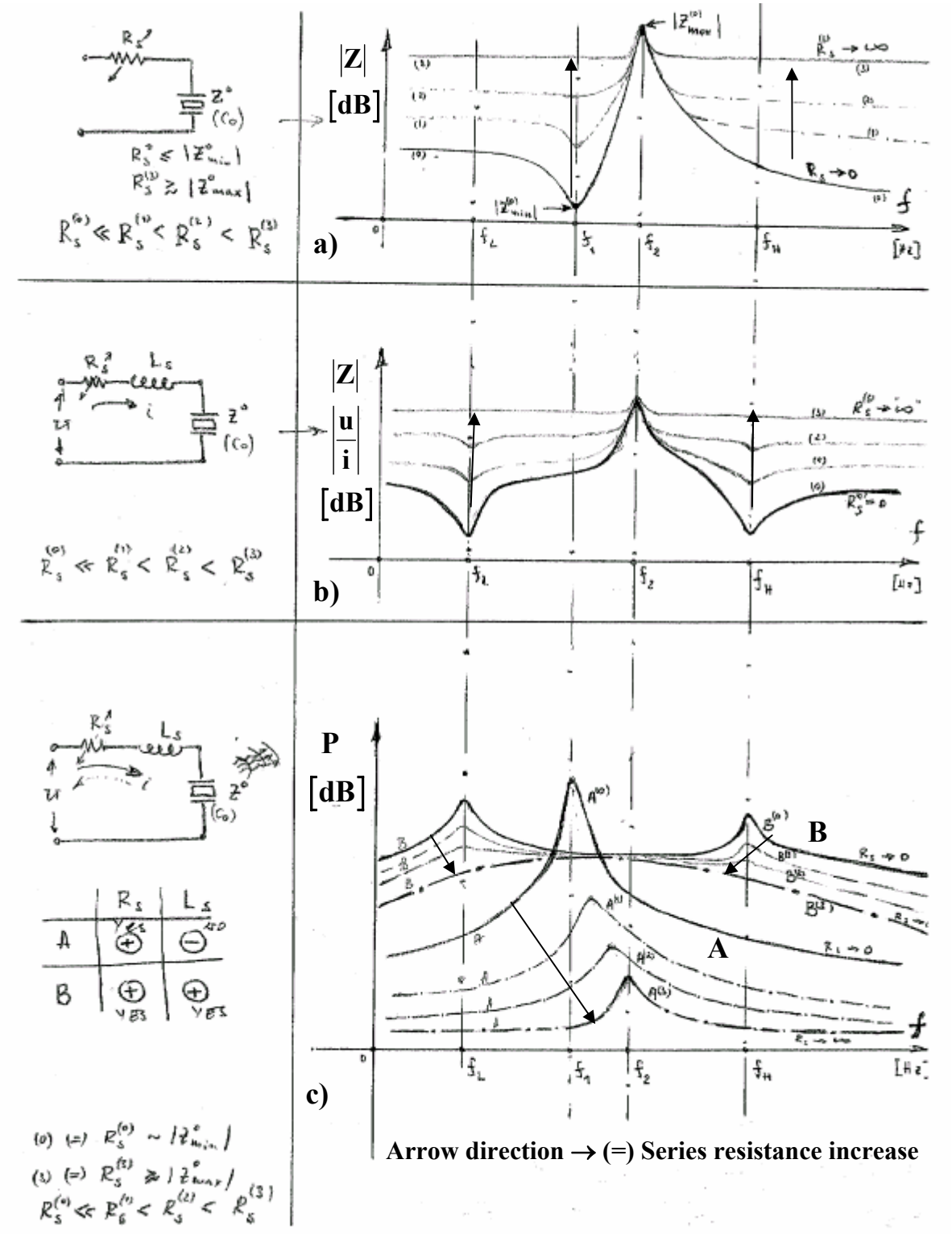

Fig. 4.1-3.4 Transmitter Tuning with Series Compensation

a) Evolution of Equivalent Converter Impedance in Series with a Resistor.

b) Evolution of Equivalent Converter Impedance in Series with a Resistor and Inductance.

c) Evolutionary Transmitting Sensors Response (or pressure generated in front of a sensor): -under a), only sensor and series resistance (=) case A; -and under b), sensor, series resistance and series inductance (=) case B.

Usually, when we use an acoustic (piezoelectric) sensor as a transmitter, we apply series inductive compensation, Fig. 4.1-3.4, since in that case the sound field pressure in front of such sensor is maximized (why this is the case, it will be explained).

We can notice that in case when we have only a sensor in series connection with a variable resistance (Fig. 4.1-3.4, a)), by increasing resistance we are practically eliminating or attenuating sensor series resonance, and only parallel resonance area remains active (see Fig. 4.1-3.4, c), case **A**).

In case if we have series resistance and series inductance connected to a sensor (Fig. 4.1-3.4, b)), we shall get similar equivalent impedance as presented on Fig. 4.1-3.1, c), and with resistance increase, again, only sensor parallel resonance area will remain active.

Now, if we connect such sensor-transmitter (first with series resistance = Case **A** = untuned sensor, and then with series resistance and series inductance = Case **B** = tuned sensor) to a constant rms. voltage-source with variable frequency sinusoidal signal, (Fig. 4.1-3.4, c)), and if we measure the sound pressure in front of the sensor (in function of frequency), we shall see that **pressure peaks are always produced in zones where equivalent impedance (sensor impedance + resistor, or sensor + resistor + inductance) is minimal, or in all impedance zones where a kind of series resonance is present**. All series resonance zones (or zones of minimal impedance: in $\mathbf{f_1}$, when sensor is non-tuned, and in $\mathbf{f_{SL}}$, $\mathbf{f_{SH}}$ when sensor is series inductance tuned) are high current consuming, because sensor current increases with equivalent-impedance decrease, and by analogy CURRENT-FORCE, we can conclude that **sensor in series resonance will be a high (or dominant) force-source** (or high pressure source, since pressure is equal to force per surface area).

Obviously, applying VOLTAGE-VELOCITY analogy, we can also conclude that piezoelectric **sensors or converters driven in zones of high equivalent impedances, or in zones of parallel resonances ($\mathbf{f_{PL}}$, $\mathbf{f_2}$, $\mathbf{f_{PH}}$), are presenting dominant velocity-sources**.

On the Fig. 4.1-3.4, c) we can see that series-resistance increase will produce in case **A**), when we have only a sensor with series resistance, progressive diminishing of output pressure and frequency shift (of maximal pressure) toward sensor parallel resonant-frequency $\mathbf{f_2}$, and in case **B**), when we have sensor, series resistance and series inductance, certain diminishing of output pressure, and pressure-curve flattening will be experienced (applicable in cases when we need to create a more-linear transmitter response-function: see also Fig. 4.1-3.3, a)).

Parallel Compensation

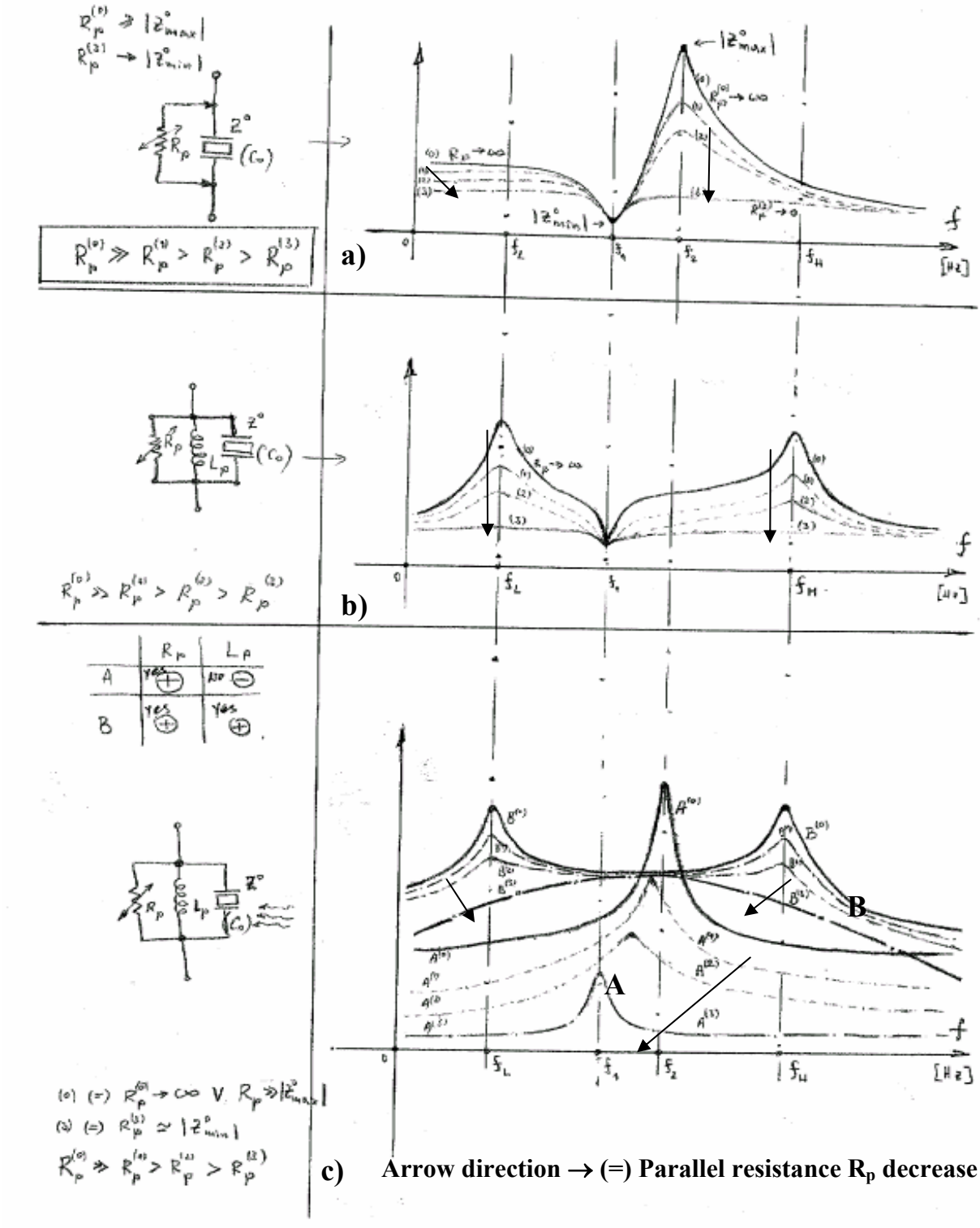

Fig. 4.1-3.5 Receiver Tuning with Parallel Compensation

a) Evolution of Equivalent Converter Impedance in Parallel with a Resistor.

b) Evolution of Equivalent Converter Impedance in Parallel with a Resistor and Inductance.

c) Evolutionary Receiving Sensors Response (or voltage output generated by sensor): -under a), only sensor and parallel resistance (=) case A; -and under b), sensor, parallel resistance and parallel inductance (=) case B.

When we use an acoustic (piezoelectric) sensor as a receiver, we apply parallel inductive compensation, Fig. 4.1-3.5, since in that case the voltage output and receiving sensitivity of such sensor is maximized (why this is the case, it will be explained).

We can notice that in case when we have only a sensor in parallel connection with a variable resistance (Fig. 4.1-3.5, a)), by decreasing resistance we are practically eliminating or attenuating sensor parallel resonance, and only series resonance area remains active (see Fig. 4.1-3.5, c), case **A**).

In case if we have parallel resistance and parallel inductance connected to a sensor (Fig. 4.1-3.5, b)), we shall get similar equivalent impedance as presented on Fig. 4.1-3.2, c and Fig. 4.1-3.3 c), and with resistance decrease, again, only sensor series resonance area will remain active.

Now, if we test such sensor (first with parallel resistance = Case **A** = non-tuned sensor, and then with parallel resistance and parallel inductance = Case **B** = tuned sensor) as a receiver of variable-frequency, sinusoidal pressure-signal, (Fig. 4.1-3.5, c)), and if we measure the voltage output produced by sensor-receiver (in function of frequency), we shall see that **output voltage peaks are always produced in zones where equivalent impedance (sensor impedance + parallel resistor, or sensor + parallel resistor + parallel inductance) is maximal, or in all impedance zones where a kind of parallel resonance is present**. All parallel resonance zones (or zones of maximal impedance: in $\mathbf{f_2}$, when sensor is non-tuned, and in $\mathbf{f_{PL}}$, $\mathbf{f_{PH}}$, when sensor is parallel inductance tuned) are low current consuming, because sensor current decreases with equivalent-impedance increase (and voltage on the sensor input terminals will increase), and by analogy VELOCITY-VOLTAGE, we can conclude that **sensor in parallel resonance will be a dominant velocity-sensitive sensor (or receiver)**.

Obviously, applying FORCE-CURRENT analogy, we can also conclude that piezoelectric **sensors or converters (used as receivers), in zones of low equivalent impedances, or in zones of series resonances ($\mathbf{f_{SL}}$, $\mathbf{f_1}$, $\mathbf{f_{SH}}$), are presenting dominant (oscillatory) force-receivers.**

On the Fig. 4.1-3.5, c) we can see that parallel-resistance decrease will produce in case **A**), when we have only a sensor with parallel resistance, progressive diminishing of output sensor-voltage and frequency shift (of maximal, detected voltage) toward sensor series resonant-frequency $\mathbf{f_1}$, and in case **B**), when we have sensor, parallel resistance and parallel inductance, certain diminishing of output voltage, and sensitivity-curve flattening will be experienced (applicable in cases when we need to create a more-linear receiver response-function: see also Fig. 4.1-3.3, b)).

For sensors and converters coupling and inductive matching purposes (presented on Fig. 4.1-3.1 until Fig. 4.1-3.5), we often need to shift characteristic Low and High-frequency resonant frequencies, $\mathbf{f_L}$, $\mathbf{f_H}$. If we take as referent points converter's natural series and parallel resonance/s ($\mathbf{f_1}$, $\mathbf{f_2}$), it can be found (experimentally and by software simulation, or calculating using Electric Circuits rules) that, when series

and/or parallel inductance/s (L_s, L_p) is/are increasing, then f_L, f_H are coincidently decreasing (f_H would asymptotically decrease from certain high frequency point toward f_2, and f_L would decrease toward very low frequencies, below f_1), see Fig. 4.1-3.6. In the same time, the interval $f_H - f_L$ would stay almost constant, regardless from L_s, L_p.

In other words, when making series inductive compensation, regardless of the value of L_s, parallel resonant frequency f_2 will always stay the same (constant, or unchanged by L_s), and only f_{SH} & f_{SL} will be influenced (shifted) by variable L_s, but their difference will stay almost constant, $f_{SH} - f_{SL} \approx \mathbf{Const.}$.

Also, when making parallel inductive compensation, regardless of the value of L_p, series resonant frequency f_1 will always stay the same (constant, or unchanged by L_p), and only f_{PH} & f_{PL} will be influenced (shifted) by variable L_p, but their difference will stay almost constant, $f_{PH} - f_{PL} \approx \mathbf{Const.}$.

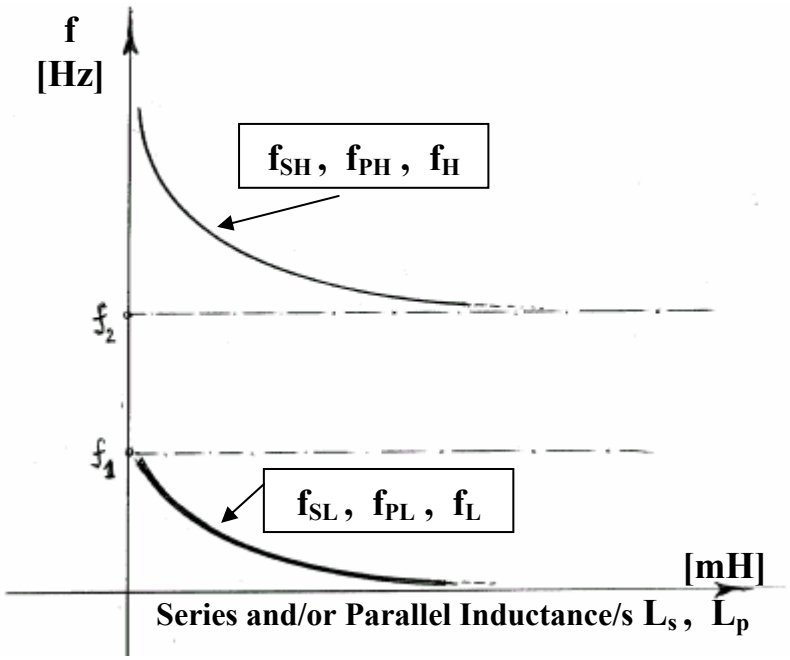

Fig. 4.1-3.6 Additional Resonances Generated by Inductive Compensation In Function of L_s and L_p (only qualitatively presented, and applicable to all situations from: Figs. 4.1-3.1 until 4.1-3.5)

Even experienced people working in Ultrasonic engineering are sometimes considering that they are changing series or parallel resonant frequency, f_1, f_2, by adjusting the values of parallel or series inductances, L_p, L_S, but in realty they are only changing (or shifting) f_L & f_H, and often operating converters in some of the side-band frequencies f_L **or** f_H, being convinced that converter is operating on its series or parallel resonant frequency (because, depending on the selected value/s of L_p, L_S, it can happen that either $f_L \approx f_1$ or $f_H \approx f_2$). This situation is very much typical for ultrasonic cleaning converters, when many (of mutually similar) converters

are connected in parallel, and **when relatively low value of series inductive compensation is applied**, effectively realizing that the best operating frequency would be $\mathbf{f_{oper.} = f_{SL} \approx f_1}$ (and this looks like series resonance operating regime).

Also in cases of heavily-attenuated transducers and sensors (like sonar transducers, or NDT transducers…), using Impedance-Phase measurements, we could realize that such structures are dominantly reacting like being capacitive components (with internal losses), and we often find in literature and ultrasonic engineering publications an oversimplified transducers' modeling, using only two components: a series or parallel connection between a capacitance and resistance (treated as dual, mutually equivalent models). Accepting this non-selective approach, inductive compensation becomes just a matter of neutralizing series or parallel capacitance for certain operating frequency, but comparing such simplified methodology with the methodology described in this paper, we can realize how much of essential matter regarding optimal transducer matching and maximal transducers' efficiency is simply lost.

4.2 Piezoelectric Converters Operating High Power

All models and theoretical conclusions regarding different inductive matching situations, presented on Fig. 4.1-1, until Fig. 4.1-3.6, are equally valid for all piezoelectric converters, sensors, transmitters and receivers.

The important difference between sensor operating regimes and high power regimes is mostly in belonging power-supply electronics. In case of sensors, we usually have very low electric-power consumption (in the range of mW or μW), and sensor would never make problems to driving electronics regarding optimal impedance and power matching, or regarding questions like: how much of active power we are delivering to the sensor-transmitter, and how much of reactive power is reflected back to driving electronics (since sensor voltages and currents would be too low, or too far from the safe operating limits of involved electronics).

The situation becomes quite different when we should apply hundreds or thousands of watts of output electric power to a single (high mechanical quality factor) converter. In such situations we prefer to deliver almost all electric-power as the Real or Active Power, and to have minimal Reactive Power reflected back to driving electronics (in order to avoid converter overheating and damaging high power electronic components). Practically, we should find a way to compensate a converter (loaded or unloaded) to present purely resistive load (or purely resistive impedance) to its driving electronics (in the operating frequency zone), of course while driving electronic output impedance can also be considered as resistive. There are different impedances and power-matching techniques to realize optimal and maximal power transfer conditions.

The most widely known converter resonant operating regimes are when converter operates exactly in its series, or parallel mechanical resonance, which will be analyzed in details. Also, converter can operate high power in certain (relatively large) frequency interval/s if we find a way to make resistive (or zero phase) impedance and power matching between the generator and converter (in such frequency interval/s).

Converter Operating High Power in Series Resonance

Applying parallel inductive compensation $\mathbf{L_p}$, we shall enable converter to operate in its series mechanical resonance $\mathbf{f_1}$ (or in impedance minimum zone). From Fig. 4.1-3.2, c) and d), we can see that equivalent impedance of **Converter & Parallel Inductance** has resistive character only when phase function, Fig. 4.1-3.2, d), is crossing zero line in $\mathbf{f_1}$. Consequently, applying PLL (for resonant frequency control), in order to keep the input current and voltage in phase, at $\mathbf{f_1}$ (measured on the input of the equivalent impedance, Fig. 4.1-3.2, c)), we shall make such (equivalent) load being low resistive impedance. The next important design task, regarding optimal power transfer, is that equivalent load impedance should be matched (or should be equal) to the internal impedance of driving electronics (of ultrasonic power supply, or ultrasonic generator, or power oscillator). This objective we usually realize designing proper primary-to-secondary-ratio of a ferrite-transformer, and adjusting low load impedance to the level of the internal impedance of driving electronics. In order to control output converter power (or output force) under loading, we should also find the best way to extract the motional current $\mathbf{i_m}$ from the output power circuit, and bring this voltage as the feedback to the main supply, or DC supply voltage control unit, effectively keeping $\mathbf{i_m}$ constant (most often by means of PWM regulation), regardless of load variations.

Since converter impedance in no-load conditions, and in series resonance (in air) is usually very low, converter can dissipate relatively high energy, and it cannot continuously oscillate long time without applying forced cooling, or without electronic protection circuit that will reduce converter's current (usually by means of PWM). When converter is mechanically loaded (operating in series resonance), its equivalent impedance is increasing, proportionally with the increase of applied load. Consequently, when converter is operating **in series resonance, we should first apply the load, and then start oscillations** (or at least apply the load and start oscillating converter in the same time), and we should know that **this operating regime is convenient for moderate and heavy-duty, relatively stable acoustical loads.**

We could also operate converter (with parallel inductive compensation) in two of its side-band parallel-resonance frequencies $\mathbf{f_{PL}}$ **or** $\mathbf{f_{PH}}$, but only operating in $\mathbf{f_{PH}}$ can give relatively acceptable results (efficient and stable, high power output) in cases when we adjust parallel inductance to produce $\mathbf{f_{oper.} = f_{PH} \approx f_2}$ (see Fig. 4.1-3.6). Also the philosophy of output ultrasonic power regulation, when operating a converter in $\mathbf{f_{PL}}$ **or** $\mathbf{f_{PH}}$, would not be the same as operating it in $\mathbf{f_2}$.

Let us now analyze a parallel-inductance compensated converter, operating on its series resonant frequency. The equivalent circuit of such operating regime, valid only for very close vicinity of converter's series resonance is presented on Fig. 4.2-1. The meaning of parallel inductive compensation in this case is to eliminate all reactive circuit elements such as capacitances and inductances (of course only for a constant frequency $\mathbf{f_1}$, when circuit is operating in resonant regime). This can be realized on the way that $\mathbf{L_p}$ should be chosen to create parallel resonance with $\mathbf{C^*_{op}}$ on $\mathbf{f_1}$ (when $\mathbf{L_p}$ and $\mathbf{C^*_{op}}$ would present very high equivalent impedance), and

naturally (in the same time) $\mathbf{L_1}$ and $\mathbf{C_1}$ would create series resonance, on $\mathbf{f_1}$, that has very low (or zero) equivalent impedance.

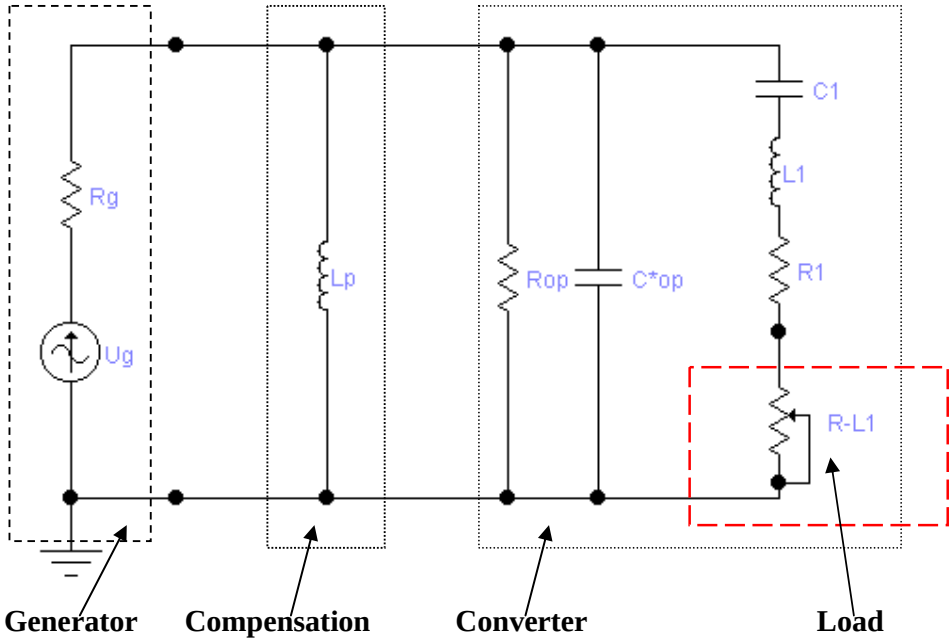

Fig. 4.2-1 Converter inductively compensated to operate in series resonant frequency $(\mathbf{L_p C_{op} \cong L_1 C_1) \cong 1 / 4\pi^2 f_1^2}$

This way, we can practically eliminate all reactive elements $\mathbf{L_p}$, $\mathbf{C^*_{op}}$, $\mathbf{L_1}$ and $\mathbf{C_1}$ from the circuit given on Fig. 4.2-1 (by satisfying $(\mathbf{L_p C_{op} \cong L_1 C_1) \cong 1 / 4\pi^2 f_1^2}$), and create a more simplified equivalent circuit (which has only resistive elements), given on Fig. 4.2-2, a). Since $\mathbf{R_{op}}$ usually presents very high resistance (in the range of several MΩ, or higher), we can additionally approximate the same circuit to its final version given on the Fig. 4.2-2, b).

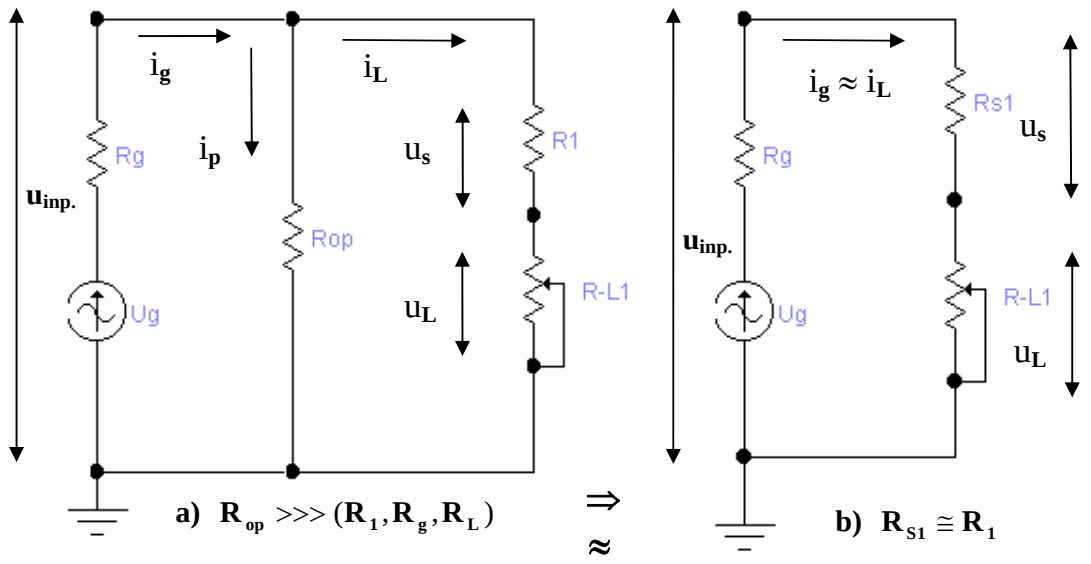

Fig. 4.2-2 Compensated converter operating on series resonant frequency

Now we can analyze circuits presented on Fig. 4.2-1 and Fig. 4.2-2, and find all characteristic currents and voltages,

$$\mathbf{i_g = i_p + i_L = \frac{u_{inp.}}{R_{op}\|(R_1+R_L)} \cong \frac{u_{inp}}{R_1+R_L} \cong i_L, (R_L = R_{L-1})}$$

$$\mathbf{u_{inp.} = U_g - R_g i_g = R_{op} i_p = (R_1+R_L) i_L =}$$

$$\mathbf{= \frac{R_{op}\|(R_1+R_L)}{R_g + R_{op}\|(R_1+R_L)} U_g \cong \frac{R_1+R_L}{R_g+R_1+R_L} U_g = \frac{R_1+R_L}{R_i+R_L} U_g, (R_i = R_g + R_1)} \qquad (4.2\text{-}1)$$

$$\mathbf{u_s = \frac{R_1}{R_1+R_L} u_{inp.} \cong R_1 i_g, u_L = \frac{R_L}{R_1+R_L} u_{inp.} \cong R_L i_g}$$

Electrical power losses dissipated on the parallel resistance $\mathbf{R_{op}}$ can be found as,

$$\mathbf{P_{eo} = R_{op} i_p^2 = \left[\frac{R_1+R_L}{R_1+R_L+R_{op}}\right]^2 i_g^2 = \frac{u_{inp.}^2}{R_{op}} =}$$

$$\mathbf{= \frac{1}{R_{op}\left[1+\frac{R_g}{R_1+R_L}\left(1+\frac{R_1+R_L}{R_{op}}\right)\right]} U_g^2 \cong \frac{(R_1+R_L)^2}{R_{op}(R_g+R_1+R_L)^2} U_g^2 =} \qquad (4.2\text{-}2)$$

$$\mathbf{= \frac{(R_1+R_L)^2}{R_{op}(R_i+R_L)^2} U_g^2 \approx \frac{(0.5R_i+R_L)^2}{R_{op}(R_i+R_L)^2} U_g^2}$$

Mechanical, internal converter power-losses, are presented by power dissipated on the resistance $\mathbf{R_1}$,

$$\mathbf{P_{m1}} = \mathbf{R_1 i_L^2} = \mathbf{R_1}\left[\frac{\mathbf{1}}{\mathbf{1}+\frac{\mathbf{R_1}+\mathbf{R_L}}{\mathbf{R_{op}}}}\right]^2 \mathbf{i_g^2} = \frac{\mathbf{u_s^2}}{\mathbf{R_1}} = \frac{\mathbf{R_1}}{(\mathbf{R_1}+\mathbf{R_L})^2}\mathbf{u_{inp.}^2} =$$

$$= \frac{\mathbf{1}}{\mathbf{R_1}\left[\mathbf{1}+\frac{\mathbf{R_L}}{\mathbf{R_1}}+\frac{\mathbf{R_g}}{\mathbf{R_1}}(\mathbf{1}+\frac{\mathbf{R_1}+\mathbf{R_L}}{\mathbf{R_{op}}})\right]^2}\mathbf{U_g^2} \cong \qquad (4.2\text{-}3)$$

$$\cong \frac{\mathbf{R_1}}{(\mathbf{R_g}+\mathbf{R_1}+\mathbf{R_L})^2}\mathbf{U_g^2} = \frac{\mathbf{R_1}}{(\mathbf{R_i}+\mathbf{R_L})^2}\mathbf{U_g^2} \approx \frac{\mathbf{0.5R_i}}{(\mathbf{R_i}+\mathbf{R_L})^2}\mathbf{U_g^2}$$

Total power dissipation in a converter is equal to the sum of (electrical and mechanical) loses presented by (4.2-2) and (4.2-3),

$$\mathbf{P_d} = \mathbf{P_{eo}} + \mathbf{P_{m1}} = \mathbf{R_1 i_L^2} = \left[\frac{\mathbf{1}}{\mathbf{R_{op}}} + \frac{\mathbf{R_1}}{(\mathbf{R_1}+\mathbf{R_L})^2}\right]\mathbf{u_{inp.}^2} =$$

$$= \left[\frac{(\mathbf{R_1}+\mathbf{R_L})^2}{\mathbf{R_{op}}} + \mathbf{R_1}\right]\frac{\mathbf{U_g^2}}{(\mathbf{R_g}+\mathbf{R_1}+\mathbf{R_L})^2} \cong \qquad (4.2\text{-}4)$$

$$\cong \frac{\mathbf{R_1}}{(\mathbf{R_g}+\mathbf{R_1}+\mathbf{R_L})^2}\mathbf{U_g^2} = \frac{\mathbf{R_1}}{(\mathbf{R_i}+\mathbf{R_L})^2}\mathbf{U_g^2} = \mathbf{P_{m1}} \approx \frac{\mathbf{0.5R_i}}{(\mathbf{R_i}+\mathbf{R_L})^2}\mathbf{U_g^2}$$

Useful acoustical (active) output power is only the power given to a load resistance $\mathbf{R_{L1}} = \mathbf{R_L}$,

$$\mathbf{P_L} = \mathbf{R_L i_L^2} = \frac{\mathbf{u_L^2}}{\mathbf{R_L}} = \frac{\mathbf{R_L}}{(\mathbf{R_1}+\mathbf{R_L})^2}\mathbf{u_{inp.}^2} =$$

$$= \frac{\mathbf{1}}{\mathbf{R_L}\left[\mathbf{1}+\frac{\mathbf{R_1}}{\mathbf{R_L}}+\frac{\mathbf{R_g}}{\mathbf{R_L}}(\mathbf{1}+\frac{\mathbf{R_1}+\mathbf{R_L}}{\mathbf{R_{op}}})\right]}\mathbf{U_g^2} \cong \qquad (4.2\text{-}5)$$

$$\cong \frac{\mathbf{R_L}}{(\mathbf{R_g}+\mathbf{R_1}+\mathbf{R_L})^2}\mathbf{U_g^2} = \frac{\mathbf{R_L}}{(\mathbf{R_i}+\mathbf{R_L})^2}\mathbf{U_g^2}$$

Now we can calculate the internal electromechanical conversion-efficiency of loaded, $\eta_{\mathbf{emL}}$, and unloaded, $\eta_{\mathbf{emo}}$, converter as,

$$\eta_{emL} = \eta_{em} = \frac{P_{m1}}{P_{m1} + P_{eo}} = \frac{1}{1 + \frac{R_1 + R_L}{R_{op}}},$$

$$\eta_{emo} = (\mathbf{Lim}\,\eta_{emL})_{R_L \to 0} = \mathbf{Lim}\left(\frac{P_{m1}}{P_{m1} + P_{eo}}\right)_{R_L \to 0} = \tag{4.2-6}$$

$$= \mathbf{Lim}\left(\frac{1}{1 + \frac{R_1 + R_L}{R_{op}}}\right)_{R_L \to 0} = \frac{1}{1 + \frac{R_1}{R_{op}}} \cong 1$$

The internal mechanical-to-acoustical conversion-efficiency of loaded converter, η_{ma} is,

$$\eta_{ma} = \frac{P_L}{P_{m1} + P_L} = \frac{R_L}{R_1 + R_L} = \frac{1}{1 + \frac{R_1}{R_L}} \quad . \tag{4.2-7}$$

The total electro-acoustical conversion-efficiency of loaded converter, η_{ea}, is,

$$\eta_{ea} = \eta_{em}\eta_{ma} = \frac{P_{m1}}{P_{m1} + P_{eo}} \frac{P_L}{P_{m1} + P_L} =$$

$$= \frac{R_L}{(R_1 + R_L)(1 + \frac{R_1 + R_L}{R_{op}})} \cong \frac{R_L}{R_1 + R_L} = \tag{4.2-8}$$

$$= \frac{1}{1 + \frac{R_1}{R_L}} = \eta_{ma} \cong \frac{P_L}{P_d + P_L} = \frac{P_L}{P_{eo} + P_{m1} + P_L}.$$

A converter itself, even if it has very high electro-acoustic efficiency, is not sufficient to realize high power output (of acoustic or ultrasonic energy). It is very important to realize proper impedance matching between the generator (as a source of electrical excitation) and the converter, in order to produce high acoustical power output.

Let us first find thermal power losses on the internal generator resistance R_g,

$$P_g = R_g i_g^2 = \frac{R_g}{\left[R_g + \frac{R_1 + R_L}{1 + \frac{R_1 + R_L}{R_{op}}}\right]^2} U_g^2 \cong \tag{4.2-9}$$

$$\cong \frac{R_g}{\left[R_{op} \| (R_1 + R_L)\right]^2} u_{inp.}^2 \cong \frac{R_g}{(R_1 + R_L)^2} u_{inp.}^2$$

The total thermal power losses in generator and converter are,

$$\mathbf{P_{d-tot.}} = \mathbf{P_g} + \mathbf{P_d} = \mathbf{P_g} + \mathbf{P_{eo}} + \mathbf{P_{m1}} =$$
$$= \frac{\mathbf{R_g}}{\left[\mathbf{R_{op}} \| (\mathbf{R_1} + \mathbf{R_L})\right]^2} \mathbf{u}^2_{\mathbf{inp.}} + \left[\frac{\mathbf{1}}{\mathbf{R_{op}}} + \frac{\mathbf{R_1}}{(\mathbf{R_1} + \mathbf{R_L})^2}\right] \mathbf{u}^2_{\mathbf{inp.}} =$$
$$= \frac{\mathbf{R_g} + \mathbf{R_1}}{(\mathbf{R_g} + \mathbf{R_1} + \mathbf{R_L})^2} \mathbf{U}^2_{\mathbf{g}} = \frac{\mathbf{R_i}}{(\mathbf{R_i} + \mathbf{R_L})^2} \mathbf{U}^2_{\mathbf{g}} \cong \mathbf{P_d} + \frac{\mathbf{R_g}}{(\mathbf{R_i} + \mathbf{R_L})^2} \mathbf{U}^2_{\mathbf{g}} \cong \quad (4.2\text{-}10)$$
$$\cong \frac{\mathbf{R_g} + \mathbf{R_1}}{(\mathbf{R_1} + \mathbf{R_L})^2} \mathbf{u}^2_{\mathbf{inp.}} = \frac{\mathbf{R_i}}{(\mathbf{R_1} + \mathbf{R_L})^2} \mathbf{u}^2_{\mathbf{inp.}} \cong \frac{\mathbf{R_i}}{\mathbf{R_L}} \mathbf{P_L} \ , \ (\mathbf{R_i} = \mathbf{R_g} + \mathbf{R_1})$$

The total electromechanical conversion-efficiency of loaded and unloaded converter, connected to generator, $\eta_{\mathbf{em-tot}}$, is,

$$\eta_{\mathbf{em-tot}} = \frac{\mathbf{P_{m1}}}{\mathbf{P_{m1}} + \mathbf{P_g} + \mathbf{P_{eo}}} \cong \frac{\mathbf{P_{m1}}}{\mathbf{P_{m1}} + \mathbf{P_g}} = \frac{\mathbf{R_1}}{\mathbf{R_1} + \mathbf{R_g}} = \frac{\mathbf{R_1}}{\mathbf{R_i}},$$
$$\eta_{\mathbf{emo-tot}} = \mathbf{Lim}(\eta_{\mathbf{em-tot}})_{\mathbf{R_L \to 0}} = \mathbf{Lim}\left(\frac{\mathbf{P_{m1}}}{\mathbf{P_{m1}} + \mathbf{P_g} + \mathbf{P_{eo}}}\right)_{\mathbf{R_L \to 0}} \cong \quad (4.2\text{-}11)$$
$$\cong \frac{\mathbf{R_1}}{\mathbf{R_1} + \mathbf{R_g} + \frac{\mathbf{R_1^2}}{\mathbf{R_{op}}}} \cong \frac{\mathbf{R_1}}{\mathbf{R_1} + \mathbf{R_g}} = \frac{\mathbf{1}}{\mathbf{1} + \frac{\mathbf{R_g}}{\mathbf{R_1}}} = \frac{\mathbf{R_1}}{\mathbf{R_i}}$$

The total mechanical-acoustical conversion-efficiency of loaded converter connected to generator, $\eta_{\mathbf{ma-tot}}$, is,

$$\eta_{\mathbf{ma-tot}} = \frac{\mathbf{P_L}}{\mathbf{P_{m1}} + \mathbf{P_L}} = \frac{\mathbf{R_L}}{\mathbf{R_1} + \mathbf{R_L}} = \eta_{\mathbf{ma}} \ , \quad (4.2\text{-}12)$$

The total electro-acoustical conversion-efficiency of loaded converter connected to a generator, $\eta_{\mathbf{ea-tot}}$, is,

$$\eta_{\mathbf{ea-tot}} = \eta_{\mathbf{em-tot}} \cdot \eta_{\mathbf{ma-tot}} = \eta_{\mathbf{tot}} =$$
$$= \frac{\mathbf{P_L}}{\mathbf{P_g} + \mathbf{P_{eo}} + \mathbf{P_{m1}} + \mathbf{P_L}} = \frac{\mathbf{P_L}}{\mathbf{P_d} + \mathbf{P_L}} =$$
$$= \frac{\mathbf{R_L}}{(\mathbf{R_L} + \mathbf{R_1})(\mathbf{1} + \frac{\mathbf{R_L} + \mathbf{R_1}}{\mathbf{R_{op}}}) + \mathbf{R_g}\left[\frac{\mathbf{R_L} + \mathbf{R_1}}{\mathbf{R_{op}} \| (\mathbf{R_L} + \mathbf{R_1})}\right]^2} \cong \quad (4.2\text{-}13)$$
$$\cong \frac{\mathbf{R_L}}{\mathbf{R_g} + \mathbf{R_1} + \mathbf{R_L}} = \frac{\mathbf{1}}{\mathbf{1} + \frac{\mathbf{R_g} + \mathbf{R_1}}{\mathbf{R_L}}} = \frac{\mathbf{1}}{\mathbf{1} + \frac{\mathbf{R_i}}{\mathbf{R_L}}} \ (< \eta_{\mathbf{ea}} = \frac{\mathbf{R_L}}{\mathbf{R_1} + \mathbf{R_L}})$$

We also know that mechanical quality factor uniquely qualifies converter power-conversion efficiency and internal losses, and for the converter operating on series resonance, Fig. 4.2-1, can be found as,

$$\mathbf{Q_{m1o}} = \frac{\mathbf{X_{C1}}}{\mathbf{R_1}} = \frac{\mathbf{X_{L1}}}{\mathbf{R_1}} = \frac{\mathbf{1}}{\mathbf{2\pi f_1 C_1 R_1}} = \frac{\mathbf{2\pi f_1 L_1}}{\mathbf{R_1}} = \frac{\mathbf{1}}{\mathbf{R_1}}\sqrt{\frac{\mathbf{L_1}}{\mathbf{C_1}}}\ \mathbf{(non-loaded\ case)},$$

$$\mathbf{Q_{m1L}} = \frac{\mathbf{X_{C1}}}{\mathbf{R_1+R_L}} = \frac{\mathbf{X_{L1}}}{\mathbf{R_1+R_L}} = \frac{\mathbf{1}}{\mathbf{2\pi f_1 C_1 (R_1+R_L)}} = \frac{\mathbf{2\pi f_1 L_1}}{\mathbf{R_1+R_L}} = \tag{4.2-14}$$

$$= \frac{\mathbf{R_1}}{\mathbf{R_1+R_L}}\mathbf{Q_{m1o}} = \frac{\mathbf{1}}{\mathbf{(R_1+R_L)}}\sqrt{\frac{\mathbf{L_1}}{\mathbf{C_1}}}\ \mathbf{(for\ loaded\ converter)},$$

In order to present all (above-found) efficiency, energy and quality parameters of a piezoelectric converter on the very general unique and dimensionless way, in the function of converter's mechanical load, let us make normalization of above found particular expressions, creating the table T. 4.2-1.

T. 4.2-1 Loaded Converter Quality and Efficiency Parameters

Basic expressions	Normalized expressions	Equation
$\mathbf{P_L} = \frac{\mathbf{R_L}}{\mathbf{(R_i+R_L)^2}}\mathbf{U_g^2} \cong \frac{\mathbf{R_L}}{\mathbf{R_i}}\mathbf{P_{d-tot}}$	$\frac{\mathbf{R_i}}{\mathbf{U_g^2}}\mathbf{P_L} = \frac{\mathbf{R_L/R_i}}{\mathbf{(1+R_L/R_i)^2}} \cong \frac{\mathbf{R_L}}{\mathbf{U_g^2}}\mathbf{P_{d-tot}}$	(4.2-5)
$\mathbf{P_{d-tot.}} = \frac{\mathbf{R_i}}{\mathbf{(R_i+R_L)^2}}\mathbf{U_g^2} \cong$ $\cong \mathbf{P_d} + \frac{\mathbf{R_g}}{\mathbf{(R_i+R_L)^2}}\mathbf{U_g^2} \cong \frac{\mathbf{R_i}}{\mathbf{R_L}}\mathbf{P_L}$	$\frac{\mathbf{R_i}}{\mathbf{U_g^2}}\mathbf{P_{d-tot.}} = \frac{\mathbf{R_i^2}}{\mathbf{(R_i+R_L)^2}} =$ $= \frac{\mathbf{1}}{\mathbf{(1+R_L/R_i)^2}} \cong \frac{\mathbf{R_i^2}}{\mathbf{R_L}}\frac{\mathbf{P_L}}{\mathbf{U_g^2}}$	(4.2-10)
$\eta_{\mathbf{ea-tot}} \cong \frac{\mathbf{R_L}}{\mathbf{R_L+R_i}} = \frac{\mathbf{R_L/R_i}}{\mathbf{R_L/R_i+1}}$	$\eta_{\mathbf{ea-tot}} \cong \frac{\mathbf{R_L}}{\mathbf{R_L+R_i}} = \frac{\mathbf{R_L/R_i}}{\mathbf{R_L/R_i+1}}$	(4.2-13)
$\mathbf{P_L} \cong \frac{\mathbf{R_L}}{\mathbf{R_i}}\mathbf{P_{d-tot.}}$	$\frac{\mathbf{P_L}}{\mathbf{P_{d-tot.}}} \cong \frac{\mathbf{R_L}}{\mathbf{R_i}}$	(4.2-10)
$\mathbf{Q_{m1L}} \cong \frac{\mathbf{R_1}}{\mathbf{R_1+R_L}}\mathbf{Q_{m10}}$	$\frac{\mathbf{Q_{m1L}}}{\mathbf{Q_{m10}}} \cong \frac{\mathbf{R_1}}{\mathbf{R_1+R_L}} \approx \frac{\mathbf{1}}{\mathbf{1+2R_L/R_i}}$	(4.2-14)
$\mathbf{Q_{m2L}} \cong \frac{\mathbf{R_2 \| R_L}}{\mathbf{R_2}}\mathbf{Q_{m20}}$	$\frac{\mathbf{Q_{m2L}}}{\mathbf{Q_{m20}}} \cong \frac{\mathbf{R_2 \| R_L}}{\mathbf{R_2}}$	(4.2-28)

For purposes of mathematical conveniences, sum of internal generator resistance, $\mathbf{R_g}$, and internal mechanical-circuit converter-resistance, $\mathbf{R_1}$, in most of above given expressions is presented as a new resistive (generator and converter specific) parameter $\mathbf{R_i = R_g + R_1}$, since, later we will see that we can easily present mechanical load $\mathbf{R_L}$ in the function of $\mathbf{R_i}$, or as a number of $\mathbf{R_i}$ units, or in a normalized and dimensionless form as $\mathbf{x = R_L / R_i}$. This way, the resistance $\mathbf{R_i}$ would become the mechanical-load unit. In practice, resistances $\mathbf{R_1}$, and $\mathbf{R_g}$ are of the same order of magnitude, $\mathbf{R_g \approx R_1}$, both in the range (for most of cases) between 5Ω and 50Ω (and when we do not have a better choice, for the purposes

of making approximations, we shall consider $\mathbf{R_i = R_g + R_1 \approx 2R_g \approx 2R_1}$). For instance, if we introduce as normalized mechanical load the ratio $\mathbf{x = \frac{R_L}{R_i}}$, table T. 4.2-1 will become T. 4.2-2.

T. 4.2-2 Loaded Converter Quality and Efficiency Parameters

$\mathbf{x = \frac{R_L}{R_i}}$, $\mathbf{x \in (0,\infty)}$ **(=) Normalized Load**	**Normalized Power and Quality Parameters Expressions F(x)**	**Equation**
Y = F(x)	$\mathbf{\frac{R_i}{U_g^2} P_L = \frac{x}{(1+x)^2}}$	(4.2-5)
	$\mathbf{\frac{R_i}{U_g^2} P_{d-tot.} = \frac{1}{(1+x)^2}}$	(4.2-10)
	$\mathbf{\eta_{ea-tot} \cong \frac{x}{1+x}}$	(4.2-13)
	$\mathbf{\frac{P_L}{P_{d-tot.}} \cong x}$	(4.2-10)
	$\mathbf{\frac{Q_{m1L}}{Q_{m10}} \approx \frac{1}{1+2x}}$	(4.2-14)

Let as now calculate all normalized expressions from T. 4.2-1 and T. 4.2-2 in the function of mechanical load units, when mechanical load is taking values: $\mathbf{R_L \in (0, 10R_i ...)}$, and create new table T. 4.2-3.

T. 4.2-3 Numerical Values of Loaded Converter Quality and Efficiency Parameters

$\mathbf{R_L \Rightarrow}$	**0**	$\mathbf{0.5R_i}$	$\mathbf{R_i}$	$\mathbf{1.5R_i}$	$\mathbf{2R_i}$	$\mathbf{3R_i}$	$\mathbf{10R_i}$	∞
$\mathbf{x = \frac{R_L}{R_i}}$	**0**	**0.5**	**1**	**1.5**	**2**	**3**	**10**	∞
$\mathbf{\frac{R_i}{U_g^2} P_L}$	**0**	**0.22**	**0.25**	**0.24**	**0.22**	**0.187**	**0.083**	**0**
$\mathbf{\frac{R_i}{U_g^2} P_{d-tot.}}$	**1**	**0.44**	**0.25**	**0.16**	**0.11**	**0.0625**	**0.083**	**0**
$\mathbf{\eta_{ea-tot}}$	**0**	**0.33**	**0.5**	**0.6**	**0.667**	**0.75**	**0.909**	**1**
$\mathbf{\frac{P_L}{P_{d-tot.}}}$	**0**	**0.5**	**1**	**1.5**	**2**	**3**	**10**	∞
$\mathbf{\frac{Q_{m1L}}{Q_{m10}}}$	**1**	**0.5**	**0.333**	**0.25**	**0.2**	**0.143**	**0.0476**	**0**

Now, based on functions and results from T. 4.2-2 and T. 4.2-3, we can present all (normalized) power and quality parameters of a converter on the same multi-functional graph, Fig. 4.2-3 (where x axis is normalized mechanical load, and Y = F(x) presents normalized expressions from T. 4.2-2).

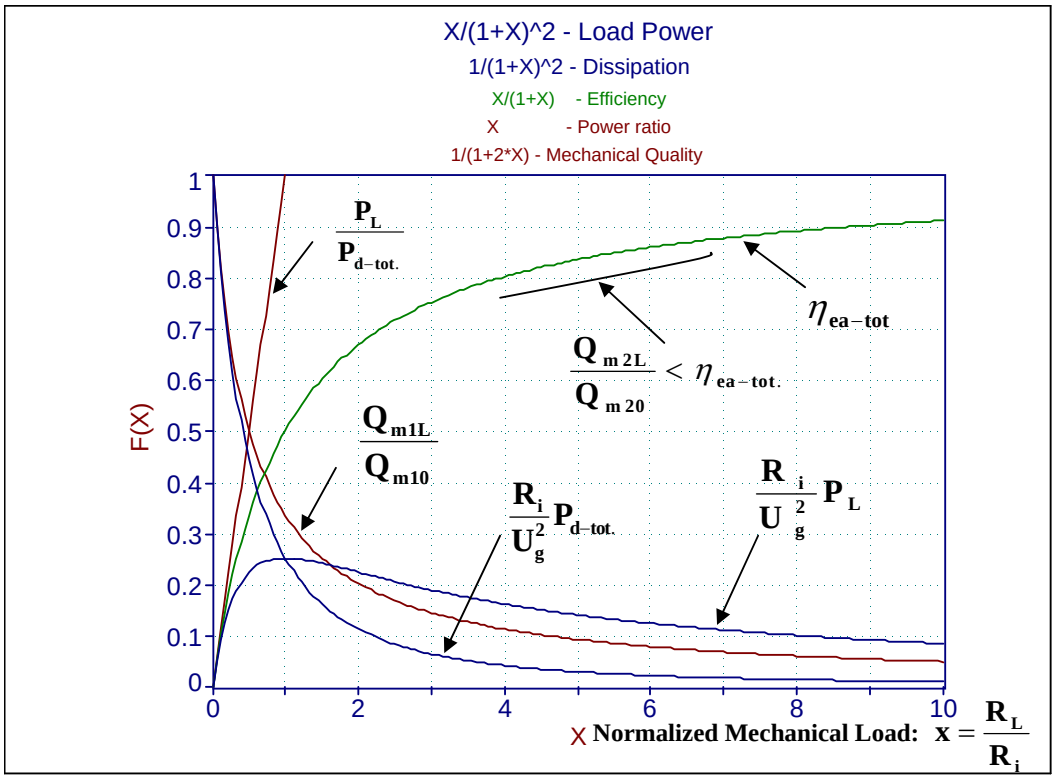

Fig. 4.2-3 Normalized Converter Power and Quality Parameters, F(x), vs. Normalized Mechanical Load, x

Before we draw any conclusion based on results summarized by Fig. 4.2-3, we shall repeat the same process for a converter operating in parallel resonance. It will be shown that in case of parallel resonance we shall again get the same normalized functions as presented on Fig. 4.2-3, except that mechanical loading will have opposite direction (compared to a converter operating in series resonance).

In series resonance, using the equivalent converter circuit on the way as presented on Fig. 4.2-1, equivalent mechanical load (here expressed as load resistance $\mathbf{R_L}$=$\mathbf{R_{L1}}$) is starting from zero, for no-load conditions, and increasing progressively with mechanical load increase (theoretically until infinity), and in parallel resonance the loading character has the opposite direction (starts for no-load conditions from very high value, or infinity, and decreases with load increase, under condition that we use converter model as presented on Fig. 4.2-4). We usually analyze only resistive mechanical loads, because this is the preferable case for making optimal power conversion and to reach high efficiency under high power output. Even if certain mechanical load cannot be presented as a resistive load, by making proper inductive (or some other compensation), and well selecting operating frequency interval, we should locally arrive to the conditions when equivalent mechanical load impedance would be presentable as a resistive impedance, or to make that converter including its compensation presents an equivalent resistive impedance (in the same frequency interval).

Converter Operating High Power in Parallel Resonance

Applying series inductive compensation $\mathbf{L_s}$, we shall enable converter to operate in its parallel mechanical resonance $\mathbf{f_2}$ (or in impedance maximum zone). From Fig. 4.1-3.1, c) and d), we can see that equivalent impedance of **Converter & Series Inductance** has resistive character only when phase function, Fig. 4.1-3.1, d), is crossing zero line in $\mathbf{f_2}$. Consequently, applying PLL (for resonant frequency control), in order to keep the input current and voltage in phase, at $\mathbf{f_2}$ (measured on the input of the equivalent impedance, Fig. 4.1-3.1 c)), we shall make an equivalent load being high resistive impedance. The next important design task, regarding optimal power transfer, is that equivalent load impedance should be matched (or should be equal) to the internal impedance of driving electronics (of ultrasonic power supply, or ultrasonic generator, or power oscillator). This objective we usually realize designing a proper primary-to-secondary-ratio of a ferrite-transformer, and reducing high load impedance to the level of the internal impedance of driving electronics. In order to control output converter power (or output velocity) under loading, we should also find the best way to extract the motional voltage $\mathbf{u_m}$ from the output power circuit, and bring this voltage as the feedback to the main supply, or DC supply voltage control unit, effectively keeping $\mathbf{u_m}$ constant (most often by means of PWM regulation), regardless of load variations.

Since converter impedance in no-load conditions and in parallel resonance (in air) is usually very high, converter is dissipating very low energy, and it can continuously oscillate long time without applying forced cooling. When converter is mechanically loaded (operating in parallel resonance), its equivalent impedance is decreasing, proportionally with the increase of applied load. Consequently, when converter is operating **in parallel resonance, we should start converter oscillations just before acoustical load is applied**, and we should know that **this regime is convenient for low and moderate, largely variable acoustical loads.**

We could also operate converter (with series inductive compensation) in two of its side-band series-resonance frequencies $\mathbf{f_{SL}}$ **or** $\mathbf{f_{SH}}$, but only operating in $\mathbf{f_{SL}}$ can give good results (efficient and stable, high power output) in cases when we adjust series inductance to produce $\mathbf{f_{oper.} = f_{SL} \approx f_1}$ (see Fig. 4.1-3.6). Also the philosophy of output ultrasonic power regulation, when operating a converter in $\mathbf{f_{SL}}$ **or** $\mathbf{f_{SH}}$, would be not the same as operating it in $\mathbf{f_1}$. The operation in $\mathbf{f_{oper.} = f_{SL} \approx f_1}$ is typical for driving arrays of (mutually similar) ultrasonic cleaning transducers.

Let us now analyze regular, series-inductance compensated converter, operating on its parallel resonant frequency. The equivalent circuit of such operating regime, valid only for very close vicinity of converter's parallel resonance is presented on Fig. 4.2-4. The meaning of series inductive compensation in this case is to eliminate all reactive circuit elements such as capacitances and inductances (of course only for a constant frequency $\mathbf{f_2}$, when circuit is operating in resonant regime). This can be realized on the way that $\mathbf{L_s}$ should be chosen to create series resonance with $\mathbf{C_{os}}$ on $\mathbf{f_2}$ (when $\mathbf{L_s}$ and $\mathbf{C_{os}}$ would present very low, or zero equivalent impedance), and naturally (in the same time) $\mathbf{L_2}$ and $\mathbf{C_2}$ would create parallel resonance, on $\mathbf{f_2}$, that has very high equivalent impedance.

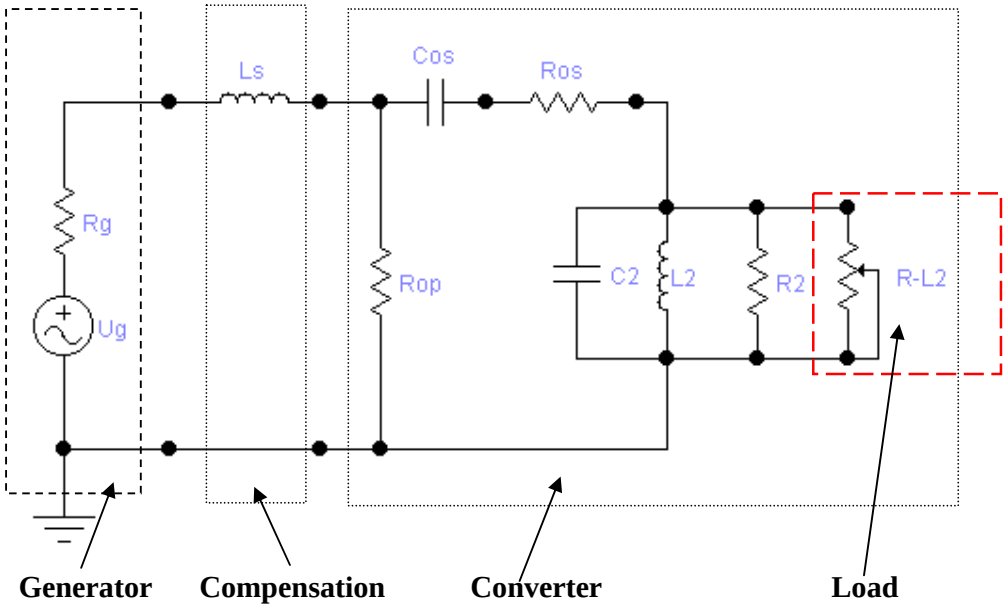

Fig. 4.2-4 Converter inductively compensated to operate in parallel resonant frequency $(L_s C_{os} \cong L_2 C_2) \cong 1/4\pi^2 f_2^2$

This way, we can practically eliminate all reactive elements L_s, C_{os}, L_2 and C_2 from the circuit given on Fig. 4.2-4 (by satisfying $(L_s C_{os} \cong L_2 C_2) \cong 1/4\pi^2 f_2^2$), and create a more simplified equivalent circuit (which has only resistive elements), given on Fig. 4.2-5, a). Since R_{op} usually presents very high resistance (in the range of several MΩ, or higher), we can additionally approximate the same circuit to its final version given on the Fig. 4.2-5, b).

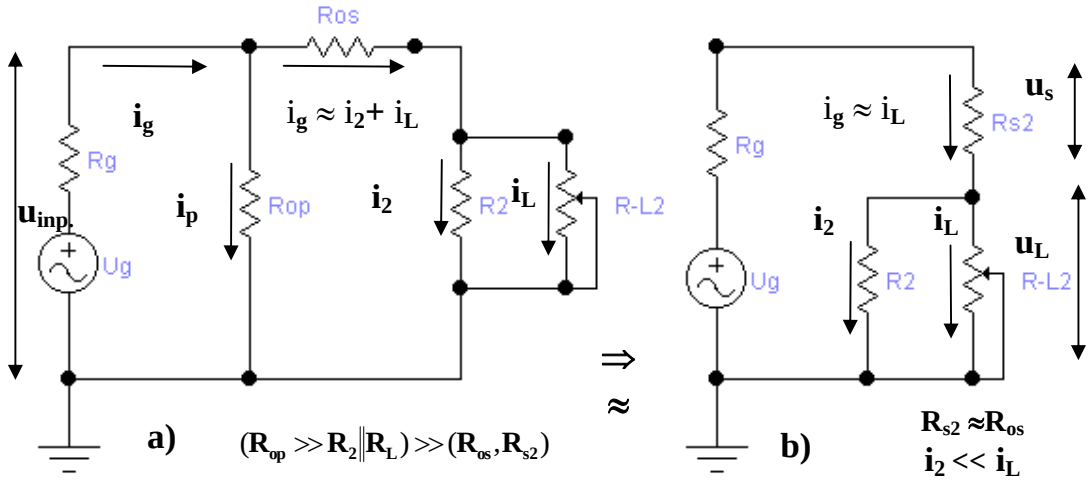

Fig. 4.2-5 Compensated converter operating on parallel resonant frequency

Now we can analyze circuits presented on Fig. 4.2-4 and Fig. 4.2-5, and find all characteristic currents and voltages,

$$\mathbf{i_g = i_2 + i_L = \frac{U_g}{(R_g + R_{os}) + (R_2 \| R_L)}}\ , (\mathbf{R_L = R_{L-2}}),$$

$$\mathbf{i_2 = \frac{R_1}{R_2 + R_L} i_g}\ ,\ \mathbf{i_L = \frac{R_2}{R_2 + R_L} i_g}\ ,$$

$$\mathbf{u_{inp.} = \frac{R_{os} + R_2 \| R_L}{(R_g + R_{os}) + (R_2 \| R_L)} u_g = (1 + \frac{R_{os}}{(R_2 \| R_L)}) u_L} \qquad (4.2\text{-}15)$$

$$\mathbf{u_L = u_2 = i_2 R_2 = i_L R_L = u_{inp.} - i_g R_{os} = \frac{R_2 \| R_L}{R_{os} + (R_2 \| R_L)} u_{inp.} =}$$

$$\mathbf{= \frac{R_2 \| R_L}{R_g + R_{os} + (R_2 \| R_L)} u_g \cong u_{inp.}\ ,\ ((R_{os} \cong R_{s2}) << (R_2 \| R_L))}$$

Electrical power-losses, $\mathbf{P_{eo}}$ dissipated on the parallel resistance $\mathbf{R_{op}}$ (which is in the range of many MΩ) can be neglected, since we made circuit transformation from Fig. 4.2-5, a) to Fig. 4.2-5, b), where all of such loses are transferred to the loses dissipated in series resistance $\mathbf{R_{os} \cong R_{s2}}$,

$$\mathbf{P_{eo} = R_{os} i_g^2 = \frac{R_{os}}{\left[(R_g + R_{os}) + (R_2 \| R_L)\right]^2} U_g^2 =}$$

$$\mathbf{= \frac{R_{os}}{\left[R_{os} + (R_2 \| R_L)\right]^2} u_{inp.}^2 = \frac{R_{os}}{(R_2 \| R_L)^2} u_L^2 \cong \frac{R_{os}}{(R_2 \| R_L)^2} u_{inp.}^2} \qquad (4.2\text{-}16)$$

Mechanical, internal converter power-losses, are presented by power dissipated on the equivalent internal resistance of mechanical circuit $\mathbf{R_2}$,

$$\mathbf{P_{m2} = P_{R2} = R_2 i_2^2 = \frac{u_L^2}{R_2} = \frac{R_L^2}{(R_2 + R_L)^2 \left[R_g + R_{os} + (R_2 \| R_L)\right]^2} U_g^2 =}$$

$$\mathbf{= \frac{R_2 R_L^2}{(R_2 + R_L)^2 \left[R_{os} + (R_2 \| R_L)\right]^2} u_{inp.}^2 = \frac{(R_2 \| R_L)^2}{R_2 \left[R_{os} + (R_2 \| R_L)\right]^2} u_{inp.}^2 =} \qquad (4.2\text{-}17)$$

$$\mathbf{= \frac{R_2 R_L^2}{(R_2 + R_L)^2} i_g^2 = \frac{1}{R_2} \left[\frac{(R_2 \| R_L)}{R_{os} + R_g + (R_2 \| R_L)}\right]^2 U_g^2}$$

Total power dissipation in a converter is equal to the sum of (electrical and mechanical) loses presented by (4.2-16) and (4.2-17),

$$\mathbf{P_d = P_{eo} + P_{m2} = \left[R_{os} + R_2 (\frac{R_L}{R_2 + R_L})^2\right] \frac{U_g^2}{(R_g + R_{os} + R_2 \| R_L)^2}}\ . \qquad (4.2\text{-}18)$$

Useful acoustical (active) output power is only the power given to a load resistance $\mathbf{R_{L2} = R_L}$,

$$\mathbf{P_L = R_L i_L^2 = \frac{u_L^2}{R_L} = \frac{1}{R_L}\left[\frac{(R_2 \| R_L)}{R_{os} + (R_2 \| R_L)}\right]^2 u_{inp.}^2 =}$$
$$\mathbf{= \frac{1}{R_L}\frac{(R_2 \| R_L)}{R_{os} + (R_2 \| R_L)} \cdot \frac{1}{R_g + R_{os} + (R_2 \| R_L)} U_g^2 \cong}$$
$$\mathbf{\cong \frac{1}{R_L}\left[\frac{(R_2 \| R_L)}{R_g + R_{os} + (R_2 \| R_L)}\right]^2 U_g^2 \cong \frac{R_L}{(R_i + R_L)^2} U_g^2 \cong \frac{R_L}{R_i} P_{d-tot} =} \qquad (4.2\text{-}19)$$
$$\mathbf{\frac{(R_2 \| R_L)^2}{R_L} \cdot \frac{R_g + R_{os} + (R_2 \| R_L)}{R_{os} + (R_2 \| R_L)} i_g^2 \ , \ ((R_2 \| R_L) \cong R_L , R_i = R_g + R_{os})}$$

Now we can calculate the internal electromechanical conversion-efficiency of loaded, η_{emL} , and unloaded, η_{emo} , converter as,

$$\eta_{emL} = \eta_{em} = \frac{P_{m2}}{P_{m2} + P_{eo}} = \frac{P_{R2}}{P_{R2} + P_{eo}}$$
$$\eta_{emo} = (\mathbf{Lim}\,\eta_{emL})_{R_L \to \infty} = \mathbf{Lim}\left(\frac{P_{m2}}{P_{m2} + P_{eo}}\right)_{R_L \to \infty} = \frac{1}{1 + \frac{R_{os}}{R_2}} \cong 1 \qquad (4.2\text{-}20)$$

The internal mechanical-to-acoustical conversion-efficiency of loaded converter, η_{ma} is,

$$\eta_{ma} = \frac{P_L}{P_{m2} + P_L} = \frac{R_2}{R_2 + R_L} = \frac{1}{1 + \frac{R_L}{R_2}} \ . \qquad (4.2\text{-}21)$$

The total electro-acoustical conversion-efficiency of loaded converter, η_{ea} , is,

$$\eta_{ea} = \eta_{em}\eta_{ma} = \eta_{em}\frac{R_2}{R_2 + R_L} = \frac{P_L}{P_d + P_L} = \frac{P_L}{P_{eo} + P_{m1} + P_L} =$$
$$= \frac{1}{1 + \frac{R_L}{R_2} + \frac{R_{os}R_L}{\left[R_{os} + (R_2 \| R_L)\right]^2}} \cong \frac{1}{1 + \frac{R_L}{R_2}} = \eta_{ma} \ , \ (R_{os} << R_2, R_L, R_{op}). \qquad (4.2\text{-}22)$$

A converter itself, even if it has very high electro-acoustic efficiency, is not sufficient to realize high power output (of acoustic or ultrasonic energy). It is also very important to realize proper impedance matching between the generator (as a source of electrical excitation) and the converter, in order to produce high acoustical power output.

Let us now find thermal power losses on the internal generator resistance $\mathbf{R_g}$,

$$\mathbf{P_g} = \mathbf{R_g i_g^2} = \frac{\mathbf{R_g}}{\left[\mathbf{R_g} + \mathbf{R_{os}} + (\mathbf{R_2} \| \mathbf{R_L})\right]^2} \mathbf{U_g^2} =$$
$$= \frac{\mathbf{R_g}}{\left[\mathbf{R_{os}} + (\mathbf{R_2} \| \mathbf{R_L})\right]^2} \mathbf{u_{inp.}^2} \cong \frac{\mathbf{R_g}}{(\mathbf{R_2} \| \mathbf{R_L})^2} \mathbf{u_{inp.}^2} \qquad (4.2\text{-}23)$$

The total thermal power losses in generator and converter are,

$$\mathbf{P_{d-tot.}} = \mathbf{P_g} + \mathbf{P_d} = \mathbf{P_g} + \mathbf{P_{eo}} + \mathbf{P_{m2}} =$$
$$= \left[\mathbf{R_g} + \mathbf{R_{os}} + \frac{(\mathbf{R_2} \| \mathbf{R_L})^2}{\mathbf{R_2}}\right] \frac{\mathbf{u_{inp.}^2}}{\left[\mathbf{R_{os}} + (\mathbf{R_2} \| \mathbf{R_L})\right]^2} =$$
$$= \left[\mathbf{R_g} + \mathbf{R_{os}} + \frac{(\mathbf{R_2} \| \mathbf{R_L})^2}{\mathbf{R_2}}\right] \frac{\mathbf{U_g^2}}{\left[\mathbf{R_g} + \mathbf{R_{os}} + (\mathbf{R_2} \| \mathbf{R_L})\right]^2} \cong \qquad (4.2\text{-}24)$$
$$\cong \frac{\mathbf{R_i}}{(\mathbf{R_i} + \mathbf{R_L})^2} \mathbf{U_g^2} \cong \frac{\mathbf{R_i}}{\mathbf{R_L}} \mathbf{P_L} \cong \left[\frac{\mathbf{R_g}}{(\mathbf{R_2} \| \mathbf{R_L})^2} + \frac{\mathbf{1}}{\mathbf{R_2}}\right] \mathbf{u_{inp.}^2} ,$$
$$((\mathbf{R_2} \| \mathbf{R_L}) \cong \mathbf{R_L} , \ \mathbf{R_i} = \mathbf{R_g} + \mathbf{R_{os}}) .$$

The total electromechanical conversion-efficiency of loaded and unloaded converter connected to generator, $\eta_{\mathbf{em-tot}}$, is,

$$\eta_{\mathbf{em-tot}} = \frac{\mathbf{P_{m2}}}{\mathbf{P_{m2}} + \mathbf{P_g} + \mathbf{P_{eo}}} \cong \frac{\mathbf{P_{m2}}}{\mathbf{P_{m2}} + \mathbf{P_g}}$$
$$\eta_{\mathbf{emo-tot}} = \mathbf{Lim}(\eta_{\mathbf{em-tot}})_{\mathbf{R_L \to \infty}} = \mathbf{Lim}\left(\frac{\mathbf{P_{m1}}}{\mathbf{P_{m2}} + \mathbf{P_g} + \mathbf{P_{eo}}}\right)_{\mathbf{R_L \to \infty}} = \qquad (4.2\text{-}25)$$
$$= \frac{\mathbf{R_2}}{\mathbf{R_g} + \mathbf{R_{os}} + \mathbf{R_2}} = \frac{\mathbf{1}}{\mathbf{1} + \frac{\mathbf{R_g} + \mathbf{R_{os}}}{\mathbf{R_2}}} \cong \mathbf{1} , \ (\mathbf{R_2} >> \mathbf{R_g} + \mathbf{R_{os}}) .$$

The total mechanical-acoustical conversion-efficiency of loaded converter connected to generator, $\eta_{\mathbf{ma-tot}}$, is,

$$\eta_{\mathbf{ma-tot}} = \frac{\mathbf{P_L}}{\mathbf{P_{m2}} + \mathbf{P_L}} = \frac{\mathbf{R_2}}{\mathbf{R_2} + \mathbf{R_L}} = \frac{\mathbf{1}}{\mathbf{1} + \frac{\mathbf{R_L}}{\mathbf{R_2}}} = \eta_{\mathbf{ma}} , \qquad (4.2\text{-}26)$$

The total electro-acoustical conversion-efficiency of loaded converter connected to a generator, $\eta_{\mathbf{ea-tot}}$, is,

$$\eta_{ea-tot} = \eta_{em-tot} \cdot \eta_{ma-tot} = \eta_{tot} =$$
$$= \frac{\mathbf{P_L}}{\mathbf{P_g + P_{eo} + P_{m2} + P_L}} = \frac{\mathbf{P_L}}{\mathbf{P_d + P_L}} = \frac{\mathbf{1}}{\mathbf{1 + R_L\left[\frac{R_g + R_{os}}{(R_2 \| R_L)^2} + \frac{1}{R_2}\right]}} \cong \tag{4.2-27}$$
$$\cong \frac{\mathbf{1}}{\mathbf{1 + \frac{R_L}{R_2} + \frac{R_L}{R_2} + \frac{R_L(R_g + R_{os})}{(R_2 \| R_L)}}} \cong \frac{\mathbf{R_L}}{\mathbf{R_L + R_i}} = \frac{\mathbf{R_L / R_i}}{\mathbf{R_L / R_i + 1}}.$$

We also know that mechanical quality factor uniquely qualifies converter power-conversion efficiency and internal losses, and for the converter operating on parallel resonance, Fig. 4.2-4, can be found as,

$$\mathbf{Q_{m2o}} = \frac{\mathbf{R_2}}{\mathbf{X_{C2}}} = \frac{\mathbf{R_2}}{\mathbf{X_{L2}}} = \mathbf{2\pi f_2 C_2 R_2} =$$
$$= \frac{\mathbf{R_2}}{\mathbf{2\pi f_2 L_2}} = \mathbf{R_2}\sqrt{\frac{\mathbf{C_2}}{\mathbf{L_2}}} \quad (\textbf{for non} - \textbf{loaded converter}),$$
$$\mathbf{Q_{m2L}} = \frac{(\mathbf{R_2} \| \mathbf{R_L})}{\mathbf{X_{C2}}} = \frac{(\mathbf{R_2} \| \mathbf{R_L})}{\mathbf{X_{L2}}} = \mathbf{2\pi f_2 C_2 (R_2} \| \mathbf{R_L}) = \frac{(\mathbf{R_2} \| \mathbf{R_L})}{\mathbf{R_2}} \mathbf{Q_{m2o}} = \tag{4.2-28}$$
$$= \frac{(\mathbf{R_2} \| \mathbf{R_L})}{\mathbf{2\pi f_2 L_2}} = (\mathbf{R_2} \| \mathbf{R_L})\sqrt{\frac{\mathbf{C_2}}{\mathbf{L_2}}} = \frac{\mathbf{Q_{m2o}}}{\mathbf{1 + \frac{R_2}{R_L}}} =$$
$$= \frac{\mathbf{R_L / R_i}}{\mathbf{\frac{R_2}{R_i} + \frac{R_L}{R_i}}} \mathbf{Q_{m2o}} \cong \frac{\mathbf{R_L}}{\mathbf{R_2}} \mathbf{Q_{m2o}} = \frac{\mathbf{R_L / R_i}}{\mathbf{R_2 / R_i}} \mathbf{Q_{m2o}} \quad (\textbf{for loaded converter}).$$

In order to present all efficiency, energy and quality parameters of a piezoelectric converter on the very general and dimensionless way, in the function of converters mechanical load, let us make normalization of above found particular expressions (valid for converter operating in parallel resonance), creating the table T. 4.2-4.

By comparing T. 4.2-1 with T. 4.2-4, we see that all expressions inside are formally identical, or approximately identical, except different expressions for quality factors (between series and parallel resonance), and also mechanical load resistances of series and parallel resonant regimes have mutually opposite directions in relation with load increase (but shear the same load axis).

For the purposes of mathematical conveniences, sum of internal generator resistance, $\mathbf{R_g}$, and internal mechanical-circuit converter-resistance, $\mathbf{R_{os}}$, in most of above given expressions (and in the T. 4.2-4) is presented as a resistive (generator and converter specific) parameter $\mathbf{R_i = R_g + R_{os}}$, since, this way we can easily treat mechanical load $\mathbf{R_L}$ as the function of $\mathbf{R_i}$, or as a number of $\mathbf{R_i}$ units, or in a normalized and dimensionless form as $\mathbf{R_L / R_i}$. This way, the resistance $\mathbf{R_i}$ would again become the mechanical-load unit.

T. 4.2-4 Loaded Converter Quality and Efficiency Parameters

Basic expressions	Normalized expressions	Equation
$P_L \cong \frac{R_L}{(R_i+R_L)^2} U_g^2 \cong \frac{R_L}{R_i} P_{d-tot}$	$\frac{R_i}{U_g^2} P_L \cong \frac{R_L / R_i}{(1+R_L/R_i)^2} \cong \frac{R_L}{U_g^2} P_{d-tot}$	(4.2-19)
$P_{d-tot.} \cong \frac{R_i}{(R_i+R_L)^2} U_g^2 \cong$ $\cong \frac{R_i}{R_L} P_L$	$\frac{R_i}{U_g^2} P_{d-tot.} \cong \frac{R_i^2}{(R_i+R_L)^2} =$ $= \frac{1}{(1+R_L/R_i)^2} \cong \frac{R_i^2}{R_L} \frac{P_L}{U_g^2}$	(4.2-24)
$\eta_{ea-tot} \cong \frac{R_L}{R_L+R_i} = \frac{R_L/R_i}{R_L/R_i+1}$	$\eta_{ea-tot} \cong \frac{R_L}{R_L+R_i} = \frac{R_L/R_i}{R_L/R_i+1}$	(4.2-27)
$P_L \cong \frac{R_L}{R_i} P_{d-tot.}$	$\frac{P_L}{P_{d-tot.}} \cong \frac{R_L}{R_i}$	(4.2-19)
$Q_{m2L} = \frac{Q_{m2o}}{1+\frac{R_2}{R_L}}$	$\frac{Q_{m2L}}{Q_{m20}} = \frac{R_2 \Vert R_L}{R_2} = \frac{1}{1+\frac{R_2}{R_L}} =$ $= \frac{R_L/R_i}{\frac{R_2}{R_i}+\frac{R_L}{R_i}} \cong \frac{R_L}{R_2} = \frac{R_L/R_i}{R_2/R_i}$	(4.2-28)
$Q_{m1L} \cong \frac{R_1}{R_1+R_L} Q_{m10}$	$\frac{Q_{m1L}}{Q_{m10}} \cong \frac{R_1}{R_1+R_L} \approx \frac{1}{1+2R_L/R_i}$	(4.2-14)

In practice for loaded converter operating in parallel resonance we can use the following circuit elements approximations: $(R_2 \Vert R_L) \approx R_L$, $R_2 > (R_i = R_g + R_{os})$, $R_L \le R_2$. For instance, if we introduce as normalized mechanical load the ratio $x = \frac{R_L}{R_i}$, table T. 4.2-4 will become T. 4.2-5. Also, when we compare T. 4.2-5 with T. 4.2-2 we will find that all expressions in both of them are either mutually identical or approximately identical, and that only difference between them is related to functions describing mechanical quality factors ratios.

T. 4.2-5 Loaded Converter Quality and Efficiency Parameters

$x = \frac{R_L}{R_i}$, $x \in (0,\infty)$ (=) Normalize Load	Normalized Power and Quality Parameters Expressions F(x)	Equation
Y = F(x)	$\frac{R_i}{U_g^2} P_L \cong \frac{x}{(1+x)^2}$	(4.2-19)
	$\frac{R_i}{U_g^2} P_{d-tot.} \cong \frac{1}{(1+x)^2}$	(4.2-24)
	$\eta_{ea-tot} \cong \frac{x}{1+x}$	(4.2-27)

	$\frac{P_L}{P_{d-tot.}} \cong x$	(4.2-19)
	$\frac{Q_{m1L}}{Q_{m10}} \approx \frac{1}{1+2x}$	(4.2-14)
	$\frac{Q_{m2L}}{Q_{m20}} = \frac{x}{\frac{R_2}{R_i}+x} < \frac{x}{1+x} = \eta_{ea-tot} \le 1$	(4.2-28)

Let as now calculate all normalized expressions from T. 4.2-4 and T. 4.2-5 in the function of mechanical load units, when mechanical load is taking values: $R_L \in (0, 10R_i ...)$, and create new table T. 4.2-6, which is almost identical to T. 4.2-3,

T. 4.2-6 Numerical Values of Loaded Converter Quality and Efficiency Parameters

$R_L \Rightarrow$	0	$0.5R_i$	R_i	$1.5R_i$	$2R_i$	$3R_i$	$10R_i$	∞
$x = \frac{R_L}{R_i}$	0	0.5	1	1.5	2	3	10	∞
$\frac{R_i}{U_g^2} P_L$	0	0.22	0.25	0.24	0.22	0.187	0.083	0
$\frac{R_i}{U_g^2} P_{d-tot.}$	1	0.44	0.25	0.16	0.11	0.0625	0.083	0
η_{ea-tot}	0	0.33	0.5	0.6	0.667	0.75	0.909	1
$\frac{P_L}{P_{d-tot.}}$	0	0.5	1	1.5	2	3	10	∞
$\frac{Q_{m1L}}{Q_{m10}}$	1	0.5	0.333	0.25	0.2	0.143	0.0476	0
$\frac{Q_{m2L}}{Q_{m20}}$	0	< 0.33	< 0.5	< 0.6	< 0.667	< 0.75	< 0.909	1

Now, based on functions and results from T. 4.2-5 and T. 4.2-6, we can again present all (normalized) power and quality parameters of a converter operating in parallel resonance on the same multi-functional graph, Fig. 4.2-3, which is already made for a converter operating in series resonance (where x axis is normalized mechanical load, and Y = F(x) presents normalized expressions from T. 4.2-5). Of course, conclusions based on Fig. 4.2-3 should be drawn differently, regarding mechanical loading, for a case when converter is operating in series or in parallel resonance. In series resonance with an increase of mechanical load, R_L is also increasing, and in parallel resonance when mechanical load is increasing, R_L is decreasing (here we should make a difference between R_L and mechanical load resistance: R_L only represents a quantitative equivalent, or analogical replacement, for real mechanical load). Of course, this explanation regarding character of mechanical loading is strictly related to the use of dual converter models (inductively compensated in series or parallel) presented on Fig. 4.2-1 and Fig. 4.2-4.

The next conclusion from Fig. 4.2-3 is that if converter is operating in series resonance, with its load increase, the total electro-acoustical efficiency is also progressively increasing, total power dissipation decreasing, and until certain maximum (x = 1) the output load power is increasing and then slowly decreasing. Consequently, we can conclude that series resonance regime is very good for moderate and heavy loads, since when load is zero or very small (x < 0.5), total power dissipation is maximal, efficiency minimal, and output power minimal. Practically, it is preferable that converter operating in series resonance is always reasonably or highly (mechanically) loaded (for instance in applications like ultrasonic metal welding).

If converter is operating in parallel resonance, with its load increase, the total electro-acoustical efficiency is also progressively, but slowly decreasing, total power dissipation is slowly increasing, and until certain maximum (x = 1) the output load power is increasing, and then slowly decreasing. Consequently, we can conclude that parallel resonance regime is very good for low and moderate loads, since when load is zero or very small (x > 10), total power dissipation is minimal, efficiency maximal, and output power still reasonably high. Practically, converter in parallel resonance is perfectly operating in no-load or moderate loading conditions (like in ultrasonic atomizers, majority of applications in ultrasonic plastic welding etc.). It is also very important to notice that useful loading interval (Δx), where converter efficiency is relatively high, power losses minimal, load power almost constant… is significantly larger in cases of parallel resonance regime than in cases of series resonance regime.

We should also pay attention on loading $\mathbf{R_i} = \mathbf{R_g} + \mathbf{R_s}$ units, which are quantitavelly different for series and parallel resonance regimes (regardless that normalized diagrams presented on Fig. 4.2-3 are looking the same for series and parallel resonance). In cases of series resonance, $\mathbf{R_i}$ units are relatively small (typically in the range of several ohms), and in cases of parallel resonance $\mathbf{R_i}$ units can be 10 to 100 times higher (typically in the range between 100 to 1000 ohms). This is related to realizing maximal real-power transfer, when generator internal resistance should be equal (or closely matched) to the load resistance, $\mathbf{R_L} = \mathbf{R_g}$. Since $\mathbf{R_L}$ in series resonance takes values between $\mathbf{0\ \Omega}$ (for no-load situation) and few hundreds of $\mathbf{\Omega}$, for heavy loaded situation, and in parallel resonance $\mathbf{R_L}$ varies between infinity (for no-load) and a few hundreds of $\mathbf{\Omega}$, for heavy loaded situation, it is clear that loading $\mathbf{R_i}$ units of series and parallel resonance circuits would be mutually different (at least for the order of magnitude). After understanding the nature of mechanical loading of piezoelectric converters (regarding the order of magnitude/s of $\mathbf{R_i}$ units) we are in a position to understand why parallel resonance regime has much wider loading interval (delivering reasonably high power, under reasonably low losses), than series resonance operating regime. Of course, there are some other, exceptional (mutually exclusive) advantages (and disadvantages) of both regimes, sometimes making only one of them particularly more useful in certain of critical applications.

If we would like to create converter models where in series and parallel resonance, both load resistances $\mathbf{R_L}$ would proportionally grow with mechanical load increase, we should make circuit modification/s in the converter model given on Fig. 4.2-4 (see Fig. 4.2-6).

For instance, operating only with dual converter models proposed in the first chapter, and again presented on Fig. 4.2-6, a), will give us the chance to treat mechanical (or acoustical) load uniquely, as a mobility, **or velocity divided by force**, measured on the element where output power is dissipated, and in both cases (of series and parallel resonances), with an increase of mechanical loading, $\mathbf{R_L}$ (= $\mathbf{R_{Ls1}}$ **or** $\mathbf{R_{Ls2}}$) would proportionally increase.

Also, when using only dual converter models given on Fig. 4.2-6, b), will give us another chance to treat mechanical (or acoustical) load uniquely, too, as a mechanical impedance, **or force divided by velocity**, measured on the element where output power is dissipated, and in both cases (of series and parallel resonances), with an increase of mechanical loading, when we are measuring input, equivalent, AC impedance of a loaded converter, operating in series resonance, we find that it starts with low impedance values for no-load conditions and it increases with mechanical loading increase, meaning that Fig. 4.2-1 is a natural modeling for such situations. (= $\mathbf{R_{Lp1}}$ or $\mathbf{R_{Lp2}}$) would proportionally decrease.

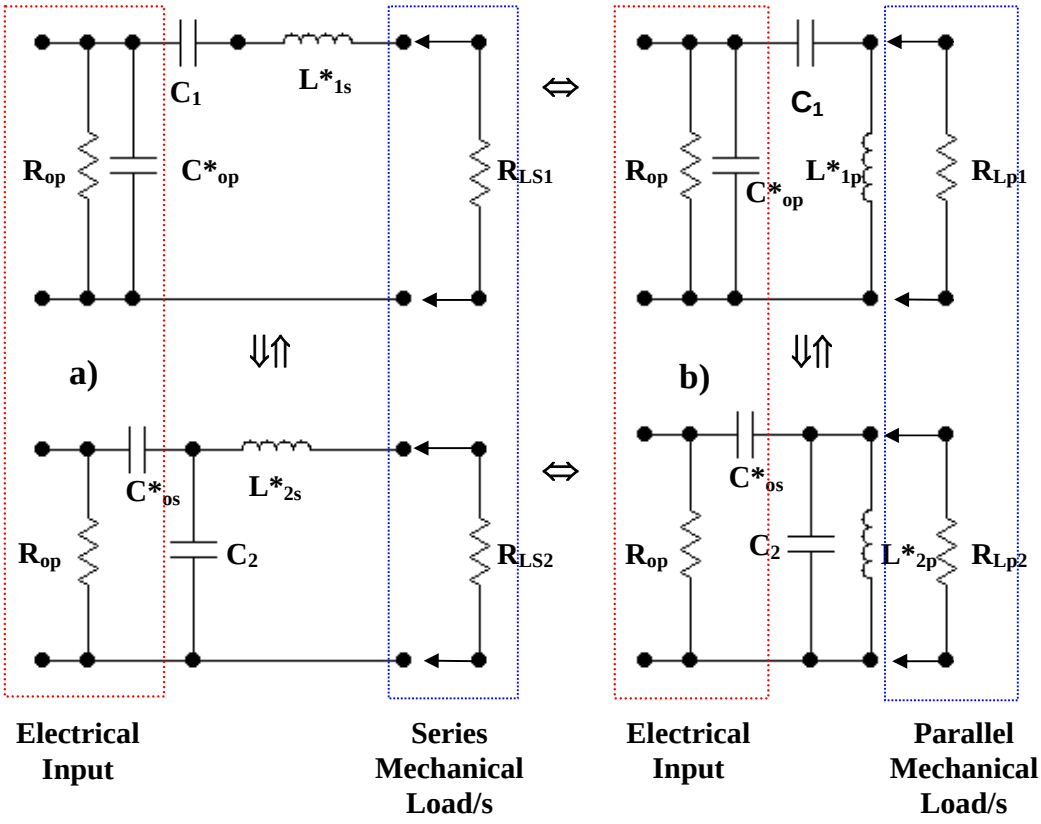

Fig. 4.2-6 Single-Mode, Series and Parallel, Resistive Load-Impedance, Dual and mutually equivalent, Piezoelectric Converter Models:

a) $\mathbf{R_{Ls1}}$ **and** $\mathbf{R_{Ls2}}$ **are increasing with load increase**

b) $\mathbf{R_{Lp1}}$ **and** $\mathbf{R_{Lp2}}$ **are decreasing with load increase**

Elements marked with asterisk (*) are presenting real capacitances and inductances with internal resistive losses (as already explained in the first chapter).

Of course, the most logical and most natural situation would be to use only mobility based analogies and models presented on the Fig. 4.2-6, a), (left side), and to treat mechanical loading-increase as an increase of $\mathbf{R_L}$ (= $\mathbf{R_{Ls1}}$ or $\mathbf{R_{Ls2}}$).

In existing literature, models on Fig. 4.2-1 and Fig. 4.2-4 are more often found (just because of historical reasons of their development and because of certain intellectual rigidity against radical changes in already accepted methodology and logic regarding converters modeling).

The other, more tangible reason for using models on Fig. 4.2-1 and Fig. 4.2-4 is in the fact that when we are measuring input, equivalent AC impedance of a loaded converter, operating in series resonance, we will find that it starts with low impedance values for no-load conditions, and it increases with mechanical loading increase, meaning that Fig. 4.2-1 presents the natural modeling for such situations, since $\mathbf{R_L} = \mathbf{R_{L1}}$ is also increasing with loading. Also when we are measuring input, equivalent AC impedance of a loaded converter, operating in parallel resonance, we will find that it starts with very high impedance values for no-load conditions, and it decreases with mechanical loading increase, meaning that Fig. 4.2-4 presents the natural modeling for such situations, since $\mathbf{R_L} = \mathbf{R_{L2}}$ is also decreasing with loading.

The same problematic becomes more complicated if generator and load impedances are not resistive (for instance, instead of $\mathbf{R_g}$ we could have $\mathbf{Z_g} = \mathbf{R_g} + \mathbf{jX_g}$ and instead of $\mathbf{R_L}$, $\mathbf{Z_L} = \mathbf{R_L} + \mathbf{jX_L}$). In such situations, $\mathbf{Z_L}$ is contributing to the input complex impedance of a loaded-converter, making that free no-load converter impedance would become a new complex impedance $\mathbf{Z_c} = \mathbf{R_{cL}} + \mathbf{jX_{cL}}$. Now, maximal power transfer (from generator to the converter) would be realized when we find a way to make $\mathbf{R_{cL}} = \mathbf{R_g}$ and $\mathbf{X_{cL}} = -\mathbf{X_g}$. Matching condition $\mathbf{X_{cL}} = -\mathbf{X_g}$ we usually name as reactive impedance matching, or reactive elements compensation (in fact elimination of all reactive circuit elements), which can be realized only for certain discrete (resonant) frequencies, or sometimes for limited frequency intervals. After realizing $\mathbf{X_{cL}} = -\mathbf{X_g}$ we enable generator to send only the active power to its load (regardless if the power transfer is maximal or not). A matching condition $\mathbf{R_{cL}} = \mathbf{R_g}$ we can qualify as an active generator-to-load impedance and power matching, when we shall obtain maximal active power transfer from generator to its load.

Start-up (or initiation) time of a converter operating in series resonance is usually significantly longer, compared to start-up times of converters operating in parallel resonance. For instance, in ultrasonic plastic welding applications we could expect to realize few welding per second (when converter is operating in series resonance), and until several times more of welding operations per second if converter is operating in its parallel resonance. In the same time we should not forget that in series resonance piezoelectric converter can be much more heavily (high force-pressure) loaded compared to (high velocity) loading in parallel resonance regime.

Converter Operating High Power between Series and Parallel Resonance

Applying convenient inductive compensation $\mathbf{L_p}$ and/or $\mathbf{L_s}$ (and other Electric Filters circuit combinations) we can enable converter (on a number of different ways) to oscillate in a stable and efficient, high power regime, between its series and parallel mechanical resonances $\mathbf{f_1}$ and $\mathbf{f_2}$ (between its minimal and maximal impedance), or even to extend this frequency interval towards lower and higher frequencies (outside of interval $\mathbf{f_1}$ - $\mathbf{f_2}$). Basically, by making convenient series and/or parallel inductive compensation we can realize that equivalent converter's electrical impedance, including all compensating elements, would have close-to-resistive character in a desired frequency band (for instance between $\mathbf{f_1}$ and $\mathbf{f_2}$, or in a bit wider interval). Of course, similar design strategy can be applied if piezoelectric converter is used as a sensor (to become an efficient detector of mechanical vibrations in a certain frequency interval). Such **Mixed-mode resonant regimes (of conveniently compensated converters operating high power, over certain frequency interval) can unite advantages of single resonant-frequency operating regimes, with an excellent electromechanical efficiency (practically without using PLL for resonant frequency control).** In order to control output converter power in a mixed-mode regime under loading conditions, we should also find the best way to extract representative motional current $\mathbf{i_m}$ and motional voltage $\mathbf{v_m}$ from the output power circuit (in order to represent an active power or mechanical amplitude signal), and bring them as the feedback to the main supply or to switching-transistors driving circuit (usually realized by means of PWM regulation). The most promising future of piezoelectric converters (and sensors) applications will be experienced in mixed-mode, fixed and/or sweeping-frequency resonant regimes.

Mixed-mode resonant operating regimes can also be found (unintentionally and by game of chance) in traditional ultrasonic cleaning systems when many of similar ultrasonic converters are connected (electrically and mechanically) in parallel, or in other familiar situations regarding sensors composed of number of transducers. Since in a group of converters (in parallel connection) each of them is usually slightly different than any other, after coupling them mechanically to an ultrasonic cleaning bath, small initial differences (in electric and mechanical characteristics) are becoming even much higher (because of number of geometrical and acoustical coupling factors). After connecting all single converters in parallel electrical connection, it can happen that particular Impedance-Phase characteristics of every single converter are mutually (and randomly) shifted in frequency scale, making that inductive areas of certain converters are partially overlapping capacitive areas of others. Naturally, overall equivalent phase characteristic of the converter group can be equal (or close) to zero in certain frequency intervals, making that (equivalent) converters' group impedance becomes resistive in the same (zero-phase) areas, producing high power output when driven inside of such intervals. The design strategy in ultrasonic cleaning, regarding transducers can be:

a) To take similar, but not well selected converters (slightly different by frequency and impedance), what minimizes the production cost and slightly reduces overall efficiency of electro-acoustic conversion, making simple and easy high power, frequency sweeping operation, and

b) To take perfectly frequency and impedance selected converter group (of almost mutually identical converters, what will increase production cost), make proper external inductive compensation, and produce high electro-acoustic efficiency on a single resonant frequency, but the frequency sweeping becomes less power-efficient than in the first case, and driving electronics should be more sophisticated, compared to the case under a).
c) In cases, a) and b), single resonant frequency (series or parallel) and mixed-mode resonant regimes (operating between average series and parallel resonant frequency or in wider frequency interval) can be produced by proper external inductive (as well capacitive) compensation (basically applying methods of electric filters theory).

If converters group is composed of highly mutually-dissimilar-converters (case a)), equivalent impedance of such group looks similar to certain series or parallel connection between a capacitive and resistive (frequency dependant) components, and if all converters are almost identical (case b)), equivalent impedance of such group looks similar to a typical piezoelectric impedance of a single transducer (with clear presence of series and parallel resonances).

4.3 Acoustically Sensitive Zones of Piezoelectric Converters

In order to experimentally support conclusions regarding piezoelectric (acoustic) FORCE and VELOCITY-sensitive zones, let us take the same piezoelectric converter (see Fig. 4.3-1), as already presented on T. 4.1-1, Figs. 4.1-2, 4.1-3.1 and 4.1-3.2. When we measure Impedance-Phase curves using Network Impedance Analyzer and relatively high sinusoidal frequency-sweeping signal $\mathbf{u_{sweep.}} \geq 1$ V-rms, we shall get the typical piezoelectric converter curves such as presented on Fig. 4.3-1.

If we now make the same Impedance-Phase measurements reducing the amplitude of the sinusoidal frequency-sweeping signal to $\mathbf{u_{sweep.}} = 0.1$ V-rms, we shall get similarly looking curves, presented on Fig. 4.3-2. We can already notice (on Fig. 4.3-2) that Impedance and Phase curves in the zone of high impedance are no more as smooth and perfectly continuous lines, as curves on Fig. 4.3-1. The cause of getting such result is still not well recognizable, but as we will see later, by reducing amplitude of the frequency-sweeping signal, we are approaching closer to the environmental acoustic-noise excitation of the laboratory where we make measurements (in this case measurements were performed in Branson Ultrasonic Corp. in USA). In other words, if the same piezoceramic were used as a receiver, it would detect certain laboratory (background, building vibrations) acoustic-noise, and produce voltage output that becomes (in its peak values) comparable to 0.1 V-rms.

If we now again make the same Impedance-Phase measurements, once more reducing the amplitude of the sinusoidal frequency-sweeping signal to $\mathbf{u_{sweep.}} = 0.01$ V-rms, we shall get new Impedance-Phase curves, presented on Fig. 4.3-3. We can now notice (on Fig. 4.3-3) that Impedance and Phase curves in the zone of high impedance are very much influenced by background, laboratory acoustic-noise. In other words, the piezoceramic converter in question is now detecting the laboratory (background) acoustic-noise, which can easily be compared to sinusoidal frequency sweeping signal $\mathbf{u_{sweep.}} = 0.01$ V-rms.

After reducing the sinusoidal frequency-sweeping signal to $\mathbf{u_{sweep.}} = 0.001$ V-rms, we shall get new Impedance-Phase curves, presented on Fig. 4.3-4. We can now notice (on Fig. 4.3-4) that the background, laboratory acoustic-noise, has no influence on Impedance and Phase curves in the zone of low impedance, but in all other frequency zones, we would not be able to recognize the shape of typical piezoelectric Impedance-Phase curves. In other words, now, the piezoceramic converter in question is non-selectively detecting the laboratory (background) acoustic-noise in a very wide frequency band (completely loosing phase information), and basically we cannot consider such operating sensor regime as engineering-wise useful (and obviously, in this latest case, the background-noise is behaving stochastically, and it is producing much higher voltage than $\mathbf{u_{sweep.}} = 0.001$ V-rms).

As the conclusion based on measurements presented on Fig. 4.3-1 until Fig. 4.3-4, we can say that converter parallel-resonance (high impedance) area is very much VELOCITY-VOLTAGE sensitive. We also see, based on the same measurements that **converter series resonance (low impedance) area is totally insensitive on VELOCITY-VOLTAGE background-excitation,** but we could also find that **series resonance (low impedance) area is very much FORCE-**

CURRENT sensitive. Of course, here we are talking about oscillating-velocity and force signal forms.

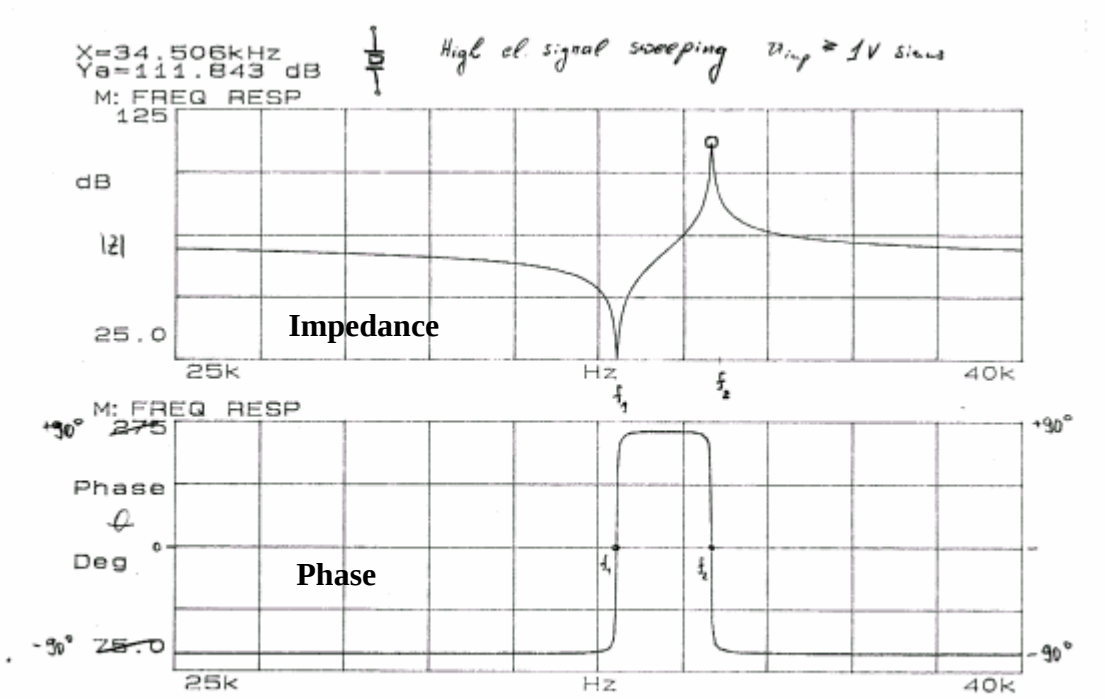

a)

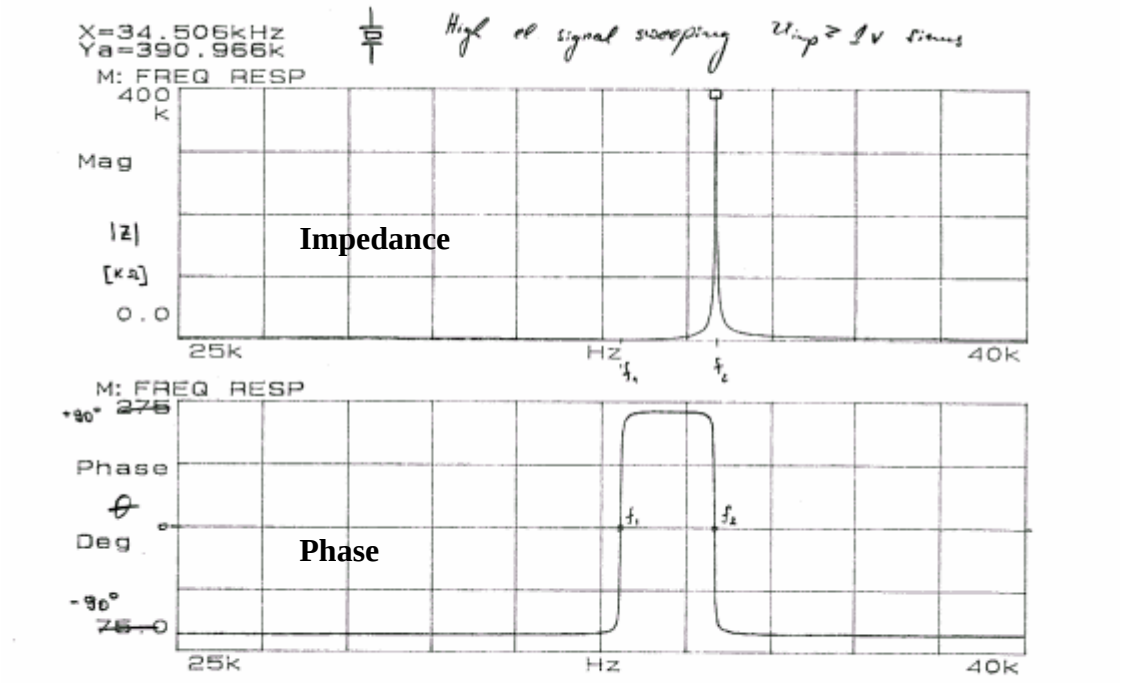

b)

Fig. 4.3-1 Piezoelectric Impedance-Phase Curves ($u_{sweep.} \geq 1$ V-rms)
a) Logarithmic Impedance-amplitude (in dB)
b) Linear Impedance-amplitude of the same converter

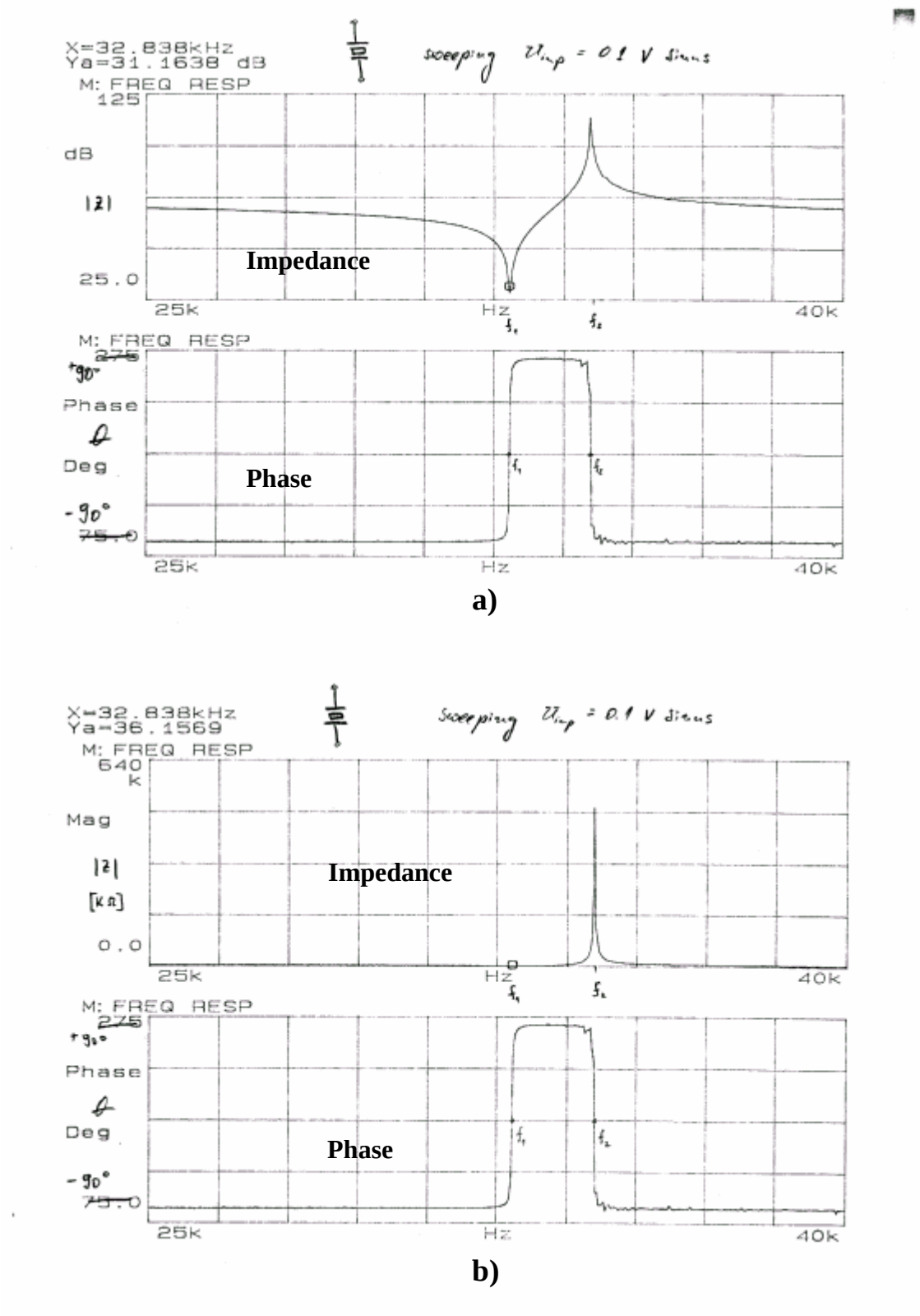

Fig. 4.3-2 Piezoelectric Impedance-Phase Curves ($u_{sweep.}$ = 0.1 V-rms)
a) Logarithmic Impedance-amplitude (in dB)
b) Linear Impedance-amplitude of the same converter

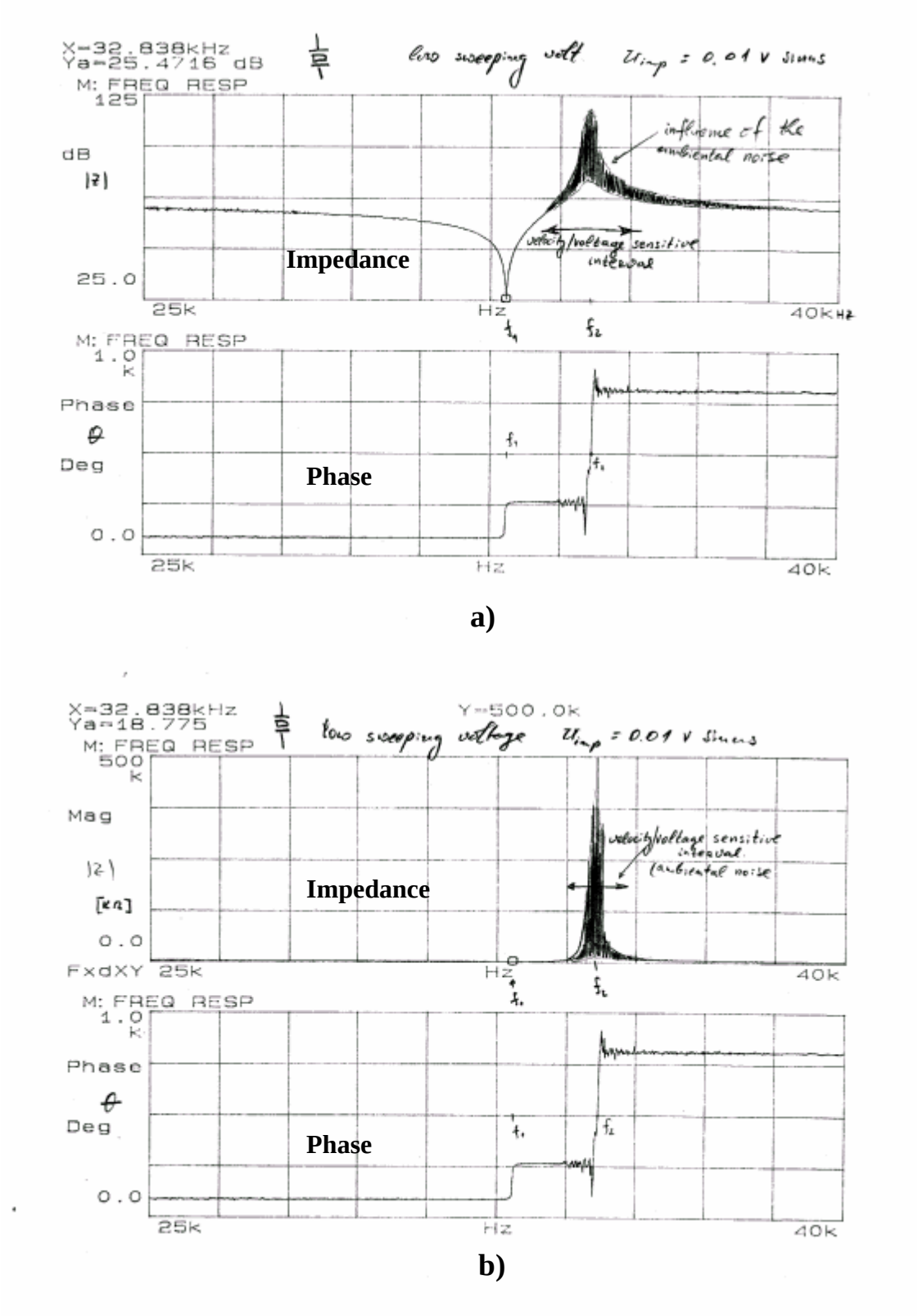

Fig. 4.3-3 Piezoelectric Impedance-Phase Curves ($u_{sweep.}$ = 0.01 V-rms)
a) Logarithmic Impedance-amplitude (in dB)
b) Linear Impedance-amplitude of the same converter

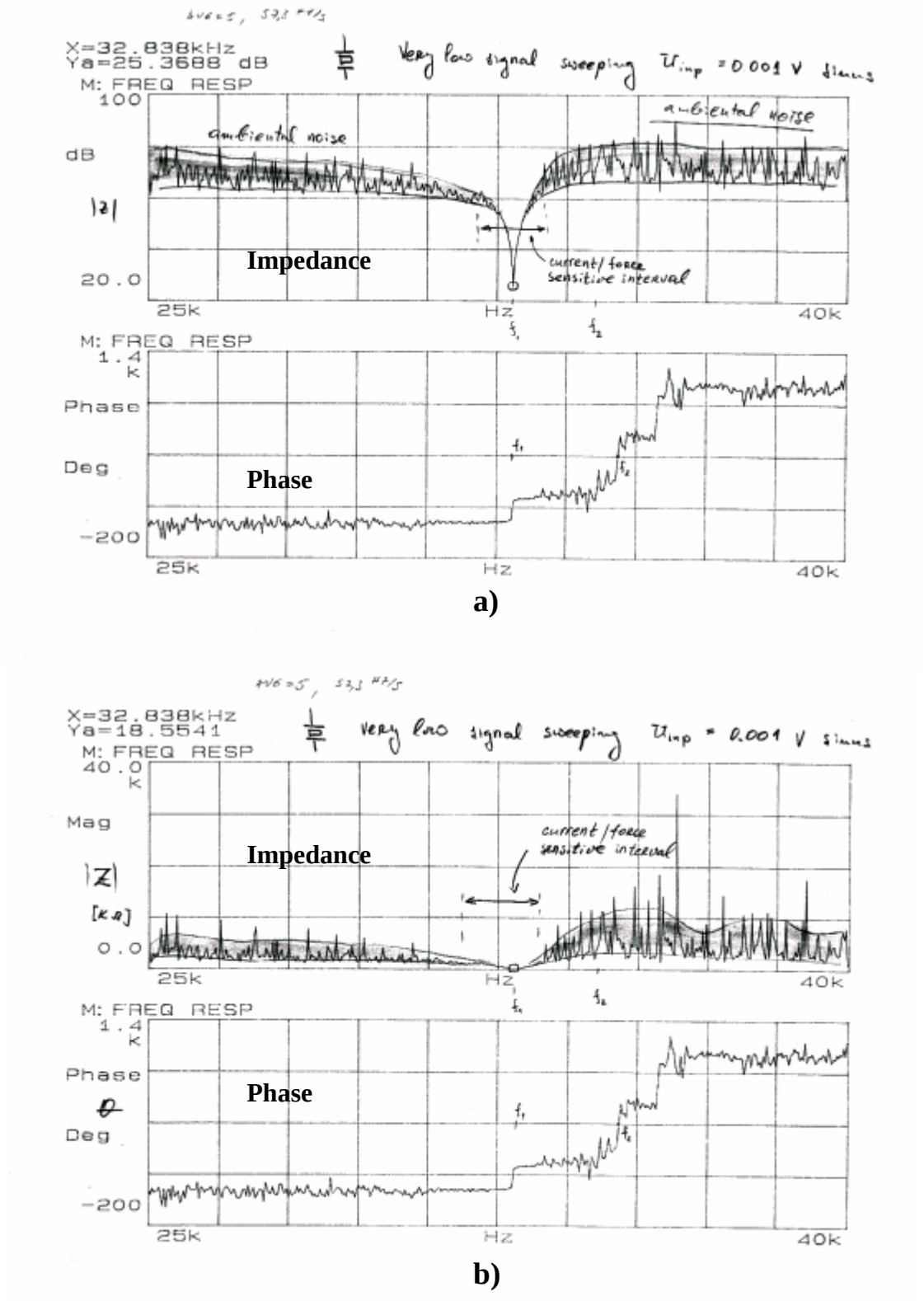

Fig. 4.3-4 Piezoelectric Impedance-Phase Curves ($u_{sweep.}$ = 0.001 V-rms)
a) Logarithmic Impedance-amplitude (in dB)
b) Linear Impedance-amplitude of the same converter

Let us again take the same piezoelectric converter, as already presented on T. 4.1-1, Figs. 4.1-2, 4.1-3.1, 4.1-3.2 and 4.3-1, inductively compensated in series and/or in parallel, and make similar sensitivity detection as before (measuring equivalent Impedance-Phase curves, and reducing sinusoidal frequency-sweeping signal, starting from $\mathbf{u_{sweep.}} \geq 1$ V-rms, until $\mathbf{u_{sweep.}} = 0.01$ V-rms; -see Fig. 4.3-5 until Fig. 4.3-8).

Again, we can consistently conclude that **all parallel-resonance (and high impedance) zones are VELOCITY-VOLTAGE sensitive,** regardless if this is the natural, parallel resonance of a single piezoceramic, or equivalent high-impedance, where piezoceramic is in certain connection with some other passive electrical components (see Fig. 4.1-3.5). We also see, again based on the same measurements (Figs. 4.3-5 – 4.3-8), that all **equivalent series resonances (low impedance zones) are totally insensitive on VELOCITY-VOLTAGE background-noise excitation,** but we can also conclude that **series resonance/s (low impedance/s) zone/s are very much FORCE-CURRENT sensitive** (regarding alternative velocity and force signal forms), since all series resonance zones are producing high-pressure acoustic fields; - see Fig. 4.1-3.4 (and, of course, we can also base our conclusions on electro-mechanical analogies, CURRENT-FORCE & VOLTAGE-VELOCITY, and on dual-circuits', equivalent models).

In order to increase piezoelectric-sensor receiving or transmitting-sensitivity (to operate in the band between two of its impedance peaks, or between $\mathbf{f_L}$ and $\mathbf{f_H}$) we can simply play with connecting parallel and/or series resistances to it, as presented on Figs. 4.1-3.4 and 4.1-3.5.

There are some other possibilities regarding how to increase sensor sensitivity in the frequency areas outside of the resonant frequency couple ($\mathbf{0 \leq f < f_1}$ & $\mathbf{f_2 \leq f}$), when using capacitance connected in series to a piezoelectric sensor or converter, Fig. 4.3-9 (meaning that such sensor will have increased sensitivity starting from very low frequency (close to zero Hz) until series resonance $\mathbf{f_1}$, and again starting from parallel resonance $\mathbf{f_2}$ toward higher frequencies, and it will not be significantly sensitive in the frequency interval between series and parallel resonant frequency). It is interesting to notice that only if series capacitance, $\mathbf{C_s}$, is smaller than static (low frequency) capacitance of a piezoelectric sensor, $\mathbf{C_o}$, the resulting sensitivity will increase (testing sensitivity on the same way as before, by reducing sinusoidal frequency-sweeping signal of Network Impedance Analyzer, starting from $\mathbf{u_{sweep.}} \geq 1$ V-rms, until $\mathbf{u_{sweep.}} = 0.01$ V-rms). For instance, the highest increase of sensitivity (of the same piezoelectric converter presented on T.1, Figs. 4.1-2, 4.1-3.1, 4.1-3.2 and 4.3-1) will be measured if series capacitance is approximately equal to ½ of the static sensor capacitance, $\mathbf{C_s} \cong 0.5\ \mathbf{C_o}$, see Fig. 4.3-10. Surprisingly, when $\mathbf{C_s} \cong \mathbf{C_o}$, this would make sensor-sensitivity non-selective, behaving randomly, and almost useless (phase curve would become unrecognizable, at least in the example of piezoceramics tested here; - given in T. 4.1-1). And again, when $\mathbf{C_s} >> \mathbf{C_o}$, such sensor would behave as sensor without series capacitance.

Generalizing the conclusions about converters activity and/or sensitivity, once more, we can see that everything we are talking about, here, is related to generator-to-load matching (where internal generator or receiver impedance should be close to the

load impedance), and where complex impedance of the load should be reactively compensated in order to become closer to resistive impedance.

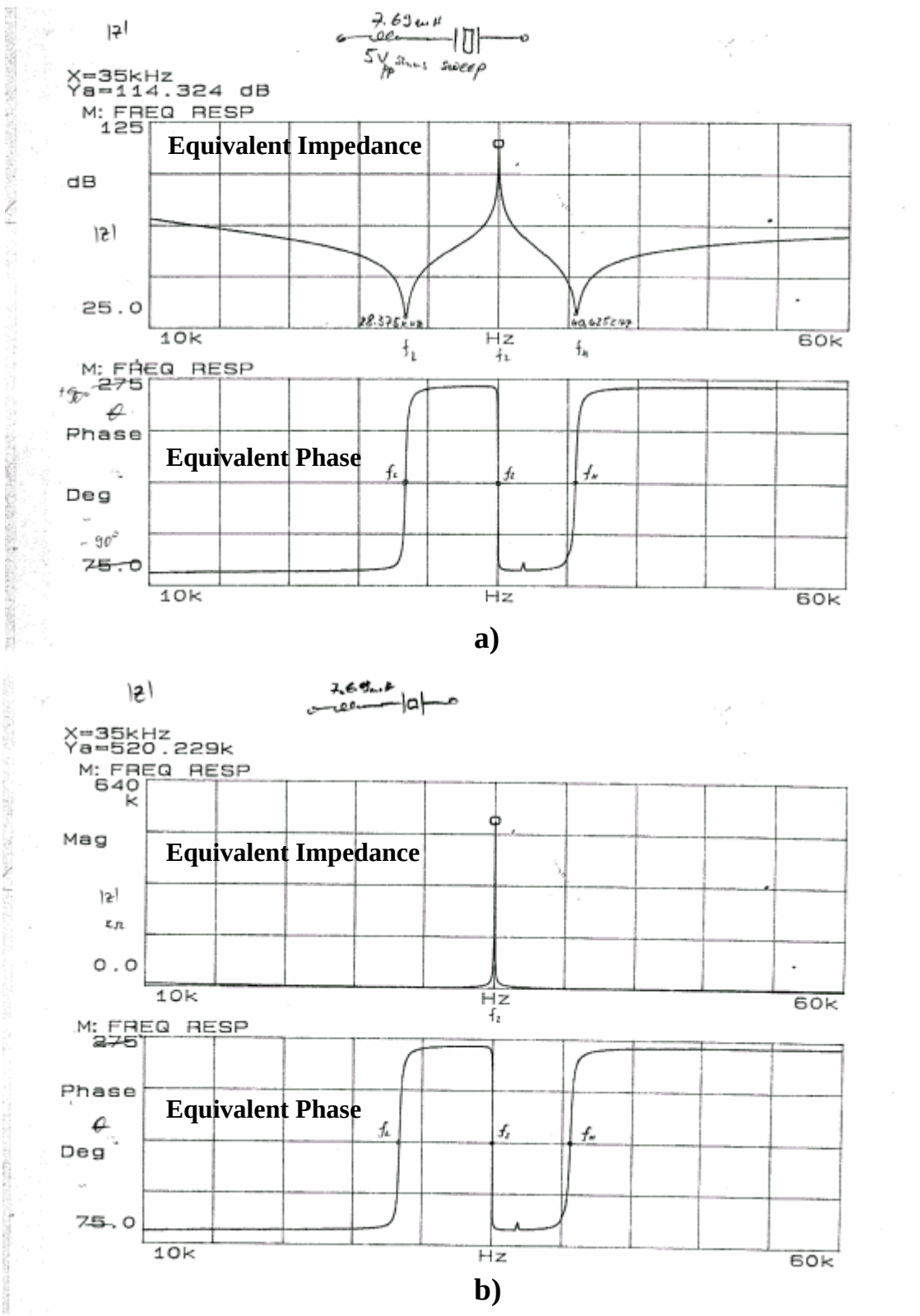

Fig. 4.3-5 Converter with Series Inductive Compensation
L_s = 7.69 mH ($u_{sweep.} \geq 1$ V-rms)

a) Logarithmic Impedance-amplitude (in dB)
b) Linear Impedance-amplitude of the same converter

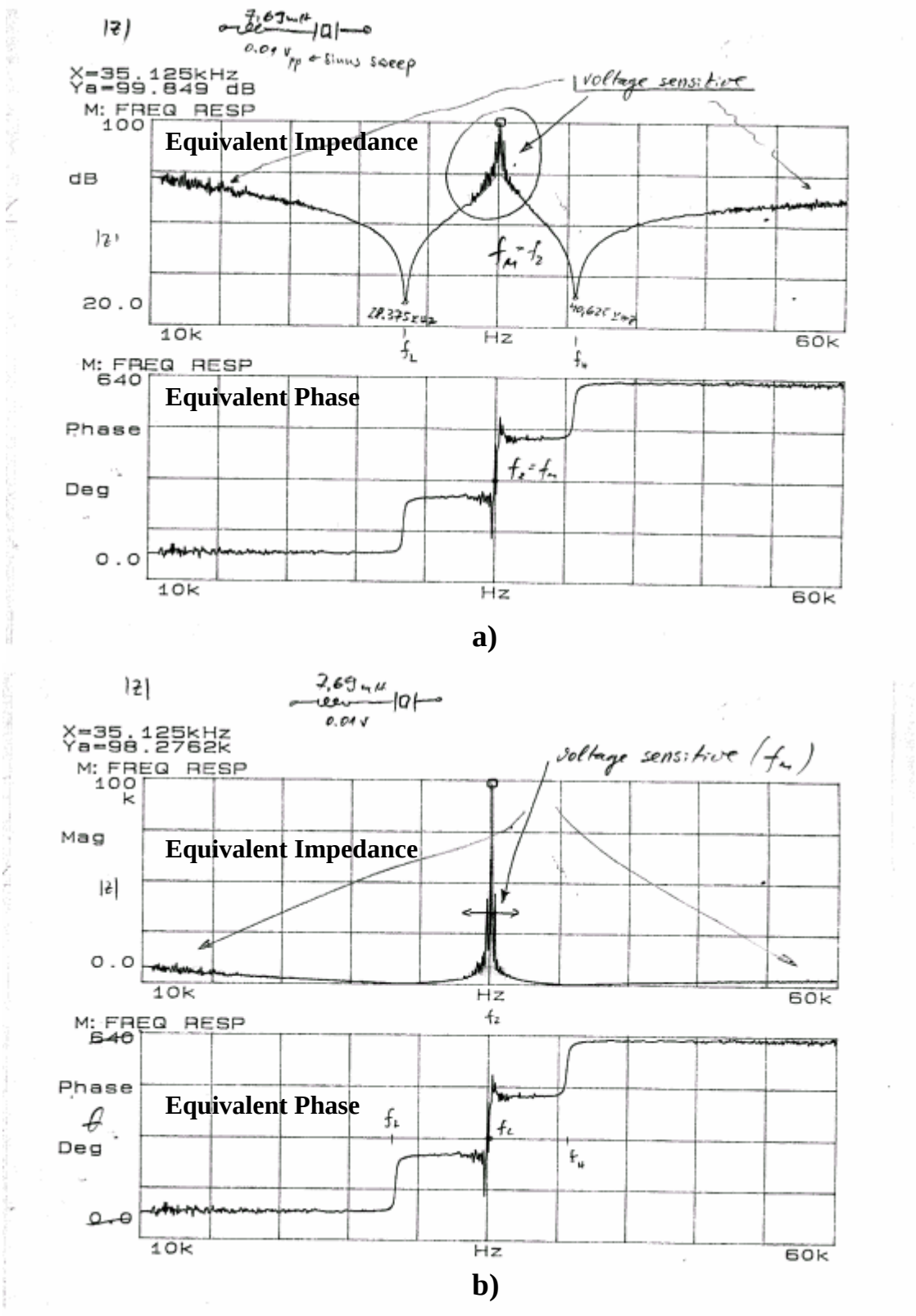

Fig. 4.3-6 Converter with Series Inductive Compensation
L_s = 7.69 mH ($u_{sweep.}$ = 0.01 V-rms)
a) Logarithmic Impedance-amplitude (in dB)
b) Linear Impedance-amplitude of the same converter

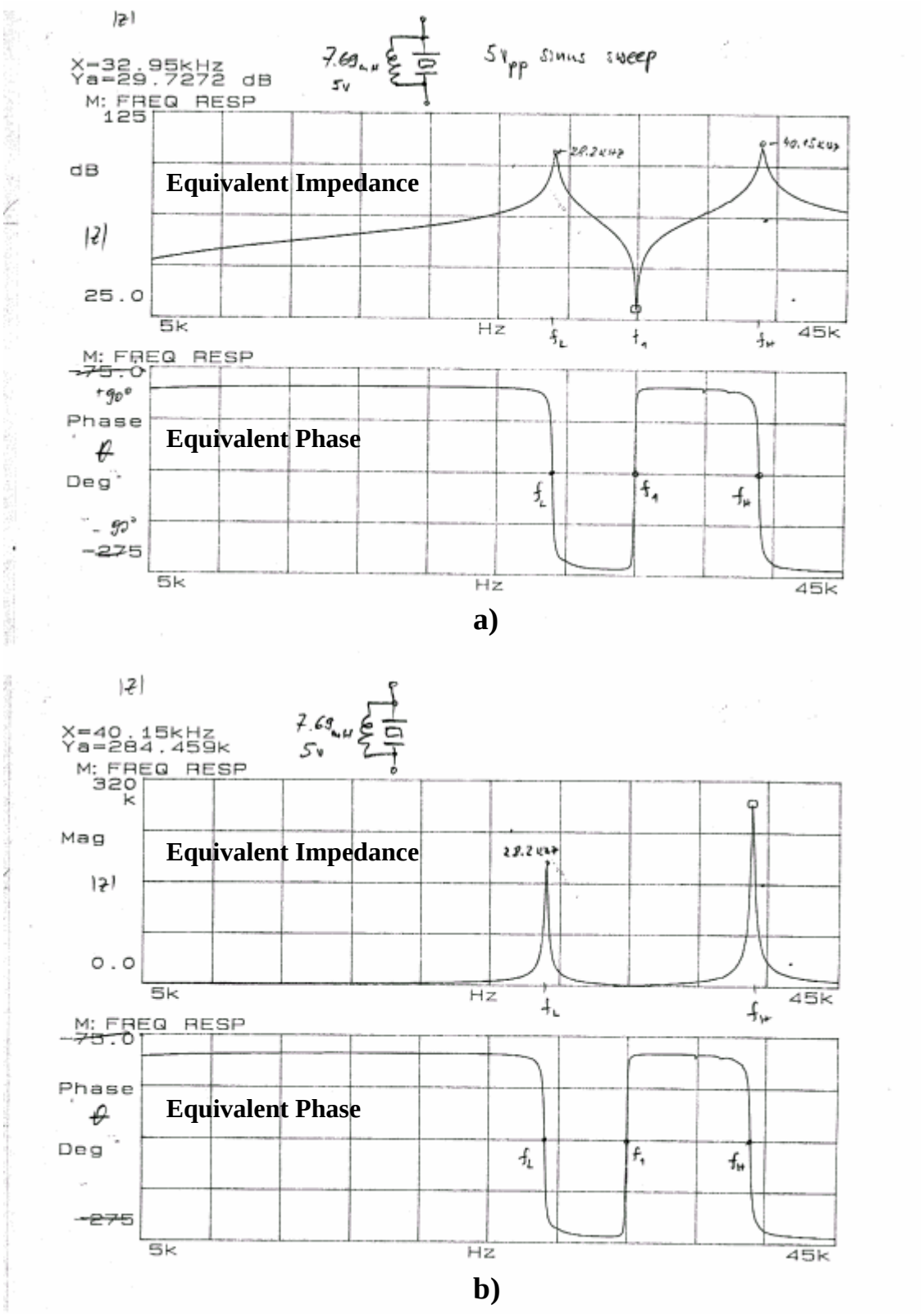

Fig. 4.3-7 Converter with Parallel Inductive Compensation
L_p = 7.69 mH ($u_{sweep.} \geq 1$ V-rms)
a) Logarithmic Impedance-amplitude (in dB)
b) Linear Impedance-amplitude of the same converter

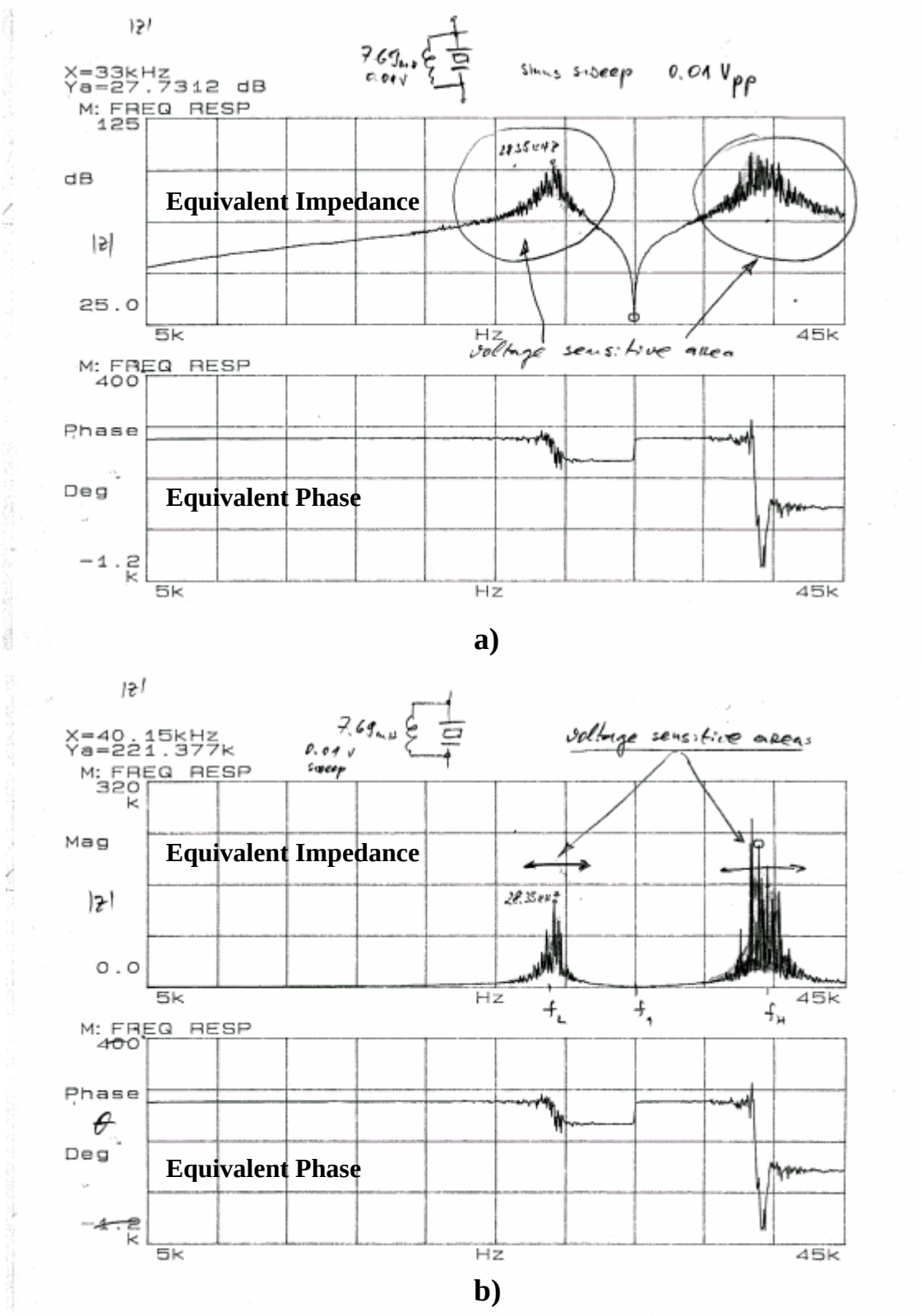

Fig. 4.3-8 Converter with Parallel Inductive Compensation
L_p = 7.69 mH ($u_{sweep.}$= 0.01 V-rms)
a) Logarithmic Impedance-amplitude (in dB)
b) Linear Impedance-amplitude of the same converter

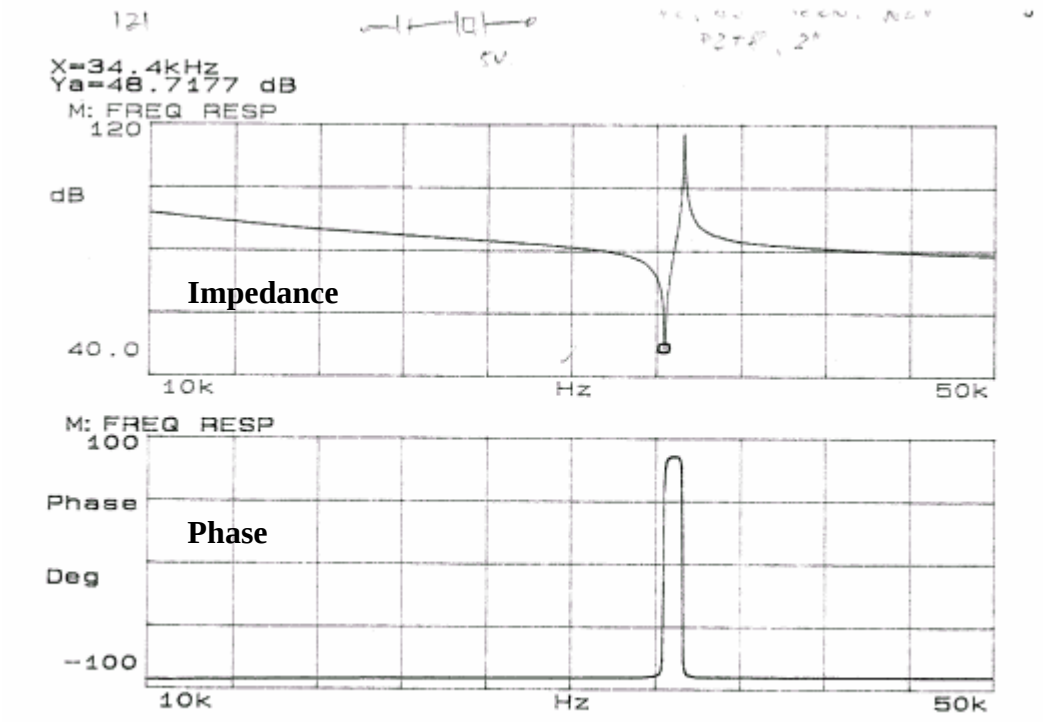

a)

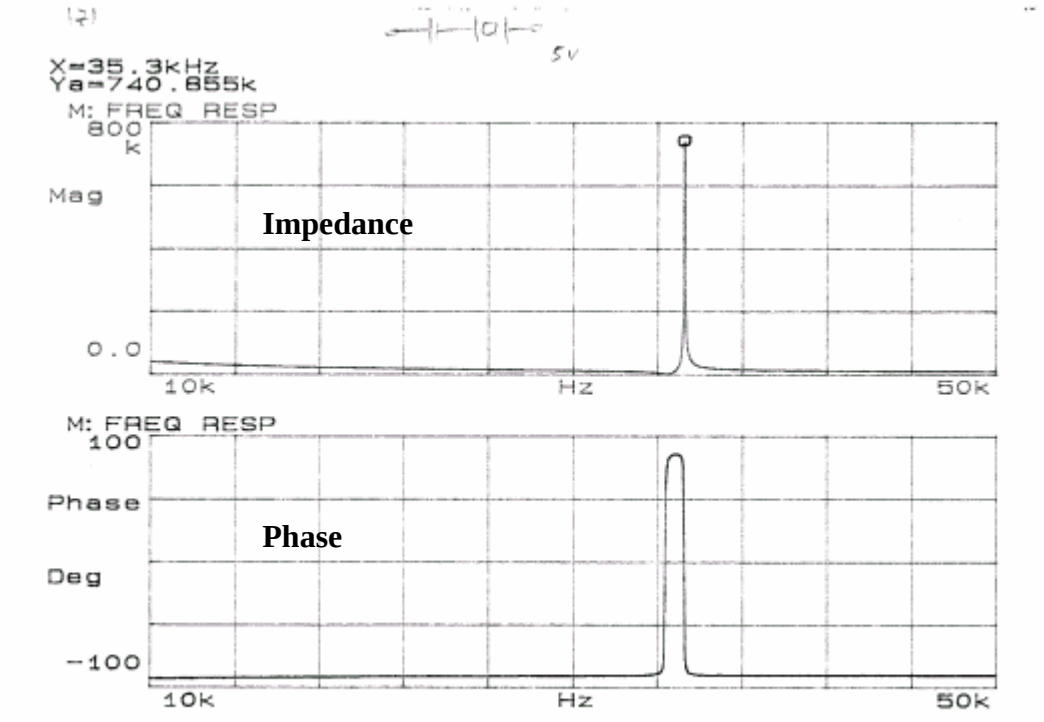

b)

Fig. 4.3-9 Converter (from T. 4.1-1& Fig. 4.1-2) with Series Capacitance, C_s = 1.368 nF, C_{os} = 3.0221 nF ($u_{sweep.} \geq 1$ V-rms)

a) Logarithmic Impedance-amplitude (in dB)

b) Linear Impedance-amplitude of the same converter

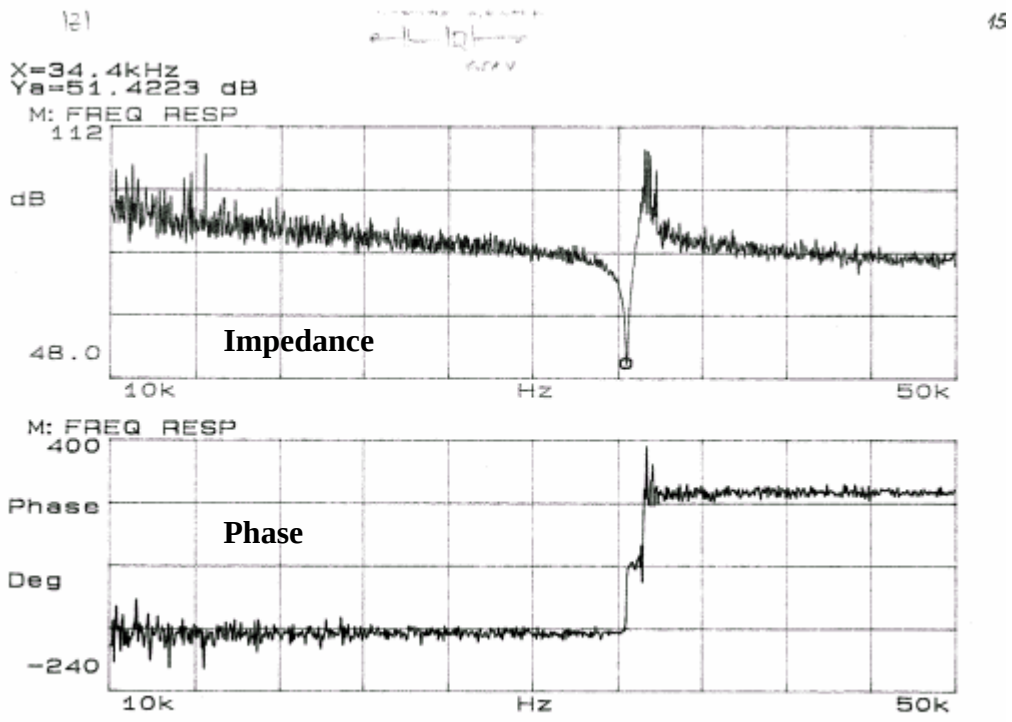

a)

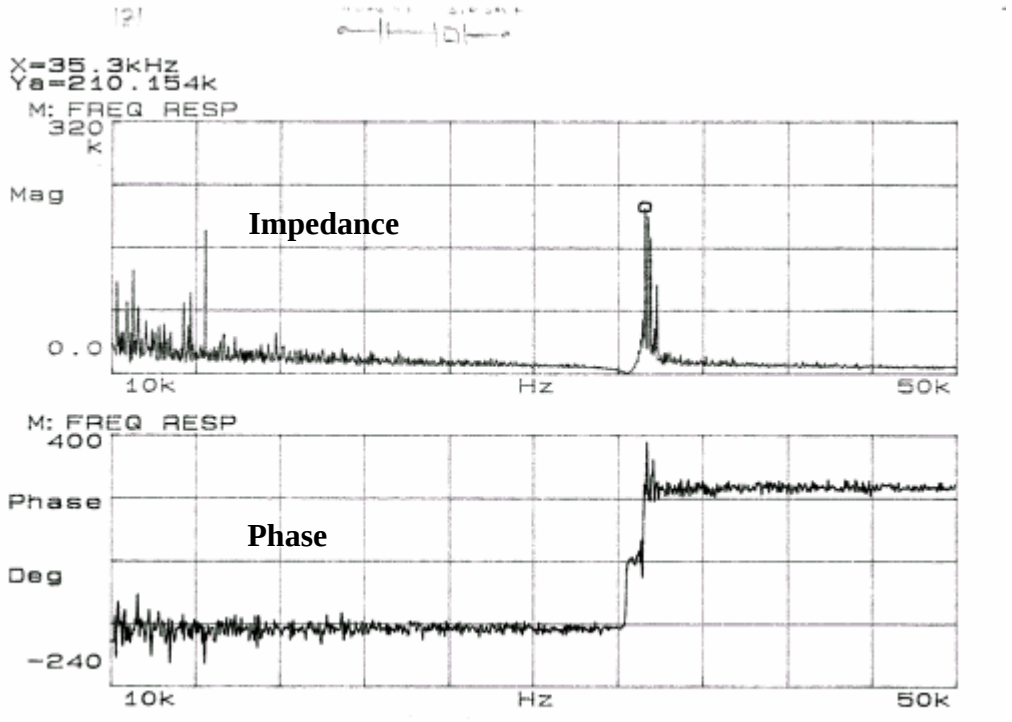

b)

Fig. 4.3-10 Converter with Series Capacitance ($u_{sweep.}$= 0.01 V-rms)
C_s = 1.368 nF, C_{os} = 3.0221 nF

a) Logarithmic Impedance-amplitude (in dB)
b) Linear Impedance-amplitude of the same converter

4.4 Practical and simplified procedure for inductive impedance compensation, optimal impedance and optimal power matching of arrays of ultrasonic cleaning transducers

1. Find the input capacitance of a single transducer measured on 1 kHz, $C_p(1kHz) = C_p$ = ___(nF), and multiply it by number of transducers, **n = 1, 2, 3…**, that will be assembled in parallel connection (on the same ultrasonic tank). $C_{pn}(1kHz) = C_{pn} = \mathbf{n}C_p(1kHz)$ = ___(nF). Use LRC-meter.

2. Find the total input capacitance of the transducer group (**n** transducers in parallel electrical connection, glued to ultrasonic tank) measured on 1 kHz. $C_{pn}(1kHz) = C_{pn}$= ___(nF). This value should be very similar to the value of $C_{pn}(1kHz)$, calculated in point 1. Use LRC-meter.

3. Find the resonant frequency and resonant impedance of a free and single transducer (not loaded, measured in air) f_r = fr = ___kHz (at minimum impedance Z_r = Zr = ___Ω). This should be the value declared by the producer of a transducer. Check if your measurement is in agreement with declared value. If you cannot make your own frequency and impedance measurements, take data from producer's catalogue. For measurements it is necessary to have recommended IEC circuit arrangement, or HP 4194A Network Impedance Analyzer. The simple improvisation for measurements is possible to be organized using sinus function generator, oscilloscope and IEC resistive network circuit.

4. Find the resonant frequency and resonant impedance of all transducers (as a group) when they are in parallel connection (**n** = number of transducers), glued to ultrasonic tank or to immersible transducer box (and when tank, or immersible transducer box are fully water loaded): $\mathbf{f_{rn}}$ = frn = ___kHz (at minimum impedance Z_{rn} = Zrn = ___Ω). This could also be the value declared by the producer of transducers, but if it is not declared, it would be found in the vicinity of about 10% lover frequency than resonant frequency measured under 3. Check if your measurement is in agreement with declared value/s. If you cannot make your own measurements (missing instruments), take data from producer catalogue. If producer did not give any data, take this frequency as an approximate number that will be equal 0.9 multiplied by frequency **fr** found under 3. ⇒ frn = 0.9fr ___kHz. If possible, find resonant impedance of the transducer group (when fully water loaded) Z_{rn} = Zrn = ___Ω. Zrn should be in the range of value measured under point 3., or more precisely in the range $10Zr/\mathbf{n} \le Zrn \le 100Zr/\mathbf{n}$ (for efficient transducer group, and for good gluing-bonding technology). For above-mentioned measurements it is necessary to have recommended IEC circuit arrangement, or HP 4194A Network Impedance Analyzer. The improvisation is possible to be organized using sinus function generator, oscilloscope and IEC resistive network circuit.

5. Calculate the approximate (maximal) value of necessary inductive compensating coil using the formula: $\mathbf{Ls \le 1/(4\pi^2 f_{rn}^2 C_{pn})}$ = ___(μH or mH) (in order to cancel the static capacitance of the transducer group). Resonant frequency $\mathbf{f_{rn}}$ is taken from 4., and parallel capacitance Cpn is taken from 2. Make, adjust and fix compensating inductance **Ls**, changing the air gap in the ferrite core. In real operation, the best ultrasonic power will be found adjusting a bit lower inductance **Ls** than previously calculated (but sometimes, the **real inductive compensation has until 2 times smaller value than here calculated Ls**, because of non-linear and self-compensating, interference-coupling effects between transducers in high power operation, especially when transducers have well operating higher harmonics, and when large frequency sweeping is applied; -since in certain limited frequency band/s every particular piezoelectric transducer reacts like inductive element, while other transducers are dominantly capacitive, and not all of them from the same group are mutually 100% identical, enabling mutual inductive compensation). Use LRC-meter for inductance measurements (usually on 1 kHz), or HP 4194A, or HP 4195A.

6. Optimal ultrasonic power (on ultrasonic transducers, operating on lowest basic series resonant frequency) will be achieved when: **a)** High frequency current and voltage measured on the primary input side of the ferrite (output power) transformer are mutually in phase, and **b)** When generator current reaches its maximum (measured on the primary side of the ferrite transformer, or

Miodrag Prokic, Marais 36, CH-2400, Le Locle, e-mail: mpi@bluewin.ch

(approximately speaking) on the main supply input of generator). **c)** In the same time when conditions **a)** and **b)** would be satisfied, the input power factor (cosines theta) on the main supply, low frequency power input (115/230 VAC, 50/60 Hz) should be very close to 1 (to one), since ultrasonic generator would consume only active power. High frequency transducers' current measured on the primary or secondary side of the ferrite transformer has sinusoidal shape. Voltage shape measured on the primary side of ferrite transformer has rectangular shape (usually 1:1, or 50% Duty Cycle, except when PWM signal is used for direct transducers driving). **For highly efficient transducers operation (and for good impedance matching) it is extremely important to oversize the primary windings cross-section area of the Litz wire (on the output, high power ferrite transformer). For instance, select the Litz wire with the total cross section surface, that corresponds to the RMS primary current of: 2.5 until 1.5 A/mm^2. To avoid any heating in output ferrite transformer, the best would be to use criteria 1.5 A/mm^2. Similar logic is valid for inductive compensating choke, and for secondary windings of the ferrite transformer (less rms. current per mm^2 is always a better choice). For inductive compensating inductance we can apply the criteria 2.5 until 2 A/mm^2 and for secondary transformer windings, 2 until 1.5 A/mm^2 (always based on RMS primary or secondary current). *The most important of all above-mentioned conditions is to increase the cross section area of primary transformer windings, in order to minimize heating in output transformer.***

7. The natural or forced aging of ultrasonic transducers is extremely important process (in ultrasonic cleaning or welding applications, when operating in any of resonant or multifrequency regimes). For instance, after assembling a group of cleaning transducers (after gluing/bonding to a cleaning tank), it is necessary to make minimum 24 hours of continuous-operating aging: Start with about 30% of ultrasonic power-loading (of an ultrasonic tank filled with water), and after several hours increase the tank power until 100% of ultrasonic generator power (and keep this way during long time: in total minimum 24 hours). Material aging and vibrating-surfaces micro-friction would stabilize transducers parameters, as well as stabilize adhesive bonding layers. Some famous ultrasonic companies are often performing 7 days (24 hours a day) forced aging of their cleaning tanks (and immersible transducer boxes). During the process of forced aging the water level in the tank should be kept on the same level (adding water when necessary). After certain time of such operation, it appears significantly noticeable that operating regime of ultrasonic transducers becomes quieter, smoother, more stable, and cleaning efficiency increases. When initial forced aging is finished, and transducers reach room temperature (for instance after 24 hours), if we perform measurements of transducers' parameters, we shall notice parameters-changes between 5% and 10% compared to measurements before forced aging. Forced aging should be performed using certain (maximally acceptable) level of frequency-modulation (sweeping), and applying sufficiently high amplitude modulation of ultrasonic power. **Practically, all above described measurements and tuning steps (from 1. to 6.) should be repeated in order to make new and final frequency and impedance tuning and matching. This way we avoid the situation that transducers aging would be naturally finalized when ultrasonic cleaner is sold to a customer (because usually a customer is not able to make retuning and new impedance matching).** The aging is finalized successfully if after 24 hours (when transducers again reach room temperature) we get the same full-power operating-conditions as during the final tuning. A similar aging procedure should be applied to single plastic-welding transducers operating on parallel or series resonance (only the conditions for treatment, acoustic loading, and time intervals should be optimally adjusted for every specific situation). **Once (after long empirical data collection) when we know the final and optimal operating regimes for certain transducer configurations, we can apply direct settings for best frequency and impedance matching, and immediately start with optimal artificial aging.**

8. In the case when transducer group is operating on some higher-harmonic frequency, we could easily have the case that transducers' current has 2 to 4 times higher frequency than the frequency of the voltage applied on primary side of ferrite transformer. Such (ringing and high frequency) resonant regimes are not described here. The inductive compensation **Ls** for such situations can be calculated similar as for basic frequency (see point 5) and then experimentally adjusted for the best ultrasonic operation on the high frequency harmonic, increasing the gap of the ferrite core of **Ls**, what is equivalent to decreasing the **Ls**. For the operation on high frequency harmonics it is necessary to apply relatively wide band frequency sweeping voltage input into output ferrite

transformer (and to produce well balanced ON-OFF signal group modulation in order to give sufficient OFF time to transducer group to produce high frequency, self-generated ringing current response). Ultrasonic transducers operating on higher harmonics usually have strong acoustic coupling between number of higher harmonics and basic (lowest frequency) resonant mode. If we are driving transducer on its basic resonant mode, it will also be possible to excite all other, coupled, higher frequency modes (just giving them sufficient OFF time to produce self-generated, ringing current signals). Knowing this, we also know that inductive compensation should be (first) well made for basic resonant mode, and later on, manually tuned (reduced to lower value) to enable transducers operating on higher frequency modes.

9. Optimal high frequency RMS-voltage (ultrasonic frequency RMS-voltage) measured directly on input side of ultrasonic transducers (on piezoceramics) should never be higher than 50 Volts (RMS) per each millimeter of single piezoceramic ring thickness (measured using high frequency and wide band, AC, RMS voltmeter, in any possible operating regime). For instance, if one transducer has two piezoceramic rings (in parallel electrical connection, as usual), each of them t = 5mm thick, than RMS-voltage measured directly on ceramics (PZT4 and PZT8) should be $u_t \leq 50 \times t = 50x5 = 250$ V (RMS). If we cannot measure RMS voltage on ultrasonic frequency (missing RMS voltmeter), then using oscilloscope we can (approximately) find maximum (half period peak) transducer voltage as $u_{tpeak} \leq 1.41 \times 50 \times t \cong 70 \times t$, or we can also find peak-to-peak transducer voltage as $u_{tpeak\text{-}to\text{-}peak} \leq 2 \times 1.41 \times 50 \times t \cong 2 \times 70 \times t \cong 140 \times t$. For the same example when thickness of one piezoceramic ring is 5mm, it will be: $u_{tpeak} \leq 1.41 \times 50 \times t \cong 70 \times 5 = 350$ V, $u_{tpeak\text{-}to\text{-}peak} \leq 2 \times 1.41 \times 50 \times t \cong 2 \times 70 \times 5 \cong 140 \times 5 = 700$ V. In any other case, if we try to make different frequency and impedance adjustments, it would become destructive for ultrasonic transducers to increase voltage on piezoceramics for more than: $u_t \leq 100 \times t$, or $u_{tpeak} \leq 1.41 \times 100 \times t$, or $u_{tpeak\text{-}to\text{-}peak} \leq 2 \times 1.41 \times 50 \times t$. Voltage and current shapes measured directly on transducers are (approximately) sinusoidal and mutually shifted between 60° and 90° angle degrees (usually shifted for almost 90° in cases of high quality transducers and good impedance matching). Transducer voltage should be adjusted by changing output (secondary side) of the ferrite transformer and slightly adjusting inductive compensation coil (changing its air gap).

10. Continuous and safe, RMS power of one single ultrasonic, cleaning transducer (when glued to ultrasonic tank and water loaded) should be in the range of 3 Watts per cubic centimeter of the total volume of piezoceramic rings for PZT4, and 4 to 5 Watts per cubic centimeter for PZT8 piezoceramics. For instance, if one single ultrasonic (cleaning) transducer has 2 of PZT4 piezoceramics, where total ceramics volume (of both ceramics) is approximately 13 cubic centimeters, its continuous and safe operating power would be $13 \times 3 \cong 40$ Watts. If the same transducer has PZT8 piezoceramic rings, then it can operate producing RMS power of $13 \times 4 = 52$ Watts, or not higher than $13 \times 5 = 65$ Watts. In a short-time loading conditions, cleaning transducers can produce up to 5 times higher ultrasonic power, providing that gluing or bonding technology is guarantying sufficiently strong mechanical coupling between transducers and ultrasonic tank (to resist such stress). Here we are talking only about real, active or RMS power that can be measured using high frequency wide band power meters (connected directly to transducers group or to the primary side of output ferrite transformer). Ultrasonic generator should be adjusted (by inductive compensation and selection of output voltage on secondary side of the ferrite transformer) not to produce higher output power than safe and continuous operating power of transducer group is (given by transducers supplier, or found empirically and tested very long time). The same transducers, when operating as plastic welding transducers could produce between 30W and 50 Watts per cubic centimeter of total piezoceramics volume installed in the sandwich transducer (valid for PZT 4 and PZT 8). **The second and extremely important criteria for efficient transducer/s operation is to achieve the maximal input power factor (cosine theta) of 1, or 0.98, or always higher than 0.9 (meaning that ultrasonic generator is consuming only the real and active power (when operating full power on its power maximum), and that input electrical energy conversion to ultrasonic energy is maximal). This will be achieved by choosing the proper inductive compensation, proper output transformer ratio, and proper filtering capacitor in the DC power diode-bridge section (input main supply AC side). When using modern PFC and PWM controller circuits for input DC power control, we can achieve the best power conversion.**

11. Every single cleaning transducer can accept the input RMS high frequency current, $\mathbf{I_t}$, in the range given by the following relation:

$$\frac{(3 \text{ until } 5)\cdot V}{100\cdot t} \le I_t(\text{Amps, RMS}) \le \frac{(3 \text{ until } 5)\cdot V}{50\cdot t}$$

(for PZT4, use 3, and for PZT8 use 5),

V = total piezoceramics volume for one single transducer (=) $[cm^3]$

t = thickness of the single piezoceramic ring (=) [mm]

The total transducers current for the group of transducers in parallel connection (operating on series resonance) is equal to the above calculated current multiplied by the number of transducers.

For welding transducers operating on parallel resonant frequency, the similar input transducer current criteria can be expressed by the equation:

$$I_t(\text{Amps, RMS}) \le \frac{(30 \text{ until } 50)\cdot V}{200\cdot t}$$

(for PZT4 ≈ Sonox P - 4, use 30, and for PZT8 ≈ Sonox P – 8 use 50),

V = total piezoceramics volume for one single transducer (=) $[cm^3]$

t = thickness of the single piezoceramic ring (=) [mm]

If welding transducer is operating on its series resonant frequency, use the criteria:

$$\frac{(30 \text{ until } 50)\cdot V}{100\cdot t} \le I_t(\text{Amps, RMS}) \le \frac{(30 \text{ until } 50)\cdot V}{50\cdot t}$$

(for PZT4 ≈ Sonox P - 4, use 30, and for PZT8 ≈ Sonox P – 8 use 50),

V = total piezoceramics volume for one single transducer (=) $[cm^3]$

t = thickness of the single piezoceramic ring (=) [mm]

12. Continuous and safe operating temperature of modern (PZT) piezoceramics (in ultrasonic cleaning) should be lower than 100°C (sometimes up to 120°C, for high temperature resistant piezoceramics), depending of water temperature in ultrasonic tank, but always lower than 150°C (for the best piezoceramics, found on the market at this time). It is recommendable to operate ultrasonic transducers on a lowest possible temperature. For welding transducers (when operating continuously in air) the piezoceramic temperature should not be higher than 50°C to 60°C (measured after very long time). The continuous operating temperature of piezoceramics can be measured using remote non-contact temperature infrared (laser beam) thermometers (directing the laser beam to the ceramics area).

ELECTRICAL SAFE OPERATING LIMITS OF PIEZOCERAMICS (PZT-8 GRADE)
(All values are in RMS and SI units)

Definitions of Piezoceramic parameters (used in T.1), which are important for transducer power calculation (valid for piezoceramic rings):

Geometry parameters:

t – thickness of the ring (=) [m] ,
R – outer radius of the ring (=) [m] ,
r – inner radius of the ring ID (=) [m] ,
S_1 – surface of one, flat side, of the ring = $\pi(R^2 - r^2)$ (=) [m^2] ,
V_1 – volume of one piezoceramic ring = $S_1 t = \pi(R^2 - r^2)t$ (=) [m^3] ,
n –Total number of PZT elements (rings) in assembled transducer (n= 2, 4, 6…).

Applied voltage and current (directly on a piezoceramic):

$u_t \leq 0.5\, u_d$ – acceptable operating (rms.) voltage on a piezoceramic (=) [v],
u_d – depolarization voltage (=) [v]

$$u'_t = \frac{u_t}{t}(=)\left[\frac{V}{m}\right] \quad - \text{Acceptable, applied electrical field on (one) piezoceramic,}$$

$$u^*_t \leq 0.9 \cdot u'_t\,(=)\left[\frac{V}{m}\right] \quad - \text{Continuous, loading / operating field applied on a piezoceramic}$$

$$I_{s1} = \frac{2 \cdot I_t}{nS_1}(=)\left[\frac{A}{m^2}\right] \quad - \text{Average Surface current density (on a PZTelectrodes)}$$

$$I_t \quad (=) \quad [A] \quad - \text{Total transducer Input current (rms)}$$

Specific ultrasonic power density:

$$P_v = \frac{P_{(r/c)-max}}{nV_1} = \frac{1}{2}u_{t1} \cdot I_{s1}(=)\left[\frac{W}{m^3}\right] \quad - \text{Average volumetric power density,}$$

$$P_{S1} = \frac{2 \cdot P_{(r/c)-max}}{nS_1}(=)\left[\frac{W}{m^2}\right] \quad - \text{Average surface power density on one flat side of a PZT}$$

Average resonant frequency (applicable for power calculation):

(For the purpose of calculation and modeling, f_{res} is taken between two characteristic resonant frequencies)

$f_{res} = (f_1 + f_2)/2 = (f_p + f_s)/2$ (=) [Hz]

ELECTRICAL SAFE OPERATING LIMITS OF BOLTED LANGEVIN TRANSDUCERS

The following table, T.1, is applicable on single and free (in air) ultrasonic (sandwich) transducers that are not bonded/glued to some other solid-state mass (data established based on measurements for the operating frequency $f_{res.} \cong 20$ kHz $\cong (f_1 + f_2) / 2$, and operating peak-to-peak, sinusoidal amplitude $a_{pp} = 20$

μm). Later on, we shall extrapolate this situation to other operating frequencies and amplitudes (as well as for cleaning transducers that are glued to a cleaning tank).

T.1

BLT is operating in series resonance: $f_s = f_1$ Current driven transducers, $Z = Z_{min.}$	**BLT is operating in parallel resonance: $f_p = f_2$ Voltage driven transducers, $Z = Z_{max.}$**

Non-Loaded (in air)	**Fully-Loaded (in water)**	**Non-Loaded (in air)**	**Fully-Loaded (in water)**
n.a.	**P_v = 60 [W/cm^3] for $P_{r\text{-}max.}$**	n.a.	**P_v = 60 [W/cm^3] for $P_{r\text{-}max.}$**
n.a.	**P_v = 30 [W/cm^3] for $P_{c\text{-}max.}$**	n.a.	**P_v = 30 [W/cm^3] for $P_{c\text{-}max.}$**
n.a.	**P_{s1} = 30 [W/cm^2] for $P_{r\text{-}max.}$**	n.a.	**P_{s1} = 30 [W/cm^2] for $P_{r\text{-}max.}$**
n.a.	**P_{s1} = 15 [W/cm^2] for $P_{c\text{-}max.}$**	n.a.	**P_{s1} = 15 [W/cm^2] for $P_{c\text{-}max.}$**
$P_{vdiss.}$ = 0.23 – 0.60 [W/cm^3]	**$P_{vdiss.}$ = 0.92 – 2.77 [W/cm^3]**	**$P_{vdiss.}$ = 0.11 – 0.35 [W/cm^3]**	**$P_{vdiss.}$ = 0.39 – 0.46 [W/cm^3]**
u'_t = 1.3 - 10 [V/mm]	**u'_t = 10 - 100 [V/mm] u^*_t = 50 - 60 [V/mm]**	**u'_t = 50 - 220 [V/mm] u^*_t = 200 [V/mm]**	**u'_t = 50 - 220 [V/mm] u^*_t = 200 [V/mm]**
$I_{s1max.}$ = 80 [A/m^2]	**I_{s1} = 80 - 1200 [A/m^2]**	**$I_{s1max.}$ = 20 [A/m^2]**	**I_{s1} = 20 - 300 [A/m^2]**
n.a.	**max.(u'_t I_{s1}) ≤ P_v**	n.a.	**max.(u'_t I_{s1})≤ P_v**
($Z_{min.}S_1/t$) ≤ (0.65 to 5) [Ωm]	n.a.	**($Z_{max.}S_1/t$) ≥ (33 to 135) [KΩm]**	n.a.

$P_{r\text{-}max.}$ [Repetitively driven, Fully-Loaded (in water)] (=) T_{on} : T_{off} = 1 : 1, pulse-repetitive train, $P_{r\text{-}max.}$ = 2 $P_{c\text{-}max.}$
$P_{c\text{-}max.}$ [Continuously driven, Fully-Loaded (in water)] (=) T_{on} = continuous, T_{off} = 0
$P_{diss.}$ (=) Thermal-dissipation power (losses)
u'_t – For variable voltage regulation, u^*_t – Constant (stable) voltage for continuous operating regime
n.a. = Not applicable

In the case if transducer/s is/are bonded/glued or differently fixed to some other solid-state mass, above given (safe-operating) maximal power limits are 5 to 10 times lower (as in the case of ultrasonic cleaning applications). The current and voltage limits (operating intervals and safe operating limits) for piezoceramics will stay the same in any situation, providing that maximal power limits are respected.

If transducer/s is/are operating in some other, frequency sweeping regime, passing over many series and parallel resonant points, all safe operating limits listed in T. 1 should be respected in the same time (max. Applied voltage, max.-Input-current, max.-Power-density). The corresponding electrical limitations, ultrasonic generator regulations and protections should be implemented. The most important criteria in such situations are to minimize reactive power of the transducer and to maximize its active power. Operating temperature of piezoceramic elements (in any operating regime) should be lover as possible (we can say between 20°C and 60°C is preferable situation, but in any case, for continuous and very long operation, no more than 90°C). If piezoceramics in operation reach temperatures between 150°C and 180°, efficiency of transducer will drop significantly.

Generally valid (semi-empirical) formula for calculating the output power of one sandwich, ultrasonic transducer (Bolted Langevin transducer = BLT) is:

$$\mathbf{P_{output}} = \eta \cdot \mathbf{a}^2{}_{\mathbf{pp}} \cdot \mathbf{f}^2{}_{\mathbf{res.}} = \mathbf{P_{r-max.}} = \mathbf{2} \cdot \mathbf{P_{c-max.}} = \mathbf{Const.} \cdot (\mathbf{Q_{em-eff}} \frac{\mathbf{M_{Piezo}}}{\mathbf{M_{converter}}} \mathbf{d_{33}} \mathbf{u_t})^2 \mathbf{f_{res.}}^2$$

(factor 2 is taken as the security margin),

a_{pp} = Transducer's front emitting surface, peak – to – peak – amplitude,

measured when transducer is oscillating harmonically (sin. oscilating function)

The most important quality parameters of power ultrasonic converters

Static & Low signal parameters; Low power parameters (converter is operating in air = no-load)

$C_{inp.}\,(\text{at}\,1\,\text{kHz}) \rightarrow \text{High enough}\ [\text{nF}]$	Total input capacitance
$E \rightarrow \text{max.}\ [\text{N/m}^2]$	Piezoceramics Young modulus
$Q_{mo1,2}\,(\text{of assembled, non-loaded converter}) \geq$ $\geq Q_{mo1,2}\,(\text{of single, non-loaded piezoceramics}) \rightarrow \text{max.}$	Relations between Mechanical Quality Factors of assembled, non-loaded converter and Quality factor of piezoceramics (that is the part of the same converter)
$Q^*_{mo} = \sqrt{Q_{mo1} \cdot Q_{mo2}} \rightarrow \text{max.},$ $(\geq 1000, \text{for instance})$	Effective mechanical quality factor (here invented parameter)
$Q^*_{emo} = \sqrt{Q^*_{mo} \cdot Q_e} \rightarrow \text{max.},$ $(\geq 1000, \text{for instance})$	Effective electromechanical quality factor (here invented parameter)
$\tan\delta\,(\text{at}\,1\,\text{kHz}) = \dfrac{1}{Q_e} \rightarrow \text{minimum}$	Dielectric loss factor Q_e = Dielectric quality factor
$d_{33} \rightarrow \text{High enough},\ 10^{-12} \cdot \left[\dfrac{m}{V} = \dfrac{C}{N}\right]$	Piezoelectric charge constant
$\left\lvert\dfrac{Z_{max.}}{1000 \cdot Z_{min.}}\right\rvert \cong \left\lvert\dfrac{R_2}{1000 \cdot R_1}\right\rvert \rightarrow \text{max.},$ $(\geq 100, \text{for example})$	Maximum to minimum impedance ratio
$T_c \rightarrow \text{High enough}\,(\text{max.}\,T_c > 300),\ [^\circ\text{C}]$	Curie temperature
$\Delta f = (f_2 - f_1) \rightarrow \text{max.}$ $\text{for ex.:}\ 100 \cdot \dfrac{\Delta f}{\langle f \rangle} \geq 10\%$	Frequency gap between series and parallel resonant frequency

Dynamic parameters in resonance
Power parameters (converter is operating in air = no-load)

$f_{res.} = f_1$, series resonance	$f_{res.} = f_2$, parallel resonance
$D_I = \dfrac{\text{Output Force}}{\text{Motional Current}} = \dfrac{F_m}{i_m} =$ $= \dfrac{4\pi^2 f_1^{\,2} a_1}{i_m} \cong \dfrac{4\pi^2 f_1^{\,2} a_1}{i_{inp.}} = \dfrac{4\pi^2 f_1^{\,2} a_1}{P_{inp.}} u_{inp.}$ $\cong \dfrac{4\pi^2 f_1^{\,2} a_1}{P_{diss.}} u_{inp.} \rightarrow \text{maximum.}$	$D_U = \dfrac{\text{Output Velocity}}{\text{Motional Voltage}} = \dfrac{V_m}{u_m} =$ $= \dfrac{2\pi f_2 a_2}{u_m} \cong \dfrac{2\pi f_2 a_2}{u_{inp.}} = \dfrac{2\pi f_2 a_2}{P_{inp.}} i_{inp.}$ $\cong \dfrac{2\pi f_2 a_2}{P_{diss.}} i_{inp.} \rightarrow \text{maximum}$
$a_1 = \text{output amplitude}$ $i_m \cong i_{inp.} = \text{motional current}$ $i_{inp.} = \text{converter's input current}$ $u_{inp.} = \text{converter's input voltage}$ $P_{inp.} \cong P_{diss.} = \text{converter's dissipation in air}$	$a_2 = \text{output amplitude}$ $u_m \cong u_{inp.} = \text{motional voltage}$ $i_{inp.} = \text{converter's input current}$ $u_{inp.} = \text{converter's input voltage}$ $P_{inp.} \cong P_{diss.} = \text{converter's dissipation in air}$

Miodrag Prokic, Marais 36, CH-2400, Le Locle, e-mail: mpi@bluewin.ch

$d_I = \frac{\text{Output Amplitude}}{\text{Motional Current}} = \frac{a_1}{i_m} \cong \frac{a_1}{i_{inp.}}$ $= \frac{D_I}{4\pi^2 f_1^{\,2}} \rightarrow \text{maximum.}$	$d_U = \frac{\text{Output Amplitude}}{\text{Motional Voltage}} = \frac{a_2}{u_m} \cong \frac{a_2}{u_{inp.}}$ $= \frac{D_U}{2\pi f_2} \rightarrow \text{maximum}$

$f_{res.} = f_1$, series resonance $u_t \approx 50\left[\frac{V}{mm}\right]$	$f_{res.} = f_2$, parallel resonance $u_t \approx 200\left[\frac{V}{mm}\right]$
$P_{output} = \eta \cdot a^2_{pp} \cdot f^2_{1.} =$ $= \eta \cdot (d_I \cdot i_m)^2 \cdot f_1^{\,2} =$ $= \eta \cdot \frac{(D_I i_m)^2}{16\pi^4 f_1^{\,2}} = \underline{\text{const}} \cdot (\frac{D_I i_m}{f_1})^2 =$ $= \text{Const.} \cdot (Q_{em-eff} \frac{M_{Piezo}}{M_{converter}} d_{33} u_t)^2 f_1^{\,2},$ $(\eta = \text{const.})$	$P_{output} = \eta \cdot a^2_{pp} \cdot f^2_{2.} =$ $= \eta \cdot (d_U \cdot u_m)^2 \cdot f_2^{\,2} =$ $= \eta \cdot \frac{(D_u u_m)^2}{4\pi} = \overline{\text{const}} \cdot (D_U u_m)^2 =$ $= \text{Const.} \cdot (Q_{em-eff} \frac{M_{Piezo}}{M_{converter}} d_{33} u_t)^2 f_2^{\,2},$ $(\eta = \text{const.})$

The most important is to respect the Safe Operating Limits of piezoceramics, as the part of BLT structure, given in T. 1.

Miodrag Prokic, Marais 36, CH-2400, Le Locle, e-mail: mpi@bluewin.ch

5. Power Performances of Ultrasonic Converters

Generally valid (semi-empirical) formula for calculating the average output power of one sandwich ultrasonic converter, when radiating into resistive mechanical load (for instance radiating in water), could be formulated as:

$$\mathbf{P_{output}} = \eta \cdot \mathbf{a}^2_{\mathbf{pp}} \cdot \mathbf{f}^2_{\mathbf{res.}} = \mathbf{P_{r-max.}} = \mathbf{2P_{c-max.}} =$$
$$= \eta \cdot \mathbf{a}^2_{\mathbf{pp}}(\mathbf{d_{33}}, \mathbf{u_t}, \mathbf{n}, \frac{\mathbf{M_{piezo}}}{\mathbf{M_{transd.}}} \cdot \mathbf{Q}^*_{\mathbf{em}}) \cdot \mathbf{f}^2_{\mathbf{res.}}, \quad (1.14)$$

where η is the converter (geometry and design related) form factor,
$\eta = \eta(\mathbf{Q}^*_{\mathbf{emo}}, \Delta\mathbf{f}, \mathbf{f_{res.}}) = \mathbf{C}(\mathbf{f_{res.}}) \cdot \mathbf{Q}^*_{\mathbf{emo}} \cdot \Delta\mathbf{f}, \ \mathbf{C}(\mathbf{f_{res.}}) = \mathbf{Const.}$
$\mathbf{P_{r-max.}}$ is the maximal acceptable pulse-repetitive (short time ON) converter power,
$\mathbf{P_{c-max.}}$ is the maximal acceptable continuous converter power (long time ON).
The factor 2 as the relation between $\mathbf{P_{r-max.}}$ and $\mathbf{P_{c-max.}}$, is taken as the (overload) security margin, and can be verified empirically, meaning that high power converter can safely deliver about 2 times higher output power ($\mathbf{P_{r-max.}}$) in a short time intervals, but if we would like to operate the same converter continuously ($\mathbf{P_{c-max.}}$), we better reduce its operating power to a half of $\mathbf{P_{r-max.}}$. For instance, we know that BRANSON 502/932R converter is able to deliver 3000 Watts (=$\mathbf{P_{r-max.}}$) in a short time intervals, but if we would like to operate it safely and continuously, very long time, we better limit its power to 1500 Watts (or maximum 2000 Watts =$\mathbf{P_{c-max.}}$, with proper air cooling).

- $\mathbf{a_{pp}} = \mathbf{a_{pp}}(\mathbf{d_{33}}, \mathbf{u_t}, \mathbf{n}, \frac{\mathbf{M_{piezo}}}{\mathbf{M_{transd.}}} \cdot \mathbf{Q}^*_{\mathbf{em0}}) = \mathbf{n} \cdot \mathbf{a_{1pp}}$ -is converter's front-emitting-surface, peak-to-peak amplitude measured when converter is oscillating harmonically.

- $\mathbf{a_{1pp}} = \mathbf{a_{pp}} / \mathbf{n}$ -is converter's average, front-emitting-surface, peak-to-peak amplitude calculated as the contribution of only one piezoceramic ring assembled in the same converter ($\mathbf{n}$ is the total number of piezoceramic rings assembled in a converter = 2,4,6…).

$\mathbf{f_{res.}} = \mathbf{resonant\ frequency\ of\ assembled\ converter} = (\mathbf{f_1} \cong \mathbf{f_s}\ \mathbf{or}\ \mathbf{f_2} \cong \mathbf{f_p})$
$\Delta\mathbf{f} = \mathbf{f_2} - \mathbf{f_1} = \mathbf{f_p} - \mathbf{f_s}\ \mathbf{(measured\ in\ air = converter\ is\ not\ under\ load)}$
$\mathbf{Q}^*_{\mathbf{mo}} = \sqrt{\mathbf{Q_{mo1}Q_{mo2}}} = \mathbf{Mechanical\ quality\ factor\ of\ assembled\ converter\ (in\ air = non\text{-}loaded)}$
$\mathbf{Q_e} = \frac{\mathbf{1}}{\mathbf{tg}\,\delta} = \mathbf{Q_{eo}} = \mathbf{Electrical\ quality\ factor\ of\ assembled\ converter\ (in\ air = no-load,\ at\ 1kHz)}$
$\mathbf{Q}^*_{\mathbf{emo}} = \sqrt{\mathbf{Q}^*_{\mathbf{mo}}\,\mathbf{Q_e}} = \mathbf{Effective\ electromechanical\ quality\ factor}$
$\mathbf{M_{piezo}} = \mathbf{n} \cdot \mathbf{M_1} = \mathbf{Total\ mass\ of\ all\ piezo\ elements\ in\ one\ assembled\ converter}$
$\mathbf{M_1} = \rho\mathbf{V_1} = \mathbf{Mass\ of\ only\ one\ piezoceramic\ element}$
$\mathbf{V_1} = \mathbf{Volume\ of\ one\ piezo\ element}$

$\mathbf{n} = \mathbf{Total\ number\ of\ piezo\ elements\ (rings)\ in\ assembled\ converter}$

$\mathbf{M_{transd.} = M_{piezo} + M_{metal} = Total\ mass\ of\ assembled\ converter}$

$\mathbf{M_{metal} = Total\ mass\ of\ metal\ parts\ /\ elements\ of\ assembled\ converter}$

Example: BRANSON 502/932R, welding converter operating in parallel resonance

BRANSON converter model 502/932R (see Fig. 17) will serve only to help us to calculate (or estimate) empirical constants of approximate formulae for power calculation, (1.14), since for this converter all relevant power and model/s parameters are already well known.

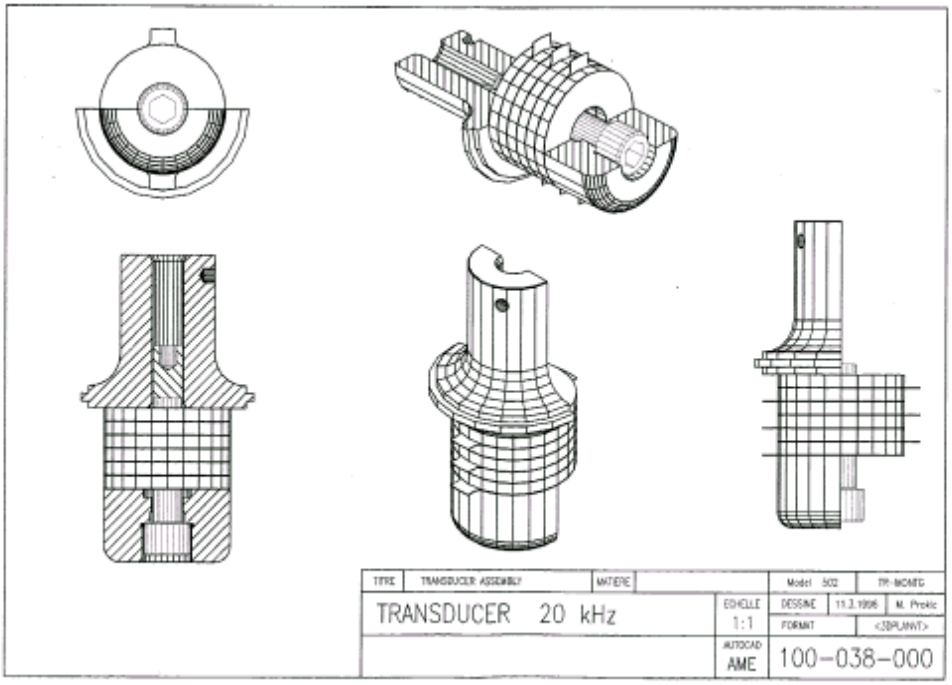

Fig. 17 BRANSON converter model 502/932R

T 1.5 BRANSON 502/932R, Typical Model Parameters Variations

	In Series Resonance	In Parallel Resonance
Model Parameters for Non-Loaded Converter (Measured on the random, standard-production-quality sample > 100 pcs. of converters, taken after assembling)	$C_{0p} \in [15.3 - 18.1]\,nF, \pm 3\%$ $C_1 \in [3.92 - 4.05]\,nF,$ $L_1 \in [17.53 - 18.7]\,mH$ $R_1 \in [1.75 - 4.6]\,\Omega, \pm 20\%$ $f_1 \in [18435 - 18905]\,Hz, \pm 0.5\%$ $Q_{m01} \in \langle Q_{m01} \rangle \pm 20\%$	$C_{0s} \in [18.7 - 22.05]\,nF, \pm 3\%$ $C_2 \in [79 - 101.53]\,nF,$ $L_2 \in [570.50 - 747]\,\mu H,$ $R_2 \in [94 - 250]\,K\Omega, \pm 20\%$ $f_2 \in [20635 - 20912]\,Hz, \pm 0.5\%$ $Q_{m02} = \langle Q_{m02} \rangle \pm 20\%$

For instance, one of well-selected (excellent quality) BRANSON 502/932R converter, Fig. 17, has the following characteristics (see T 1.6, T 1.7 and T 1.8).

T 1.6 Parameters and Properties of the Well-Selected 502/932R Converter

$T_{on} : T_{off} = 1:1$ (Pulse-Repetitive, ON-OFF regime in parallel resonance, $f_{res.} \cong f_{02}$)

$a_{pp} = 20\ \mu m = 6 \times 3.33^{*}\ \mu m = 6 \times a_{1pp}$

$a_{1pp} = (20/6)\ \mu m = 3.33^{*}\ 10^{-6}\ m = 0.66^{*}\ t\ 10^{-9}$ [m], $(f_1+f_2)/2 \cong 20$ kHz, $\Delta f = f_2 - f_1 \cong 2$ kHz,

$(u_t)_{rms.} \leq 1500$ V, $E_t = u_t/5 \leq 300$ V/mm (= voltage & field on the converter input)

$(u_m)_{rms.} = 930$ V, $E_m = u_m/5 \leq 186$ V/mm (= converter's motional voltage & field)

$P_{output} = 3000\ W = P_{r\text{-}max.}$ = Maximal pulse repetitive output power under load

$P_{d02} = 5$ W = Power dissipation in air (non-loaded converter; more often $P_{d02} \cong 10$ W)

$$\eta = \frac{P_{output}}{a^2_{pp} f^2_{res.}} = \frac{P_{r-max.}}{a^2_{pp} f^2_{res.}} = \frac{3000}{(20 \cdot 10^{-6} \cdot 20 \cdot 10^3)^2} = 18750\ (=) \left[\frac{W \cdot s^2}{m^2}\right] \quad \text{(see eq. (1.14))}$$

$$P_{output} = P_{r-max.} = 2 \cdot P_{c-max.} = \eta \cdot a^2_{pp} \cdot f^2_{res.} = 18750 \cdot a^2_{pp} \cdot f^2_{res.}\ (=) \left[W\right]$$

n = 6 piezoceramic rings: $\cong \phi 50 \times \phi 20 \times 5$ mm (PZT-8, Vernitron – Morgan-Matroc)

$t = 5\ mm = 0.005\ m$, $S_1 = 16.5\ cm^2 = 16.5\ 10^{-4}\ m^2$, $V_1 = S_1 \times t = 8.25\ 10^{-6}\ m^3$,

$V = 6V_1 = 49.5\ 10^{-6}\ m^3$ = total volume of piezoceramics

$d_{33} = 245 \times 10^{-12}$ [v/m] $\pm 10\%$, $k_{33} = 0.640$,

$C_{inp.}(1\ kHz) = 19.55$ nF,

$tg\ \delta\ (1\ kHz) = 0.000279$

$R_s(1\ kHz) = 56\ \Omega$, $R_p(1\ kHz) = 52\ M\Omega$

$C_{0p} = 17.32401$ nF, $C_{0s} = 21.228$ nF,

$C_1 = 3.9044$ nF, $C_2 = 97.08423$ nF,

$L_1 = 18.3335$ mH $L_2 = 595.6\ \mu H$,

$R_1 = 1.87\ \Omega$, $R_2 = 216\ K\Omega$, , $\dfrac{|Z_{02}|}{1000|Z_{01}|} \cong \dfrac{R_2}{1000 R_1} \cong (96.46, 115.51)$

$|Z_{01}| = 1.98\ \Omega$, $|Z_{02}| = 191\ K\Omega$

$f_1 = 18815$ Hz, $f_2 = 20828$ Hz,

$Q_{m01} = 1139$ $Q_{m02} = 2485$

$Q^*_{mo} = 1682$, $Q_e = 3584 = 1/tg\ \delta$, $Q^*_{emo} = 2455$

$$k_c^2 = \frac{\text{Energy stored in mechanical form}}{\text{Total input energy}} = \frac{C_1}{C_{op} + C_1} \cong \frac{C_{os}}{C_2} \cdot \frac{f_1^2}{f_2^2} \cong 0.1811,\ k_c \cong 0.4256,$$

$$\frac{k_c}{k_{33}} \cong \frac{\text{Mechanical energy stored by (assembled) converter}}{\text{Mechanical energy that can be stored (only) in piezoceramics}} \cong \frac{0.4256}{0.640} = 0.665,$$

(The ideal converter design would be when $(k_c / k_{33}) \cong 1$).

If we simply apply DC (or low frequency AC) voltage to the electrical input of BRANSON 502/932R converter, in the acceptable upper voltage limits $\mathbf{u_t} \in [\mathbf{930, 1500}]\mathbf{V}$, we shall produce converter's total elongation proportional to:

$$\Delta \mathbf{x} \cong \mathbf{6} \cdot \mathbf{d_{33}} \cdot \mathbf{u_t} = \mathbf{6} \cdot \mathbf{225} \cdot \mathbf{u_t} \cdot \mathbf{10^{-12}} = \mathbf{1350} \cdot \mathbf{u_t} \cdot \mathbf{10^{-12}} = \mathbf{d_{33-converter}} \cdot \mathbf{u_t} = \begin{cases} \mathbf{d_{33-converter}} \cdot \mathbf{u_m}\text{, or} \\ \mathbf{d_{33-converter}} \cdot \mathbf{1.6129} \cdot \mathbf{u_m} \end{cases}$$

$$\mathbf{u_t} = \mathbf{930\,V} = \mathbf{u_m} \Rightarrow \Delta \mathbf{x} \cong \mathbf{1350} \cdot \mathbf{u_m} \cdot \mathbf{10^{-12}} = \mathbf{1.2555} \cdot \mathbf{10^{-6}}\,\mathbf{m} = \mathbf{1.22555}\,\mu\mathbf{m}$$

$$\mathbf{u_t} = \mathbf{1500\,V} = \mathbf{1.6129} \cdot \mathbf{u_m} \Rightarrow \Delta \mathbf{x} \cong \mathbf{2177.419} \cdot \mathbf{u_m} \cdot \mathbf{10^{-12}} \cong \mathbf{2.025} \cdot \mathbf{10^{-6}}\,\mathbf{m} = \mathbf{2.025}\,\mu\mathbf{m}.$$

The same situation, when converter is driven with the same high voltage in parallel resonance ($\mathbf{u_m} = \mathbf{930\,V}$, $\mathbf{u_t} \in [\mathbf{930, 1500}]\mathbf{V}$) will result in converter peak-to-peak amplitude equal to:

$$\mathbf{a_{pp}} = \Delta \mathbf{x} = \frac{\mathbf{20}}{\mathbf{930}} \mathbf{u_m} \cdot \mathbf{10^{-6}} = \mathbf{21505.376} \cdot \mathbf{u_m} \cdot \mathbf{10^{-12}} = \mathbf{d_{33-resonant}} \cdot \mathbf{u_m} = \begin{cases} \mathbf{d_{33-resonant}} \cdot \mathbf{u_t}\text{, or} \\ \mathbf{d_{33-resonant}} \cdot \mathbf{0.62} \cdot \mathbf{u_t} \end{cases}$$

$$\mathbf{u_m} = \mathbf{930\,V} \Rightarrow \Delta \mathbf{x} = \mathbf{21505.376} \cdot \mathbf{930} \cdot \mathbf{10^{-12}} = \mathbf{20}\,\mu\mathbf{m}\text{ , }(\mathbf{d_{33-resonant}} = \mathbf{21505.376}).$$

Obviously, the voltage-amplitude conversion factor for BRANSON 502/932R converter in parallel resonance (**21505.376**) is for the order of magnitude greater, comparing to the voltage-amplitude conversion factor (**2177.419, or 1350**) when converter is driven the same voltage and far from resonance area (let us say below 1 kHz): **21505.376/2177.419 = 9.8765; 21505.376/1350 = 15.93**. It looks that $\mathbf{d_{33}}$ constant that is valid for non-resonant (low or DC) frequency area of piezoceramic (here for PZT8, $\mathbf{d_{33\text{-}converter}} = \mathbf{d_{33}}$ **x 6 = 225 x 6 = 1350**) should be multiplied by the factor close to 10 (or a bit higher than 10), in order to get $\mathbf{d_{33\text{-}resonant}}$ valid for parallel resonance: $\mathbf{d_{33\text{-}resonant}} \geq 10\ \mathbf{d_{33\text{-}converter}}$. This numerical example is given only for the purpose of creating an approximate picture of the order of magnitudes of converter amplitudes in DC and low frequency operating conditions, and operations in parallel resonance.

Similar calculation (with similar conclusions) should be applicable for converter operating in series resonance, but this time important amplitude conversion factors will be linked to converter motional current (as well as to converter input current).

T 1.7 Dynamic Power Parameters In Resonance (operating in air = no-load)

$\underline{f_{res.} = f_1}\ ,\ u_t = u_{inp.} \le 50\left[\frac{V}{mm}\right]$	$\underline{f_{res.} = f_2}\ ,\ u_m \le u_t = u_{inp.} \le 300\left[\frac{V}{mm}\right]$ $u_m \le 186\left[\frac{V}{mm}\right]$
a_1 = output amplitude	a_2 = output amplitude
$a_{1pp} = 2a_1$ = peak – to – peak	$a_{2pp} = 2a_2$ = peak – to – peak
$i_m \cong i_{inp.}$ = motional current	$u_m \cong u_{inp.}$ = motional voltage
$i_{inp.}$ = converter's input current	$i_{inp.}$ = converter's input current
$u_{inp.}$ = converter's input voltage	$u_{inp.}$ = converter's input voltage
$P_{inp.} \cong P_{diss.}$ = converter's dissipation in air	$P_{inp.} \cong P_{diss.}$ = converter's dissipation in air
V_m = converter's motional velocity	V_m = converter's motional velocity
F_m = converter's motional force	F_m = converter's motional force

Total Output Power Under Load

$$P_{output} = \eta_1 \cdot a^2{}_{pp} \cdot f^2{}_1 =$$

$$= \eta_1 \cdot (d_I \cdot i_m)^2 \cdot f_1{}^2 = \eta_1 \cdot (\frac{2u_{inp.}}{\pi D_{IF}})^2 =$$

$$= \text{Const.} \cdot (Q^*{}_{emo} \frac{M_{Piezo}}{M_{converter}} d_{33} u_t)^2 f_1{}^2,$$

$$(\eta_1 = \text{const.} \cong 18750 \left[\frac{W \cdot s^2}{m^2}\right]$$

for BRANSON 502 / 932R)

Total Output Power Under Load

$$P_{output} = \eta_2 \cdot a^2{}_{pp} \cdot f^2{}_2 =$$

$$= \eta_2 \cdot (d_U \cdot u_m)^2 \cdot f_2{}^2 = \eta_2 \cdot (\frac{D_{UV} u_m}{2\pi})^2 =$$

$$= \text{Const.} \cdot (Q^*{}_{emo} \frac{M_{Piezo}}{M_{converter}} d_{33} u_t)^2 f_2{}^2,$$

$$(\eta_2 = \text{const.} \cong 18750 \left[\frac{W \cdot s^2}{m^2}\right],$$

for BRANSON 502 / 932R)

Force transformation constant

$$D_{IF} = \frac{\text{Output Force}}{\text{Motional Current}} = \frac{F_m}{i_m} =$$

$$\cong \frac{2u_{inp.}}{\pi f_1 d_1 i_m} \cong \frac{2u_{inp.}}{\pi f_1 a_{1pp}} \cong \frac{2P_{diss.}}{V_m \cdot i_m} \cong$$

$$\cong \frac{2P_{diss.}}{\pi f_1 a_{1pp} \cdot i_m} \rightarrow \text{maximum}$$

$$(\cong 2 \cdot 21.6 / \pi 18815 \cdot 20 \cong 36.54 \frac{(V)_{rms} \cdot s}{m}$$

$$= 36.54 \frac{N}{(A)_{rms}}, \text{for } 502 / 932R)$$

Velocity transformation constant

$$D_{UV} = \frac{\text{Output Velocity}}{\text{Motional Voltage}} = \frac{V_m}{u_m} =$$

$$= \frac{2\pi f_2 a_2}{u_m} = \frac{\pi f_2 a_{2pp}}{u_m} = \pi f_2 d_U \rightarrow \text{max.}$$

$$(\cong \pi \cdot 20828 \cdot 20 / 930 \cong 1407.2 \cdot 10^{-6} \frac{m}{(V)_{rms} \cdot s}$$

for BRANSON 502 / 932R)

Amplitude transformation constant

$$d_I = \frac{\text{Output Amplitude}}{\text{Motional Current}} = \frac{a_{1pp}}{i_m} \cong \frac{a_{1pp}}{i_{inp.}}$$

$$\cong \frac{2u_{inp.}}{\pi f_1 D_{IF} i_m} \rightarrow \text{maximum.}$$

$$(\cong 20 / 2.98 \cong 6.71 \frac{(\mu m)_{pp}}{(A)_{rms}}, \text{for } 502 / 932R)$$

Amplitude transformation constant

$$d_U = \frac{\text{Output Amplitude}}{\text{Motional Voltage}} = \frac{a_{2pp}}{u_m} \cong \frac{a_{2pp}}{u_{inp.}} =$$

$$= \frac{D_{UV}}{2\pi f_2} \rightarrow \text{maximum}$$

$$(\cong 20 / 930 \cong 0.02 \frac{(\mu m)_{pp}}{(V)_{rms}}, \text{for } 502 / 932R)$$

T 1.8 Additional Power Parameters In Resonance (converter is non-loaded)

$\underline{f_{res.} = f_1}\ ,\ u_t = u_{inp.} \le 50\left[\frac{V}{mm}\right]$	$\underline{f_{res.} = f_2}\ ,\ u_m \le u_t = u_{inp.} \le 300\left[\frac{V}{mm}\right]$ $u_m \le 186\left[\frac{V}{mm}\right]$
Velocity transformation constant $D_{IV} = \frac{\text{Output Velocity}}{\text{Motional Current}} = \frac{V_m}{i_m} =$ $\cong \frac{P_{diss.}}{D_{IF} \cdot i^2{}_m} \cong \frac{P_{diss.}}{D_{IF} \cdot i^2{}_{inp.}} \rightarrow \text{maximum}$ $(\cong 64.368 / 36.54 \cdot 2.98^2 \cong 0.1984 \frac{m}{(A)_{rms} \cdot s}$ $P_{diss.} \cong 64.368\,W,\ \text{for}\ 502/932R)$	**Force transformation constant** $D_{UF} = \frac{\text{Output Force}}{\text{Motional Voltage}} = \frac{F_m}{u_m} =$ $\cong \frac{P_{diss.}}{u^2{}_m \cdot D_{UV}} \cong \frac{P_{diss.}}{u^2{}_{inp.} \cdot D_{UV}} \rightarrow \text{maximum}$ $(\cong 10 / 930^2 \cdot 1407.2 \cdot 10^{-6} \cong$ $\cong 8.82 \cdot 10^{-3} \frac{(A)_{rms} \cdot s}{m} = 8.82 \cdot 10^{-3} \frac{N}{(V)_{rms}}$ $P_{diss.} \cong 10\,W,\ \text{for}\ 502/932R)$

All voltages and currents in this table should be treated as RMS values.

Tables T 1.7 and T 1.8 are only establishing the definitions of important dynamic converter parameters (related to low signal and low power converters modeling), and it is obvious that such parameters should be conveniently re-defined in the function of converter's loading (starting from no-load situation until a fully loaded converter).

ELECTRICAL SAFE OPERATING LIMITS OF BOLTED LANGEVIN TRANSDUCERS

(Piezoceramics PZT-8 GRADE, All values are in RMS, and SI units)

The following table, T.1, is applicable on single and free (in air) ultrasonic (sandwich) transducers that are not bonded/glued to some other solid-state mass (data established based on measurements for the operating frequency $f_{res.} \cong 20$ kHz $\cong (f_1 + f_2) / 2$, and operating peak-to-peak, sinusoidal amplitude $a_{pp} = 20$ μm). Later on, we shall extrapolate this situation to other operating frequencies and amplitudes (as well as for cleaning transducers that are glued to a cleaning tank).

T.1

BLT is operating in series resonance: $f_s = f_1$ Current driven transducers, $Z = Z_{min.}$		BLT is operating in parallel resonance: $f_p = f_2$ Voltage driven transducers, $Z = Z_{max.}$	
Non-Loaded (in air)	**Fully-Loaded (in water)**	**Non-Loaded (in air)**	**Fully-Loaded (in water)**
n.a.	**$P_V = 60$ [W/cm^3] for $P_{r\text{-}max.}$**	n.a.	**$P_V = 60$ [W/cm^3] for $P_{r\text{-}max.}$**
n.a.	**$P_V = 30$ [W/cm^3] for $P_{c\text{-}max.}$**	n.a.	**$P_V = 30$ [W/cm^3] for $P_{c\text{-}max.}$**
n.a.	**$P_{S1} = 30$ [W/cm^2] for $P_{r\text{-}max.}$**	n.a.	**$P_{S1} = 30$ [W/cm^2] for $P_{r\text{-}max.}$**
n.a.	**$P_{S1} = 15$ [W/cm^2] for $P_{c\text{-}max.}$**	n.a.	**$P_{S1} = 15$ [W/cm^2] for $P_{c\text{-}max.}$**
$P_{vdiss.} = 0.23 - 0.60$ [W/cm^3]	**$P_{vdiss.} = 0.92 - 2.77$ [W/cm^3]**	**$P_{vdiss.} = 0.11 - 0.35$ [W/cm^3]**	**$P_{vdiss.} = 0.39 - 0.46$ [W/cm^3]**
$u'_t = 1.3 - 10$ [V/mm]	**$u'_t = 10 - 100$ [V/mm]** **$u^*_t = 50 - 60$ [V/mm]**	**$u'_t = 50 - 220$ [V/mm]** **$u^*_t = 200$ [V/mm]**	**$u'_t = 50 - 220$ [V/mm]** **$u^*_t = 200$ [V/mm]**
$I_{S1max.} = 80$ [A/m^2]	**$I_{S1} = 80 - 1200$ [A/m^2]**	**$I_{S1max.} = 20$ [A/m^2]**	**$I_{S1} = 20 - 300$ [A/m^2]**
n.a.	**$\max.(u'_t I_{S1}) \leq P_V$**	n.a.	**$\max.(u'_t I_{S1}) \leq P_V$**
$(Z_{min.} S_1/t) \leq$ (0.65 to 5) [Ωm]	n.a.	**$(Z_{max.} S_1/t) \geq$ (33 to 135) [KΩm]**	n.a.

$P_{r\text{-}max.}$ [Repetitively driven, Fully-Loaded (in water)] (=) $T_{on} : T_{off} = 1 : 1$, pulse-repetitive train, $P_{r\text{-}max.} = 2\ P_{c\text{-}max.}$
$P_{c\text{-}max.}$ [Continuously driven, Fully-Loaded (in water)] (=) T_{on} = continuous, $T_{off} = 0$
$P_{diss.}$ (=) Thermal-dissipation power (losses)
u'_t – For variable voltage regulation, u^*_t – Constant (stable) voltage for continuous operating regime
n.a. = Not applicable

In the case if transducer/s is/are bonded/glued or differently fixed to some other solid-state mass, above given (safe-operating) maximal power limits are 5 to 10 times lower (as in the case of ultrasonic cleaning applications). The current and voltage limits (operating intervals and safe operating limits) for piezoceramics will stay the same in any situation, providing that maximal power limits are respected.

If transducer/s is/are operating in some other, frequency sweeping regime, passing over many series and parallel resonant points, all safe operating limits listed in T. 1 should be respected in the same time (max. Applied voltage, max. Input current, max. Power density). The corresponding electrical limitations, generator regulations and protections should be implemented. The most important criteria in such situations are to minimize reactive power of transducer and to maximize its active power. Operating temperature of piezoceramic elements (in any operating regime) should be lover as possible (we can say between 20°C and 60°C is preferable situation, but in any case, for continuous and very long operation, no more than 90°C). If piezoceramics in operation reach temperatures between 120°C and 180°, efficiency of transducer will drop significantly.

Piezoceramic parameters (used in T.1), which are important for transducer power calculation (valid for piezoceramic rings):

t – thickness of the ring (=) [m] ,
R – outer diameter of the ring (=) [m] ,
r – inner diameter of the ring (=) [m] ,
S_1 – surface of one, flat side, of the ring $= \pi(R^2 - r^2)$ (=) $[m^2]$,
V_1 – volume of one piezoceramic ring $= S_1 t = \pi(R^2 - r^2)t$ (=) $[m^3]$,
u_t – rms. voltage on one piezoceramic (=) [v],
$f_{res.}$ – resonant frequency (=) [Hz]

$$P_v = \frac{P_{(r/c)-max}}{V_1}(=)\left[\frac{W}{m^3}\right] \text{ – volumetric power density,}$$

$$P_{S1} = \frac{P_{(r/c)-max}}{S_1}(=)\left[\frac{W}{m^2}\right] \text{ – one flat side, surface power density,}$$

$$u_{t1} = \frac{u}{t}(=)\left[\frac{V}{m}\right] \text{ – electrical field on (one) piezoceramic,}$$

$$I_{s1} = \frac{I}{S_1}(=)\left[\frac{A}{m^2}\right] \text{ – one flat side, surface current density}$$

Applied voltage and current (directly on a piezoceramic):

$u_t \le 0.5\, u_d$ – acceptable operating (rms.) voltage on a piezoceramic (=) [V],
u_d – depolarization voltage (=) [V]

$$\mathbf{u'_t = \frac{u_t}{t}(=)\left[\frac{V}{m}\right]} \quad \textbf{– Acceptable, applied electrical field on (one) piezoceramic,}$$

$$\mathbf{u^*_t \le 0.9 \cdot u'_t\,(=)\left[\frac{V}{m}\right]} \quad \textbf{– Continuous, loading / operating field applied on a piezoceramic}$$

$$\mathbf{I_{s1} = \frac{2 \cdot I_t}{nS_1}(=)\left[\frac{A}{m^2}\right]} \quad \textbf{– Average Surface current density (on a PZTelectrodes)}$$

$$\mathbf{I_t \quad (=) \quad [A]} \quad \textbf{– Total transducer Input current (rms)}$$

For rough and fast estimation of the quality and type of piezoceramics (applicable for high power BLT), we can use the following empirical criteria:

PZT-8 , SP-8 TYPE III DOD-STD-1376A (Vernitron USA)	Excellent	Very good	Good	Acceptable
$\left\|\frac{Z_{max.}}{1000 Z_{min.}}\right\| \ge$ For single piezoceramics, non-loaded, in air	80	36	18	7
$\left\|\frac{Z_{max.}}{1000 Z_{min.}}\right\| \ge$ For assembled converter, non-loaded, in air	100	75	50	20

Piezoceramic materials that have higher dielectric constants and higher (low frequency) static capacitance are generally preferable for designing high power ultrasonic transducers. Also important parameters for high power transducers are: very high Young modulus, high mechanical quality factors, very fine ceramic granulation, very low porosity of sintered piezoceramics, high d_{33}, low dielectric losses and high Curie temperature.

6. IMPORTANT COMMENTS REGARDING HIGH POWER BLT ASSEMBLING, PIEZOCERAMICS QUALITY AND TOLERANCES (BLT = Bolted Langevin Transducer)

For producing high power ultrasonic transducers it is necessary to use “hard” Piezoceramic materials (such as PZT-8 and SP8). Hard piezoceramic materials have mechanical quality factor higher than 1000 (often between 1000 and 2000). There is also a big difference among hard piezoceramics (from different sources) regarding implemented internal polarization. It is preferable to ask suppliers of piezoceramics to use maximal as possible, high DC voltage for implementing very strong internal electrical polarization-field in piezoceramics. Piezoceramics in process of implementing internal polarization are permanently connected to a very high voltage DC source, immersed in silicone oil (or some other electrically isolating liquid), and kept on elevated temperature during the poling process. After certain time, internal dipole domains of piezoceramics are sufficiently well oriented in the direction of externally applied electric field, and in order to permanently stabilize and freeze such internal polarization, oil heating is disconnected and piezoceramics and surrounding oil start cooling down, slowly, naturally, until reaching room temperature, or lower, without disconnecting the high DC polling voltage, during more than 24 hours. If piezoceramics producers were trying to accelerate this process and to reduce the costs of pooling, this would result in weaker internal polarization (consequently reducing the maximal power of assembled ultrasonic converters). A good, high-DC polarization-voltage should be close to the piezoceramic material breakdown-voltage. The next difference between hard piezoceramics from different sources is in values of materials Young Modulus, which should be sufficiently high (comparable to Vernitron-USA, PZT-8 material, and to CeramTec SP8). Higher Young Modulus will produce higher power BLTs, if all other BLT design elements are well selected. Piezoceramic materials that have higher dielectric constants and higher (low frequency) static capacitance are generally preferable for designing high power ultrasonic transducers. Also important parameters for high power transducers (in addition to very high Young modulus) are: high mechanical quality factors, as the consequence of very fine ceramic granulation and very low porosity of sintered piezoceramics (what basically makes high strength of piezoceramics), high d-33, low dielectric losses, low aging rate and high Curie temperature.

In order to accelerate natural aging of “green” piezoceramics, many suppliers are applying additional thermal aging (or thermal cycling). The best artificial aging can be realized when piezoceramic is externally in electrical short circuit, during thermal cycling, and in the same time mechanically agitated (placed on some variable-frequency, vibrating platform). Such aging arrangement should be discussed and arranged with piezoceramic supplier. There are some more innovative and excellent methods for piezoceramic artificial aging and stabilization, but not as easy applicable, as above described methods. Piezoceramic, if not well homogenized and properly sintered, could have structural defects, voids, certain porosity, non-uniform internal-stress distribution etc. The best option to check piezoceramic quality from that aspect (structural stability) is, to perform (suitable) variable-frequency mechanical agitation (on a convenient vibrating platform), when piezoceramics containing internal structural defects will brake (this way being naturally eliminated). Practically vibrations are internally accelerating the process of structural space stabilization of polarized domains, and accelerating the migration and mobility of internal defects and structural imperfections (until all of them reach final and stable conditions).

Development of modern ultrasonic generators (or power supplies) gives us the chance to use hard piezoceramic materials, not only for ultrasonic welding BLTs, but also for ultrasonic cleaning BLTs. This is possible because modern power regulation applies PWM concept for power regulation, operating frequency is automatically controlled using fast PLL, overload protection is reacting very fast, active power is maximized, reactive power minimized, etc.

The next important aspect of making high power BLTs is to know the how to determine the optimal prestress on piezoceramics (realized by central bolt) in order to have the highest operational margin for sinusoidal oscillations. Usually, on “soft” piezoceramic materials we apply static pressure on piezoceramics in the range of 25 MPa (valid for PZT-4, SP4), and for hard piezoceramics around 50 MPa (valid for Vernitron PZT-8 and for CeramTec Sonox P8, P88 materials). For any other piezoceramics, optimal prestress should be found in collaboration with piezoceramics supplier, or experimentally. We should also have in mind that every piezoceramics is much more resistant on positive, compressive-pressure than on negative, elongating-pressure (about 5 times). Applying compressive pressure (to a piezoceramic stack of a BLT) in the range of 60 MPa and higher is not recommendable. Most of piezoceramics for high power BLTs should be fastened until no more than 50 MPa. Braking or cracking point of CeramTec SP8 is +125 MPa on compressive pressure, and –25 MPa on elongation. The total length (or available pressure gap) of this interval (for SP8) is 125 + 25 = 150 MPa (where 125 MPa is below zero line and 25 MPa is above zero line). The middle pressure point of 150 MPa is 75MPa, and since, negative pressure of 25 MPa (25 MPa is the limit of piezoceramics maximal elongation or extension) should be reduced from 75 MPa, we can calculate the best optimal (static, and positive) pressure on SP8 as 75 – 25 = 50 MPa. In reality, any pressure between 40 MPa and 50 MPa, applied on SP8, and/or PZT-8 is very good, because BLT should also be able to oscillate linearly in the rest of allowed pressure interval (without damaging piezoceramics). The highest prestress pressure-limit of 50 MPa is also producing higher power BLTs. Branson is applying 51 MPa for the highest power converters. Also: 1°, as the prestress increases, the Curie temperature decreases; 2°. The prestress must be large enough to handle not only the ultrasonic stress in the ceramics due to normal axial vibration but also any stress that is caused by bending (e.g., due to an asymmetric horn).

In order to determine the optimal static pressure on certain BLT we should implement the following process: First, we shall produce a test-BLT and gradually start increasing the pressure on its piezoceramics (making impedance measurements whenever we change the static prestress). During fastening process, step-by-step, we are measuring different resonant frequencies and different belonging impedances of a test-BLT, depending on applied pressure. We should make the table of measured points and produce corresponding curves using the most suitable curve fitting method (in the function of applied pressure). When all (measured) characteristic impedances and frequencies reach their relatively stable, almost constant and saturated-like values, and when mechanical quality factor of such test-BLT reaches its maximum, we can be sure that this is the optimal static pressure for BLT under testing. The pressure found this way takes into account all design-specific parameters, quality of used piezoceramics, quality of metal masses and quality of central bolt. For such measurements we need HP-4194A Network Impedance Analyzer (or an equivalent instrument). If we continue with fastening (after optimal point is reached), applying stronger pressure, characteristic impedances, frequencies and belonging mechanical quality factor will stay relatively stable and constant only during certain (relatively short) pressure interval, and later on, with further pressure increase, mentioned BLT parameters will start changing (non-linearly) and degrading rapidly, until to the fatal ceramic or central bolt damage/s, or the bolt pulls the threads out of the front driver. Optimal static pressure should be chosen to be in the linear stability-interval of BLT parameters (in the first 50% of that interval, but not just on its starting point, because after certain time BLT will naturally loose about 10% of its initial static pressure (because of spontaneous static-stress release and natural aging of the converter). If we change something (significantly) in BLT design, above described measurement procedure should be repeated and new (optimal) static pressure should be found.

Optimum bolt diameter (considering desired preload and strength of front driver threads); undercutting bolt diameter next to ceramics to increase bolt compliance. Note: if bolt is

overly stiff, the coupling coefficient k is reduced. Optimum bolt engagement length in front driver (how many threads) → don't want fatigue of Al front driver. Best bolt mat: steel vs. Ti?

Optimum bolt-ceramic clearance (for arc protection). Undercutting bolt to give additional clearance while still retaining large threads required for static preload.

Front driver material: Aluminum (as opposed to Ti) gives higher amplitude but has lower fatigue strength and front threads (where booster attaches) wear out more quickly. Some designs have the stud permanently installed in the converter, rather than the booster, to prevent wear to front converter threads.

Design of BLT's metal masses, surface finishing, position of piezoceramics and BLT nodal plane, size and quality of central bolt could have significant influence on static and dynamic stress distribution in the structure of BLT. In the case if piezoceramic contact surfaces are non-uniformly loaded (because of bad surface finishing, voids, surface defect…), this will produce non-uniform stress and oscillating-amplitude distribution and partial piezoceramic depolarization, followed by increased thermal dissipation. Such piezoceramic (non-uniformly loaded) will easily loose a part of its piezoelectric properties. In order to uniformly equalize mechanical loading, stress and oscillating-amplitude distribution on metal and ceramic contact surfaces, some ultrasonic companies are implementing relatively simple design tricks on all surfaces of BLT end-metal masses (that are in contact with piezoceramics). They counterbore the metal mass in the central zone, around the central bolt axis (often from both sides on both metal masses in contact with piezoceramics). This looks like reducing the total front surfaces of BLT masses, introducing one empty space zone in the middle, but as a result, stress and vibration-amplitude distribution on such (reduced surface/s) will be much more uniform than if surface has only one flat level. The same reasoning is applicable on the front emitting aluminum mass that is in contact with a booster or sonotrode (reduced contact area produces uniform amplitude and stress distribution on the remaining contact surface, exciting dominantly longitudinal vibration modes of a booster). The next good reason for introducing two axial-levels in contact surfaces (removing metal in the middle zone of contact area) is in minimizing the effects of coupling between longitudinal and radial oscillating modes, and to stimulate only axial-longitudinal oscillations, since radial, or planar surface coupling is minimized if the contact surface is minimized. To be sure in previously described design modifications (how and where to apply them), we should use the Finite Elements Analysis method for BLT design optimization.

For electrode materials it is very important to use 99% nickel foils, or nickel-beryllium alloys, or some other nickel-rich alloys (which are relatively easy solderable, or where brazing can easily be applied, for creating good electrical contacts). Surface hardness of applied electrodes (empirically found as the best) should not be higher than 140 HV (Vickers) and not softer than 100 HV. Electrode-foil bands should be produced with cold drawing, without applying thermal treatment (resulting in relatively softer and more elastic alloys, with long fatigue-life). Electrode surfaces should be mirror and brilliant shiny, and extremely flat. Electrode thickness should be around 0.25mm. It is preferable not to apply any mechanical treatment on electrode surfaces (like polishing), because there is a danger to implement some hard particles in electrode surfaces (in any case, proper electrode cleaning should be applied in cases when any surface treatment is used). The best would be to buy an excellent foil material and to produce proper electrodes for BLT, without making any surface treatment.

All solid surfaces that are in contact with piezoceramics (BLT metal masses, foil-electrodes, piezoceramic metal plating) should secure/maintain:

-Maximum as possible contact surface/s,
-Excellent acoustic and mechanical coupling,
-Excellent heat transfer and very low thermal resistance,

-Very low surface-electrical-resistance, or high electrical conductivity,
-High flexibility and very low friction in planar-radial contact-zone, because different materials anyhow have different elasticity and different thermal expansion properties,
-Very long fatigue-life under vibrations,
-As well as high resistance against surface corrosion.

Nickel is an excellent material for reaching the most of above listed performances.

After assembling a BLT, when BLT is selected (after measurements) as a good one, we should apply a convenient surface coating using some protecting, liquid mass (rubber, adhesive, lacquer) that will not be able to make capillary penetration in the capillary zones of contact between piezoceramics and metal masses. For this purpose, some high quality (and relatively high density) transformer or magnet-wires lacquers could be used (usually part of the specific know-how). It is extremely important to protect external (lateral) surfaces of piezoceramics against moisture (since piezoceramic materials are known as slightly hygroscopic), without giving the chance to a coating mass (lacquer) to penetrate into internal (capillary) contact areas. Some companies apply silicone seal to electrode tabs to damp the vibration and reduce fatigue failures.

Electrode wire material and braid type: The best are highly flexible and highly electrically conductive, Nickel-rich alloys, litz-type, multiple wires. Many other, tinned or silver-plated copper-alloys wires are also in use.
Wire size (to handle amps): $\geq$ 2 A, rms., per mm^2.
Attachment method of wire to electrode tabs: Brazing, crimping, and soldering, eventually silicone coated.

SUMMARY OF THE MOST IMPORTANT ELEMENTS RELATED TO PIEZOCERAMICS ASSEMBLING PROCEDURE FOR MAKING HIGH POWER CONVERTERS

During high-power transducer assembling, piezoceramic could be damaged, especially when we apply (very) high static pressure, comparable to 40-50 MPa. In the following text, only very critical and very important aspects of piezoceramic assembling process will be summarized. It is clear that all other, standard and traditionally known technological conditions for transducer assembling should be respected (such as: tolerances of metal parts, very high quality of surface finishing, plan-parallel contact surfaces, necessary metal plating, quality of fastening bolts...). *The following procedure (given in a form of description including necessary comments) is securing the highest quality of assembled high power, BLT transducers:*

1. Some producers of ultrasonic equipment think that when they buy piezoceramics that has good mechanical tolerances and good electro-mechanical properties they can immediately assemble such piezoceramics, without any special preparation. This is not correct because metal (or silver) plated surfaces of piezoceramics usually have certain non-uniform roughness, oxides and attached solid particles. Just before transducer assembling, it is extremely recommendable to make a kind of (additional) piezoceramic fine polishing and cleaning, to eliminate any possible roughness, particles, remains of non-uniform silver plating, oxidized surface elements… For this operation, experienced ultrasonic companies are using a kind of vibrating polishing-platform that is producing only planar vibrations (X-Y vibrations). This could be a very flat metal surface driven by two electromagnets (only in x-y plane), or driven by one fast rotating electro-motor, transferring rotation to X-Y motion (via one eccentric coupling). On the surface of such vibration platform, a kind of very fine polishing paper should be placed (like silky fabric, impregnated with some very fine abrasive: quality 600 or finer). The operator, who is assembling transducers, should take every single piezoceramic ring, place it on such vibrating surface, slightly pressing on it, during 5 to 10 seconds, then change the side of piezoceramics, then apply pressurized air-jet for cleaning of remaining dust (on the ceramics surfaces), and eventually piezoceramic is ready to be assembled in the transducer. Of course, silver plating, which was mat-white, nice, uniform and clean (before such vibration polishing process), becomes much more shiny, partially covered with slightly transparent spots, and we can (almost) see certain fogy zones with the piezoceramic original color in the spots where some hard particles are removed by fine polishing (of course, silver plating should not be removed by applied polishing). This way, the remaining roughness on piezoceramic rings would be eliminated, and such piezoceramic is ready to be assembled in high power transducers (there will be no more cracking and braking of piezoceramics caused by imperfect electrode surfaces).

2. The same procedure (as specified in 1.) could be applied on metal masses and foil electrodes that will be directly in contact/s with piezoceramics (just to realize slight polishing and micro grinding to remove possible particles, roughness, sharp edges, and similar surface imperfections). Modern industrial production of ultrasonic transducers is applying high standards for mechanical surface rectification and surface finishing of metal masses (to make them plan-parallel and perpendicular to the central axis). Then, a liquid-abrasive-polishing is applied (lapping and honing), and in the end, we apply ultrasonic cleaning to remove remains of abrasive particles. It looks sufficient, but in reality, a lot of abrasive particles are mechanically implemented in such surfaces and not easy visible. This way, mechanical friction and electrical resistance of such contact surfaces is remaining higher than acceptable for assembling high power BLT. Consequently, we should once more apply dry polishing and surface cleaning. Above described procedure is important because when piezoceramics is oscillating in the structure of sandwich transducers, it is performing significant planar/radial friction with surrounding/contacting

metal masses (and foil electrodes), and this friction (and elevated electrical resistance) should be minimized. Also, because of very high pressure (40-50 MPa), applied on piezoceramics, if contact surfaces are not very flat, plan-parallel and shiny polished, piezoceramics could be damaged (because surface friction and elevated electrical resistance are producing intensive local heating on certain spots of piezoceramics). Basically, planar/radial friction between piezoceramic rings and surrounding metal masses should be minimized, and contact surface between ceramics and metal masses should be maximized. Later on, when ultrasonic generator drives assembled transducer, an additional surface self-polishing and reduction of surface electrical resistance (caused by immanent radial/planar friction between vibrating piezoceramics and metal masses) will (again) contribute to BLT structure stabilization. The first several minutes of transducer's operation are very critical, because radial surface friction and electrical resistance (between piezoceramics and metal masses) are much higher in the beginning, and getting lower (and stable) after certain time (and it would be better to start operating a converter with reduced power or reduced amplitude).

3. Using convenient metal plating and convenient foil-electrodes (in the case of very high power BLT) should also minimize radial and planar surface friction. The best metal plating (that could be applied to reach highest quality of high power ultrasonic transducers) is pure nickel (realized by galvanic plating, which gives hard nickel layer, and makes mirror shiny surfaces: 5 to 10μm thick). Some ultrasonic companies are applying shiny, hard-nickel plating, after polishing, even on aluminum masses, in order to minimize surface friction and surface contact-electrical-resistance. Nickel is an excellent material because of its mechanical properties, very low surface friction, high stability in the large temperature interval, and anticorrosion stability. In fact, any relative movement of ultrasonic components in direct contact is undesirable (i.e., all components should be essentially "welded" together, so friction should not play a role), but in all practical design situations this undesirable effects can only be minimized, but not eliminated, since different materials have different relative elongations, different elasticity, and different temperature expansion-coefficients. Most probably that some other metal-alloys could have similar surface-friction and electrical and thermal conductivity properties as Nickel.

4. The best materials for foil-electrodes of BLT are approx. 0.25mm thick foils, such as pure nickel (99%), or nickel, cooper, beryllium alloys (where nickel content is dominant). Material for production of foil electrodes should not be hardened (has to be very flat, very bright, to have almost mirror shiny surfaces, to be sufficiently soft and flexible, or half-hard, like in the case of elastic springs production: surface hardness between 100 HV and 140 HV is preferable). Foil electrodes could be produced using photo-chemical-etching technology to avoid formations of sharp edges. It is a common opinion that beryllium alloys are the best materials for contact electrodes of BLTs, but this is not correct, except if additional brilliant nickel plating, over such electrodes is applied (because beryllium itself is not sufficiently corrosion resistant, it has relatively high surface-friction coefficient, and under strong planar-radial vibrations starts degrading, separating cooper from beryllium).

5. Threaded body and head of a central bolt, that is fastening piezoceramics and metal masses, should be slightly lubricated with (high temperature stable) Molybdenum Disulphide grease, before transducer fastening, in order to minimize unnecessary friction during fastening. Sometimes, 30% to 60% of applied fastening torque/pressure is lost in metal-to-metal friction, if central bolt is not properly lubricated. We should not forget that central bolt, beside its function as a mechanical spring element, is also very important as electrical contact, connecting two sides of piezoceramic electrodes, or two end metal masses of a BLT (creating ground-mass electrode). The best method of applying consistent preload is: using torque reading versus using d-c voltage across shunt capacitor (note: we will still need to record torque to check later if preload has relaxed).

6. After transducer is assembled/fastened, in order to be sure in the stable quality of transducers, it is also very recommendable to place, just finished/assembled, transducers into an oven on 80°C to 120°C, during several hours, or longer. Such elevated temperature is performing thermal treatment/aging (on metal parts and ceramics), consequently all BLT parts are moving (or elongating) a little bit, and finding better (more stable) micro-positions in the structure of the transducer. This is in the same time a kind of residual stress deliberation in complete transducer structure. After thermal treatment, transducers should be on a room temperature (20°C, without humidity) during several hours, or 24 hours, to cool down naturally. This way, mechanical structure of transducers is again getting more stabilized and finds its optimal position. During thermal treatment (and later, during natural cooling), electrical input terminals of transducers should be permanently in a short circuit connection, in order to avoid effects of internal electrical depolarization of piezoceramics. Thermal treatment is contributing significantly to the quality and stability of assembled transducers. In order to test more severely if certain converter design is optimal, we can make gradual converter heating in an oven, on a several converters only, during one hour, until reaching 160°C, then to keep converter on this temperature during 2 hours, and then again gradually reduce the temperature until room temperature is reached (20°C). If after such severe test, piezoceramics or central bolt are not broken or differently damaged, and if static pressure on the BLT is still in the initially given range (not lower than for -10%, compared to initially realized pressure; see 9 below), we can say that such BLT is well designed (and that its components are well selected).

7. Later, when transducers are again cold, we can put them in real operation, during 10 to 20 minutes (each), on some specially made testing place, driven with real ultrasonic generator, but on low power (without mechanical loading, hanging in air). This way, transducers are performing additional structural stabilization, contact surface self-polishing, aging and more of residual stress elimination.

8. In the next step, such transducers should be tested, driven full power (or in over-power/overload), during 10 to 30 seconds. This way, vibrating transducers are forcing piezoceramic and metal parts to create additional strong friction and mutual self-polishing on their contact surfaces, making transducer structure more stable. During this test, we should control carefully if some electrical discharge, corona or micro arcing appears in the contact areas between piezoceramics and metal masses (followed by ozone creation). This is a very dangerous phenomenon that will produce local over-heating and cause crack of piezoceramics. After certain time of such self-polishing between metal masses and piezoceramics, mentioned corona and micro arcing can disappear, or if not, we should not continue forcing this situation, before we protect the lateral surfaces of piezoceramics using special coating.

9. After all above-mentioned operations, if transducers are still visibly compact (without cracks and defects on piezoceramics) an additional refastening of central bolt could be applied. This is just to check/control if previous fastening is still correct (for instance, we can again use the same torque-key (locked in the same position as before) and check if during previous thermal treatment transducer did not loose the initially realized pressure on piezoceramics (of course, without unscrewing the central bolt of transducer). Refastening should not be applied systematically, if on several randomly chosen transducer samples we find that fastening torque/pressure is still the same as before (or lower not more than 5% to 10%, compared to initial fastening). Contrary, if we find that fastening pressure (realized by a central bolt) drops more than 10%, after initial transducer assembling and its thermal treatment, this usually tell us that we have a big problem regarding used metals, components and transducer design. Fastening and refastening should be always performed on the same room temperature (when metal parts are relatively cold: 20°C).

10. Electrical and mechanical measurements should be applied after the last assembling step (as a final quality control). Transducer fastening and all measurements should be applied only in a controlled temperature (and very low humidity) environment, when all solid, transducer parts are relatively cold (say, always on 20°C to 25°C). Converters insulation resistance should be much higher than 10 MΩ, measured on 1000 V DC (it can go until 1000 MΩ on 1000 V DC). Also DC breakdown voltage of a piezoceramic stack should be measured on the assembled converter, by applying 1000 V-DC/mm test field, and converter should resist in such test conditions during 60 seconds, without producing any electrical discharge or arcing effects.

Eventually, we should protect transducer surface (against humidity and moisture, and against corona and micro arcing phenomena on electrode surfaces) using convenient (high temperature and high breakdown-voltage resistant) coating: Silicone spray, epoxy, magnet-wires lacquers... (such as Conap, etc.) This should be very fine protective layer (0.1 to 0.3 mm thick). Transducer surface coating should be applied as the last step, after connecting its electrodes to output electric terminals (and after thermal treatment). The most important is to protect externally visible area of piezoceramics and all places where moisture and humidity could penetrate into internal area of a transducer structure (because piezoceramics are slightly hygroscopic materials. A protective coating could also be done before the DC breakdown test, since one purpose of the insulation is to prevent arc-over? The bolt area passing the internal zone of piezoceramic rings should be protected by certain PTFE (teflon) cylinder, in order to prevent arc-over.

For some coatings, the converter loss may increase after the coating has first been applied. Subsequently, the converter loss may decrease for several days as the coating cures. Therefore, converter loss tests should not be conducted during this time in order to assure that the loss data is valid.

MECHANICAL TOLERANCES OF PIEZOCERAMIC RINGS

For making very high power and high efficiency ultrasonic converters (with minimal internal losses), it is extremely important to use mechanically well-finished piezoceramic rings, produced under the strongest tolerance limits.

For instance, PZT8 or SP8 piezoceramic rings used for assembling very high power ultrasonic welding converters usually have the following mechanical and surface-finishing tolerances:

T 1.6 Tolerance limits applicable on piezoceramic rings

TYPE III DOD-STD-1376A	Tolerance limits specified by BRANSON	CeramTec Catalogue (SP8)	Morgan Electro Ceramics Ruabon (PZT8)	TAMURA SA Material
Parallelism top and bottom surface	0.001"= 0.0254mm until 0.0127mm	from ≤ 0.02mm to ≤ 0.002mm	Standard Within 0.012mm ---------- Lapped Silver Within 0.007mm	0.01mm max.
Surface Flatness top and bottom surface	0.001"= 0.0254mm until 0.0127mm	0.004mm	Standard Within 0.012mm ---------- Lapped Silver Within 0.002mm to 5 light bands	0.01mm max.
Thickness	±0.005"= ±0.127mm	±0.05mm, without electrodes	Standard +/- 0.05mm Without electrodes	Standard type : -0/+0.05, High cost type : -0/+0.005, Without electrodes
Concentricity	?	max. 0.1mm	0.2mm T.I.R.	?
Outer Diameter	±0.381mm	from ±0.1mm to ±0.3mm	Standard +/- 0.15mm	± 0.4
Inner Diameter	±0.381mm	from ±0.1mm to ±0.3mm	Standard +/- 0.15mm	± 0.4
Squareness (Edge to Face)	?	?	Within 0.5^{o}	?
Surface Finish	35 micro-inches = 0.000889mm (?!)	Standard, Polished K-Schliff	Standard Within 0.003mm ---------- Lapped Silver Within 0.0005mm	Standard type: polished (#800) High cost type: polished (#2,000) Before silver electrodes are printed.
Roughness	?	≤1,6 µm (Ra – value)	?	?

Morgan Electroceramics best spec. for PZT8:

Polished Electrodes

For applications where surface flatness and surface finish to very high standards are required e.g. ultrasonic welding transducers, parts can be supplied with ("**Flat Lapped Silver**") the silver electrodes polished to the following: Surface flatness within 5 light bands Surface finish within 0.3 microns.

Evaporated Electrodes

Metal electrodes such as copper, aluminum, gold on nickel, silver on nickel applied by the evaporation process can also be supplied as an alternative to "fired-on" silver.

CeramTec spec. for piezoceramic rings (SP8):

1. For transducer rings for Ultrasonic Cleaning and Welding applications we don't specify Squareness values because they don't influence the transducer performance and would create additional costs to measure them.
2. Surface finish of the piezoceramic is not relevant because in any case a metallization is added to the piezoceramic. Only flatness and parallelism are important.
3. Standard means: Screen-printed ductile silver surface with no further treatment.
4. Polished and K- Schliff are more or less the same; there we grind the parts after the metallization process a second time to create a more flat surface over the silver. Polished is mirror - like. K-Schliff is a technical grinding which creates only a flat surface with no consideration of the visual appearance.
5. Roughness measured over metallization is ≤ 1,6 µm (Ra - value).
6. We don't specify or measure a Friction value.
7. Talking about piezoelectric parameters like capacitance, coupling coefficient, charge constant etc. if nothing special is specified we have a tolerance of +- 20 %. Basis is the data in our brochure.
8. Depending on the part and the price the tolerances for capacitance and resonance frequency can be narrowed to different levels:
   +- 15 %: Often agreed with customers for selected parameters.
   +- 10 %
   +- 5 %: Normally our tightest tolerance level
   +- 2 %: Extreme, seldom for very special parts.
9. All these data are based on high volume production (>10000 parts per year) and include "in - batch - variation" and "batch to batch - variation".

ACCEPTABLE STATISTICAL QUALITY LEVEL OF ELECTRICAL AND PIEZOELECTRIC PARAMETERS OF PIEZOCERAMICS USED FOR BLT ASSEMBLING (FOR MASS PRODUCTION OF POWER CONVERTERS)

When specifying the acceptance quality level of certain piezoceramics, we should also specify its particular electrical characteristics and piezoelectric-constants, including acceptable tolerances, using HP 4194A, (an impedance-phase network analyzer), applied on a statistical sample of ≥ 1000 pcs., for verification. All measurements should be taken on a room temperature, 20°C, and very low humidity, in an air-conditioned laboratory. For instance, PZT-8 or SP8 piezoceramic rings (OD x ID x t = 2" x 0.8" x 0.2" ≅ 50 x 20 x 5 mm), should be specified (for input factory control, on the reception) as (see Table T 2.6):

Table 2.6 Input control, acceptance limits for piezoceramic rings 2" x 0.8" x 0.2"

PZT-8 , TYPE III DOD-STD-1376A	Average Values	Maximal Tolerances	Conditions
$C_{inp.}$ (1 kHz), [nF]	3.005	± 5%	90 days after poling
$f_1 = f_s$, [Hz]	32880	± 1%	90 days after poling
$f_2 = f_p$, [Hz]	34880	± 1%	90 days after poling
$\Delta f : f_s = (f_2 - f_1) : f_s$	0.063	± 3%	90 days after poling
$\lvert Z_{min} \rvert = \lvert Z_s \rvert$, [Ω], at f_1	(≤) 13.7	± 10%	At f_s
$\lvert Z_{max} \rvert = \lvert Z_p \rvert$, [kΩ], at f_2	(≥) 245	± 20%	At f_p
Q_{m10}	(≥) 1000	± 15%	At f_s
tan δ	(≤) 0.002	± 20%	At 1 kHz
d_{33}, [E-12 C/N]	245 - 260	± 5%	Reference only
Y (Young Modulus) [N/m^2]	Short circuit: 8.1496 E+10 Open circuit: 8.9632 E+10 Poisson R = 0.31, Density: 7600 kg/m^3		Calculated using Finite Elements Analysis, based on data for f1 and f2

Silver electrodes on both surfaces
d_{33}-meter: Berlincourt, Piezo d_{33} meter, Channel Products Inc.

Table 2.6-1 Input control, acceptance limits for piezoceramic rings 1.6" x 0.8" x 0.2"

PZT-8 , TYPE III DOD-STD-1376A	Average Values	Maximal Tolerances	Conditions
$C_{inp.}$ (1 kHz), [nF]	1.86	± 5%	90 days after poling
$f_1 = f_s$, [Hz]		± 1%	90 days after poling
$f_2 = f_p$, [Hz]		± 1%	90 days after poling
$\Delta f : f_s = (f_2 - f_1) : f_s$	0.043	± 3%	90 days after poling
$\lvert Z_{min} \rvert = \lvert Z_s \rvert$, [Ω], at f_1		± 10%	At f_s
$\lvert Z_{max} \rvert = \lvert Z_p \rvert$, [kΩ], at f_2		± 20%	At f_p
Q_{m10}	≥ 1000	± 15%	At f_s
tan δ	≤ 0.002	± 20%	At 1 kHz
d_{33}, [E-12 C/N]	245 - 260	± 5%	Reference only

Table 2.6-2 Input control, acceptance limits for piezoceramic rings 0.75" x 0.25" x 0.1"

PZT-8 , TYPE III DOD-STD-1376A	Average Values	Maximal Tolerances	Conditions
$C_{inp.}$ (1 kHz), [nF]	0.90	± 5%	90 days after poling
$f_1 = f_s$, [Hz]		± 1%	90 days after poling
$f_2 = f_p$, [Hz]		± 1%	90 days after poling
$\Delta f : f_s = (f_2 - f_1) : f_s$	0.071	± 3%	90 days after poling
$\lvert Z_{min} \rvert = \lvert Z_s \rvert$, [Ω], at f_1		± 10%	At f_s
$\lvert Z_{max} \rvert = \lvert Z_p \rvert$, [kΩ], at f_2		± 20%	At f_p
Q_{m10}	≥ 1000	± 15%	At f_s
tan δ	≤ 0.002	± 20%	At 1 kHz
d_{33}, [E-12 C/N]	245 - 260	± 5%	Reference only

In cases of all other piezoceramic rings (other sizes) used for high power BLT, we can apply the following selection criteria; see Table 3.6 (again using for measurements HP 4194A, on a statistical sample ≥ 1000 pieces).

Table 3.6 Input control, acceptance limits for any-size piezoceramic rings

PZT-8 , SP-8 TYPE III DOD-STD-1376A	Excellent	Very good	Good	Acceptable
$C_{inp.}$ (1 kHz), [nF]	nominal ± 1%	nominal ± 2.33%	nominal ± 3.67%	nominal ± 5%
$f_1 = f_s$, $f_2 = f_p$ [Hz]	nominal ± 0.1%	nominal ± 0.4%	nominal ± 0.7%	nominal ± 1%
$\Delta f : f_s = (f_2 - f_1) : f_s$	nominal ± 1%	nominal ± 2.33%	nominal ± 3.67%	nominal ± 5%
$\lvert Z_{min} \rvert = \lvert Z_s \rvert$, [Ω], at f_1	nominal ± 5%	nominal ± 10%	nominal ± 15%	nominal ± 20%
$\lvert Z_{max} \rvert = \lvert Z_p \rvert$, [kΩ], at f_2	nominal ± 10%	nominal ± 16.67%	nominal ± 23.33%	nominal ± 30%
Q_{m10}	nominal ± 5%	nominal ± 10%	nominal ± 15%	nominal ± 20%
d_{33}	nominal ± 3%	nominal ± 5.33%	nominal ± 7.67%	nominal ± 10%

nominal = average or mean value,
$f_1 = f_s$, $f_2 = f_p$ first resonant frequency couple of free piezoceramics (radial-planar mode),
d_{33}-meter: Berlincourt, Piezo d_{33} meter, Channel Products Inc.
Measurements should be taken on a room temperature (20°C, very low humidity, air-conditioned).
$\mathbf{tg\delta \le 2 \cdot 10^{-3}}$, $\mathbf{Q_{m10} \ge 1000}$, **at** $\mathbf{f_{res.} = f_1 = f_s}$.
Silver electrodes applied on both surfaces.

All above given tolerances expressed in percentage-intervals (around average values), are calculated based on the Gauss, Standard, Statistical Distribution curve, where 99% of all measured cases are captured by the interval of 6 (six) standard deviations, and this criteria is in the perfect agreement with all practical situations, when measured sample is relatively large; -minimum 1000 pieces of piezoceramics.

The distinction between "Excellent", "Very good", "Good" and "Acceptable" is made by splitting the interval between “Excellent” and “Acceptable” on four, almost equal intervals (while “excellent” and “Acceptable” limits should be empirically known, in advance, after enough testing and experimental results).

T 4.6 Young modulus of different piezoceramics [N/m^2]

Source	FEM calculated	Declared in the Catalogue
Morgan: PZT8	**Short circuit: 8.1496 E+10 [N/m^2]** **Open circuit: 8.9632 E+10 [N/m^2]** **Poisson R = 0.31** **Density: 7600 kg/m^3**	**Short circuit: Y_{11}= 8.7 E+10 [N/m^2]** **Y_{33}= 7.4 E+10 [N/m^2]** **Open circuit: Y_{11}= 9.9 E+10 [N/m^2]** **Y_{33}= 11.8 E+10 [N/m^2]**
CeramTec: SP8	**Short circuit: 8.85 E+10 [N/m^2]** **Open circuit: 1.02 E+11 [N/m^2]** **Poisson R = 0.31** **Density: 7700 kg/m^3**	**Short circuit: Y_{11}= 8.77 E+10 [N/m^2]** **Y_{33}= 7.30 E+10 [N/m^2]** **Open circuit: Y_{11}= 1.00 E+11 [N/m^2]** **Y_{33}= 1.11 E+11 [N/m^2]**
Philips: PXE43	**Short circuit: 9.7 E+10 [N/m^2]** **Open circuit: 1.09 E+11 [N/m^2]** **Poisson R = 0.31** **Density: 7760 kg/m^3**	**Short circuit: Y_{11}= 9.09 E+10 [N/m^2]** **Y_{33}= 7.69 E+10 [N/m^2]** **Open circuit: Y_{11}= 8.84 E+10 [N/m^2]** **Y_{33}= 7.94 E+10 [N/m^2]**
TAMURA SA Material	**Y_{11}^E**	**$8.54 * 10^{10}$ N/m^2**
	Y_{33}^E	**$7.33 * 10^{10}$ N/m^2**
	Y_{11}^D	**$9.71 * 10^{10}$ N/m^2**
	Y_{33}^D	**$14.1 * 10^{10}$ N/m^2**
	Poisson's ratio	**0.31**
	Density	**7910 kg/m^3**

Data in this table (**red color**) probably should be corrected!!!

Piezoceramic rings used in Branson production of ultrasonic welding converters (PZT-8, SP8):

2" x 0.8" x 0.2" = 50.80 x 20.32 x 5.08 mm ≅ 50 x 20 x 5 mm
1.6" x 0.8" x 0.2" = 40.64 x 20.32 x 5.08 mm ≅ 40 x 20 x 5 mm
0.75" x 0.25" x 0.1" = 19.05 x 6.35 x 2.54 mm ≅ 19 x 6 x 2.54 mm

Piezoceramic ring and disc used in Branson production of ultrasonic cleaning converters (PZT-4, SP4):

Ring (for 40 kHz cleaning transducer):
1.5" x 0.594" x 0.2" = 38.10 x 15.0876 x 5.08 mm ≅ 38 x 15 x 5 mm

Disk (7.48 nF, for 50 kHz plate transducers):
2" x 0.1" = 50.80 x 2.54 mm ≅ 50 x 2.5 mm

Now, we can illustrate the complete impedance measurements and modeling results, realized using HP-4194A, an Impedance-Phase Network Analyzer, on the well selected (an excellent quality sample of) PZT-8, piezoceramic rings produced by Vernitron (Morgan Matroc, USA): OD x ID x t = 2" x 0.8" x 0.2" ≅ 50 x 20 x 5 mm (see T 4.7).

T 4.6 Piezoceramics measurements and Models
Piezoceramic Ring: Vernitron, PZT8, 45 / 89, ∅2" x ∅0.8" x 0.2"
First Radial Resonance Parameters

$f_1 = 32880$ Hz
$f_2 = 34880$ Hz
$|Z\ \text{min.}| = 12.8724\,\Omega$
$|Z\ \text{max.}| = 256.861\,\text{k}\Omega$
$Q_{m10} = 1129$
$Q_{m20} = 1385$

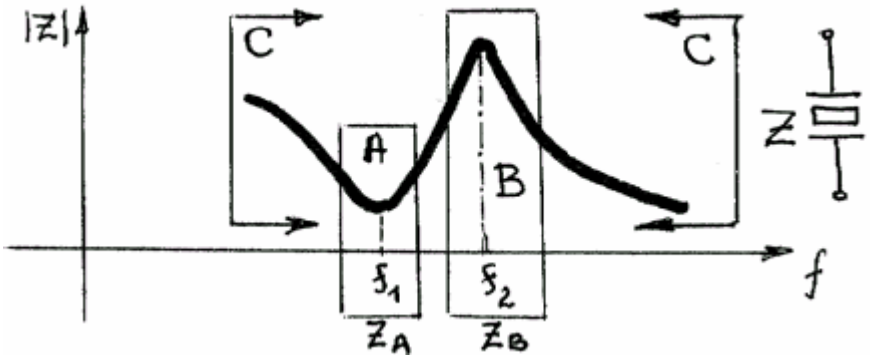

A

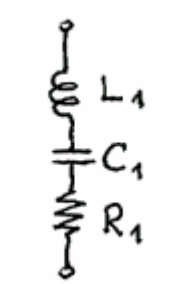

Z_A

$C_1 = 336.812$ pF
$L_1 = 69.5565$ mH
$R_1 = 12.6210\ \Omega$

⇔

A

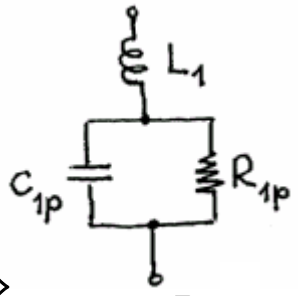

Z_A

$C_{1p} = 336.812$ pF
$L_1 = 69.5565$ mH
$R_{1p} = 16.8762\ \text{M}\Omega$

B

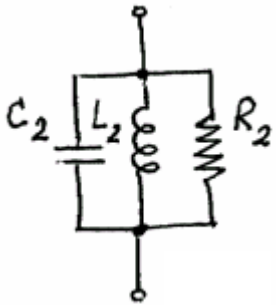

Z_B

$C_2 = 24.2667$ nF
$L_2 = 857.904\ \mu$H
$R_2 = 260.045\ \text{k}\Omega$

⇔

B

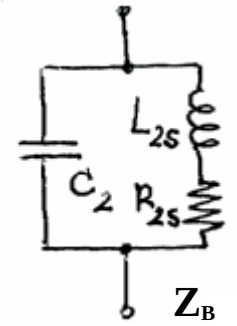

Z_B

$C_2 = 24.2667$ nF
$L_{2s} = 857.903\ \mu$H
$R_{2s} = 142.611\ \text{m}\Omega$

C

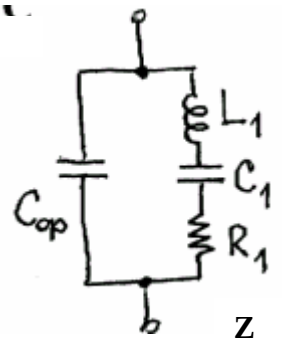

Z

$C_{op} = 2.68554$ nF
$C_1 = 336.552$ pF
$L_1 = 69.6164$ mH
$R_1 = 12.741\ \Omega$

⇔

C

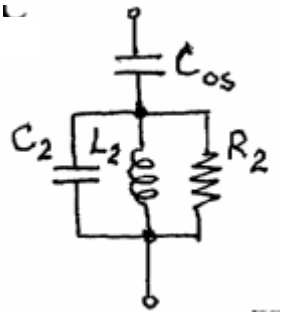

Z

$C_{os} = C_{op} + C_1 =$
$= 3.0221$ nF
$C_2 = 24.26$ nF
$L_2 = 857.9\ \mu$H
$R_2 = 260.045\ \text{k}\Omega$

The electric characteristics and tolerances of TAMURA Rings

Example: Ring dimensions (SA material): 38.0 x 15.5 x 6.2 mm

Items	Average value	Standard with tolerance
f_r	41.43 kHz	41.5 kHz ± 10%
Z_{min}	7.76 Ω	-
f_a	45.08 kHz	-
Z_{max}	649.25 kΩ	-
Δf	3.66 kHz	-
k_r	44.51 %	39.7 % min.
Q_m	2,295.87	-
C	1,818 pF	1,800 pF ± 20%
tan δ	0.18 %	-
C_{op}	1.55369 nF	-
C_1	286.77 pF	-
L_1	51.49 mH	-
R_1	5.99 Ω	-

Equivalent circuit

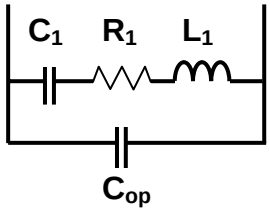

TAMURA PIEZOCERAMICS TECHNOLOGY (comments)

1. Density

Tamura applies normal, conventional sintering method to produce high-density piezoceramic. Granulated ceramic powder, which contains some kind of binder, is die-pressed to form compacts, whose green density is in the range from 4.7 to 4.8 grams per volume centimeter. Tamura powders are also fired traditionally, in the muffle furnace, after the binders were removed, to obtain the density of about 7.9 grams per cubic centimeter.

2. Specific ultrasonic power

The value of specific ultrasonic power of Tamura SA material (according to laboratory testing) must not be much different from CeramTec's (30 Watts per Centimeter Square).

3. Important parameters

The most important parameter for both of SS and SA Tamura materials is high Qm value, because they are used specially for high power converters, and its heat losses are very low.

For SA material relative permitivity is the most important parameter. The value is almost the same as the value of Japanese other big ceramic makers.

SA material's relative permitivity do not change significantly, before and after ring ceramic is assembled into BLT. This is also the reason why SA materials are suitable for ring-shaped piezoelectric transducers.

"Best" Piezoceramics

The following is from a conversation on 6/10/99 with a ceramic engineer who was previously employed by Morgan-Matroc.

His ranking of ceramic manufacturers:

a. **First tier**
   i) Morgan Matroc
   ii) Piezokinetics Inc (PKI) – buys from EDO. 4/3/00: Has special high ampl piezos designed for medical applications. Suresh Viswanathan seems very knowledgeable.
   iii) ?Valpey – buys from EDO
   iv) ?Stavley Sensors – buys from EDO

b. **Second tier**
   i) EDO
   ii) Sensor Tech
   iii) Transducer Products of South Hampton
   iv) Hoescht – material is between PZT4 and PZT8; lower loss material similar to Morgan Matroc 4S and 8M, but "odd" formulation so may not be able to obtain from other companies as secondary suppliers
   v) Unilator

c. **Third tier**
   i) APC – uses Czech ceramics; Craig had some problems
   ii) Channel

Ceramic tolerances (disks, fully machined):

Company	Parameter	Tolerance	Notes
Channel Industries (p. 13)	Diameter	±.003	Ø.125 → Ø1.500
	Thickness	±.003	.080 → .200
	Parallelism	.001"/"	Up to Ø2.000
	Flatness	.001"/"	Up to Ø2.000
	Silver electrode thickness (p. 11)	.0006 -- .001	Dimension, not tolerance
Stavley Sensors	Diameter	+.000/-.003	
	Thickness	±.0003	Up to Ø3.000
	Finish	35 (fired electrodes) 32 (electroless Ni) 8 (electroless Cu or Au)	
Valpey Fisher (p. 4)	Diameter		

	Thickness		
	Parallelism	.00005" max.	
	Flatness	.0001" max.	
EDO (p. 27)	Diameter	±.003	Ø.125 → Ø1.500
	Thickness	±.003	.080 → .200
	Parallelism		
	Flatness	Within thickness tolerance if dia/thickness < 10:1	
Vernitron (PD-9247, p. 5)	Diameter	±.015	
	Thickness	±.010	.080 → .500
	Parallelism	.007"	
	Flatness	Within thickness tolerance up to Ø1.0 and up to .080 thick; .005" above .080 thick	
	Silver electrode thickness (p. 26)	.0003 -- .001	Dimension, not tolerance
	Nickel electrode thickness (p. 26)	.00005 -- .0002	Dimension, not tolerance
Piezokinetics	Silver electrode thickness	.0005 -- .0007	Dimension, not tolerance
	Nickel electrode thickness	.0003	Dimension, not tolerance
Stavley Sensors	Diameter	±.002	
	Thickness	±.003	
	Parallelism		
	Flatness		
	Silver electrode thickness (p. 26)	.0005	Dimension, not tolerance
	Nickel electrode thickness (p. 26)	.00002	Dimension, not tolerance
	Electroless copper or gold	< 100 microns	

Channel (p. 11) – Electroless nickel is a low temperature process that gives thinner, higher resistance electrodes than silver. Used mainly for shear ceramics.

Insulation for ceramics

Loctite Lite-tak 375: brush on, ultraviolet curing in several seconds, very low mechanical loss (per Tim Meyers at Vernitron, 6/9/92).

Conap

Parylene: Vapor deposition, therefore excellent coverage (even on sharp corners and cavities) with no pinhole leaks. Masking required preventing adherence to unwanted surfaces. Thickness typically <= 1 mil. Dielectric strength 5500 – 7000 volts/mil. Used by Morgan Matroc on their ceramics (per Tim Meyers, Morgan Matroc, 4/9/96)

Others: Hysol, Master Bond (per American Piezoceramics, 3/28/93); Eccocoat 831 (Emerson & Cumming)

6.1 MECHANICAL TOLERANCES OF PIEZOCERAMIC RINGS

For making very high power and high efficiency ultrasonic converters (with minimal internal losses), it is extremely important to use mechanically well-finished piezoceramic rings, produced under the strongest tolerance limits.

For instance, PZT-8 or SP8 piezoceramic rings (OD x ID x t = 50 x 20 x 5 mm = 2" x 0.8" x 0.2"), often used for assembling very high power ultrasonic welding converters usually have the following mechanical and surface-finishing tolerances:

T 1.6 Tolerance limits applicable on piezoceramic rings: 50 x 20 x 5 mm

PZT Rings	BRANSON tolerance limits	CeramTec	Vernitron
Parallelism top and bottom surface	**0.001"= 0.0254mm until 0.0127mm**	**from ≤ 0.02mm to ≤ 0.002mm**	**0.012mm**
Surface Flatness top and bottom surface	**0.001"= 0.0254mm until 0.0127mm**	**0.004mm**	**from 0.012mm to 5 light bands**
Thickness	**±0.005"= ±0.127mm**	**±0.05mm, without electrodes**	**±0.05mm, without electrodes**
Concentricity	**?**	**max. 0.1mm**	**0.2mm T.I.R.**
Outer Diameter	**±0.381mm**	**from ±0.1mm to ±0.3mm**	**±0.15mm**
Inner Diameter	**±0.381mm**	**from ±0.1mm to ±0.3mm**	**±0.15mm**
Squareness (Edge to Face)	**?**	**?**	**Within 0.5° Max. deviation less than 1 micrometer, both on ID and OD**
Surface Finish	**35 micro-inches = 0.000889mm (?!)**	**Standard, Polished K-Schliff**	**from 0.003mm until 0.0003mm**
Roughness			
Surface Friction			

ACCEPTABLE STATISTICAL QUALITY LEVEL OF ELECTRICAL AND PIEZOELECTRIC PARAMETERS OF PIEZOCERAMICS USED FOR BLT ASSEMBLING (FOR MASS PRODUCTION OF POWER CONVERTERS)

When specifying the acceptance quality level of certain piezoceramics, we should also specify its particular electrical characteristics and piezoelectric-constants, including acceptable tolerances, using HP 4194A, applied on a statistical sample of ≥ 1000 pcs., for verification. All measurements should be taken on a room temperature, 20°C, and low humidity, in an air-conditioned laboratory.

For instance, PZT-8 or SP8 piezoceramic rings (OD x ID x t = 50 x 20 x 5 mm = 2" x 0.8" x 0.2"), should be specified (for the purpose of input control on the reception) as:

T 2.6 Input control, acceptance limits for piezoceramic rings 50 x 20 x 5 mm

PZT-8 , SP-8 TYPE III DOD-STD-1376A	Average Values	Maximal Tolerances	Conditions
$C_{inp.}$ (1 kHz), [nF]	3.005	± 5%	90 days after poling
$f_1 = f_s$, [Hz]	32880	± 1%	90 days after poling
$f_2 = f_p$, [Hz]	34880	± 1%	90 days after poling
$\Delta f : f_s = (f_2 - f_1) : f_s$	0.063	± 3%	90 days after poling
$\lvert Z_{min} \rvert = \lvert Z_s \rvert$, [Ω]	≤ 13.7	± 10%	At f_s
$\lvert Z_{max} \rvert = \lvert Z_p \rvert$, [kΩ]	≥ 245	± 20%	At f_p
Q_{m10}	≥ 1285	± 15%	At f_s
tan δ	≤ 0.002	± 20%	At 1 kHz
d_{33}, [E-12 C/N]	245 - 260	± 5%	Reference only

Silver electrodes on both surfaces
d_{33}-meter: Berlincourt, Piezo d_{33} meter, Channel Products Inc.

T 2.6-1 Input control, acceptance limits for piezoceramic rings 1.6" x 0.8" x 0.2"

PZT-8 , SP-8 TYPE III DOD-STD-1376A	Average Values	Maximal Tolerances	Conditions
$C_{inp.}$ (1 kHz), [nF]	1.86	± 5%	90 days after poling
$f_1 = f_s$, [Hz]		± 1%	90 days after poling
$f_2 = f_p$, [Hz]		± 1%	90 days after poling
$\Delta f : f_s = (f_2 - f_1) : f_s$	0.043	± 3%	90 days after poling
$\lvert Z_{min} \rvert = \lvert Z_s \rvert$, [Ω]		± 10%	At f_s
$\lvert Z_{max} \rvert = \lvert Z_p \rvert$, [kΩ]		± 20%	At f_p
Q_{m10}	≥ 1000	± 15%	At f_s
tan δ	≤ 0.002	± 20%	At 1 kHz
d_{33}, [E-12 C/N]	245 - 260	± 5%	Reference only

T 2.6-2 Input control, acceptance limits for piezoceramic rings 0.75" x 0.25" x 0.1"

PZT-8 , SP-8 TYPE III DOD-STD-1376A	Average Values	Maximal Tolerances	Conditions
$C_{inp.}$ (1 kHz), [nF]	0.90	± 5%	90 days after poling
$f_1 = f_s$, [Hz]		± 1%	90 days after poling
$f_2 = f_p$, [Hz]		± 1%	90 days after poling
$\Delta f : f_s = (f_2 - f_1) : f_s$	0.071	± 3%	90 days after poling
$\lvert Z_{min} \rvert = \lvert Z_s \rvert$, [Ω]		± 10%	At f_s
$\lvert Z_{max} \rvert = \lvert Z_p \rvert$, [kΩ]		± 20%	At f_p
Q_{m10}	≥ 1000	± 15%	At f_s
tan δ	≤ 0.002	± 20%	At 1 kHz
d_{33}, [E-12 C/N]	245 - 260	± 5%	Reference only

In cases of all other piezoceramic rings (other sizes) used for high power BLT, we should apply the following selection criteria (again using HP 4194A, on a statistical sample ≥ 1000 pieces):

T 3.6 Input control, acceptance limits for any-size piezoceramic rings

PZT-8 , SP-8 TYPE III DOD-STD-1376A	Excellent	Very good	Good	Acceptable
$C_{inp.}$ (1 kHz), [nF]	nominal ± 1%	nominal ± 2.33%	nominal ± 3.67%	nominal ± 5%
$f_1 = f_s$, $f_2 = f_p$ [Hz, kHz]	nominal ± 0.1%	nominal ± 0.4%	nominal ± 0.7%	nominal ± 1%
$\Delta f : f_s = (f_2 - f_1) : f_s$	nominal ± 1%	nominal ± 2.33%	nominal ± 3.67%	nominal ± 5%
$\lvert Z_{min} \rvert = \lvert Z_s \rvert$, [Ω]	nominal ± 5%	nominal ± 10%	nominal ± 15%	nominal ± 20%
$\lvert Z_{max} \rvert = \lvert Z_p \rvert$, [kΩ]	nominal ± 10%	nominal ± 16.67%	nominal ± 23.33%	nominal ± 30%
Q_{m10}	nominal ± 5%	nominal ± 10%	nominal ± 15%	nominal ± 20%
d_{33}	nominal ± 3%	nominal ± 5.33%	nominal ± 7.67%	nominal ± 10%

nominal = average or mean value,
$f_1 = f_s$, $f_2 = f_p$ first resonant frequency couple of free piezoceramics (radial-planar mode),
d_{33}-meter: Berlincourt, Piezo d_{33} meter, Channel Products Inc.
Measurements should be taken on a room temperature (20°C, very low humidity, air-conditioned).
$\mathbf{tg\delta \le 2 \cdot 10^{-3}}$, $\mathbf{Q_{m10} \ge 1000}$, **at** $\mathbf{f_{res.} = f_1 = f_s}$.
Silver electrodes applied on both surfaces.

All above given tolerances expressed in percentage-intervals (around average values), are calculated based on the Gauss, Standard, Statistical Distribution curve, where 99% of all measured cases are captured by the interval of 6 (six) standard deviations, and this criteria is in the perfect agreement with all practical situations, when measured sample is relatively large; -minimum 1000 pieces of piezoceramics.

Piezoceramic rings used in Branson production of ultrasonic welding converters (PZT-8, SP8):

2" x 0.8" x 0.2" = 50.80 x 20.32 x 5.08 mm ≅ 50 x 20 x 5 mm
1.6" x 0.8" x 0.2" = 40.64 x 20.32 x 5.08 mm ≅ 40 x 20 x 5 mm
0.75" x 0.25" x 0.1" = 19.05 x 6.35 x 2.54 mm ≅ 19 x 6 x 2.54 mm

Piezoceramic ring and disc used in Branson production of ultrasonic cleaning converters (PZT-4, SP4):

Ring (for 40 kHz cleaning transducer):
1.5" x 0.594" x 0.2" = 38.10 x 15.0876 x 5.08 mm ≅ 38 x 15 x 5 mm

Disk (7.48 nF, for 50 kHz plate transducers):
2" x 0.1" = 50.80 x 2.54 mm ≅ 50 x 2.5 mm

Now, we can illustrate the complete impedance measurements and modeling results, realized using HP-4194A, an Impedance-Phase Network Analyzer, on the PZT-8, piezoceramic rings produced by Vernitron (Morgan Matroc, USA): OD x ID x t = 50 x 20 x 5 mm ≅ 2" x 0.8" x 0.2".

T 4.6 Piezoceramics measurements and Models
Piezoceramic Ring: Vernitron, PZT8, 45 / 89, ∅2" x ∅0.8" x 0.2"
First Radial Resonance Parameters

$f_1 = 32880$ Hz
$f_2 = 34880$ Hz
$|Z\ \text{min.}| = 12.8724\,\Omega$
$|Z\ \text{max.}| = 256.861\,\text{k}\Omega$
$Q_{m10} = 1129$
$Q_{m20} = 1385$

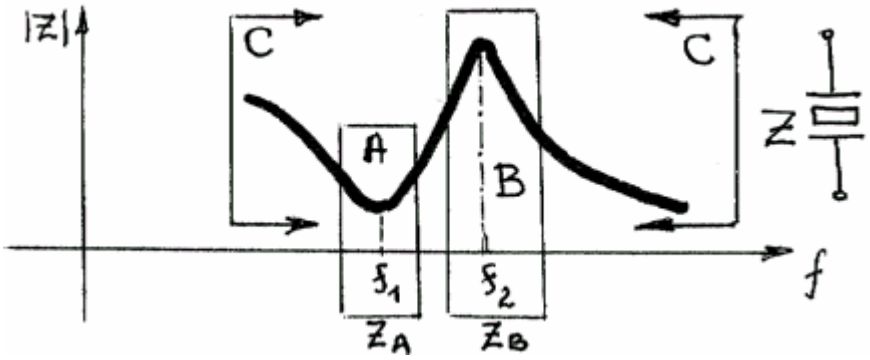

A

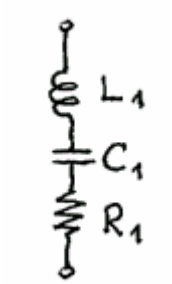

Z_A

$C_1 = 336.812$ pF
$L_1 = 69.5565$ mH
$R_1 = 12.6210\ \Omega$

⇔

A

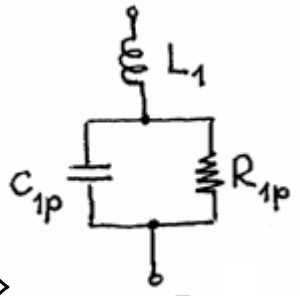

Z_A

$C_{1p} = 336.812$ pF
$L_1 = 69.5565$ mH
$R_{1p} = 16.8762\ \text{M}\Omega$

B

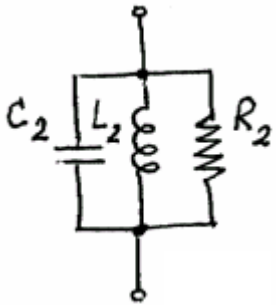

Z_B

$C_2 = 24.2667$ nF
$L_2 = 857.904\ \mu$H
$R_2 = 260.045\ \text{k}\Omega$

⇔

B

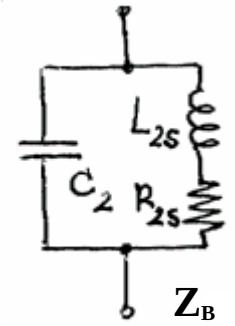

Z_B

$C_2 = 24.2667$ nF
$L_{2s} = 857.903\ \mu$H
$R_{2s} = 142.611\ \text{m}\Omega$

C

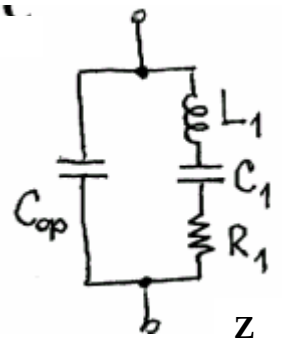

Z

$C_{op} = 2.68554$ nF
$C_1 = 336.552$ pF
$L_1 = 69.6164$ mH
$R_1 = 12.741\ \Omega$

⇔

C

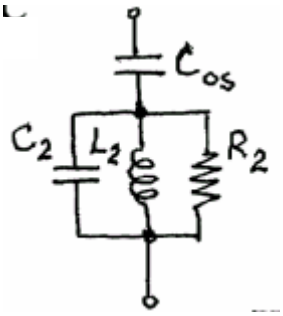

Z

$C_{os} = C_{op} + C_1 =$
$= 3.0221$ nF
$C_2 = 24.26$ nF
$L_2 = 857.9\ \mu$H
$R_2 = 260.045\ \text{k}\Omega$

THE ULTRASONIC HAMMER TRANSDUCER

Miodrag Prokic*
*MP Interconsulting, Marais 36, CH-2400 LeLocle, Switzerland
Jon Tapson [γ]
[γ] Department of Electrical Engineering, University of Cape Town, Rondebosch 7701, South Africa
Bruce J.P. Mortimer [•]
[•] Centre for Instrumentation Research, Cape Technikon, PO Box 652, Cape Town 8000, South Africa

Abstract – A new high power ultrasonic transducer is described. This transducer consists of a front mass and rear mass and two piezoelectric drivers on either side of a center mass which is also the dominating resonance mass. The characteristics of the transducer resemble a force transducer combined with the small signal characteristics of a sandwich transducer. Several variations can be achieved by manipulating the mechanical coupling as well as the electrical connections. The transducer is suitable for driving high mass loads such as the contents of pipes.

I. INTRODUCTION

Conventional Langevin or sandwich transducers [1] (Figure 1) are well known and are widely used in high power piezoelectric sonar and ultrasonic applications. These transducers are usually characterized by a relatively narrow resonant frequency bandwidth (or a relatively high Q) and a resonant characteristic that is coupled to the load i.e. its resonance is affected by changes in the medium. Most conventional ultrasonic systems account for this variation by employing various frequency and motional locking schemes to insure that the load is optimally driven within the limits of the transducer and the energy supply [2].

In spite of the popularity of the Langevin transducer, these transducers cannot effectively drive certain loads such as those contained within thick-walled pipes. This is due the load mass being directly connected to the front oscillating mass and thereby introducing an additional order of complexity into the system as well as an increase in lumped element mass. This problem has become more prevalent as many emerging applications such as sonochemistry or high pressure cleaning [3], require ultrasonic energy to be transmitted through thick walled vessels.

A separate problem with conventional ultrasonic cleaning and liquid processing systems is that one generally requires a uniform coverage over the treatment vessel. Since the transducers used have of relatively narrow resonant characteristics, standing waves usually form. Many systems make use of some frequency sweeping, amplitude modulation or a combination of different transducers to reduce this effect. However, this usually results in some compromise on the transducer efficiency. Increasing the transducer system frequency response would therefore have the potential to couple energy into the load without the formation of standing waves, but this is not practical with conventional sandwich transducer systems.

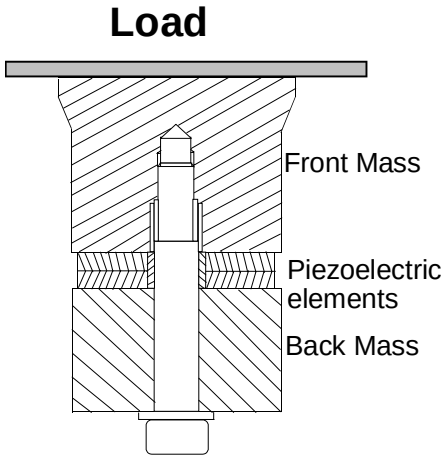

Figure 1 : Conventional Langevin transducer. The front mass is coupled to the back mass via a tensional bolt and the piezoelectric ring elements in the middle of the transducer. The load is coupled to the front mass and therefore influences the resonance response.

This paper presents a novel configuration that we have termed the hammer transducer [4]. The transducer has a resonant mass element that is independent of the acoustic load and, in certain circumstances, this configuration has a multi-resonant characteristic that is well suited to multi-frequency driving (over a significant bandwidth).

II. THE HAMMER TRANSDUCER

This transducer uses a minimum of two series driven piezoelectric elements to drive a fixed resonator mass element that is clamped between the piezoelectric rings. The piezoelectric elements are in turn sandwiched between a front and back mass and held together by a central bolt (which is also used to pretension the piezoelectric elements) as shown in Figure 2.

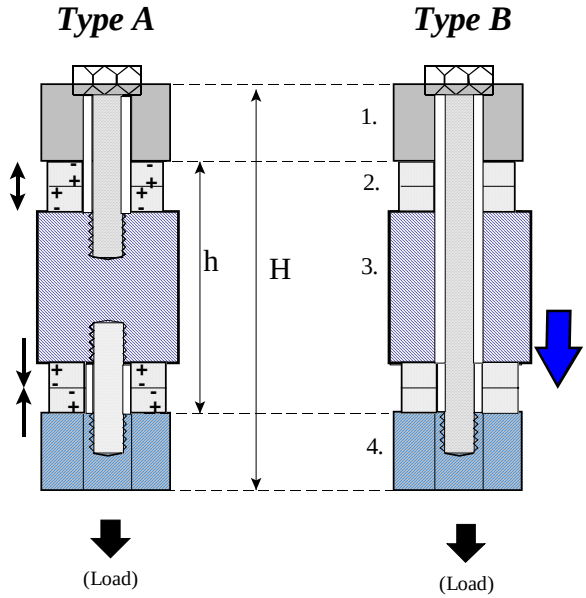

Figure 2 : Schematic of the Hammer transducer showing 1) tail mass, 2) four piezoelectric rings, 3) hammer mass and 4) front mass that is usually coupled to the load. Two configurations are possible: *Type A* - Center mass connected directly to bolt and *Type B* - Center mass moves independently of the bolt.

Although the construction of the transducer is similar to a conventional sandwich transducer, the operation is different as the central mass is usually designed to be the predominant resonant mechanism. This mass is in turn forced in one direction and then the other as a consequence of the piezoelectric elements being driven in series – as one disk contracts the other expands (in thickness mode). We have termed this type of transducer a "hammer transducer" as the central mass "hammers" the front and back masses [4].

Two different constructions are possible; firstly *Type A* the central bolt mechanically connects all masses and participates as an important (spring and mass) element of the total mechanical oscillating circuit (all three masses are oscillating) and secondly, *Type B* where the middle mass is not mechanically (directly) connected to the central bolt and central bolt can be approximately considered as the rigid connection between two end metal masses (only the middle mass is oscillating).

III. TRANSDUCER OPERATION

An approximate mechanical-equivalent oscillating circuit demonstrating the different hammer transducers configurations is shown in Figure 3. Mechanical excitation is symbolically represented as a mechanical generator/s, $e_m(F,V)$, where F and V are the force and the velocity respectively.

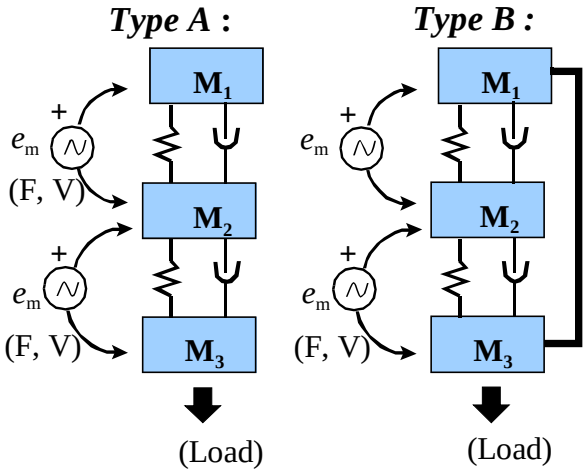

Figure 3 : Simplified equivalent oscillation system for the Hammer transducer options.

In the *Type A* resonator, we create a double resonant, 3 degree of freedom system. This can be rather complex to analyze (especially if the load interacts

with M_3). This configuration is similar to a hybrid magnetorestrictive / piezoelectric combinational transducer that has been reported to be capable of achieving a significantly greater bandwidth than conventional tonpilz type transducers [5].

In *Type B* we have a hammer-mode where we can assume that only the middle metal mass is moving (in piston-mode with the end masses confined by the central bolt). With suitable parameter selection, *Type A* resonators can be designed with a dominant central mass, also approximating hammer-mode resonance. In this case, the end-masses are also oscillating, but significantly less (power-wise) than the middle-mass.

Hammer-mode resonance :

The total length of the active transducer stack *h* (the length of the central mass and two piezo-ceramic layers, without counting the end metal) remains approximately constant and fixed by the bolt. This is because the two piezo-ceramic layers are mechanically identical and are in opposite electrical polarization (and equally driven). When the first piezo-ceramic layer is contracting, the second one is extending by the same displacement (and vice versa) mutually compensating the total displacement of the active middle-stack length. Of course, the total transducer length, including both end-masses will not stay absolutely constant, except in case/s of fully symmetrical hammer transducer structure where upper and lower end-masses, and piezo-ceramic layers are identical.

An unusual property of the hammer transducer is that the dynamic center of mass, or center of inertia also oscillates. This is in contrast with conventional transducers where the center of mass will remain in a stable position.

The overall hammer-mode vibration is as a force transducer as opposed to a displacement transducer. This property means that the transducer will require a coupling to a load (such as a cavity resonator), but the characteristics of the load will not necessarily affect the resonance of the hammer.

Electrical driving options :

There are two basic configurations in which the hammer transducers electrical terminals can be connected; piezoelectric elements series driven and piezoelectric parallel driven. This is demonstrated by drawing the system in the format of a two-port network [6]. This is shown for the case of a hammer *Type B* with piezoelectric elements driven in series in Figure 4 and for parallel driving in Figure 5.

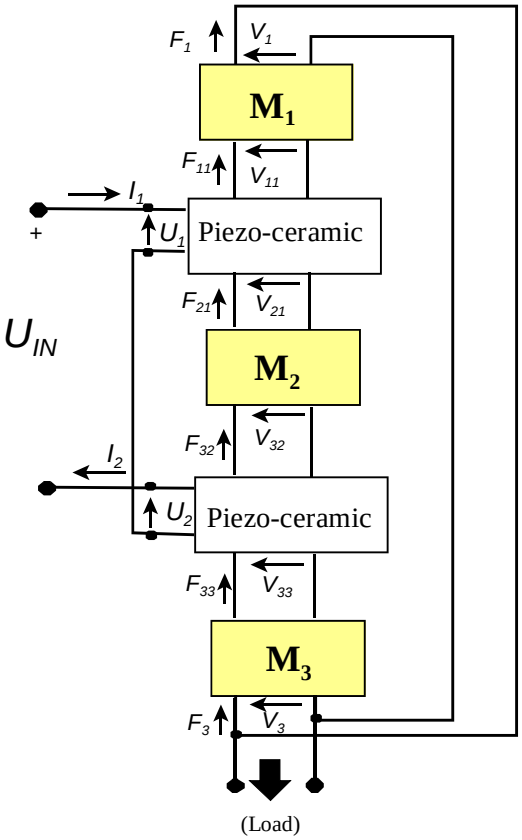

Figure 4 : Two-port system representation [6] showing piezoelectric elements driven in series. In this case, $F_1 \approx F_3$, $V_1 \approx V_3$, $F_{21}=F_{32}$, $V_{21}=V_{32}$, $I_1=I_2$ and $U_1=U_2=0.5U_{in}$

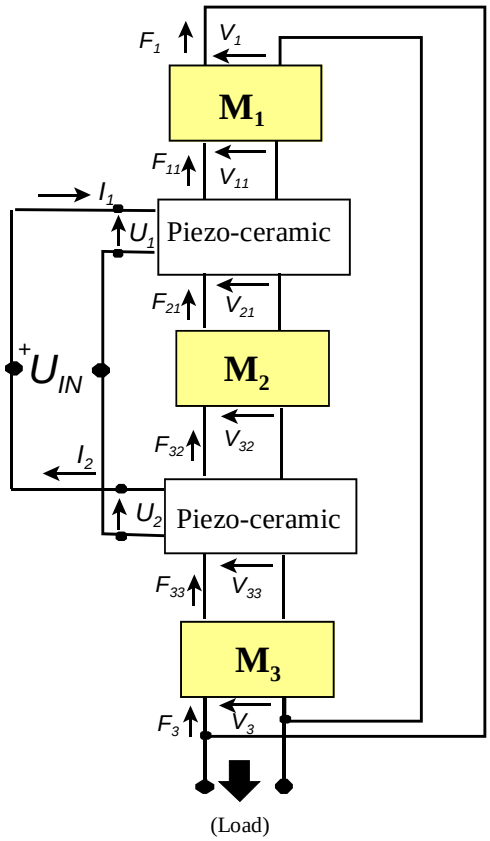

Figure 5 : Two-port system representation of a Type B hammer transducer [6] showing piezoelectric elements driven in parallel. In this case, $F_1 \approx F_3$, $V_1 \approx V_3$, $F_{21}=F_{32}$, $V_{21}=V_{32}$ and $U_1=U_2=U_{in}$

The two electrical configurations shown in Figure 4 and 5 allow for various driving options (including motional current and motional voltage). A complete analysis however, must take into account the transmission line characteristics of the components (including the load).

IV. EXPERIMENTAL RESULTS

Hammer transducers have been tested in various metal stamping, forging and high pressure cleaning [3] applications. Coupling from the hammer transducer to the load was via an aluminum or steel bar and in the case of high pressure cleaning, an additional acoustical coupling ring (round the exterior of the liquid filled pipe).

Variations in the load have very little effect on the operation of this transducer. Further the drive frequency can be modulated in a much wider frequency interval than in the case of traditional two-mass transducers (sometimes up to ±30% around central operating frequency), without dropping mechanical quality factor.

V. CONCLUSIONS

Several configurations of a force transducer, termed the hammer transducer have been presented. A central mass is the dominant resonant mechanism and the transducer has several advantages; namely a certain degree of isolation from the load, a transducer capable of generating large forces in an attached work-piece (even of high mass) and the potential of driving over a wide power bandwidth. Two electrical configurations are possible, each resulting in a complex system filter characteristic that cannot be accurately represented as a lumped equivalent circuit.

VI. REFERENCES

[1] A.P. Hulst, “On a family of high-power transducers”, Ultrasonics International Conference Proceedings, 1973.

[2] B. Mortimer, T. du Bruin, J. Davies, J. Tapson, “High power resonant tracking amplifier using admittance locking”, Ultrasonics, vol. 39, pp. 257-261, 2001.

[3] M. Prokic, “Multifrequency Ultrasonic Actuators with Special Application to Ultrasonic Cleaning in Liquid and Supercritical CO_2”, UIA Conference, Atlanta, 10-12 October 2001.

[4] European Patent Application: EP 1 060 798 A1, Miodrag Prokic, 2400 Le Locle Switzerland, Date of publication: 20.12.2000, Bulletin 2000/51, (patent pending in several countries).

[5] S. Butler, F. Tito, “A broadband hybrid magnetorestrictive piezoelectric transducer array”, MAGSOFT UPDATE, vol. 7, No. 1 1-7 2001.

[6] R. S. Woollett, Scientific and Engineering Studies : Section II The Longitudinal Vibrator, Naval Underwater Systems Centre, Newport, Rhode Island, pp 66-79.